Report No. 4: 2D UHRS Survey Geomodel Integrated with CPT and BH Data, Full Site

Danish Offshore Wind 2030 | North Sea 1, Denmark

F217715-REP-004 [02] | 21 November 2025

Final

Energinet Eltransmission A/S

Document Control

Document Information

Project Title	Danish Offshore Wind 2030
Document Title	Report No. 4: 2D UHRS Survey Geomodel Integrated with CPT and BH Data, Full Site
Fugro Project No.	F217715
Fugro Document No.	F217715-REP-004
Issue Number	[02]
Issue Status	Final
Fugro Legal Entity	Fugro Netherlands Marine Limited
Issuing Office Address	Prismastraat 4, Nootdorp, 2631 RT, The Netherlands

Client Information

Client	Energinet Eltransmission A/S
Client Address	Tonne Kjærsvej 65, DK-7000 Fredericia, Denmark
Client Contact	Anna Bondo Medhus and Pieter Oudshoorn

Document History

Issue	Date	Status	Comments on Content	Prepared By	Checked By	Approved By
01	19 September 2025	For Review	Awaiting client comments	DS/TC/CS	JW	LOL/CS
02	7 November 2025	Final	Addressing client comments	DS/TC/CS	JW	CS
03	21 November 2025	Final	Update following final client comments	DS/TC	JW	CS

Project Team

Initials	Name	Role
AP	A. Padwalkar	Project Director
AL	Alistair Leighton	Project Manager
MN	Malgorzata (Gosia) Nowak	Reporting and Deliverables Project Manager
CS	Chris Steven	Principal Engineering Geologist
LO	Lorraine O'Leary	Engineering Geology and Geohazards Team Lead
JW	Jordan Wilson	Senior Engineering Geologist
DS	Devan Scanlan	Supervising Engineering Geologist
TC	Tom Cookson	Project Engineering Geologist

FUGRO
Fugro Netherlands Marine Limited
Prismastraat 4
Nootdorp
2631 RT
The Netherlands

Energinet Eltransmission A/S
Tonne Kjærsvej 65
DK-7000 Fredericia
Denmark

21 November 2025

Dear Ms Medhus and Mr Oudshoorn

We are pleased to submit Report No. 4: 2D UHRS Survey Geomodel Integrated with CPT and BH Data, Full Site for the Danish Offshore Wind 2030 project. This report presents the results of the geological site survey with geotechnical Cone Penetration Test (CPT) and Borehole (BH) survey results integrated for the full North Sea 1 site including Sub-Area 2 geotechnical data collected in 2025.
We hope that you find this report to your satisfaction; should you have any queries, please do not hesitate to contact us.

Yours sincerely

Chris Steven
Principal Engineering Geologist

Frontispiece

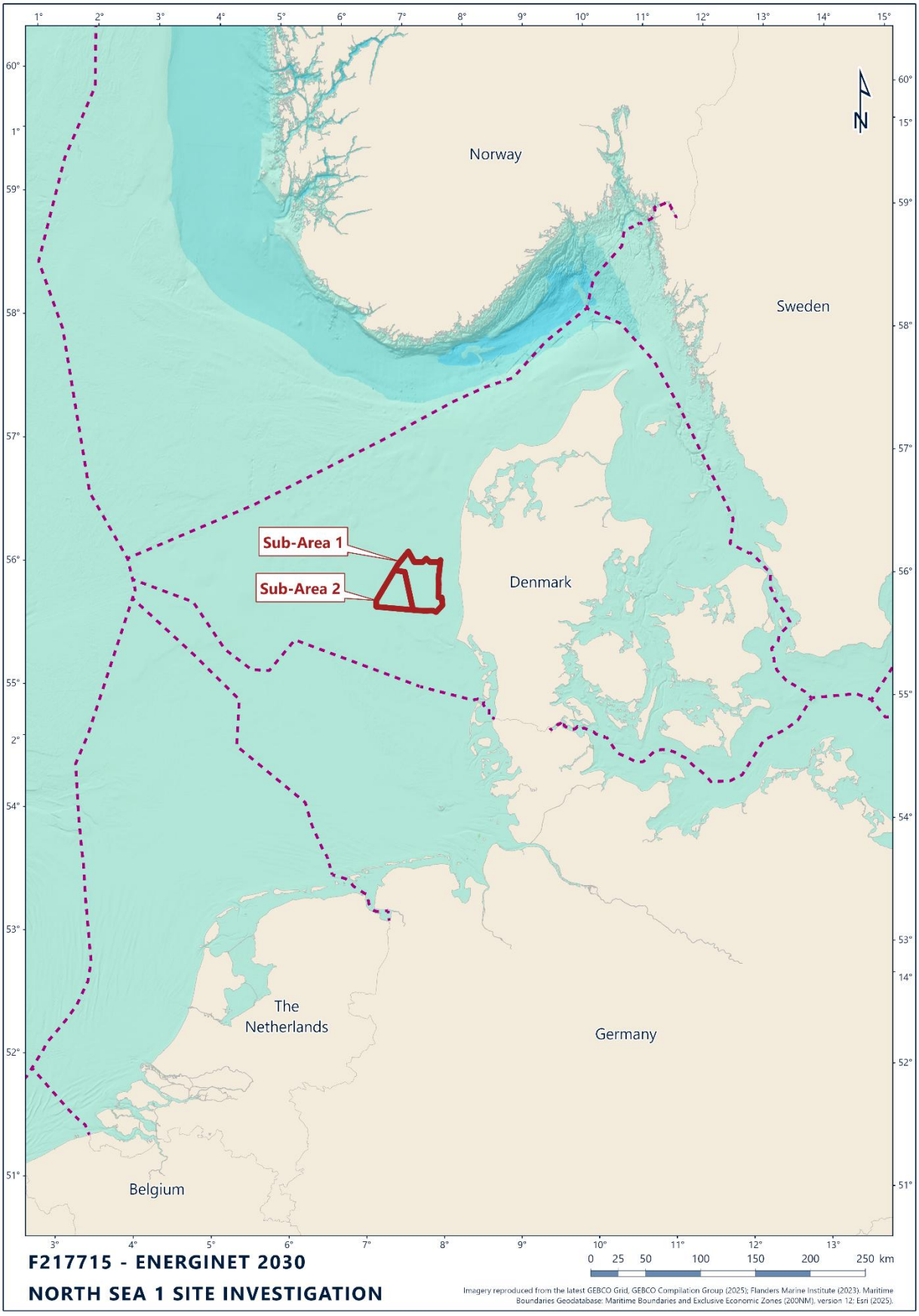

Executive Summary

Interpretative Site Investigation	
Survey Dates	10 June to 13 November 2023 (geophysical); 27 October 2023 to 25 July 2025 (geotechnical)
Equipment	Geophysical: multibeam echosounder (MBES), sub-bottom profiler (SBP); 2D ultra high resolution (2D UHR) seismic. Geotechnical: cone penetrometers, seismic cone penetrometers and borehole sampling
Coordinate System	Datum: European Terrestrial Reference System 1989 (ETRS89) Projection: Universal Transverse Mercator (UTM) Zone 32N, CM 3°E
Vertical Datum	Mean Sea Level [MSL]
Bathymetry	
Elevation at the time of the survey ranged from 12.27 m to 33.51 m below Mean Sea Level (MSL). In the south of the site is a sand bank with north-north-west to south-south-east orientation. To the west of this are several south-west to north-east and north-west to south-east oriented ridges (Ocean Infinity, 2024).	
Regional Geological History	
During the Miocene to Middle Pleistocene (23 million to 781 thousand years), marine, deltaic and fluvial deposits (geological units Base Seismic Unit (BSU) and Unit U90) were deposited at the site as a result of the progradation of the Eridanos river system. During the Elsterian glaciation, tunnel valleys and their infill (geological unit U70) were formed, and the BSU was glacially deformed. In the Holstenian interglacial period, glacial lacustrine deposits infilled valleys formed during the Elsterian glaciation (geological unit U69). During the Saalian glacial period, tunnel valley infills, glacial deposits (geological unit U65) and glacio-fluvial sediments (geological units U60 and U65) were deposited. During the Eemian interglacial period marine clays (geological units U36 and U50) were deposited. During the Weichselian glacial period, glacio-fluvial (geological units U30 and U35) and glacio-lacustrine (geological unit U30) sediments were deposited. During the final stages of the last glacial period, channels were eroded which were filled during the Late Pleistocene (geological unit U35) to early Holocene (geological unit U20). During the Holocene, marine sediments (geological unit U10) were deposited during the marine transgression.	
Geological Features and Geohazards	
Peat and/or organic clay	Peat and/or organic clay is present locally in geological units U20, U30, U50 and BSU.
Low strength clays	Soft clays are present in geological unit U20.
Shallow gas	There is evidence for the presence of shallow gas in the form of acoustic blanking and/or signal attenuation on the 2D UHR seismic data in geological unit U20 and to a lesser extent in geological unit U50.
Coarse material	Gravel and cobbles may be present in shallow marine (geological unit U10), glacio-fluvial deposits (geological units U30, U35, U60 and U90). Gravel, cobbles and boulders may be present in glacial deposits (geological units U65 and U70).
Buried channels and tunnel valleys	Geological units U20, U30, U35, U50 and U60 locally form channel infills. Geological units U70 and partially geological unit U65 represent the infill of tunnel valleys. Geological units U35, U60, U65, U70 and U90 contain internal erosion surfaces and channels.
U65 Variability	High variability in composition, and soil strengths due to variable depositional nature of the unit, making extrapolation of data from geotechnical sources less reliable.
Glacial deformation	Thrust faults were observed in geological units U65, U70, and the BSU, and are interpreted to be the result of glacio-tectonism.
Faults	Normal faults are present in the BSU in a small area in the south-east of the site. Thrust faults are present across the site in BSU. They may also be present in U70 due to flank collapse.
Geological Model	

Unit 10	Geological unit U10 is present throughout most of the site and forms a layer of Holocene marine sand with a maximum thickness of 10 m.
Unit 20	Geological unit U20 forms infill of spatially variable channels and overbank sand (Subunit 20a) and clay (Subunit 20b) deposits, and has a maximum thickness of 30 m. This unit is more prominent in NS1 Sub-Area 1 within channelised and overbanking deposits. It appears in Sub-Area 2 in channels, mainly in the north of Sub-Area 2.
Unit 30	Geological unit U30 is a locally present sand unit with a sheet-like geometry, often with a clay bed at its base, and has a maximum thickness of 12 m. This unit is predominantly limited to the north of the NS1 Sub-Area 1 site, with smaller localised deposits in Sub-Area 2.
Unit 35	Geological unit U35 comprises fluvial sand with a sheet-like to channelised geometry, and has a maximum thickness of 24 m. This unit is widely found in NS1 Sub-Area 1 and in the north and south-west of Sub-Area 2.
Unit 36	Geological unit U36 is transitional between units U35 and U50, with internal dipping reflectors comprising silt and sand, and has a maximum thickness of 24 m. This unit is spatially limited to the south-east of NS1 Sub-Area 1.
Unit 50	Geological unit U50 is a marine clay with a sheet-like to channelised geometry. There is a bed of sand at its base, and it has a maximum thickness of 50 m. This unit is mainly found on the east side of the NS1 Sub-Area 1 site, but can also be found in localised patches in Sub-Area 2.
Unit 60	Geological unit U60 is a fluvial sand with a sheet-like to channelised geometry, and has a maximum thickness of 77 m. This unit is only found on the eastern edge of the NS1 Sub-Area 1 site.
Unit 65	Geological unit U65 is a glacial unit comprising clay, sand and till, with a maximum thickness of more than 158 m. This unit is more prominent in the NS1 Sub-Area 2 site, however some overbank and channelised deposits are present in the Sub-Area 1 site.
Unit 69	Geological unit U69 is glacio-lacustrine and comprises clay sediments with a thickness of more than 105 m. This unit is only present in the north-east of the NS1 Sub-Area 1 site, overlying geological U70 in a channelised area.
Unit 70	Geological unit U70 is a tunnel valley infill comprising clay, sand and till, with a maximum thickness of more than 157 m. This unit is mainly present in the NS1 Sub-Area 1 site within a large channel deposit which extends into the south-east of Sub-Area 2.
Unit 90	Geological unit U90 is a fluvial sand, with a maximum thickness of more than 108 m. This unit is present predominantly in NS1 Sub-Area 2, with localised deposits in Sub-Area 1.
BSU (Base Seismic Unit)	The BSU is a stratified Miocene clay and sand, which is locally deformed by various types of faults. BSU is present within the depth of interest across much of the central and western side of the NS1 site and locally on the east, it is outside the depth of interest in the channelised areas in Sub-Area 1 and far western edge of Sub-Area 2.

Geotechnical Data

A total of 389 geotechnical locations were sampled using seafloor cone penetration tests (CPT) and seismic CPTs (SCPT) equipment to sample sediments between 0.4 m and 54.2 m below seafloor (BSF). A further 102 geotechnical locations (including, where applicable, results from downhole sampling, downhole in situ testing, borehole geophysical logging, and laboratory testing) between seafloor and 70.8 m BSF were acquired. Geotechnical datasets were unitised and correlated with geophysical data to create an integrated model for the study area. Geotechnical datasets were collected in all geological units. A number of geotechnical subunits were observed in certain geological units (geological units U20, U50, U65 and U70).

Correlation between geotechnical unit boundaries and geophysical horizons was generally observed to be consistent. Currently correlations use a simple time-to-depth conversion with an assumed seismic velocity of 1730 m/s.

Three groupings of units were observed in the geotechnical data, and these can be linked to the geological history of the site. Shallow geological units U10 to U20 are largely from a postglacial environment. Geological units U35 to U60 are expected to have been deposited in a glacial environment but not to have been ice loaded. Geological units U65 and below may contain ice-loaded sediments as well as glacial till deposits.

Geotechnical Zone

Fifteen geotechnical zones were defined across the study area. These divide the site based on two factors:

- The first is the thickness of geological unit U20 sediments, with four intervals determined. Thicker areas of geological unit U20 may result in deposits of low-strength clays that could affect future foundations due to lower axial capacity;
- The second is the depth to the top of glacial units U65 and U70. These represent the shallowest/youngest units and are associated with a period in the site's history where direct glacial action is expected to have affected the geotechnical properties, resulting in greater variability in sediment properties. Four conditions subdivide this factor, selected based on their relevance to foundation types.

Combined, these factors result in 16 possible zone scenarios; however, conditions for one of these were mutually exclusive conditions, resulting in 15 zones.

The zonation work highlights that the most frequent zone was Geotechnical Zone 2a, which covers 28% of the site. The ground conditions within this zone show that geological unit U20 sediments were absent, and the top of glacial sediments (geological units U65 and U70) were less than 10 m below seafloor. It is predominantly found in Sub-Area 2.

Contents

Appendices

Figures in the Main Text

Tables in the Main Text

Abbreviations

2D UHR	Two-dimensional ultra high resolution (As agreed via TQ – 038, throughout the report and charts the name of 2D UHRS has been used, while 2D UUHRS in digital deliverables)
BH	Borehole
BP	Before present
BSF	Below seafloor
BSU	Base Seismic Unit
CM	Central meridian
CPT	Cone penetration test
DOW2030	Danish Offshore Wind 2030
ETRS89	European Terrestrial Reference System 1989
GNSS	Global Navigation Satellite System
ka	1000 years ago
LGM	Last Glacial Maximum
MBES	Multibeam echosounder
MIS	Marine isotope stage
MSL	Mean Sea Level
MSS	Mean Sea Surface
OWF	Offshore wind farm
SBP	Sub-bottom profiler
SCPT	Seismic cone penetration test
SSS	Side scan sonar
SVT	Seismic velocity test
UTM	Universal Transverse Mercator
WGS84	World Geodetic System 1984

1. Introduction

1.1 General

Energinet Eltransmission A/S (Energinet) contracted Fugro to perform an offshore geological site survey for the Danish Offshore Wind 2030 (DOW2030) project at the North Sea 1 (NS1) site. NS1 is one of several areas of investigation and covers an area of approximately 2200 km^2 in the North Sea west of Jutland, roughly between the Horns Rev and Thor offshore wind farm (OWF) areas. Water depths at the site range from 12 m to 40 m.

This report builds on the previous Fugro integrated reports (Fugro 2024a; 2024h), integrating the new geotechnical borehole survey locations acquired in Sub-Area 2 with the mainline survey subsurface data and Cone Penetration Test (CPT) locations for the NS1 site and the borehole locations collected for Sub-Area 1.

The borehole survey for Sub-Area 1 took place between 27 February and 16 July 2024 from the geotechnical vessels Excalibur, Gargano and Fugro Voyager. The borehole survey for Sub-Area 2 took place between 15 March to 25 July 2025 using the Fugro Synergy, RS Alegranza and Fugro Zenith. The data were acquired from downhole boreholes and CPTs at locations chosen from the baseline survey data and mainline survey line plan.

Table 1.1 displays the reporting sequence for the work packages associated with this project, including the geophysical, geotechnical and integration reports that were used as input to this report

Table 1.1: Overview of reports, including geophysical, geotechnical and integration reporting

Type	Deliverable				
Integrated Geoconsulting Reports (See Table 1.2)	217715-REP-002 2D UHRS Survey Geomodel Integrated with CPT Data, Full Site	217715-REP-003 Sub-Area 1 CPT, Borehole & Seismic Integrated Report	217715-REP-004 Full Site CPT, Borehole & Seismic Integrated Report		
Geotechnical Reports	F217703/01 Geotechnics investigation report – Sub-Area 1 Seafloor In Situ Test Locations	F217703/02 Geotechnics investigation report – Sub-Area 2 Seafloor In Situ Test Locations	F217703/03 Geotechnics Investigation report – Seafloor In Situ Test Locations (Jack-up)	F217703/04 Geotechnics Investigation report – Sub-Area 1 Geotechnical Borehole Locations	F217703/05 Geotechnics Investigation report – Sub-Area 2 Geotechnical Borehole Locations
Geophysical Reports	217715-REP-001 Baseline Geophysical	217715-REP-002 Mainline Report			
Notes Reports highlighted in light green constitute input reports for this document. This report is highlighted in dark green. To be completed reports are highlighted in Tan					

Table 1.2 explains the purpose of the main four geophysical and integrated reports.

Table 1.2: Overview and purpose of geophysical and geoconsulting integrated reports

Report Number	Report Name	Purpose
217715-REP-001	2D UHRS baseline survey	Identify large scale geology and use geophysical data to suggest geotechnical locations to investigate relevant units
217715-REP-002	2D UHRS survey geomodel integrated with CPT data, full site	Provide a detailed understanding of the site geology from an in-depth geophysical survey, including an integrated 3D geomodel based on seismic and CPT data available at time of submission
217715-REP-003	2D UHRS Survey Geomodel integrated with CPT and BH data, Area 1	Update integrated 3D geomodel created in the Mainline report with geotechnical information from borehole locations in Sub-Area 1
217715-REP-004	2D UHRS Survey Geomodel integrated with CPT and BH data, Full Site	Updated integrated 3D geomodel created in the Mainline report with geotechnical information from borehole locations across the entire site

Notes
This report is highlighted in green
UHRS = Ultra high resolution Seismic
CPT = Cone penetration test
BH = Borehole

1.2 Study Area

The project area is located offshore Denmark, approximately 45 nautical miles north-west of Esbjerg (Figure 1.1).

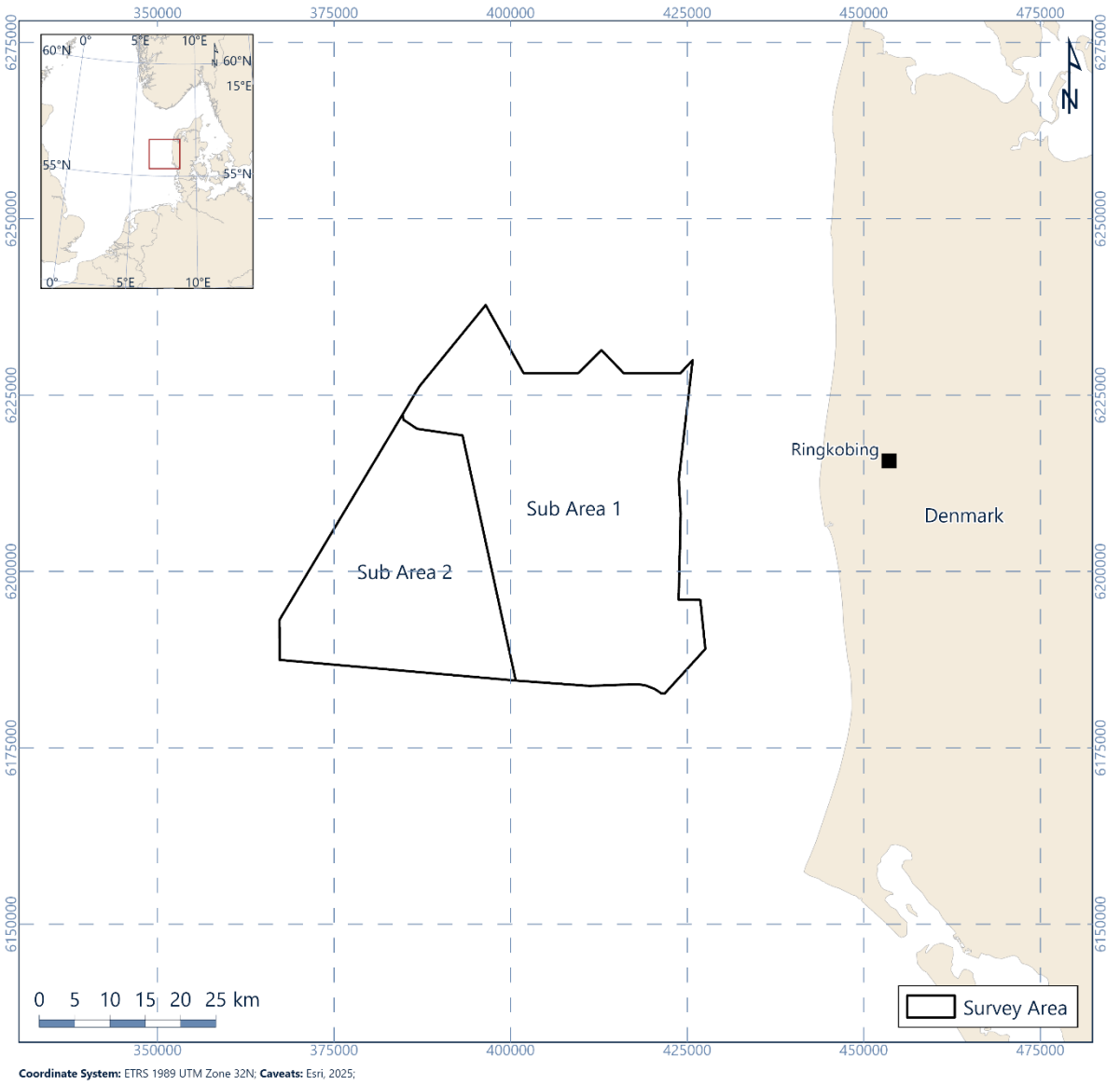

Figure 1.1: Project location with NS1 site split

Sub-Area 1 is also split into three areas; Nord, Mid and Syd. These are displayed in Figure 1.2. In Section 4, the seafloor depths and gradients are split by these three areas to provide more context; however no further interpretation is performed based on this subdivision.

Figure 1.2: Sub-Area 1 split

1.3 Scope of Work

This report follows both the geophysical baseline and mainline surveys and the geotechnical CPT full site campaign and borehole surveys for both Sub-Area 1 and Sub-Area 2. This report integrates the data previously collected to create a full integrated report for the NS1 site. To achieve this, the following scope of work items were completed:

- **Acquisition data review and methodology:** review of all available and recently acquired geological, geophysical and geotechnical data for the site, acquisition vessel information, methodology and data quality;
- **Geological setting:** a regional geological setting has been developed, providing context for the depositional environments and geology expected;

- **Seafloor conditions:** produce a description of seafloor conditions in the area using bathymetry, gradient, and seafloor features;
- **Geological model:** A conceptual model was developed integrating the seafloor and sub-seafloor conditions, integrated geophysical and geotechnical data from CPTs and borehole locations. Providing predicted soil profiles down to 60 m below seafloor (BSF) and associated soil provinces. This section also provides a quantitative geohazard inventory and anthropogenic constraints;
- **Geotechnical parameters:** predicted geotechnical parameters have been derived to a depth of 70 m per unit, with low estimate (LE), best estimate (BE) and high estimate (HE) values for each. Where possible, the parameters for each soil unit include:
  - Submerged unit weight;
  - Water content;
  - Minimum and maximum density values;
  - Atterberg limit test values;
  - Cone resistance;
  - Relative density;
  - Undrained shear strength.

1.4 Geodetic Parameters

The project geodetic and projection parameters are summarised in Table 1.3. Unless stated otherwise, geodetic coordinates presented in this report are as per the datum in Table 1.3.

Table 1.3: Project geodetic parameters

GNSS Geodetic Parameters	
Datum	ETRS89
EPSG code	25832
Semi major axis	6 378 137.00 m
Reciprocal flattening	298.257222101
Project Projection Parameters	
Grid projection	UTM
UTM zone	32 N
Central meridian	009° 00’ 00.000” E
Latitude of origin	00° 00’ 00.000” N
False easting	500 000 m
False northing	0.000 m
Scale factor on central meridian	0.9996
EPSG code	16032
Units	Metres
Notes GNSS = Global Navigation Satellite System ETRS89 = European Terrestrial Reference System 1989 UTM = Universal Transverse Mercator	

1.5 Vertical Datum

The vertical datum used was Mean Sea Level (MSL). All water depths were referenced to MSL using post-processed Global Navigation Satellite System (GNSS) height data collected in real time onboard vessels. GNSS heights were referenced to MSL by means of the World Geodetic System 1984 (WGS84) to Technical University of Denmark Mean Sea Surface (DTU21 MSS) ellipsoidal to datum separation model.

1.6 Guidelines on Use of Report

Appendix A outlines the limitations of this report in terms of a range of considerations including, but not limited to, its purpose, its scope, the data on which it is based, its use by third parties, possible future changes in design procedures and possible changes in the conditions at the site with time. It represents a clear exposition of the constraints which apply to all reports issued by Fugro. It should be noted that the Guidelines do not in any way supersede the terms and conditions of the contract between Fugro and Energinet Eltransmission A/S.

2. Acquisition Data

2.1 Data Review

2.1.1 Geophysical Data Acquired by Ocean Infinity

Between 3 April and 17 September 2023, Ocean Infinity carried out a geophysical survey of the NS1 site. This included collecting multibeam echosounder (MBES) bathymetry, side scan sonar (SSS), sub-bottom profiler (SBP) and magnetometer data. The scope of this survey was to provide full coverage of data across the site.

Within this report, Fugro used the processed MBES data for the seafloor elevation presented in Section 4, which visually represents seafloor conditions, including sediments and features. The associated reporting (Ocean Infinity, 2024) contains detailed interpretation of the shallow geology relevant for site characterisation of the inter-array cables. Fugro has not interpreted or integrated these data further as part of this report.

2.1.2 Fugro Acquired Geophysical Data

Between 14 and 19 April 2023, Fugro carried out a full site baseline survey using SBP and 2D ultra high resolution (UHR) 10 km spaced lines. A geophysical mainline survey of 250 m spaced mainline and 1 km spaced crosslines was subsequently performed, acquiring further SBP and 2D UHR data. The data from these surveys were used to understand sub-seafloor conditions and for integration with the CPT and borehole locations to provide a more confident geological ground model.

Refer to Section 2.2.1 and Fugro (2023c, 2024a) for further information on the geophysical data, vessels and equipment used.

2.1.3 Fugro-Acquired Geotechnical Data

There have been three main phases of geotechnical data acquisition at the NS1 site.

Between 27 October 2023 and 6 March 2024, Fugro acquired data from 368 CPT and SCPT locations selected using the results of the baseline survey and the interim soil zonation (Fugro, 2023c). These data were integrated with the 2D UHR data from the baseline and mainline surveys to create a more confident geological ground model. Refer to Section 2.2.2.1 and Fugro (2024b, 2024c, 2024d) for further information on this survey.

Between 27 February and 16 July 2024, following the CPT campaign, Fugro undertook a borehole survey within Sub-Area 1. This involved collecting samples and data from 69 borehole locations, including results from downhole sampling, downhole in-situ testing and borehole geophysical logging (where applicable), and laboratory testing. These data were integrated into this report, building on the data from the CPT campaign. Refer to Section 2.2.2.2 and Fugro (2024g) for further details on the vessel and equipment used in the Sub-Area 1 borehole campaign.

Between 15 March and 25 July 2025, the Sub-Area 2 borehole campaign was undertaken. This involved collecting samples and data from 33 borehole locations, including results from downhole sampling and downhole in-situ testing. No offshore advanced laboratory testing was carried out during this campaign. The field data were integrated into this report, incorporating the full site CPT and Sub-Area 1 borehole campaigns to produce a full site geomodel. Refer to Section 2.2.2.3 and Fugro (2026a) for further details on the vessel and equipment used in the Sub-Area 2 borehole campaign.

2.2 Acquisition Details

This section summarises the data acquisition and resulting deliverables used in the integration reporting.

2.2.1 Geophysical Acquisition

2.2.1.1 Baseline Survey

The baseline survey was performed from the MV Arctic between 14 and 19 April 2023. Figure 2.1 shows the survey track lines. The data were acquired using MBES, SBP and 2D UHR seismic. Further details can be found in the operations report (Fugro, 2023a).

The MV Arctic scope of work for this project was to survey the geophysical baselines. The survey grid was covered 10 km x 10 km lines, creating 100 km^2 boxes (Figure 2.1).

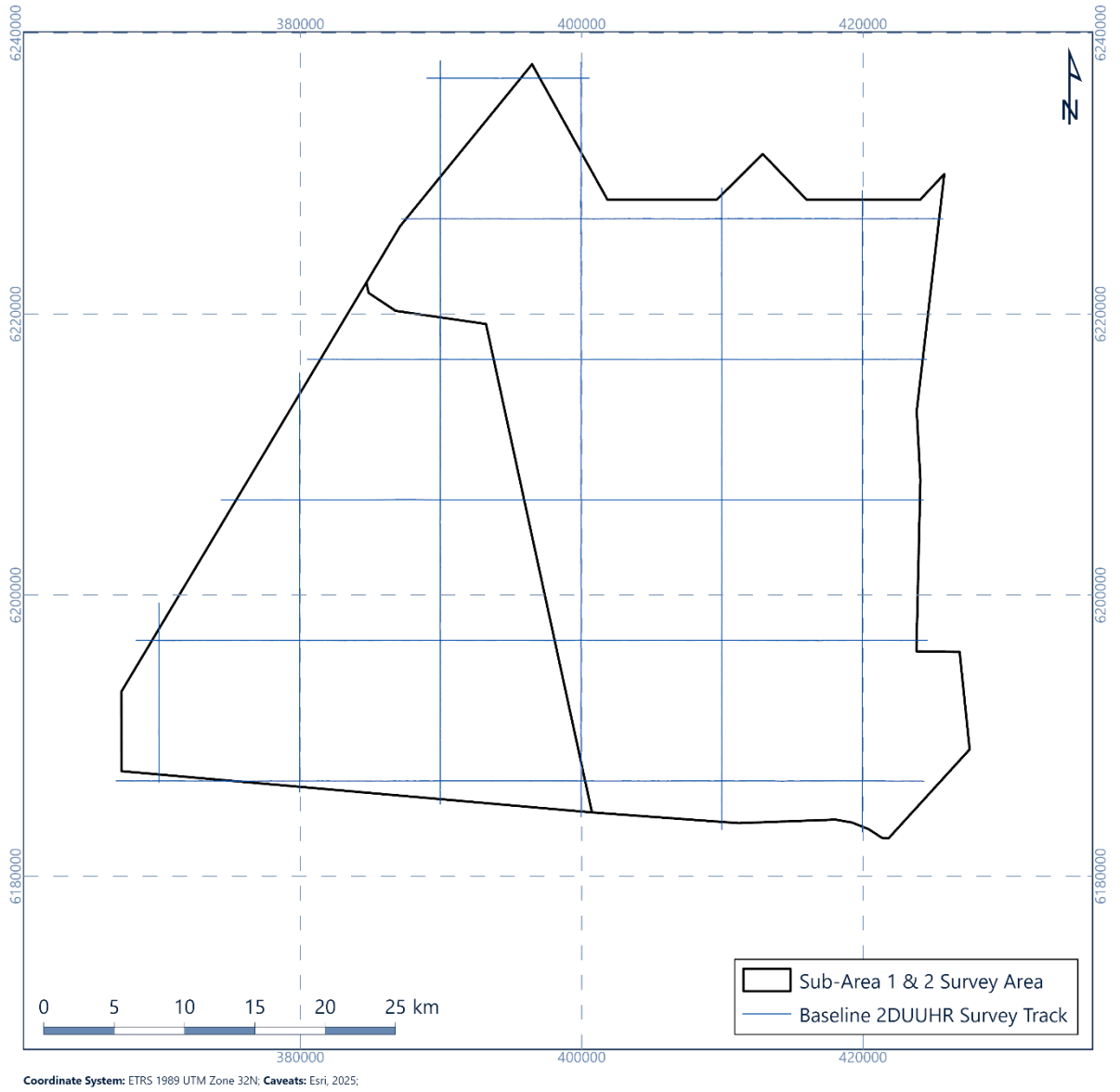

Figure 2.1: Baseline survey track lines

2.2.1.2 Mainline Survey

The mainline geological survey was undertaken between 10 June and 13 November 2023 performed by vessel MV Fugro Pioneer. The data were acquired using MBES, SBP and 2D UHR seismic. Further details can be found in the operations report (Fugro 2023b).

The MV Fugro Pioneer scope of work for this project was to survey the main lines and cross lines. The survey grid was covered by main lines with 250 m line spacing and cross lines with 1000 m line spacing. Some main lines were not surveyed due to a combination of bad weather, limited daylight hours as the survey progressed and a high density of fishing gear in the southern area of the NS1 site. This is presented in Figure 2.2 where gaps in the survey area can be observed.

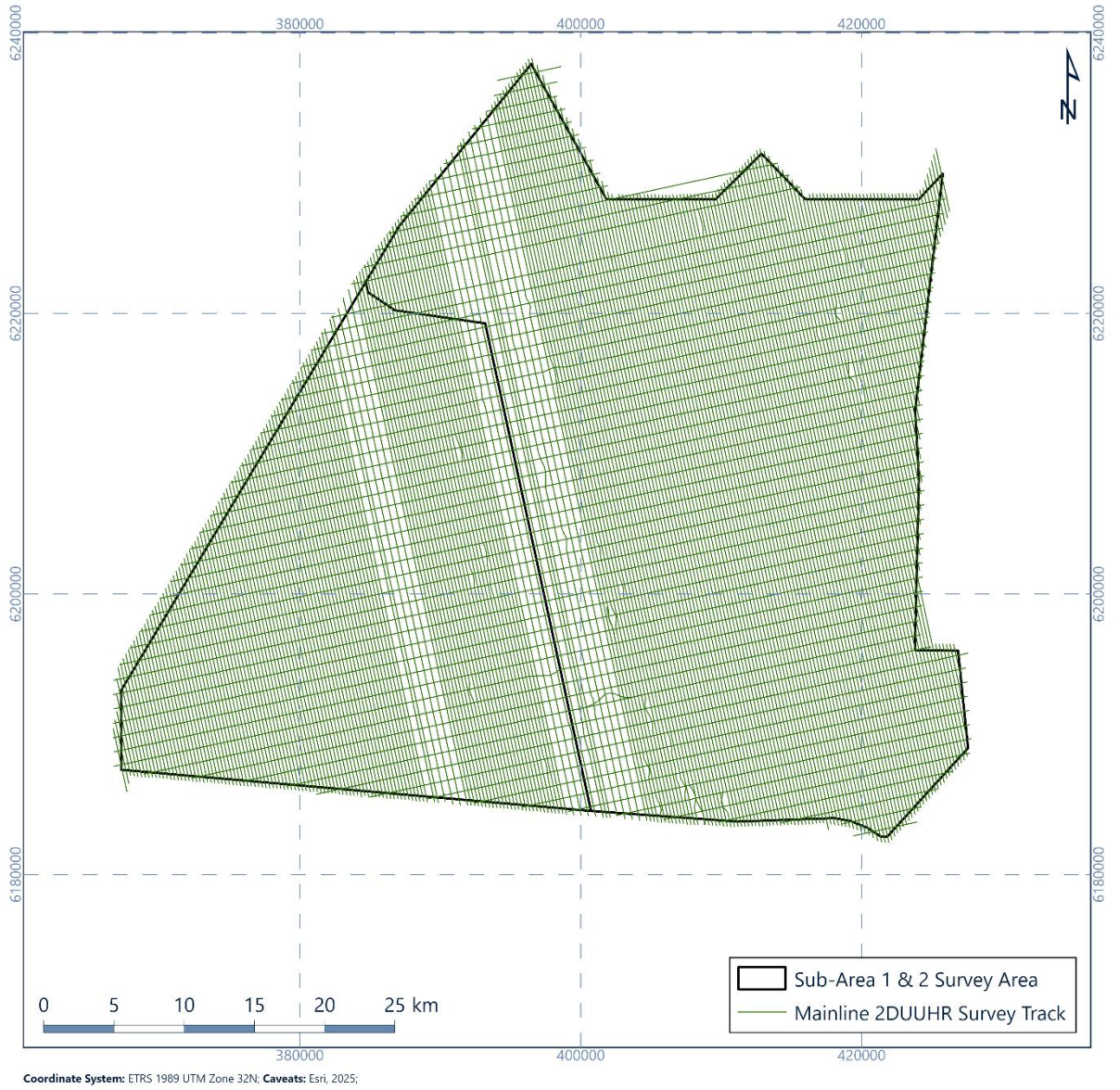

Figure 2.2: Mainline survey track lines

2.2.2 Geotechnical Acquisition

2.2.2.1 CPT Campaign

The CPT campaign was undertaken between 27 October 2023 and 6 March 2024 from the multipurpose survey vessel MV Normand Mermaid.

The Normand Mermaid scope of work was to carry out a seafloor CPT geotechnical investigation for Sub-Areas 1 and 2, including:

- 353 seafloor CPTs;
- 15 seismic CPTs (SCPTs), 12 of which included seismic velocity tests (SVTs).

Figure 2.3 shows the geotechnical locations collected across Sub-Areas 1 and 2.

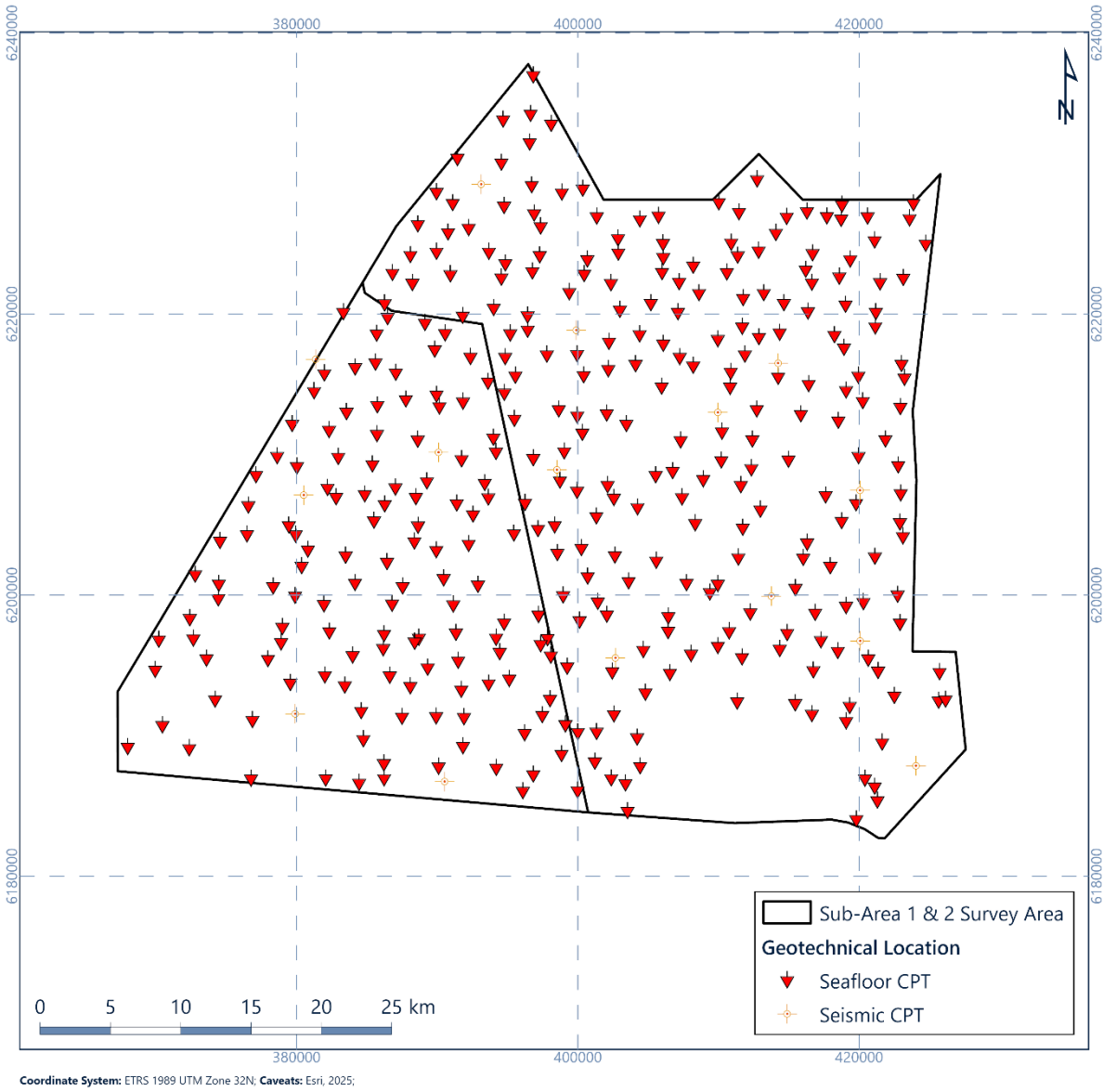

Figure 2.3: CPT and SCPT locations

2.2.2.2 Borehole Campaign Sub-Area 1

The Sub-Area 1 borehole campaign took place from 27 February to 16 July 2024 from the Excalibur jack-up barge and the MV Gargano and Fugro Voyager. Figure 2.4 presents the borehole locations and Figure 2.5 the locations per vessel.

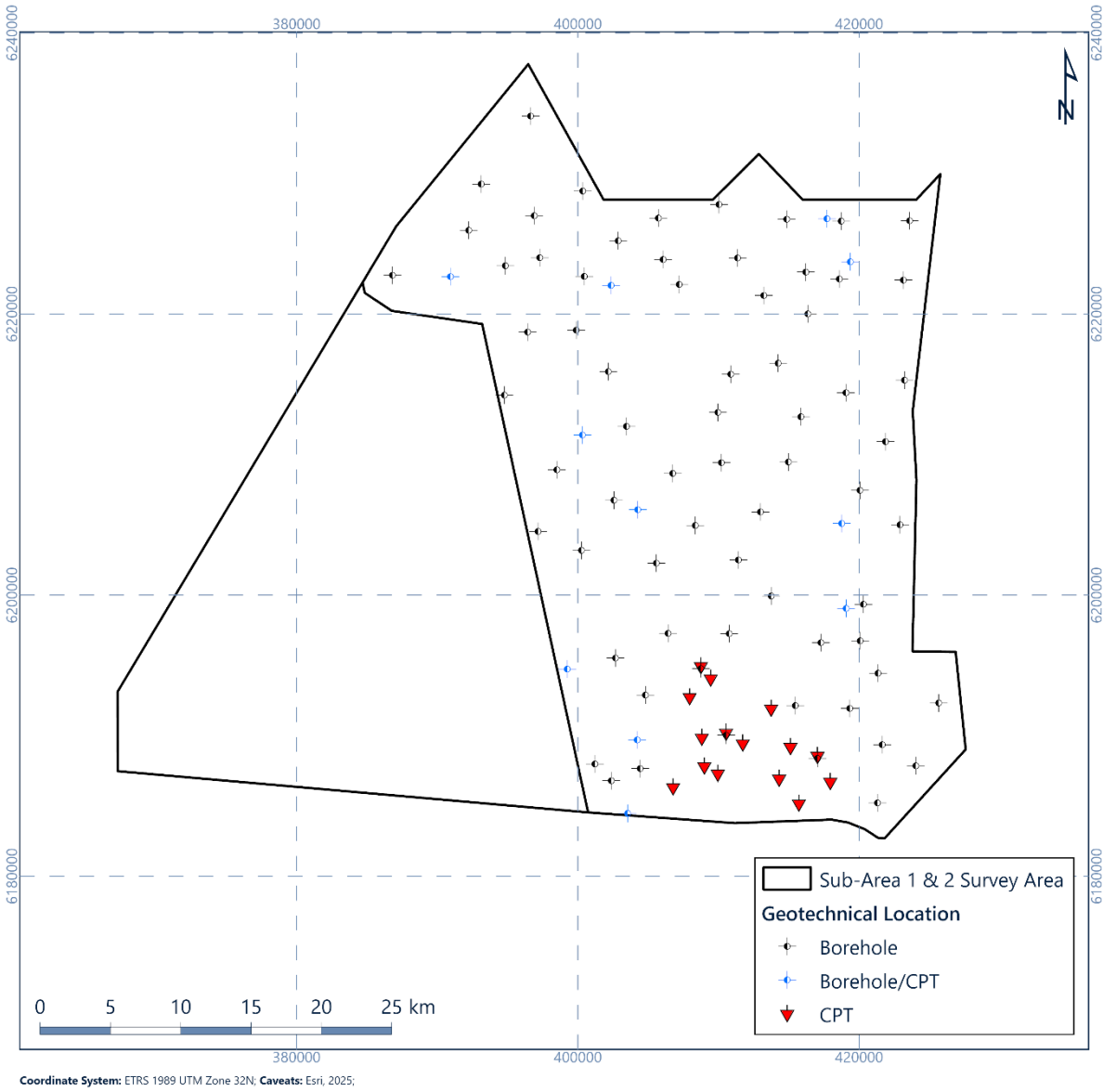

Figure 2.4: Sub-Area 1 geotechnical locations

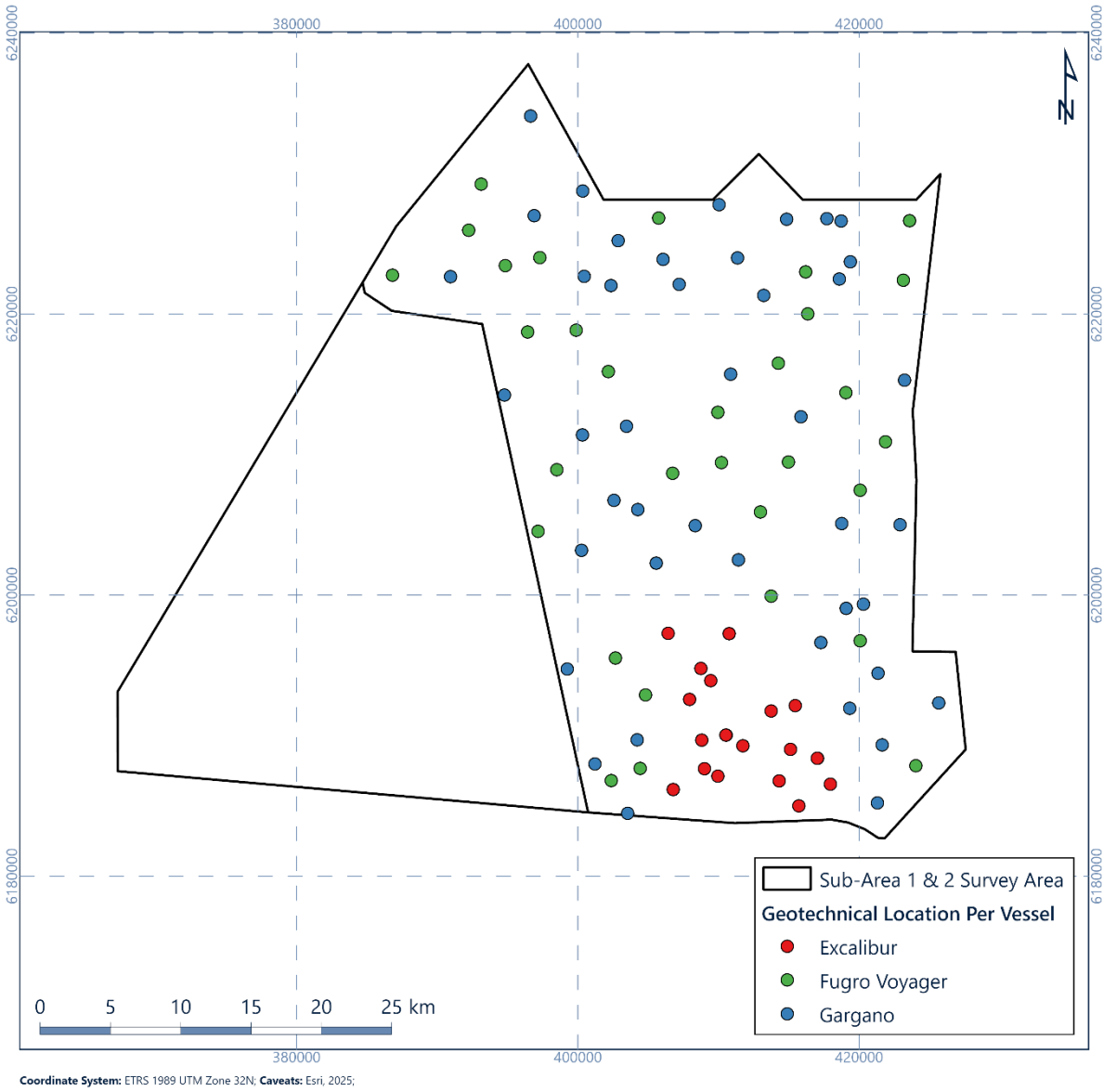

Figure 2.5: Sub-Area 1 geotechnical locations per vessel

Excalibur

The Excalibur barge operated between 30 April and 25 June 2024, collecting the following geotechnical locations:

- 16 seafloor CPTs to a target depth of 55 m BSF;
- 6 geotechnical boreholes to a target depth of 70 m BSF;
- 2 geotechnical boreholes, including blind drilling from seafloor to refusal depth of the seafloor CPT, and downhole CPT to a target depth of 55 m BSF.

Refer to Fugro (2024d) for details of the work conducted from the Excalibur and the equipment used.

MV Gargano

The drilling vessel MV Gargano operated between 1 March and 1 July 2024, collecting the following geotechnical locations:

- 27 borehole sampling locations;
- 4 combined borehole sampling and downhole CPT locations;
- 18 downhole CPT locations.

Refer to Fugro (2024e) for details of the work conducted from the Gargano and the equipment used.

Fugro Voyager

The geotechnical drilling vessel Fugro Voyager operated between 12 March and 16 July 2024, collecting the following geotechnical locations:

- 28 geotechnical boreholes with semi-continuous sampling to a target depth of 70 m BSF, including 10 boreholes with geophysical logging to a target depth of 70 m BSF;
- 2 geotechnical boreholes, including blind drilling from seafloor to refusal depth of the seafloor CPT and downhole CPT to a target depth of 55 m BSF;
- 4 geotechnical boreholes with combined downhole sampling and downhole CPTs to a target depth of 55 m BSF.

Refer to Fugro (2024f) for details of the work conducted from the Fugro Voyager and the equipment used.

Fugro's enhanced offshore laboratory (EOL) was mobilised on the Fugro Voyager, allowing additional offshore tests to be carried out as follows:

- Particle size (via dynamic image analysis): 340 tests;
- Minimum and maximum density: 400 tests;
- Atterberg limits: 200 tests;
- Incremental loading oedometer: 140 tests.

The results of the EOL tests were used where applicable, including to inform the geotechnical characteristic values in Section 7.3.

2.2.2.3 Borehole Campaign Sub-Area 2

The Sub-Area 2 borehole campaign took place from 15 March to 25 July 2025 from the Fugro Synergy, Fugro Zenith and RS Alegranza. Figure 2.6 shows the boreholes collected and Figure 2.7 presents the boreholes per vessel.

Figure 2.6: Sub-Area 2 borehole locations

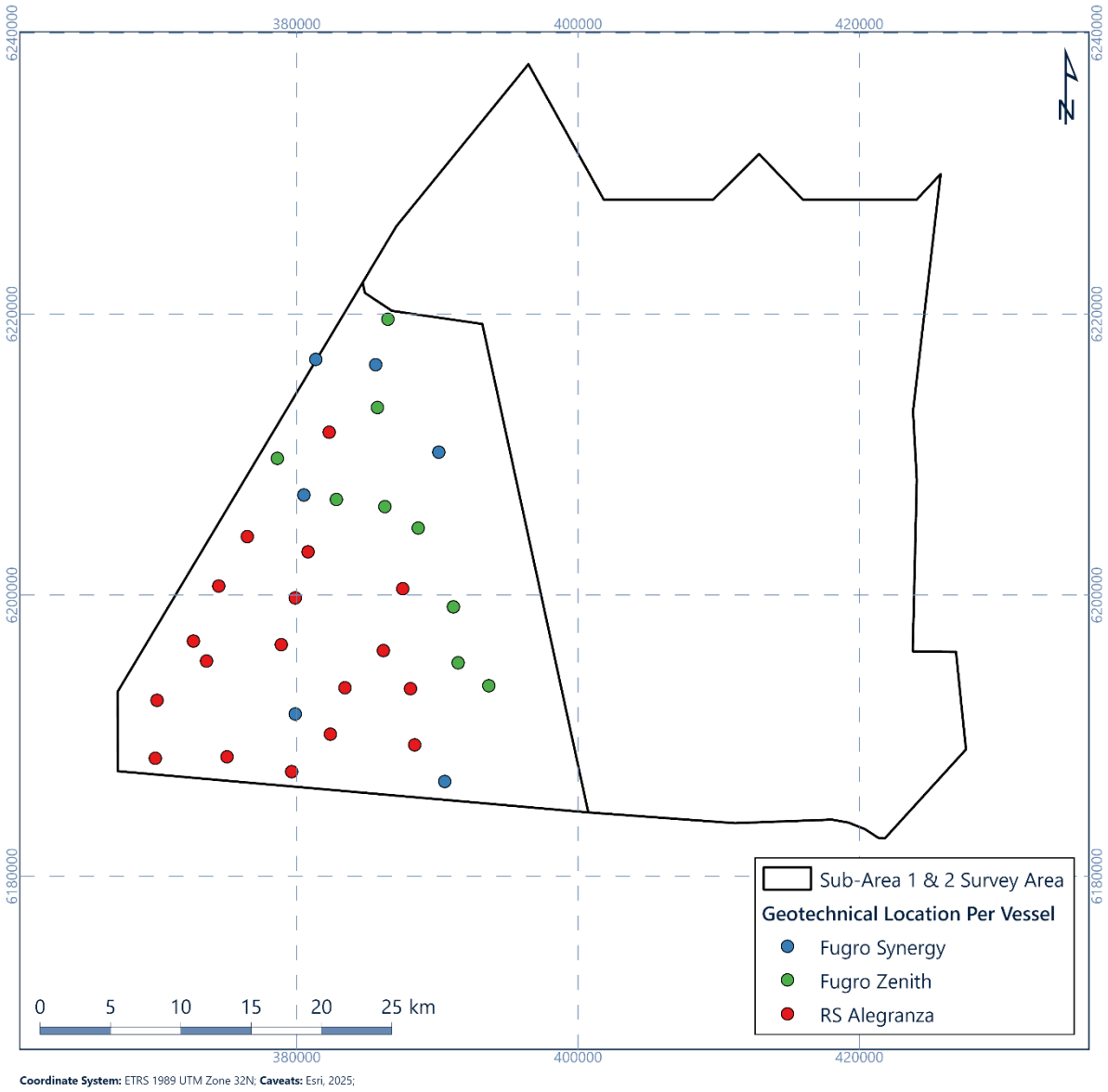

Figure 2.7: Sub-Area 2 borehole locations collected per vessel

Fugro Synergy

Between 15 March and 1 April 2025, the geotechnical drilling vessel Fugro Synergy collected the following geotechnical locations:

- 5 geotechnical boreholes with continuous logging to target depth of 70 m BSF;
  - Including 5 locations logged with geophysical logging to target of 70 m BSF;
- 1 geotechnical borehole with continuous logging to target depth of 70 m BSF;
  - Including 1 blind drilling in a separate hole from seafloor to refusal depth of seafloor CPT and downhole CPT to target depth of 55 m BSF.

Refer to Fugro (2025a) for details of the work conducted from the Fugro Synergy and the equipment used.

Fugro Zenith

Between 2 May and 16 June 2025, the Fugro Zenith collected the following geotechnical locations:

- 10 geotechnical boreholes with continuous sampling to target depth of 70 m BSF.

Refer to Fugro (2025b) for details of the work conducted from the Fugro Zenith and the equipment used.

RS Alegranza

Between 5 May and 24 July 2025, the RS Alegranza collected the following geotechnical locations:

- 9 geotechnical boreholes with downhole sampling to target depth of 70 m BSF.
- 3 geotechnical boreholes including combined downhole sampling and downhole CPT's from seafloor to a target depth of 55m BSF, continue semi-continuous sampling from 55m to target depth of 70m BSF.
- 4 geotechnical boreholes including blind drilling from seafloor to refusal depth of the seafloor CPT and downhole CPT to target depth 55m BSF.

Refer to Fugro (2025c) for details of the work conducted from the RS Alegranza and the equipment used.

2.3 Data Quality

2.3.1 Seismic Data

SBP and 2D UHR seismic data quality was monitored throughout the survey and deemed to be good. The technical requirements of the survey with regards to resolution and penetration were met.

The typical penetration depth of the 2D UHR seismic data was approximately 150 m BSF. For a detailed description of the quality of the 2D UHR seismic data collected during the survey, refer to Fugro (2024a).

Comments on the quality of the SBP data are as follows:

- The penetration depth is closely related to the geology, and may vary depending on lateral variation in sub-seafloor conditions. Typical penetration depth was approximately 10 m BSF, with a maximum of approximately 20 m BSF;
- Penetration was limited in relatively dense units composed predominantly of sand (e.g. Units U10, U35, U60 and U90);
- Penetration was greater in units where the soil conditions were expected to comprise higher percentages of clay (e.g. Units U20, U30 and U50);

- Horizon H10 (the first interpreted geophysical horizon below the seafloor) forms the base of Unit U10 (see Section 6.2) and was always within the penetration depth of the SBP data.

2.3.2 Geotechnical Data

Geotechnical data quality was considered suitable for the purposes of the current work stage. The geotechnical data quality will only be improved once a location-specific geotechnical data and laboratory testing data are acquired, for designing turbine and substation locations, as well as along potential cable routes.

Further details on the geotechnical data and the use of this data are presented in Section 2.5.

2.4 Methodology

2.4.1 Seismic Interpretation

The strategy for SBP and 2D UHR seismic data interpretation was as follows:

- Compiling historical geotechnical, geophysical and geological data from client-provided sources, Fugro's internal database, the ongoing Fugro campaign and the public domain (e.g. Jensen et al., 2008; COWI, 2021; Fugro, 2023a);
- Loading SEG-Y files (2D UHR seismic and SBP data) into Kingdom Suite version 2023, SQL server express version 2016;
- Loading seafloor CPT data acquired into Kingdom Suite;
- Loading borehole data acquired into Kingdom Suite;
- Interpretation of seismically distinct horizons, which form the bases of seismic units in the depth-domain. The interpreted horizons take into account and were adjusted based on available seafloor CPT data and borehole data, where required;
- Identification and interpretation of key geological features, which can be potential (geo)hazards for offshore infrastructure.

Comments are as follows:

- Geophysical horizon H10 was interpreted on the SBP data. All other horizons were interpreted on the 2D UHR seismic data;
- In areas where geophysical horizons were interpreted to be deeper than the maximum depth of penetration of the seismic data (e.g. Horizons H65, H70, H90), horizons were picked at the base of the available seismic section;
- The '2D Hunt and Fill' options were used in Kingdom where clear reflectors were present. These options follow the peak or trough of each trace, resulting in high accuracy but giving the reflector a serrated appearance. Where the reflector was less distinct or the boundary between units was in the form of a change in seismic character, these tools were less effective and horizons were picked manually;
- Time-to-depth conversion of horizons, grids and geological features interpreted on the SBP and 2D UHRS data used a constant velocity of 1730 m/s in the subsurface. This

velocity was based on the 141 seafloor CPTs available when the velocity model was determined;
- Horizons were gridded in Kingdom Suite 2023 with the following settings: minimum (0) curvature; midway (6) smoothness; cell size 5 m × 5 m; search distance 400 m; gridding extent controlled with polygons, which outline the area where the horizon is interpreted to be present;
- Seismic anomalies and acoustic blanking were gridded in Kingdom Suite 2023 with the following settings: minimum (0) curvature; midway (6) smoothness; cell size 5 m × 5 m; search distance 150 m;
- Isochore grids were calculated by subtracting the grid of the top of the unit from the grid of the base of the unit;
- In the report main text, thickness is used as a synonym for isochore.

2.4.2 Integration

The geophysical and geotechnical data were integrated following initial interpretation (Fugro 2024a, 2024h), to ensure that the geophysical interpretation, where available, considers any revisions to the geotechnical properties. Refer to Table 1.2 for details of the reporting for these work phases.

The geotechnical (CPT, SCPT and borehole) data were interpreted based on the previous and newly available data (using CPT, borehole correlation and borehole description as presented in Section 6). Only one geotechnical interpretation was carried out for each location, including those locations where multiple CPT tests or boreholes had been performed. This interpretation considered changes to derived and measured parameters, and significant changes to geotechnical descriptions that could indicate change across a wider area.

Following further geotechnical interpretation, the seismostratigraphic units which combine the variations observed in the geotechnical data with seismic character changes were defined by importing the CPT and borehole data into Kingdom Suite.

CPT log data and offshore laboratory testing included:

- Submerged unit weight [kN/m^3];
- Water content [%];
- Cone resistance [q_c];
- Sleeve friction [f_s];
- Pore pressure [u_2];
- Friction ratio [R_f].

Borehole data included only formation tops as per geotechnical descriptions and unitisation presented in Fugro (2024g, 2026a, *in press*).

As part of the assessment of geotechnical data, significant geotechnical or lithological changes were unitised and identified before being compared with the initial interpretation of the geophysical and geotechnical data. This process was carried out in near-real time to

ensure the work was updated as data were collected. A process flow of the integration work is provided in Figure 2.8.

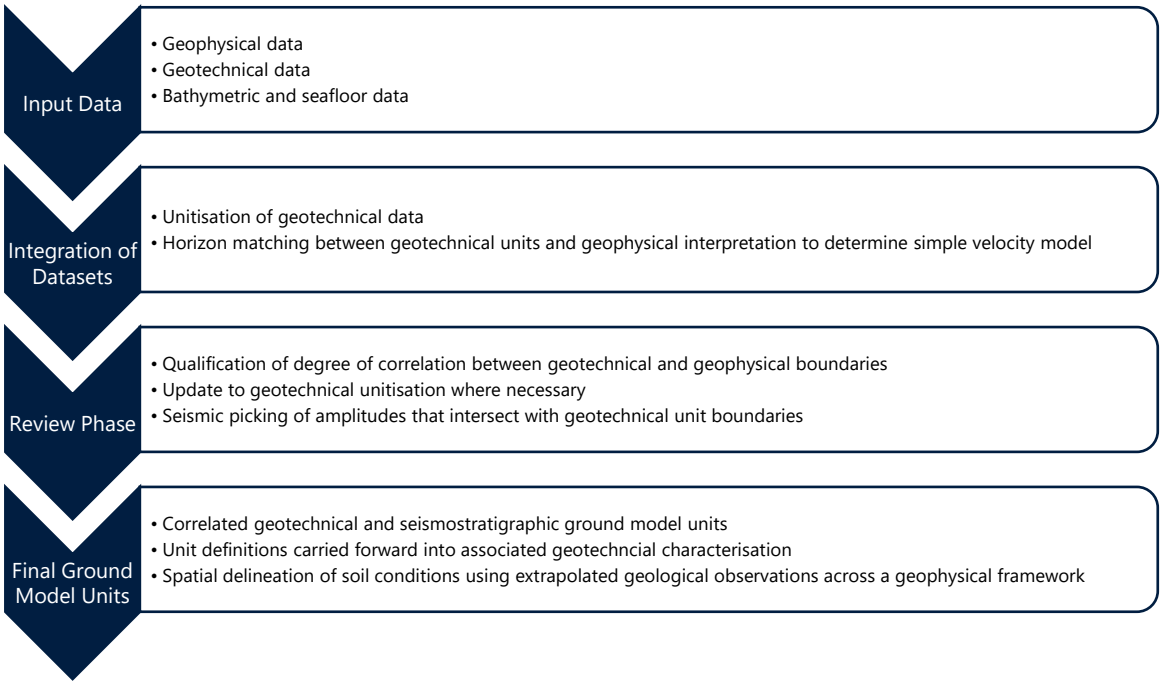

Figure 2.8: Integration of geotechnical and geophysical data workflow

Misalignments between the soil units and the interpreted horizons were addressed at workshops held with both the geophysical and geotechnical interpretation teams. Some formation bases were re-evaluated, and horizons were partially adjusted. Discrepancies between geotechnical units and geophysical horizons can be due to several factors, including:

- Offset between geotechnical locations and geophysical survey data;
- Depth conversion of geophysical data;
- Gradation between geotechnical properties.

As a result, some inconsistencies between geophysical changes and geotechnical units were observed and are detailed in Section 6.2. This allowed ground model integration work to be utilised for assignment of laboratory test data.

2.5 Geotechnical Data for Integration

2.5.1 CPT Geotechnical Correlations

Measured data were collected from the in-situ geotechnical tests.

Derivation parameters were defined from these measured parameter values. Classification parameters then be defined from the derived parameters. An example of these parameters is shown in the CPT log in Figure 2.9. The approach and methodology for the derivation of CPT and classification parameters is described in Appendix B.

The undrained shear strength terms presented in this report are from ISO 14688-2:2018 (ISO, 2018b), using the derived CPT parameters and offshore test data, and are presented in Table 2.1. Table 2.2 details the relative density terms for the description of sand units based on relative density ranges (Lambe & Whitman, 1969).

Table 2.1: Consistency terms for undrained shear strength (ISO, 2018a, 2018b)

Strength Term (BS 5930: 2010)	Undrained Shear Strength [kPa]
Extremely low	< 10
Very low	10–20
Low	20–40
Medium	40–75
High	75–150
Very high	150–300
Extremely high	300–600
Ultra high*	> 600
Notes * - This is not part of the standard for strengths, this is defined by Fugro	

Table 2.2: Ranges of relative density for the description of sand units (Lambe & Whitman, 1969)

Relative Density Term	Relative Density [%]
Very loose	0–15
Loose	15–35
Medium dense	35–65
Dense	65–85
Very dense	85–100

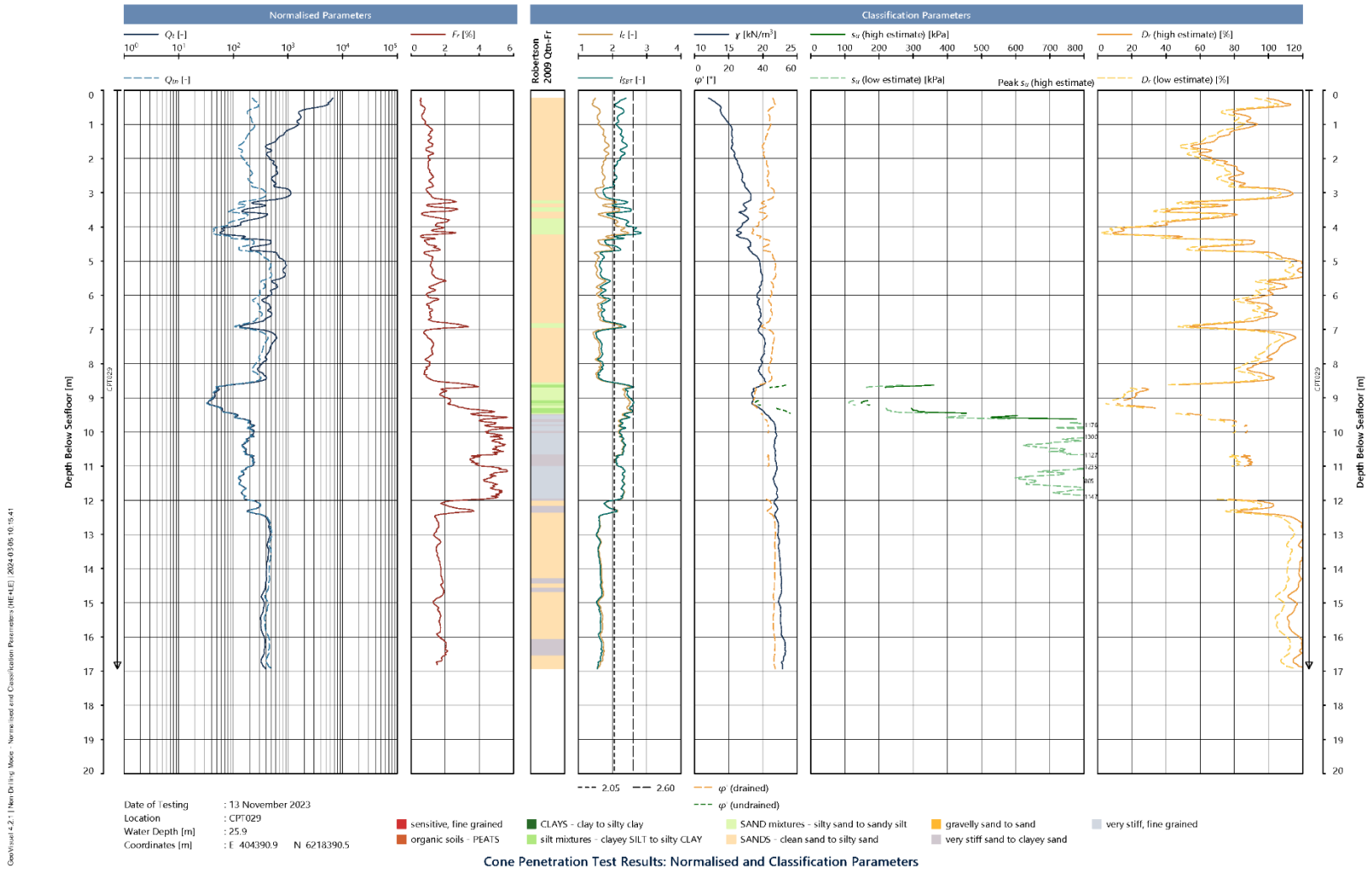

Figure 2.9: Presentation of CPT data including classification parameters

Geotechnical properties are described per unit in Section 6.

3. Regional Geological History

3.1 General

During the Cenozoic, up to 3 km thick sediment successions were deposited in the North Sea basin (Knox et al., 2010). Quaternary deposits increase in thickness from the margins of the North Sea basin towards its centre (Arfai et al., 2018); as NS1 is located at the margin, thinner Quaternary deposits are therefore expected.

The Cenozoic comprises three major depositional phases in the North Sea basin:

1. From the Paleocene to Middle Pleistocene, deposition took place in marine and fluvio-deltaic depositional environments (Section 3.2);
2. During the Middle to Late Pleistocene, several periods of ice sheet advance and retreat took place, resulting in complex glacial and periglacial depositional environments (Section 3.3);
3. A marine transgression followed the Last Glacial Maximum (LGM), resulting in marine depositional environments (Section 3.4).

3.2 Paleocene to Middle Pleistocene

During this period, a fluvial system (the Eridanos river) drained the Baltic Sea basin in the direction of the North Sea basin (Cohen et al., 2014; Gibbard & Cohen, 2015; Gibbard & Lewin, 2016). Throughout the Paleocene to Middle Pleistocene, this river system and its associated depositional environments prograded into the North Sea basin. Marine clays were deposited at the site during the Miocene (Figure 3.1; EMODnet, 2023). Eventually the prograding delta reached the site, and marine and fluvial sands were deposited during the Early to Middle Pleistocene (Figure 3.2; Gibbard & Lewin, 2016).

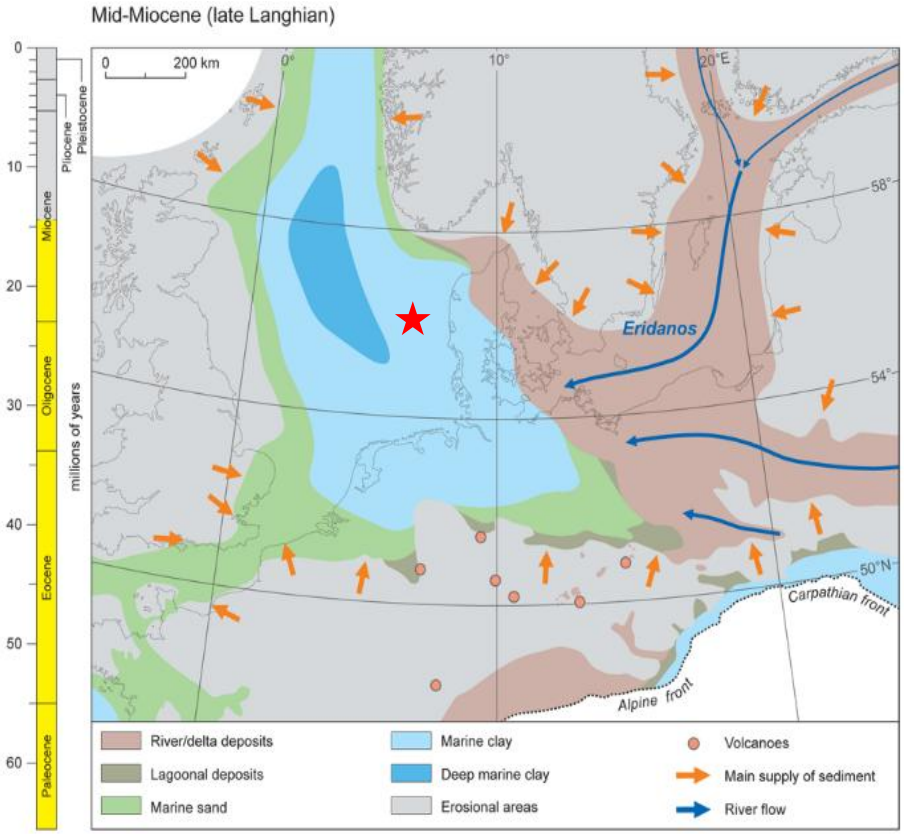

Figure 3.1: Palaeogeography of the North Sea during the Miocene (after Gibbard & Lewin, 2016). The red star indicates the site location

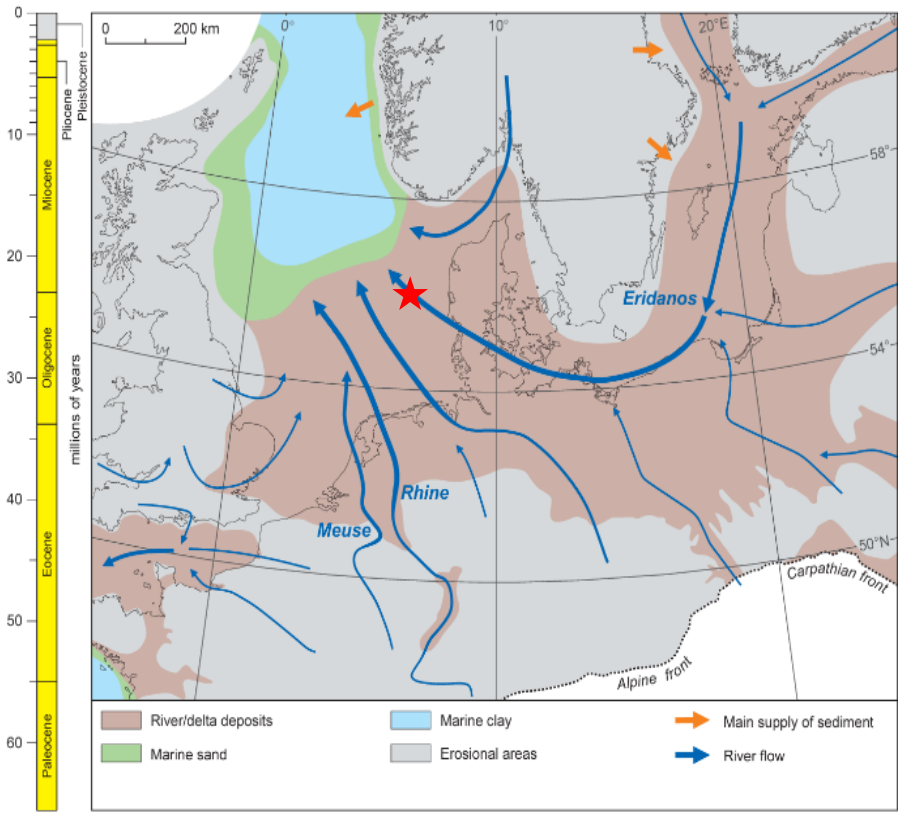

Figure 3.2: Palaeogeography of the North Sea during the Early to Middle Pleistocene (after Gibbard & Lewin, 2016). The red star indicates the site location

3.3 Middle to Late Pleistocene

Ice sheets advanced into the North Sea basin during several glacial periods during the Middle to Late Pleistocene, with marine deposition intervening during interglacial periods. Figure 3.3 illustrates the change in stable marine oxygen isotope ratios over time. High ratios (grey) correspond with glacial periods, low ratios (white) with interglacial periods (Hughes et al., 2020). The glacial and interglacial periods named at the bottom of Figure 3.3 correspond to geomorphologic units in north-west Europe, and are were recognised as morphologic units in the subsurface.

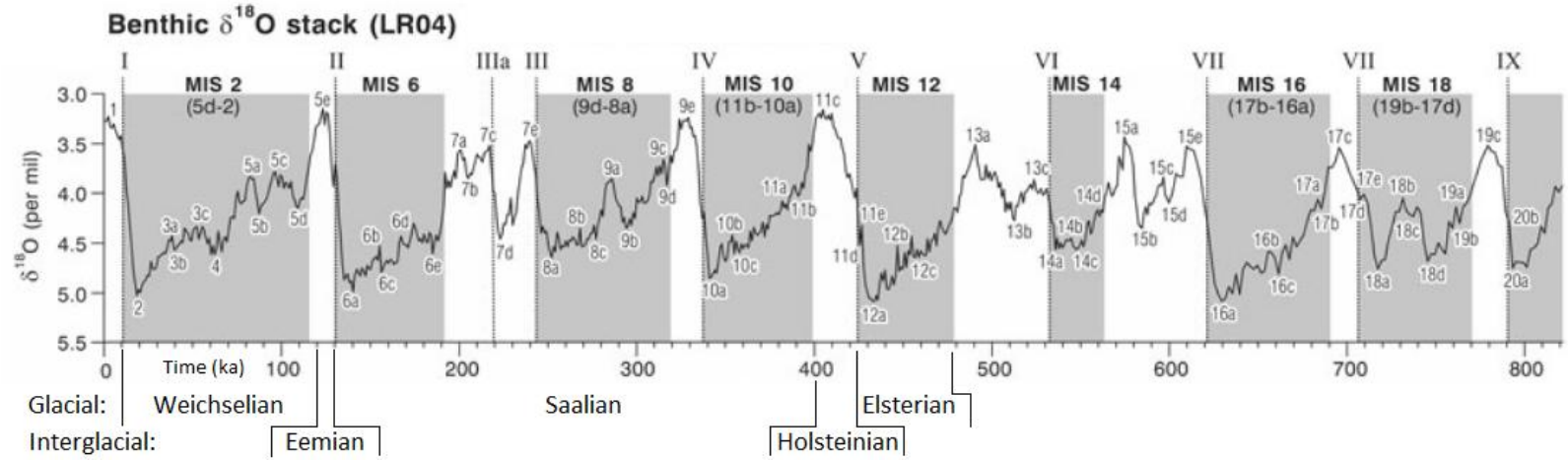

Figure 3.3: Graph illustrating the marine isotope stages used for geological dating (modified after Hughes et al., 2020). The grey areas indicate glacial periods with higher O_{18}, and the white areas indicate interglacial periods with lower O_{18}

3.3.1 Elsterian Glacial Period

The Elsterian glacial period corresponds with the marine isotope stage (MIS) 12 (Figure 3.3); Gibbard & Cohen, 2015) and was the first significant ice advance into the North Sea basin. At its peak, the ice sheet covered Scandinavia, the United Kingdom, and most of the North Sea basin, including NS1 (Figure 3.4). During this period, subglacial tunnel valleys eroded into the underlying sediment (Figure 3.5). As the ice sheets began to retreat, the channels were progressively filled with clays, silts and sands which were subsequently overconsolidated by successive glacial stages (Huuse & Lykke-Andersen, 2000b; Kirkham et al., 2021).

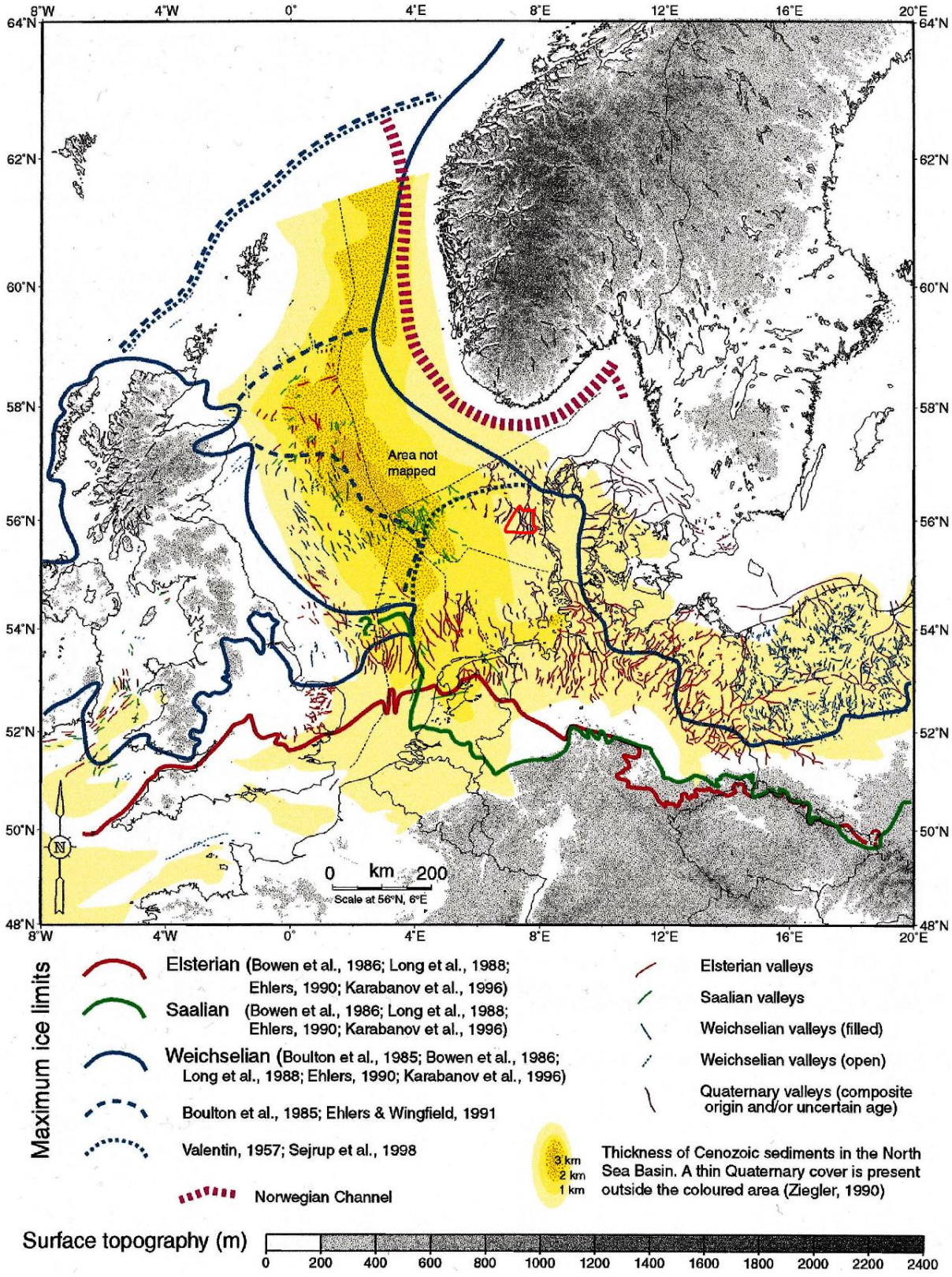

Figure 3.4: Extent of ice sheets and tunnel valleys during the Pleistocene in the North Sea (after Huuse & Lykke-Andersen, 2000b). The site location is indicated in red

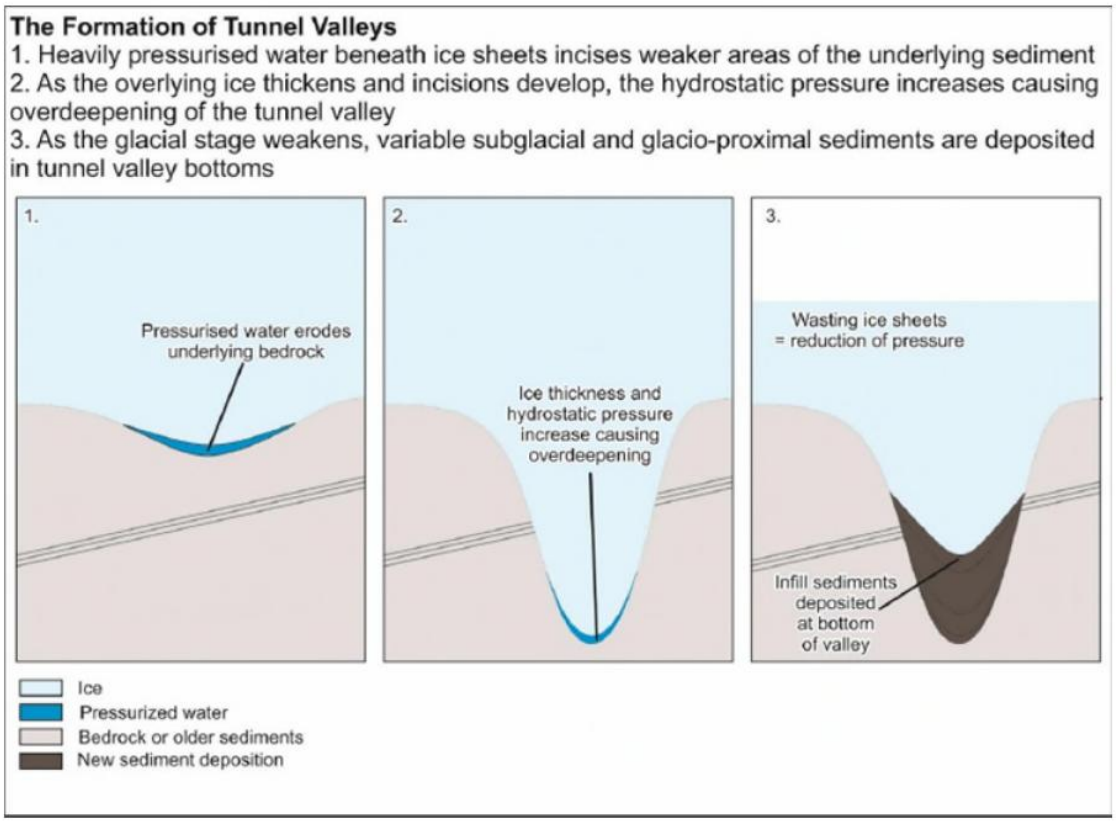

Figure 3.5: Glacial tunnel valley formation

3.3.2 Holsteinian Interglacial Period

The Holsteinian interglacial period corresponds to MIS 11 (Figure 3.3; Hughes et al., 2020; Cohen et al., 2014) and follows the Elsterian glacial period. The Holsteinian represents a period of global rise in temperatures and the retreat of the Elsterian ice sheets. During the marine transgression, the area offshore Denmark was likely characterised by shallow and later deep marine environments (Gibbard & Lewin, 2016). Deposits from the Holsteinian filled the tunnel valleys of the Elsterian glacial period. Holsteinian marine clays are reported to be present in the Horns Rev area to the south of the NS1 site (Jensen et al., 2008) and were also observed within the NS1 site.

3.3.3 Saalian Glacial Period

The Saalian glacial period comprises multiple stadials and interstadials and corresponds to MIS 6 to MIS 10 (Figure 3.3; Lang et al., 2018; Hughes et al., 2020; Gibson et al., 2022). Three major stadials are identified, MIS 6, MIS 8, and MIS 10, separated by interstadials MIS 7 and MIS 9.

The Saalian ice sheet coverage varied significantly over time. Its extent in Europe during the Early and Middle Saalian is poorly understood because very little evidence has been confidently linked to the period (Batchelor et al., 2019; Hughes et al., 2020). The ice sheet reached its maximum extent during the Late Saalian, when the Danish sector of the North Sea was completely covered by ice (Figure 3.4; Lang et al., 2018, 2019).

Several types of deposit are related to the Saalian glacial period:

1. Sets of tunnel valleys formed below the Saalian ice sheet (Huuse & Lykke-Andersen, 2000b; Nielsen et al., 2008);
2. Sediments deformed by glacio-tectonics during the Saalian as a result of ice sheet advance folding previously deposited sediments (Huuse & Lykke-Andersen, 2000a; Larsen & Andersen, 2005; Høyer et al., 2013; Winsemann et al., 2020; Cartelle et al., 2021);
3. Several periglacial deposits related to the Saalian glacial period, such as fluvial outwash plains (Friborg, 1996) and pro-glacial lakes (Lang et al., 2018). Onshore Denmark, in south-west Jutland, the Saalian landscape has been preserved as several hill islands (bakkeø) comprising glacial till deposits (Figure 3.6; Friborg, 1996).

3.3.4 Eemian Interglacial Period

The Eemian interglacial period corresponds to MIS 5 (Figure 3.3; Cohen et al., 2022; Wohlfarth, 2013) and followed the Saalian glacial period. During the Eemian interglacial period, the global temperature increased and the ice sheets melted, resulting in eustatic sea level rise (Figure 3.3). After a brief period of fluvial depositional environments at the end of the Saalian glacial period (Friborg, 1996), the Danish sector of the North Sea was flooded (Figure 3.6) with a transition from lacustrine environments with peat deposition (Cohen et al., 2022) to open marine environments with clay deposition.

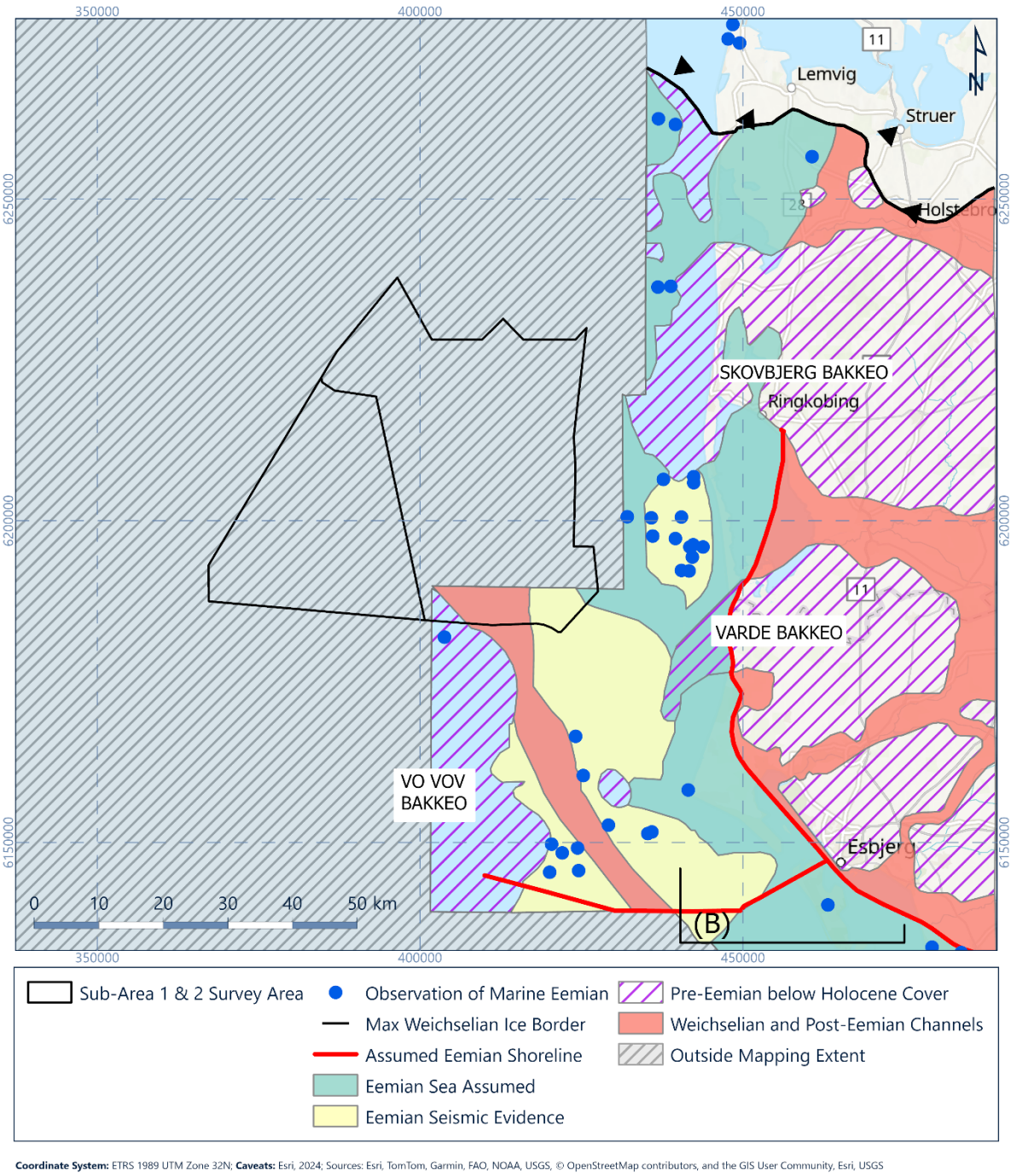

Figure 3.6: Map of south-west Jutland and nearshore areas during the Eemian transgression. Adapted from Konradi et al, 2005.

3.3.5 Weichselian Glacial Period

The Weichselian glacial period corresponds to MIS 2 to MIS 4 (Hughes et al., 2015) and followed the Eemian interglacial period (Figure 3.3). During this period, the global temperature and sea level began to decrease and, as a result, the Danish sector of the North Sea was exposed subaerially and fluvial systems developed (Figures 3.7 and 3.8; Houmark-Nielsen, 2011; Möller et al., 2020).

Northern Europe was then subjected to several major pulses of glacial expansion and retreat during this period (Houmark-Nielsen, 2011). The ice sheet was at its maximum extent during the LGM, when it reached Jutland and the northern part of the Danish sector of the North Sea. However, it is not interpreted to have covered the site (Figure 3.6).

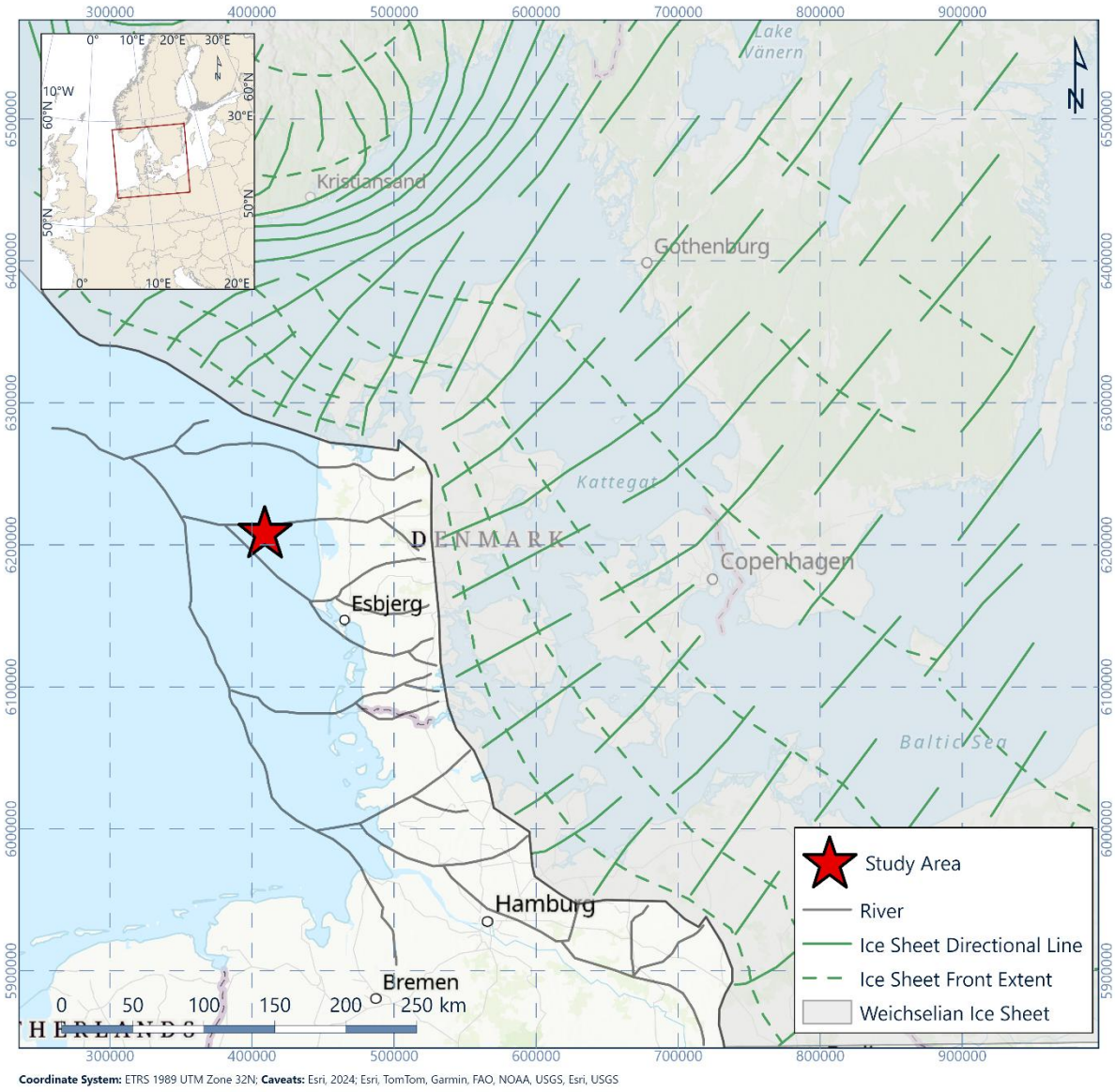

Figure 3.7: Denmark during the LGM (22 to 20 ka BP) (Houmark-Nielsen, 2011)

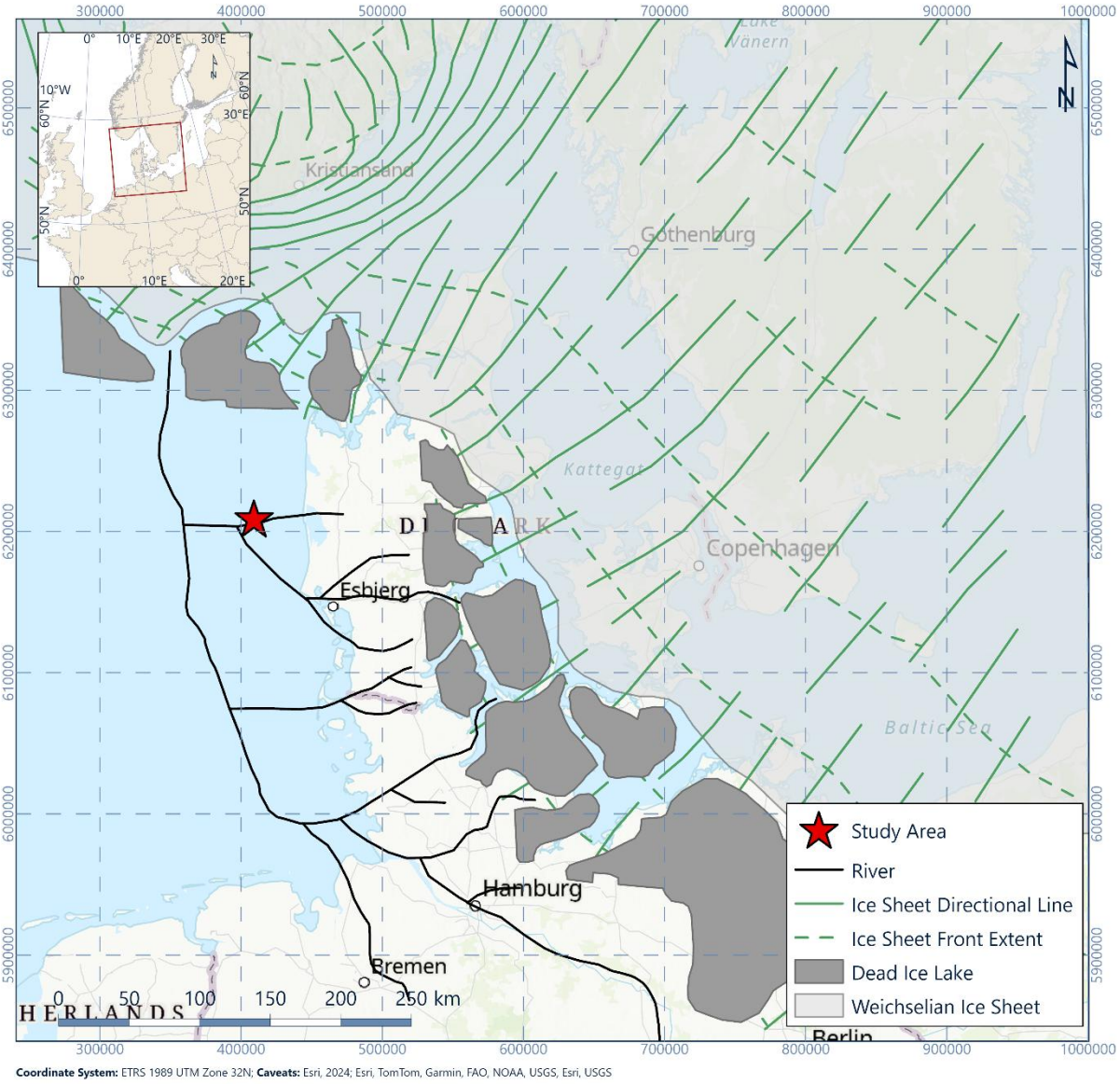

Figure 3.8: Denmark just after the Last Glacial Maximum (20 to 19 ka BP) (Houmark-Nielsen, 2011)

3.4 Holocene

Global temperatures started to increase during the Holocene. Melting ice sheets led to a rise in sea levels (Harrison et al., 2018). Terrestrial environments were gradually flooded (Houmark-Nielsen, 2011; Möller et al., 2020), transitioning to lacustrine and coastal environments until they were eventually drowned by the rising sea levels.

The coastline reached the site approximately 8000 years Before Present (BP) (Figure 3.9; Walker et al., 2020). The site was completely drowned by the marine transgression approximately 7000 years BP (Walker et al., 2020), and the depositional environment gradually changed to marine (Figure 3.10).

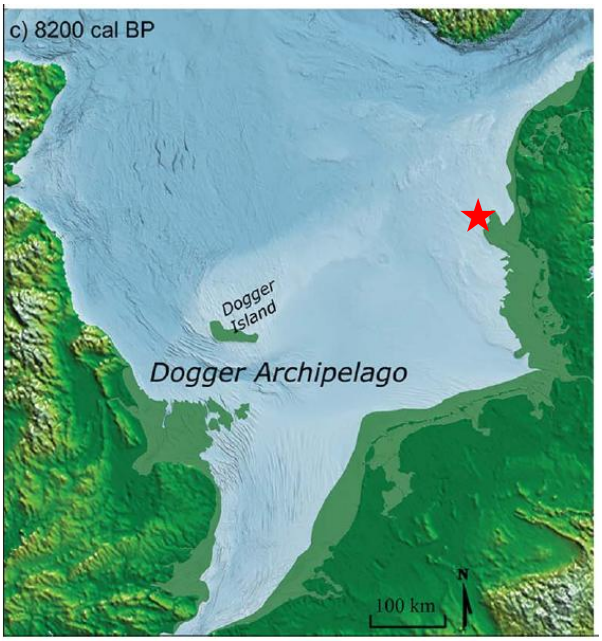

Figure 3.9: Map of the North Sea 8200 cal BP (Walker et al., 2020). The red star indicates the site location

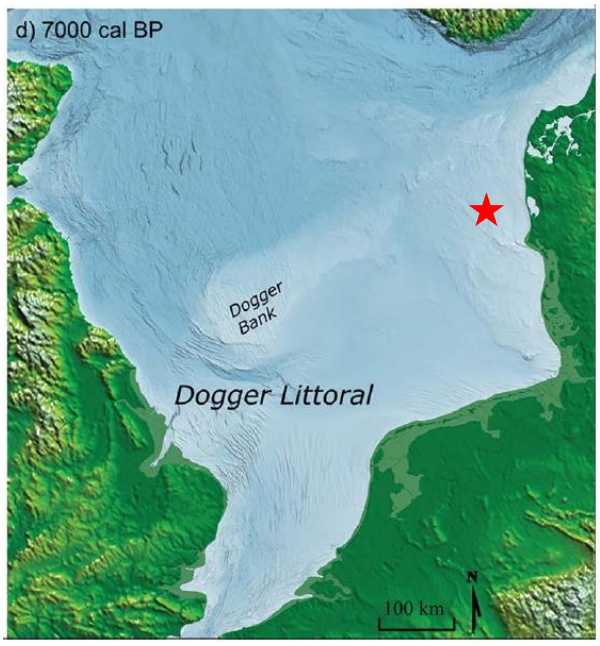

Figure 3.10: Map of the North Sea 7000 cal BP (Walker et al., 2020) . The red star indicates the site location

4. Seafloor Conditions

4.1 Bathymetry

Based on the final bathymetry data received from Ocean Infinity (Figure 4.1), elevation ranges are outlined in Table 4.1. A north-north-west and south-south-east oriented bank is present in the south of the Sub-Area 1 with a smaller bank present in the east side of Sub-Area 2. Across the site there are several additional south-west to north-east and north-west to south-east oriented ridges (Ocean Infinity, 2024).

Table 4.1: Bathymetry [m below MSL] from Ocean Infinity (2024)

Area	Minimum Depth [m below MSL]	Maximum Depth [m below MSL]	Average Depth [m below MSL]
Full NS1 Site	12.3	39.1	26.9
Sub-Area 1	12.3	33.5	25.5
Sub-Area 1 Nord	23.6	33.7	28.8
Sub-Area 1 Mid	20.5	32.1	25.7
Sub-Area 1 Syd	12.3	27.6	22.0
Sub-Area 2	20.5	39.1	29.4
Notes MSL = Mean Sea Level			

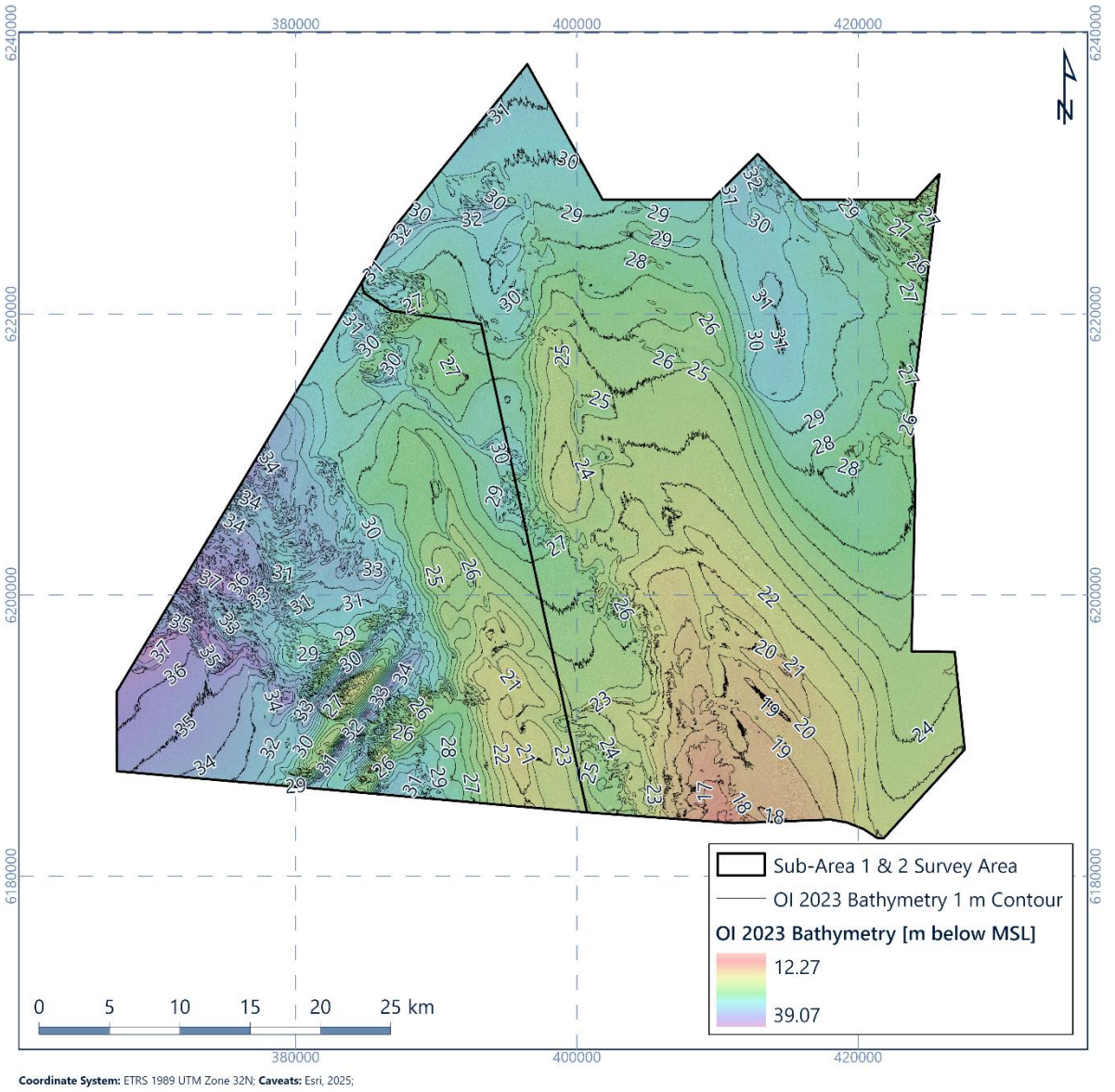

Figure 4.1: Full site bathymetry [m below MSL] (Ocean Infinity, 2024)

4.2 Seafloor Gradient

The seafloor gradient (Figure 4.2) was derived from the Ocean Infinity bathymetry data. The range of seafloor gradients across the site are presented in Table 4.2. There are small, isolated locations where the slope angle is greater than 5°, some of which reaching 65° in Sub-Area 2. These are not visible at the scale in Figure 4.2 (Ocean Infinity, 2024). The cell size used for the calculation of seafloor gradient was 1 m, the same as the bathymetry. Seafloor gradient is dependent on the cell size of the input data, therefore the detail in which steep features are highlighted can vary.

Table 4.2: Seafloor Gradient from Ocean Infinity (2024)

Area	Minimum Seafloor Gradient [°]	Maximum Seafloor Gradient [°]	Average Seafloor Gradient [°]
Full NS1 Site	0	65.1	0.4
Sub-Area 1	0	64.9	0.4
Sub-Area 1 Nord	0	55.9	0.3
Sub-Area 1 Mid	0	53.0	0.4
Sub-Area 1 Syd	0	64.9	0.5
Sub-Area 2	0	65.1	0.5
Notes MSL = Mean Sea Level			

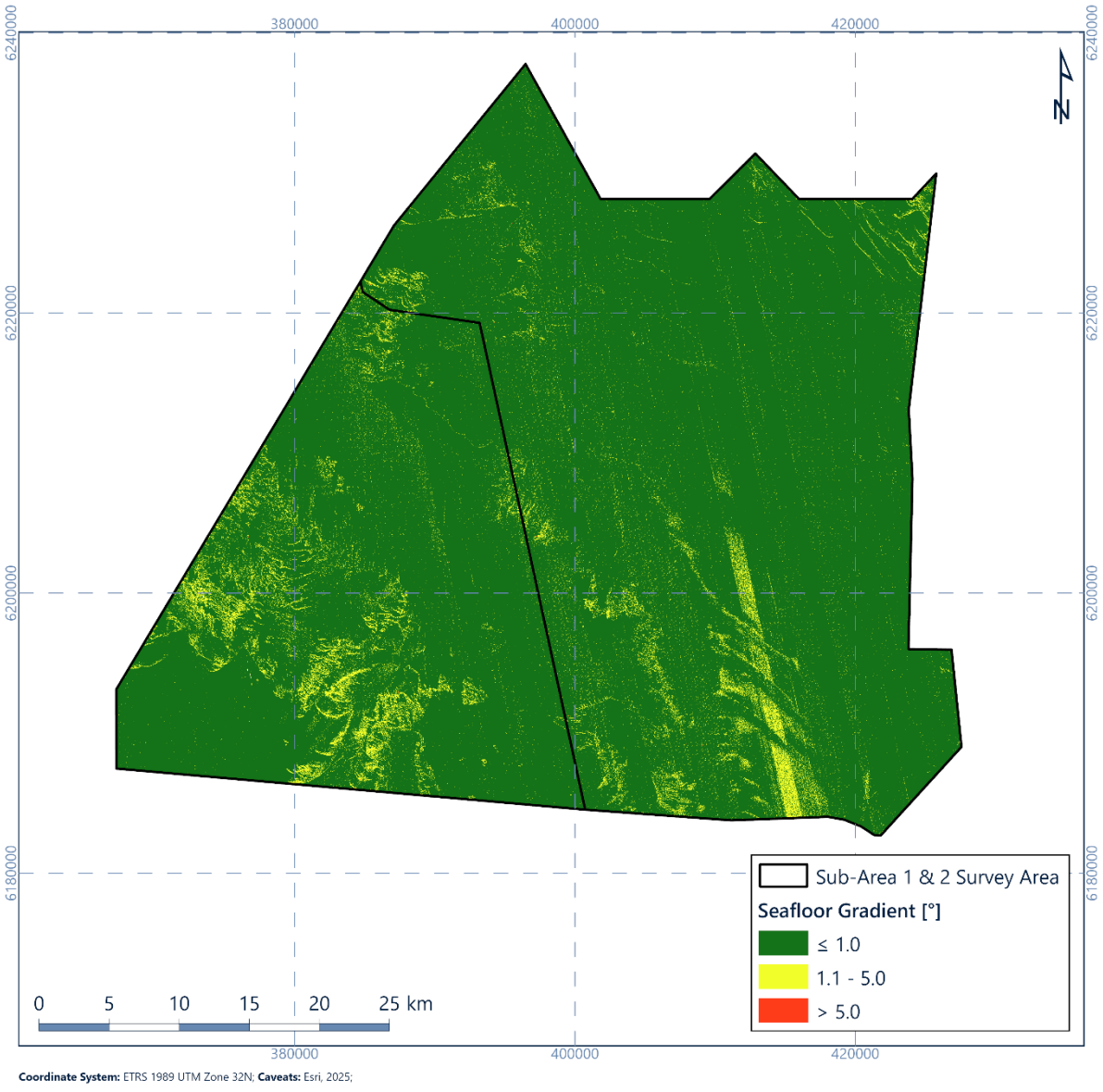

Figure 4.2: Full site seafloor gradient (Ocean Infinity, 2024)

4.3 Seafloor Features

Figure 4.3, Figure 4.4 and Figure 4.5 present the seafloor interpretation of seafloor sediments and features completed by Ocean Infinity (2024).

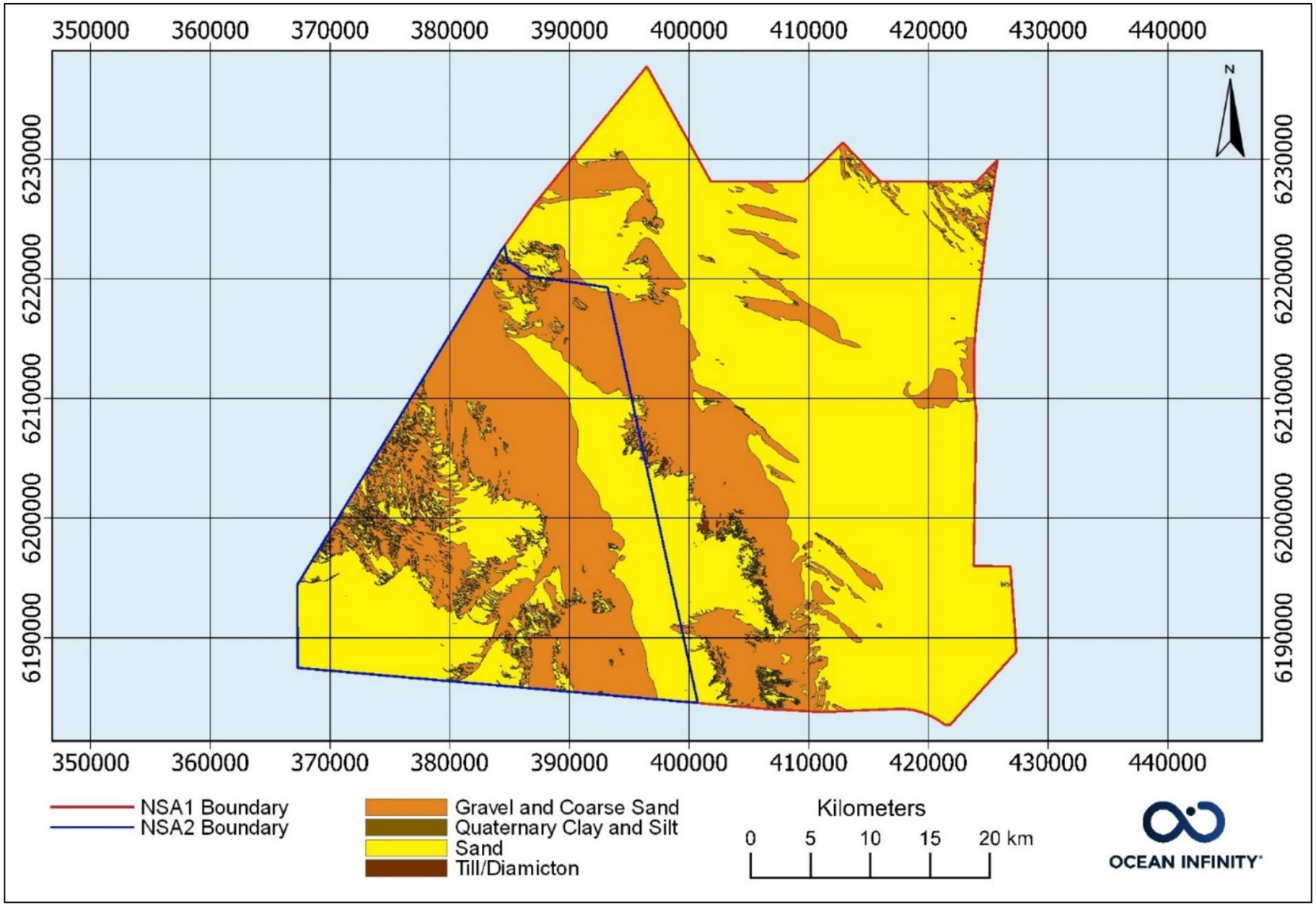

Figure 4.3: Seafloor sediments mapped by Ocean Infinity (2024)

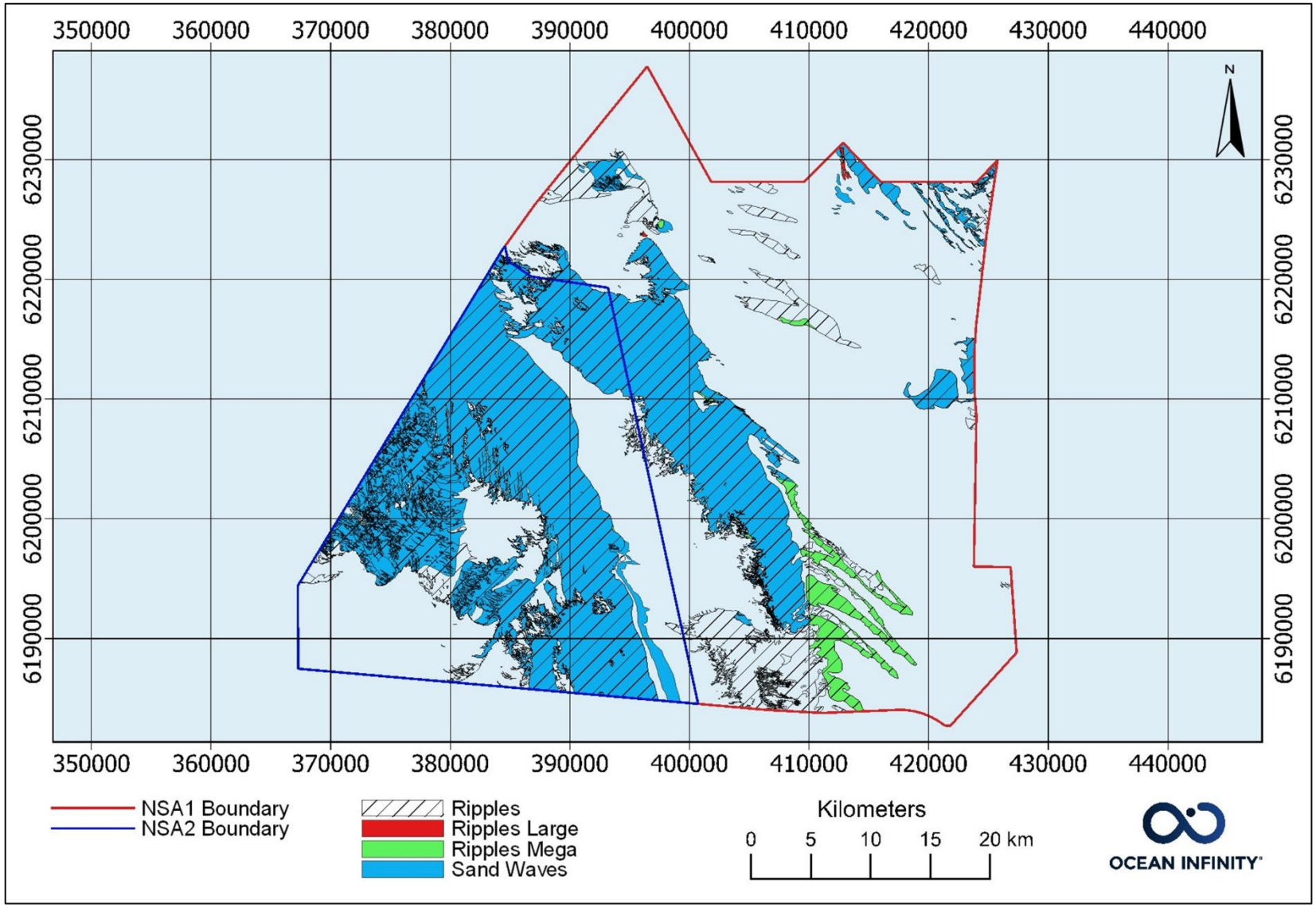

Figure 4.4: Seafloor mobile features mapped by Ocean Infinity (2024)

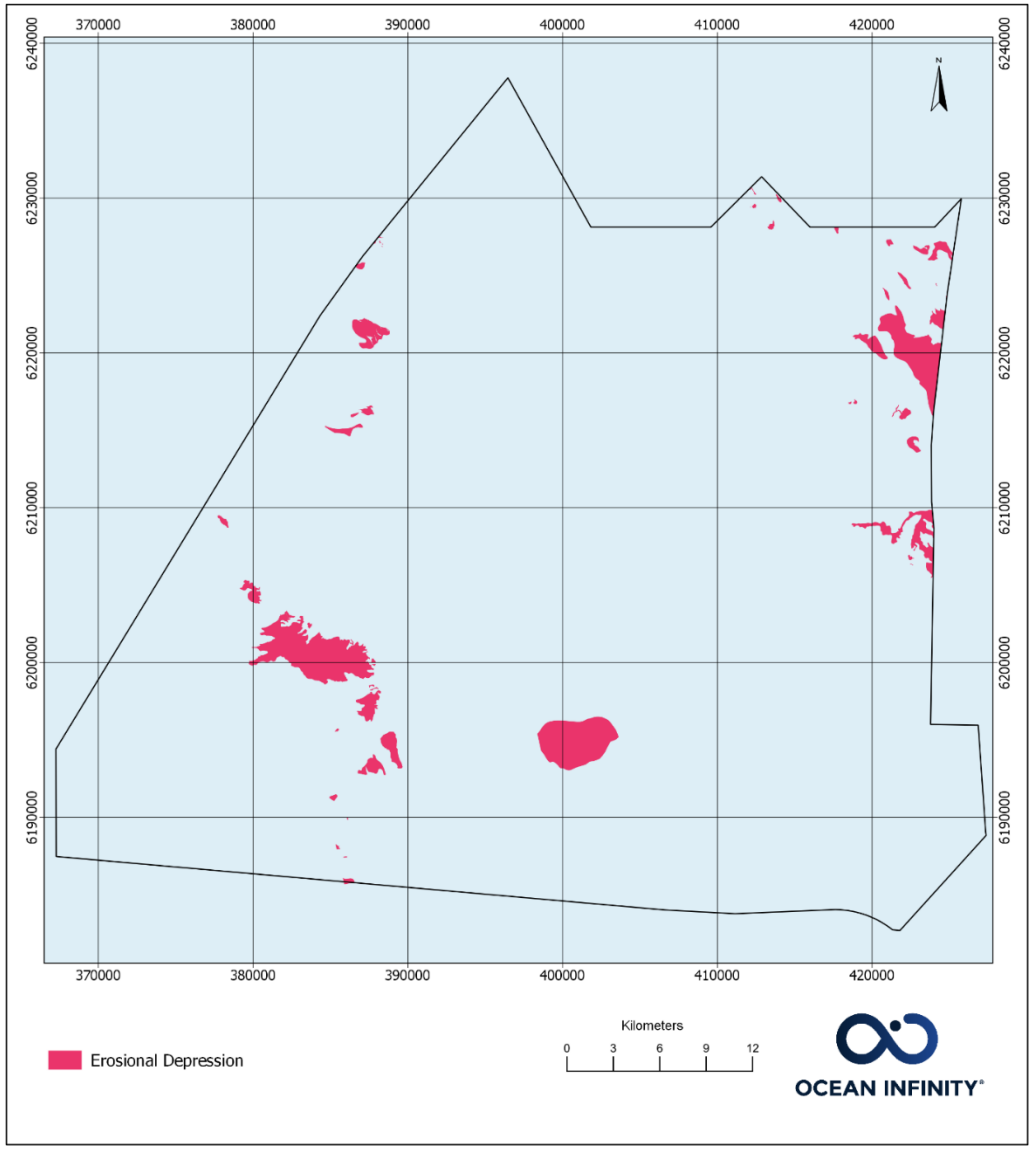

Figure 4.5: Erosional depression mapped by Ocean Infinity (2024)

5. Conceptual Geological Model

5.1 General

This section outlines how the geological model for the study area was derived to spatially delineate the integrated geotechnical and geophysical datasets. A series of integrated geological units were defined across the study area, as described in Section 2.4.2. The geophysical and geotechnical data were integrated together across the teams, without any separate initial interpretation of the geotechnical data.

Figure 5.1 and Table 5.1 provide a conceptual model of the interpreted geophysical horizons and associated geological units.

Eleven geophysical horizons were interpreted and delineate the base of 11 geological units. A further unit is present below the basal horizon.

The depositional environment, age and stress history (Table 5.1) are interpreted based on the geological setting, combined with the geophysical character of the seismic facies, soil type and geotechnical properties.

Table 5.1: Geological stress history

Stress History*	Description
A	Normally consolidated
B1	Possibly overconsolidated as a result of subaerial exposure
B2	
C1	Overconsolidated as a result of glacial loading
C2	
D	Pre-Quaternary, therefore possibly lithified
Notes * - Number is attributed to how many subaerial exposures or periods of ice cover	

It should be noted that:

- Geological units U35, U60, part of U65 and U90 have a similar depositional environment and expected soil type and are interpreted as fluvial deposits. Their architecture is complex and locally difficult to distinguish from each other;
- Units U65 and U70 both form the infill of tunnel valleys and are locally difficult to distinguish from each other;
- Geophysical horizons are defined by the grids derived for each unit. Grids may simplify some units where the associated geological processes are expected to be variable and complex. This is likely to be the case for geological unit U20;
- The previous two points are particularly relevant to the west of the NS1 site where these units are relatively thin and only locally present.

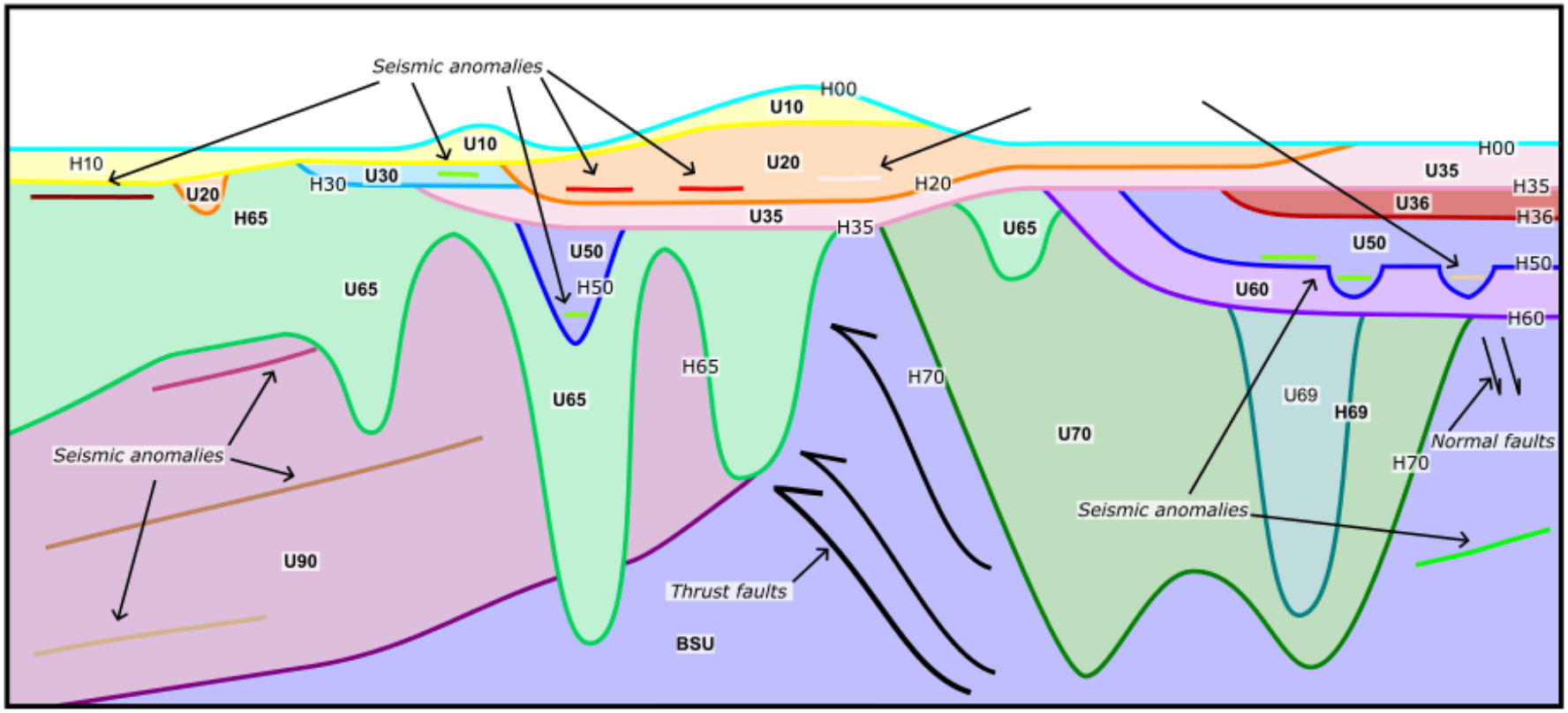

Figure 5.1: Conceptual model of the interpreted geophysical horizons (e.g. H20) and geological units (e.g. U20) in the top 200 m below seafloor

Table 5.2: Overview of interpreted horizons and soil units

Geological Unit	Horizon Base	Seismic Character	Soil Type†	Depositional Environment‡	Age‡	Stress History#
U10	H10	Acoustically transparent with point reflectors	SAND, fine to coarse, poorly sorted to well-sorted, slightly silty to very silty, occasionally slightly gravelly, with frequent fine-grained organic matter, with few to occasionally many shell fragments, occasionally with mica crystals, light olive brown to very dark grey, non-calcareous	Marine	Postglacial	A
U20a	H20	Stratified to acoustically transparent; locally forms channel infill ^	SAND, fine to medium, sorted, slightly silty to very silty, occasionally clayey, occasionally slightly gravelly, with frequent fine-grained organic matter, with few to occasionally many shell fragments, olive grey to very dark grey, non-calcareous locally calcareous	Freshwater to marine	Postglacial	A
U20b			SAND, fine to medium, poorly sorted to sorted, slightly clayey to clayey, slightly silty to very silty, occasionally with fine-grained organic matter, with few shell fragments, occasionally with few mica crystals, grey to dark grey, non-calcareous to slightly calcareous transitioning to CLAY, low to high plasticity, silty, slightly sandy to sandy, with few pockets of fine-grained organic matter, with few shells and shell fragments, olive grey to very dark grey, slightly calcareous transitioning to PEAT, slightly decomposed, occasionally decomposed to strongly decomposed, clayey, occasionally sandy to very sandy, dark brown to black			
U30	H30	Complex – stratified to chaotic, with locally internal erosion surfaces and high amplitude positive polarity internal reflectors	SAND, fine, occasionally fine to medium, poorly sorted to sorted, silty, with few fine-grained organic matter, light olive brown to very dark grey, non-calcareous to slightly calcareous, with a thick to very thick bed of CLAY, low to high plasticity, silty, with pockets of fine-grained organic matter, with mica crystals, dark grey to very dark grey, calcareous	Meltwater Freshwater	Glacial (Weichsalian)	B1
U35	H35	Complex with locally internal erosion surfaces and high amplitude positive polarity internal reflectors; locally forms channel infill	SAND, fine to medium, occasionally coarse, sorted, slightly silty to silty, slightly gravelly to gravelly, with fine-grained organic matter, occasionally with mica crystals, grey to dark grey, non-calcareous to slightly calcareous, with occasional thick beds of CLAY, low to medium plasticity, slightly to very sandy, occasionally silty, grey to dark grey, slightly to highly calcareous	Meltwater	Glacial (Weichsalian)	B1
U36	H36	Stratified, locally with clinoforms	SAND fine to medium, sorted, slightly silty to very silty, occasionally slightly gravelly, occasionally with pockets of fine-grained organic matter, occasionally with few shells and shell fragments, greenish grey to dark greenish grey, non-calcareous to slightly calcareous with occasional very thick beds of CLAY, low to medium plasticity, slightly to very silty, occasionally sandy, with pockets of fine-grained organic matter, with few shells and shell fragments, greenish grey to dark greenish grey, slightly calcareous to calcareous	Deltaic Marine	Interglacial (Eemian) to Glacial (Weichsalian)	B1
U50	H50	Acoustically transparent; locally forms stratified channel infill	CLAY, low to high plasticity, slightly to very silty, sandy to very sandy, occasionally slightly gravelly, with pockets of fine-grained organic matter, with few shell fragments, dark to very dark grey, slightly calcareous to calcareous Basal thick bed of SAND, fine to medium, poorly to well sorted, silty to very silty, occasionally with shell fragments, grey to dark grey, non-calcareous to calcareous	Marine	Interglacial (Eemian)	B1
U60	H60	Complex – with internal erosion surfaces and high amplitude positive internal reflectors; locally forms channel infill	SAND, fine to medium, occasionally coarse, poorly sorted to sorted, occasionally well sorted, occasionally slightly silty, occasionally slightly gravelly to gravelly, with few pockets of fine-grained organic matter, with rare wood fragments, occasionally with few shell fragments, occasionally with mica crystals, grey to dark grey, non-calcareous to slightly calcareous, with a basal medium bed to thick bed of GRAVEL, fine to coarse, unsorted to poorly sorted, occasionally sandy to very sandy, multi-coloured, non-calcareous	Meltwater	Glacial (Saalian)	B2
U65	H65	Variable from acoustically transparent, stratified to acoustically complex with internal erosion surfaces and inclined stratification	SAND, fine to coarse, poorly sorted to well sorted, slightly silty to very silty, slightly gravelly to gravelly, with laminae to layers of clay, with few to many shell fragments, with laminae to pockets of fine grained organic material, with few wood fragments, with few mica crystals, greyish brown, grey to dark grey, non-calcareous to calcareous CLAY, low to high plasticity, slightly sandy to very sandy, slightly silty to very silty, slightly gravelly to very gravelly, with laminae to few pockets of fine-grained laminae, with few shell fragments, with few to many mica crystals, dark grey to very dark grey, non-calcareous to highly calcareous GRAVEL, fine to coarse, unsorted to poorly sorted, slightly sandy to very sandy, with few shell fragment to shell fragments, various lithologies, multicoloured, non-calcareous	Marine Freshwater Meltwater Glacier	Glacial (Saalian)	C1
U69	H69	Well stratified. Forms upper part of tunnel valley infill	CLAY, low to high plasticity, occasionally very high plasticity, slightly to very silty, sandy to very sandy, occasionally slightly gravelly, with few pockets of silt or sand, occasionally with few shell fragments, with few mica crystals, dark greenish grey to dark grey, calcareous	Lacustrine	Interglacial (Holstenian)	C1
U70	H70	Acoustically chaotic. Forms lower part of tunnel valley infill	Medium to very thickly interbedded CLAY, low to high plasticity, occasionally very high plasticity, sandy to very sandy, occasionally slightly silty to silty, occasionally slightly gravelly, with few pockets of silt or sand, with few pockets of fine-grained organic matter, occasionally with mica crystals, blocky or slickensided, dark grey to very dark grey, slightly calcareous to calcareous and SAND, fine to medium, occasionally coarse, poorly sorted to sorted, slightly silty to very silty, occasionally slightly clayey to clayey, occasionally slightly gravelly to gravelly, with few laminae of fine-grained organic matter, occasionally with layers and laminae of clay, grey to dark grey, non-	Marine Freshwater Meltwater Glacier	Interglacial (Holstenian) and glacial (Elsterian)	C2

			calcareous to slightly calcareous, occasionally with STONES, occasionally with basal thick to very thick beds of CLAY TILL to SILT TILL, low to high plasticity, occasionally very high plasticity, slightly sandy to sandy, slightly gravelly to gravelly, with few pockets of sand, dark greyish brown to very dark greyish brown, calcareous			
U90	H90	Complex – chaotic to transparent (horizontal and inclined reflectors), with internal erosion surfaces	SAND, fine to medium, occasionally coarse, sorted, occasionally slightly silty to silty, occasionally slightly gravelly, with few laminae of fine-grained organic matter, grey to dark greyish brown, non-calcareous	Meltwater to freshwater	Glacial (Pre-Elsterian)	C2
BSU	n/a	Well stratified, locally the stratification is less well defined	Medium to very thickly interbedded CLAY, medium to high plasticity, slightly silty to silty, occasionally slightly sandy, occasionally slightly gravelly, with few fine-grained organic matter and layers of PEAT, with few laminae of silt, occasionally with few shell fragments, slickensided, very dark grey to black, non-calcareous and SAND, fine, poorly sorted to well sorted, very silty, occasionally very clayey, occasionally slightly gravelly, with laminae of clay and silt, grey to very dark grey, non-calcareous to slightly calcareous	Marine	Miocene	D

Notes
† = Soil type based on borehole data collected in across the whole site
‡ = Depositional environment and age according to the Danish standard (Larsen et al., 1995)
# = A: normally consolidated; B: possibly overconsolidated as a result of subaerial exposure; C: overconsolidated as a result of glacial loading; D: Pre-Quaternary, therefore possibly lithified; number of subaerial exposures or number of periods with ice cover
^ = No single horizon can be mapped to delineate the geotechnical subunits
BSU = Base seismic unit
n/a = not applicable

6. Integrated Geological Model

6.1 Introduction

This section presents the geological model derived from integrating NS1 datasets. Sections 6.3 to 6.14 present each geological unit and Section 6.15 details the geological features and geohazards. Section 8.3.1 presents a summary of the charts and data deliverables, including additional geotechnical integration plates associated with the integrated geological model.

6.2 Integration of Datasets: Confidence and Uncertainties

Section 2.4.2 describes the methodology used to integrate datasets and create geological units across the study area. This section outlines the confidence in the data and the uncertainties that remain following this process. Some uncertainty in the modelling due to dataset coverage is inevitable.

Refer to the plates in Section 8.3.1 for the integration of the locations.

6.2.1 Unit Gridding

Integrated geophysical horizons were gridded as part of the spatial ground modelling (Section 2.4.1). Some uncertainty can be expected due to the density of the input datasets.

Line spacing of inline 2D UHR data was greater than the 250 m line plan in limited areas of the NS1 site. This is visible in the west of the site where data collection line spacing was increased to 500 m in two sections, presented in Figure 2.2. In some localised areas of the NS1 site, line spacing greater than 250 m is associated with acquisition challenges and limited infill opportunities. This results in greater extrapolation within grid data and may increase uncertainty in spatial model units.

It should be noted that where there is an increase in geophysical line spacing, the depths to surfaces are more less certain, particularly in channelised areas due to more interpolation. This certainty is reduced as channelised units can vary considerably over short distances. Given the likely depositional processes, the base of channelised units often have highly complex geometries. 2D UHR data acquisition is unlikely to capture these complexities fully. Figure 6.1 shows an example of an area where the 2D UHR lines have a wider spacing within the geological unit U70.

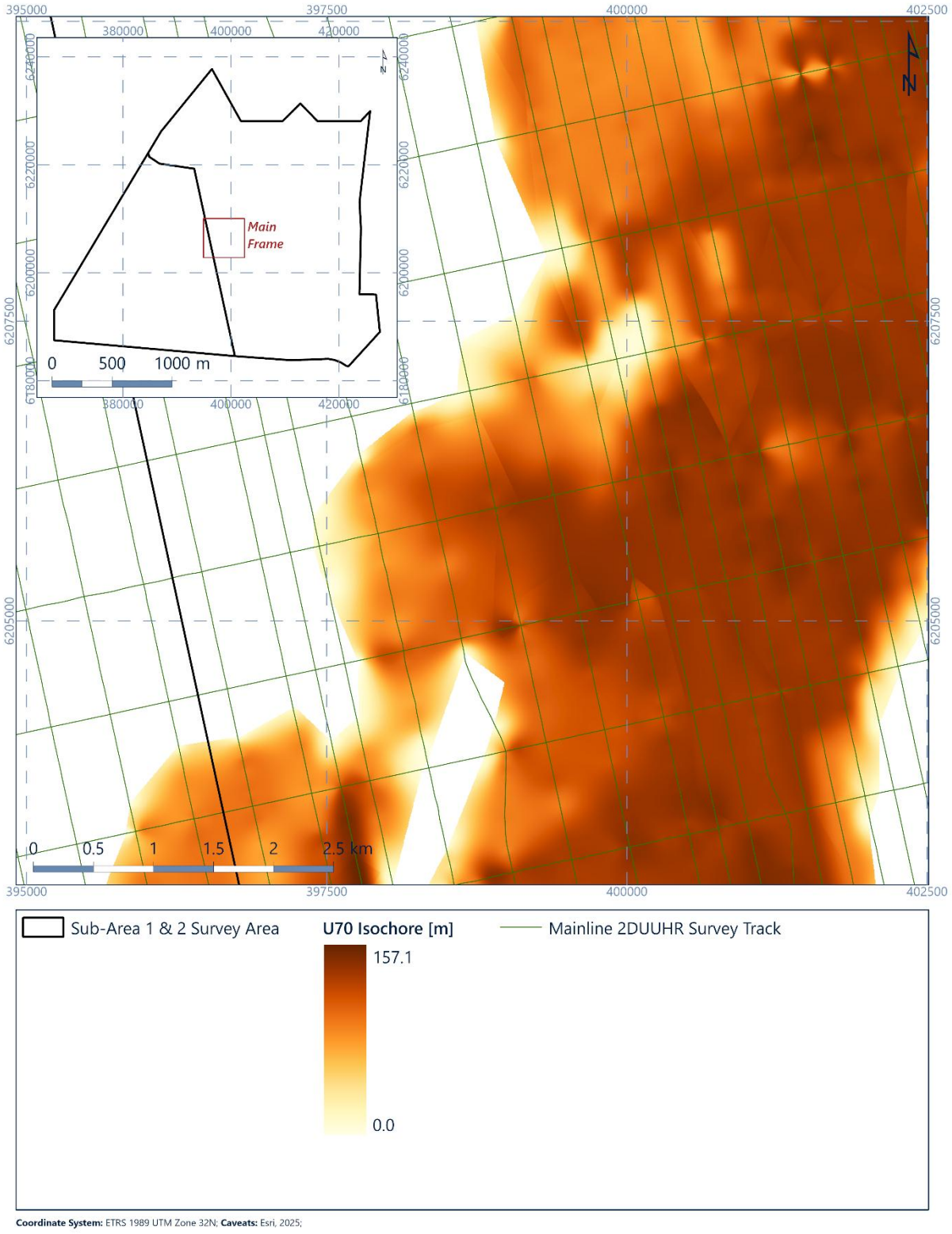

Figure 6.1: Gridding around channelised units – geophysical unit U70 example

6.2.2 Time Depth Conversion

Geophysical data were depth converted using a single seismic velocity of 1730 m/s (Section 2.4.1). This value was based on correlations between geotechnical and geophysical data for

all units, however variability within unit velocities is expected. Information on unit boundaries for geophysical and geotechnical datasets are presented as part of borehole integration charts and in Appendix B. Offsets between datasets vary based on multiple factors such as the velocity model, offsets between geophysical lines and geotechnical data locations and grid uncertainty. Further revision to the velocity model is recommended once refinement to the study area occurs and sub-areas are designated, (Section 1.2). This will allow greater focus on selected units and ground conditions within designated sub-areas.

6.3 Geological Unit – Unit U10

6.3.1 Seismic Character

Geological unit U10 occurs across almost the entire NS1 site (Figure 6.2). It is locally absent, most notably in the east and north of the site. This unit has an average thickness of less than 1.8 m, locally it is thicker, reaching a maximum thickness of 10 m in Sub-Area 2 (Figure 6.3). This is due to mobile sediments present within the site, especially on the western side (Figure 4.4).

Within Sub-Area 1 the thickness is less than 5 m. In Sub-Area 2, geological unit U10 is more consistently present and has a thickness of up to 10 m. The thickest areas of geological unit U10 mostly correspond to bathymetric highs, especially in Sub-Area 2 (Figure 4.1). In the south of the site geological unit U10 forms a series of ridges and banks. The largest of these is a north-north-west to south-south-east oriented sand bank, approximately 10 km wide in Sub-Area 2. Around this sand bank there is a series of north-east to south-west oriented ridges up to 3 km wide, and north-west to south-east oriented ridges up to 1.5 km wide.

The basal horizon of geological unit U10 is flat to undulating and generally a medium to high amplitude positive reflector. Where geological unit U10 overlies geological unit U20, in the north and east of the site, the basal horizon H10 gradually becomes difficult to distinguish from internal reflectors within geological unit U20. In those areas the shallowest laterally continuous reflector was interpreted as horizon H10. In Sub-Area 2, geological unit U10 is generally overlying geological unit U65.

Geological unit U10's internal seismic character is acoustically transparent with point reflectors. (Figure 6.4).

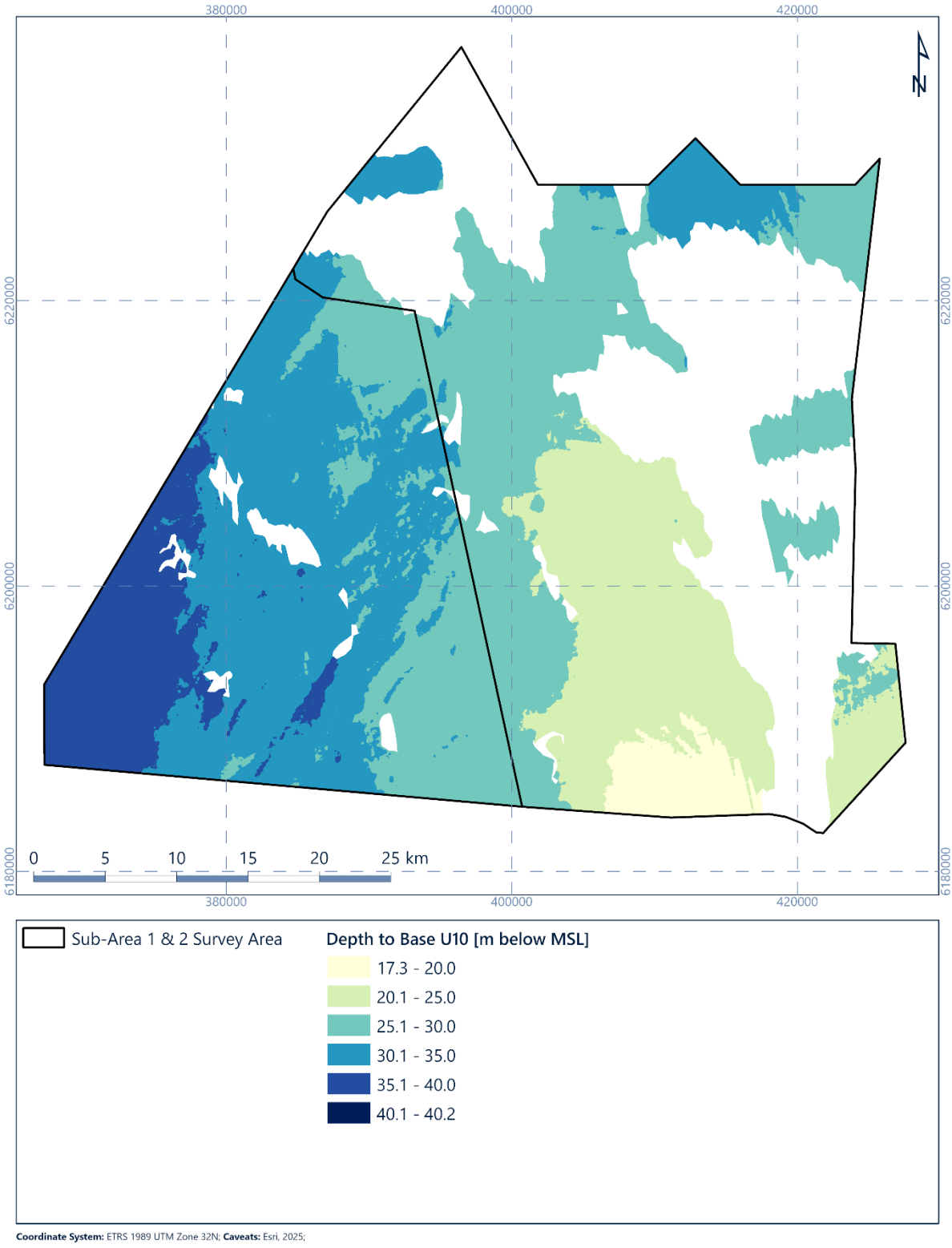

Figure 6.2: Depth [m below MSL] to horizon H10 (base of geological unit U10)

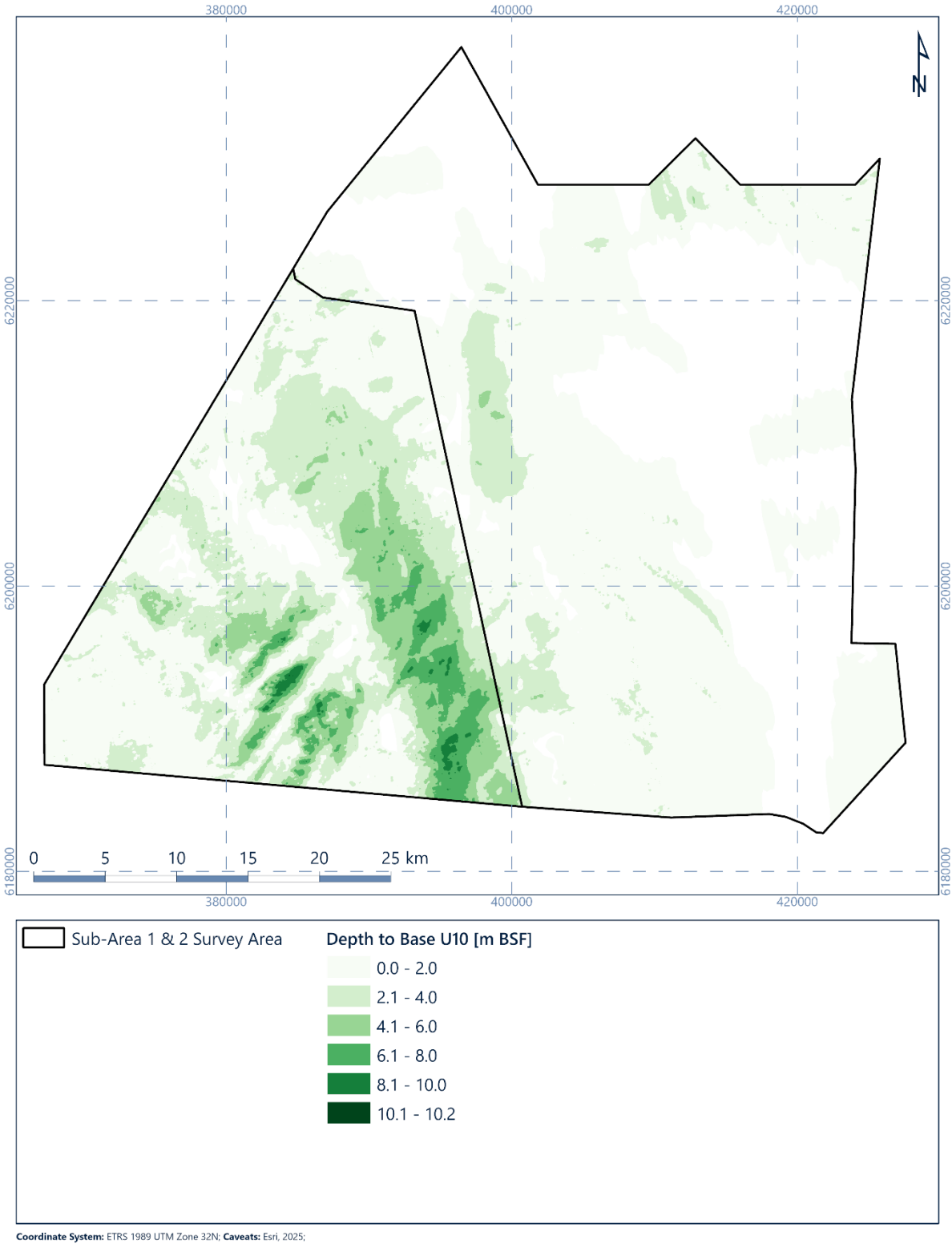

Figure 6.3: Depth [m BSF] to horizon H10 (base of geological unit U10)

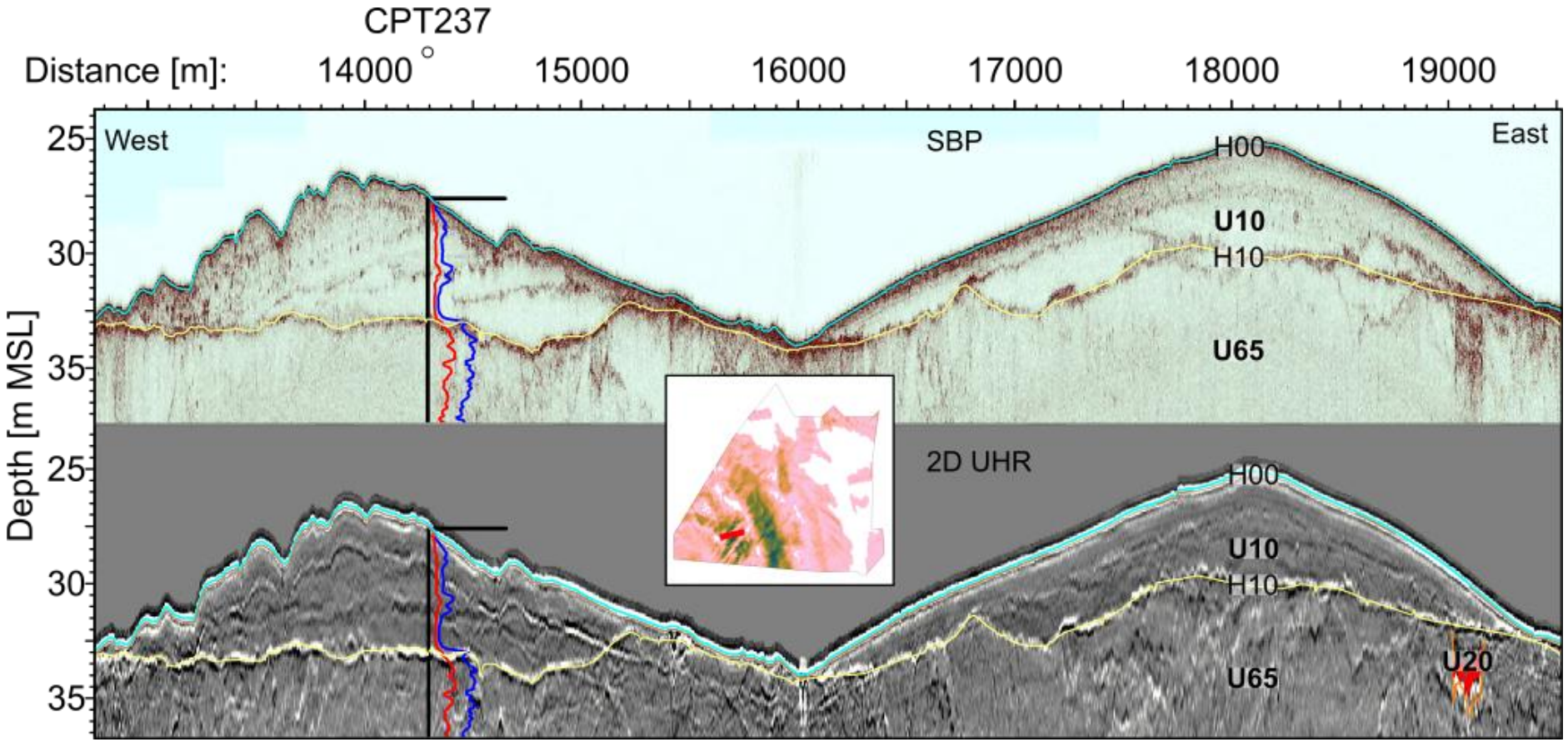

Figure 6.4: SBP and 2D UHR seismic data example of geological unit U10. Line EAXC405P1, CPT237. CPT scale: blue is q_c with a scale from 0 MPa to 80 MPa; red is f_s with a scale of 0 MPa to 2 MPa. Examples are from Sub-Area 2, but show good seismic response and geotechnical data

6.3.2 Integration and Interpretation

The most recent sediments at the site belong to the Holocene marine period. Site conditions are characterised by those present at the site today, with similar depositional processes and metocean processes being active. Sediments deposited during this time belong to geological unit U10. In the centre of the site a large sand bank is present, is interpreted to be a palaeo-coastline, formed around the bathymetric highs between 8.2 and 7.0 ka BP (Figures Figure 3.8 and Figure 3.9). Figure 6.5 presents a schematic diagram of this period of deposition. A gradual transition from non-marine into marginally marine and fully marine environments is interpreted where geological unit U10 overlies geological unit U20.

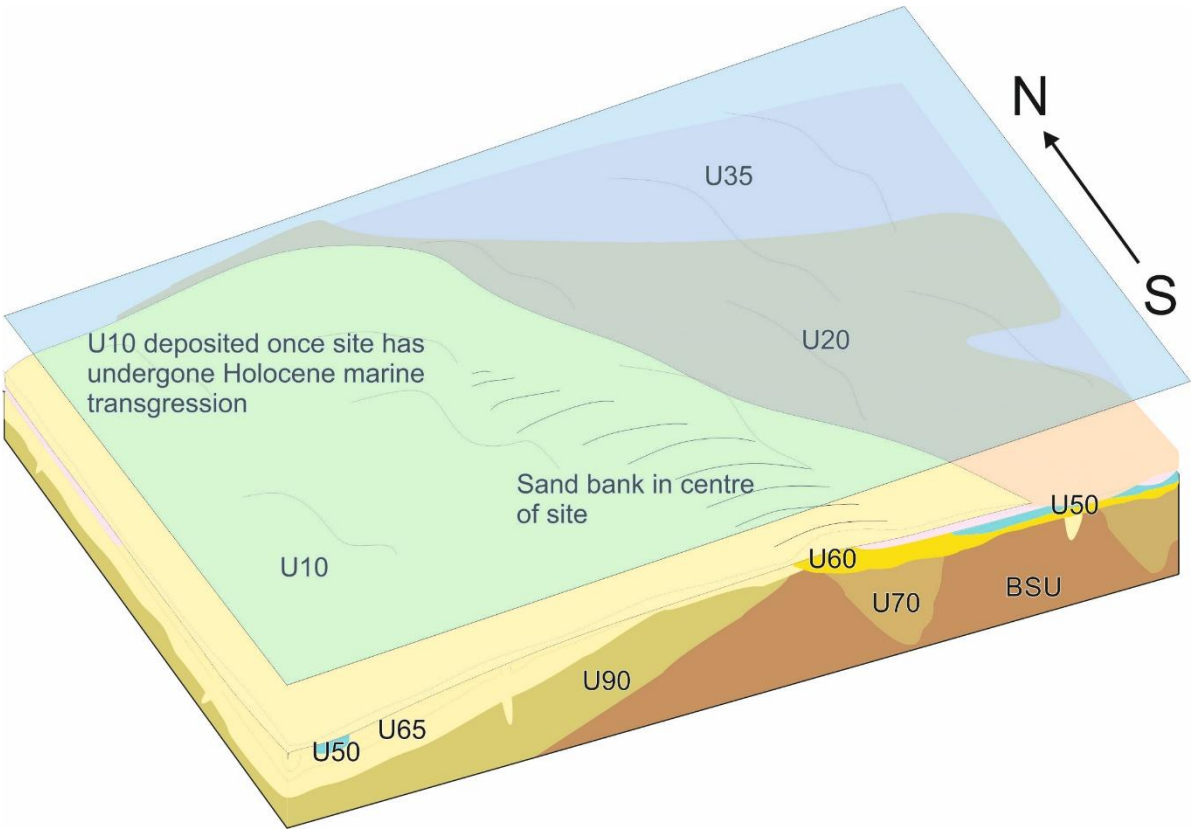

Figure 6.5: Depositional processes associated with U10

The correlation between seismic data and seafloor mapping (Section 4.3) suggests that greater thicknesses of geological unit U10 correspond to areas of gravels and coarse sands, supporting environmental depositional interpretations associating geological unit U10 with higher energy shallow marine environments than the underlying geological unit U20 sediments. Figure 6.6 displays the correlation between the geological interpretation and geotechnical locations. Integration between geophysical and geotechnical datasets is generally suitable. The limited inconsistencies observed are interpreted to be a result of areas where very thin deposits of geological unit U10 observed in geotechnical data were not mapped in the geophysical data.

Geological unit U10 is almost exclusively observed as a sand unit, with grain sizes ranging from fine to coarse. Organic matter and shell fragments are both noted in the sample data, highlighting the material's possible reworking from underlying older sand sediments.

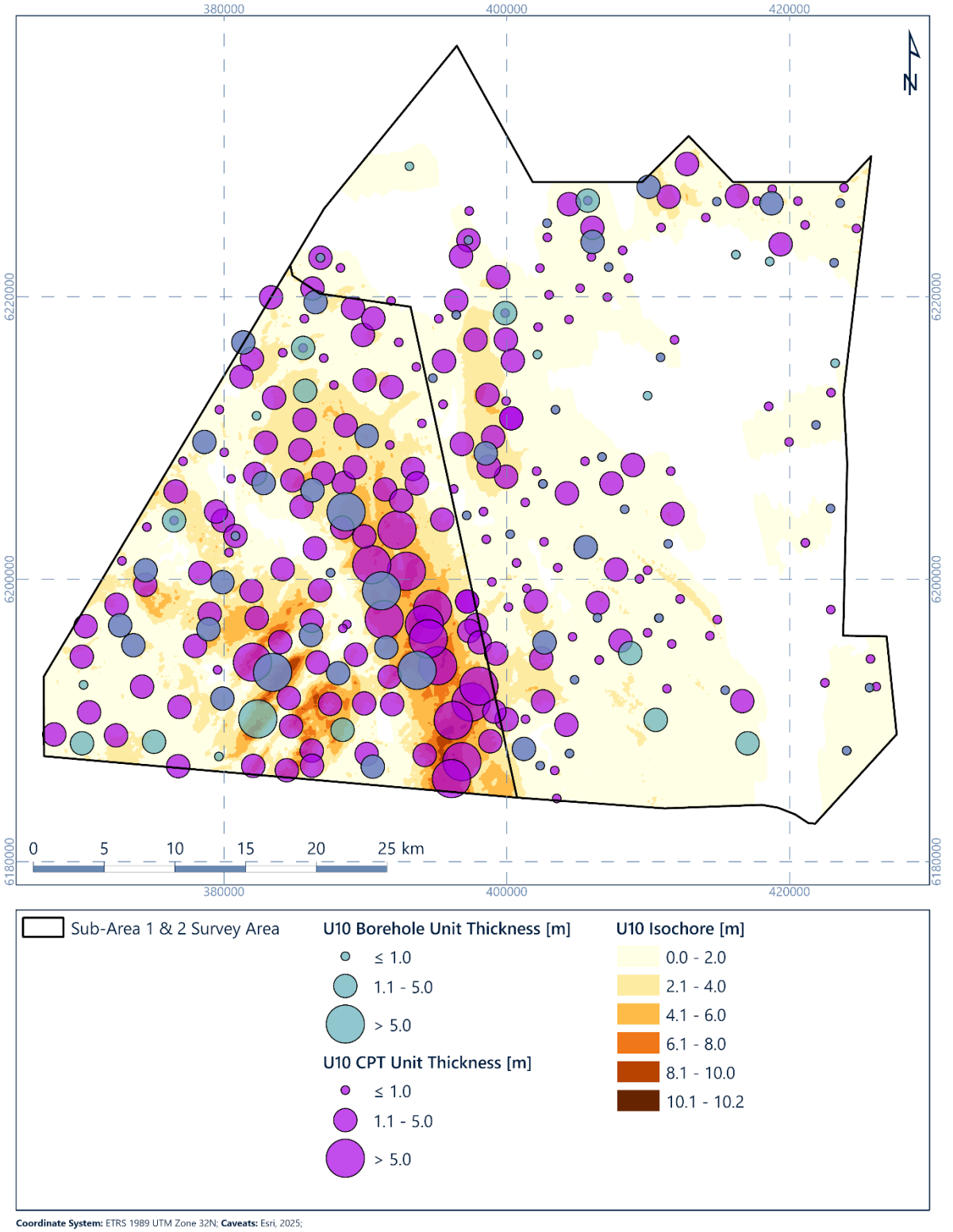

Figure 6.6: Isochore for geological unit U10 correlated with geotechnical data recoveries

6.4 Geological Unit – Unit U20

6.4.1 Seismic Character

Geological unit U20 forms the infill of spatially variable channels and their overbank deposits up to 10 km wide, with a west to east or north-west to south-east orientation forming a tributary network (Figure 6.7 and Figure 6.8). The thickness of geological unit U20 reaches approximately 30 m (Figure 6.9 and Figure 6.10). The infill of narrow (less than 1 km) tributary channels is less than 10 m thick (Figure 6.11). Beyond the confinement of the main channels, this unit forms a relatively thin layer up to approximately 5 m thick.

Geological unit U20's base is marked by horizon H20, a low to high amplitude positive reflector. Geological unit U20 is generally associated with, and directly overlies, geological unit U35.

Internally, geological unit U20 is acoustically transparent or stratified with low to medium amplitude reflectors dipping towards the east (Figure 6.11). The seismic character is more variable at the base and margins of channels. The base of the geological unit is frequently formed by a seismic anomaly with a negative polarity (Section 6.15.1); indicating peat or organic-rich material at the boundary (Section 6.15.1). Where the unit is relatively thick, a seismic anomaly associated with acoustic blanking is often present (Section 6.15.3); this could indicate the presence of shallow gas (Section 6.15.3).

Fugro reviewed whether further horizons within geological unit U20 could be picked across the study area, but found that no consistent horizons delineating the geotechnical transitions observed within the geological unit U20 sediments could be consistently mapped.

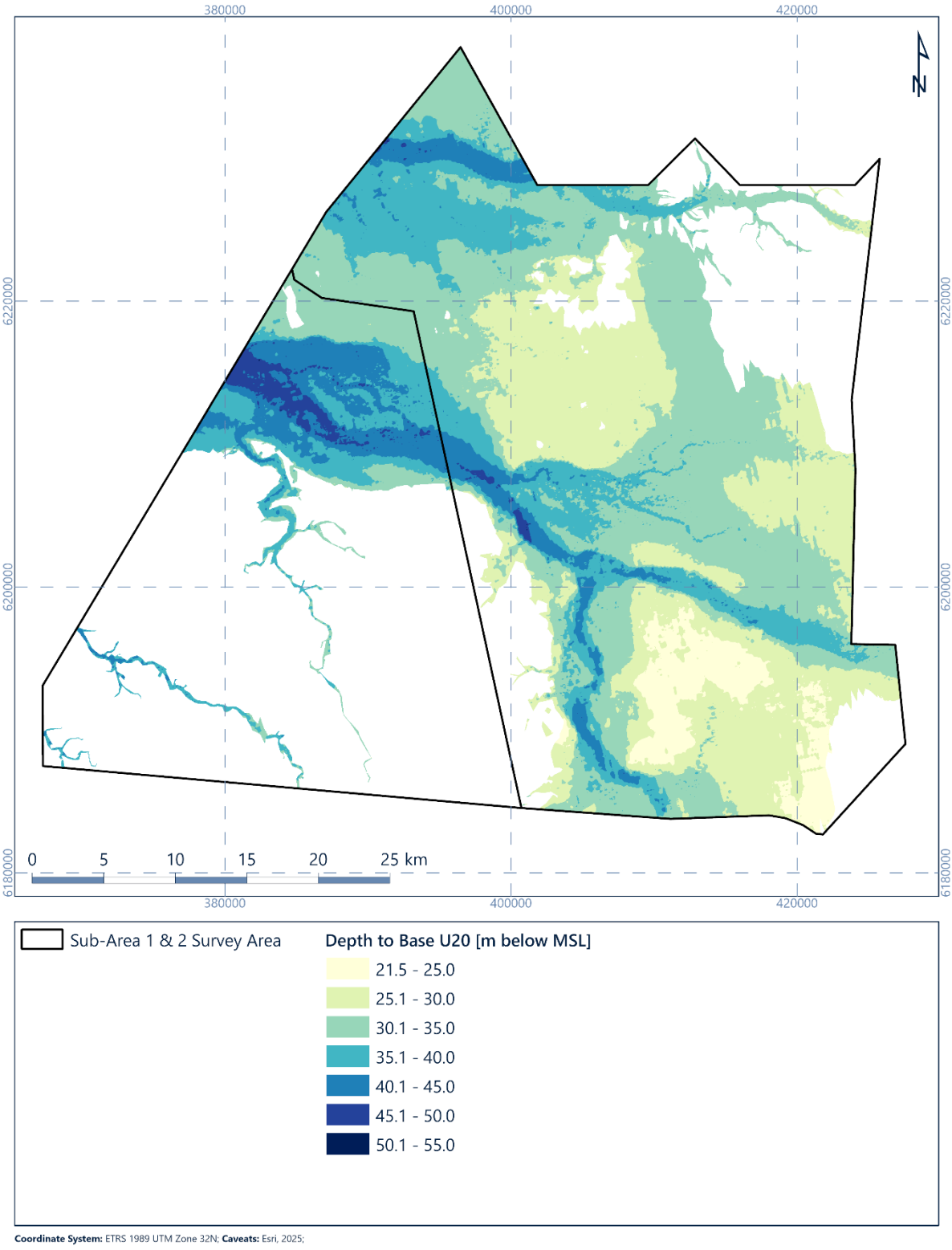

Figure 6.7: Depth [m below MSL] to horizon H20 (base of geological unit U20)

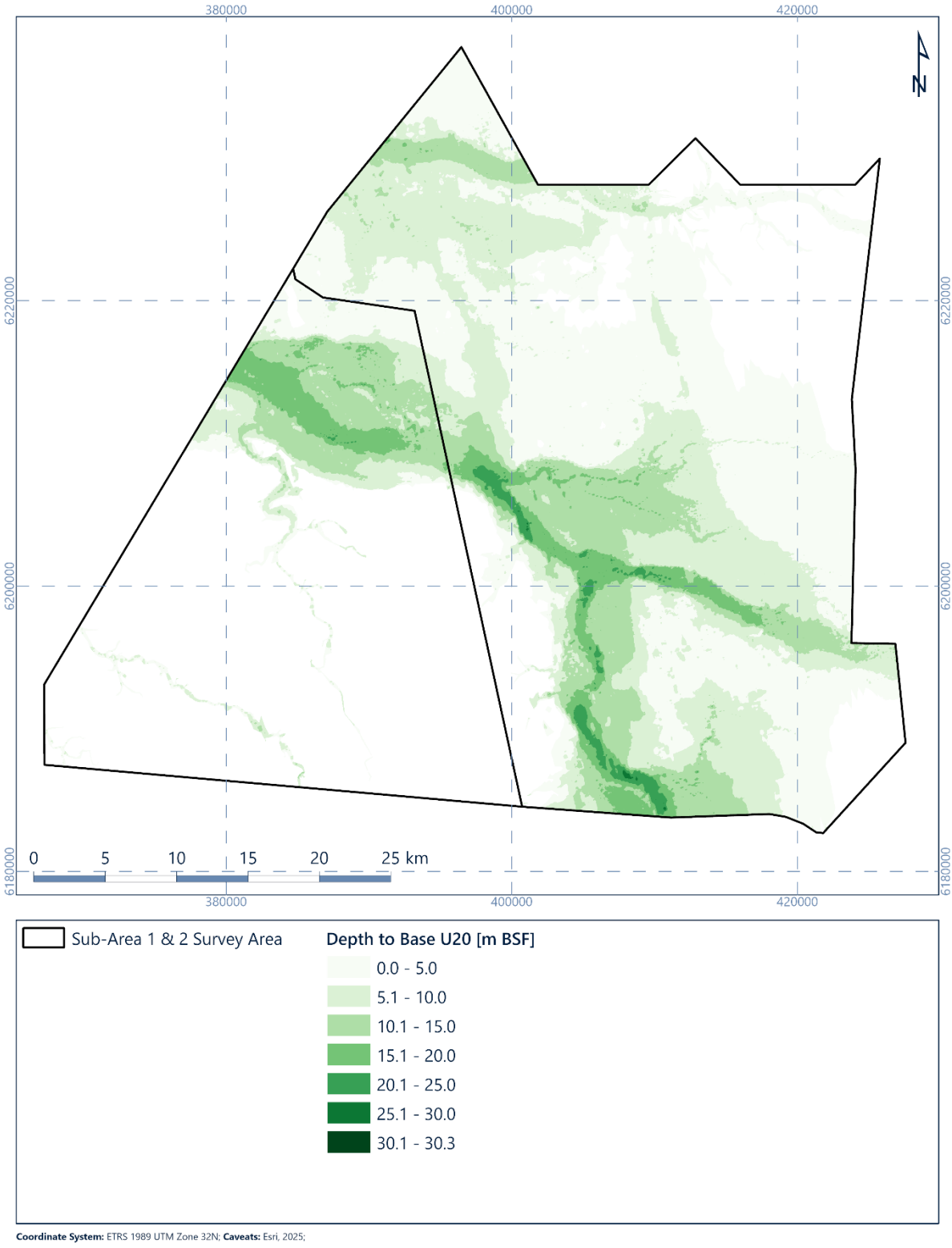

Figure 6.8: Depth [m BSF] to horizon H20 (base of geological unit U20)

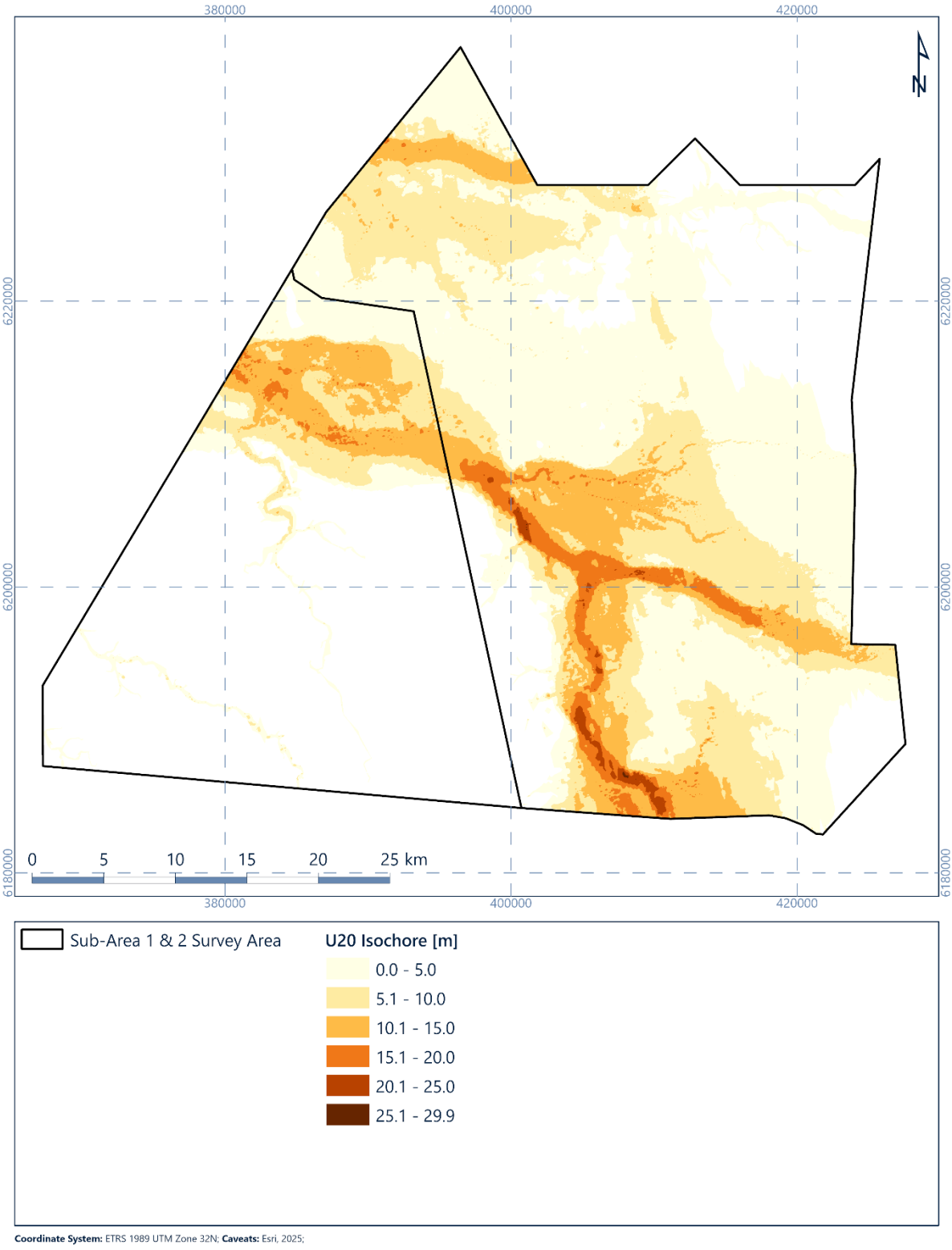

Figure 6.9: Isochore of geological unit U20 [m]

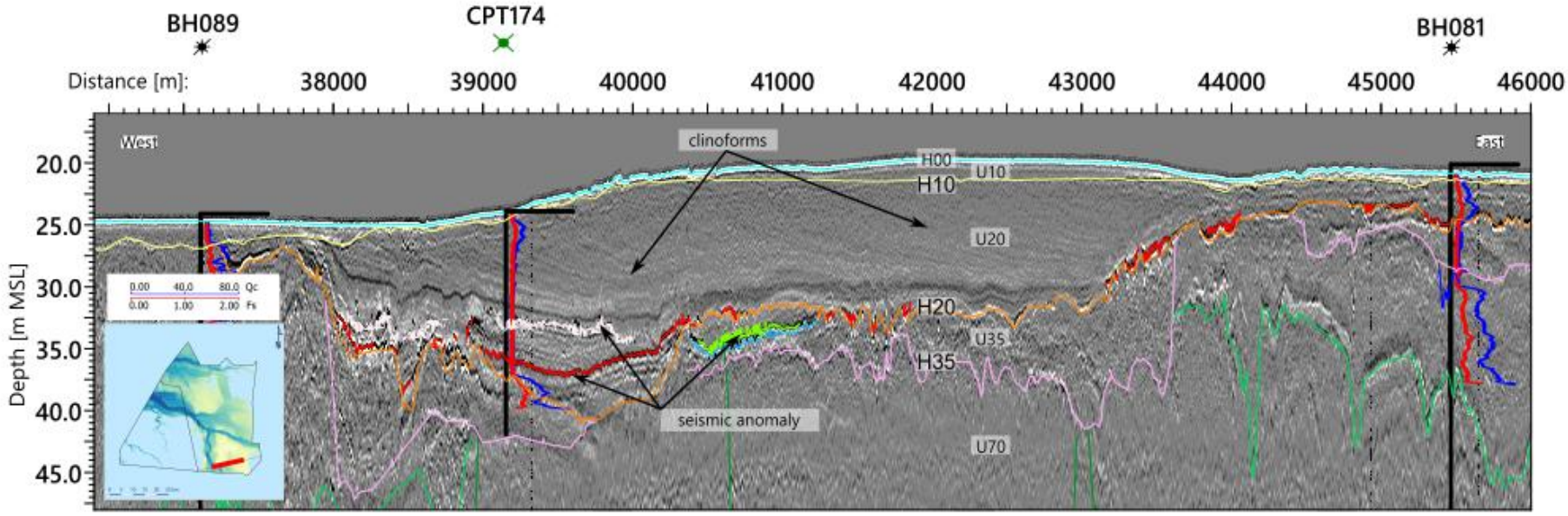

Figure 6.10: 2D UHR seismic data example showing the wide and deep channel of Unit U20

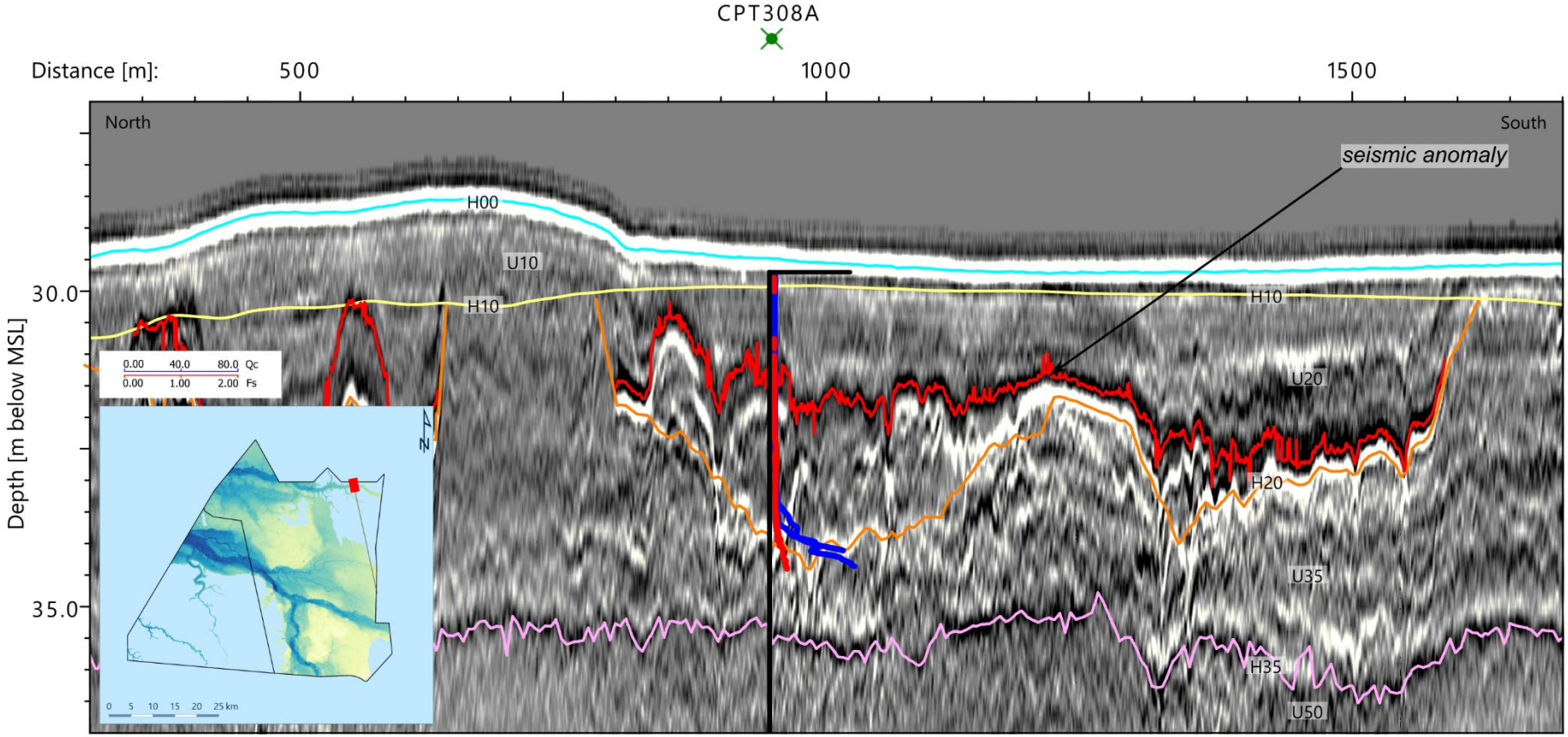

Figure 6.11: 2D UHR seismic data example showing a small channel of Unit U20

6.4.2 Integration and Interpretation

At the end of the Weichselian, a global marine transgression occurred associated with the retreat of ice sheets following the LGM. As a result, deposition at the NS1 site is predicted to have changed from glacio-fluvial to fluvial and then gradually to a marine setting (Section 3). During this period of transition, sediments from geological unit U20 are predicted to have been deposited; comprising a network of three main channels and several secondary distributary channels. Figure 6.12 presents an evolutionary model for the deposition of geological unit U20.

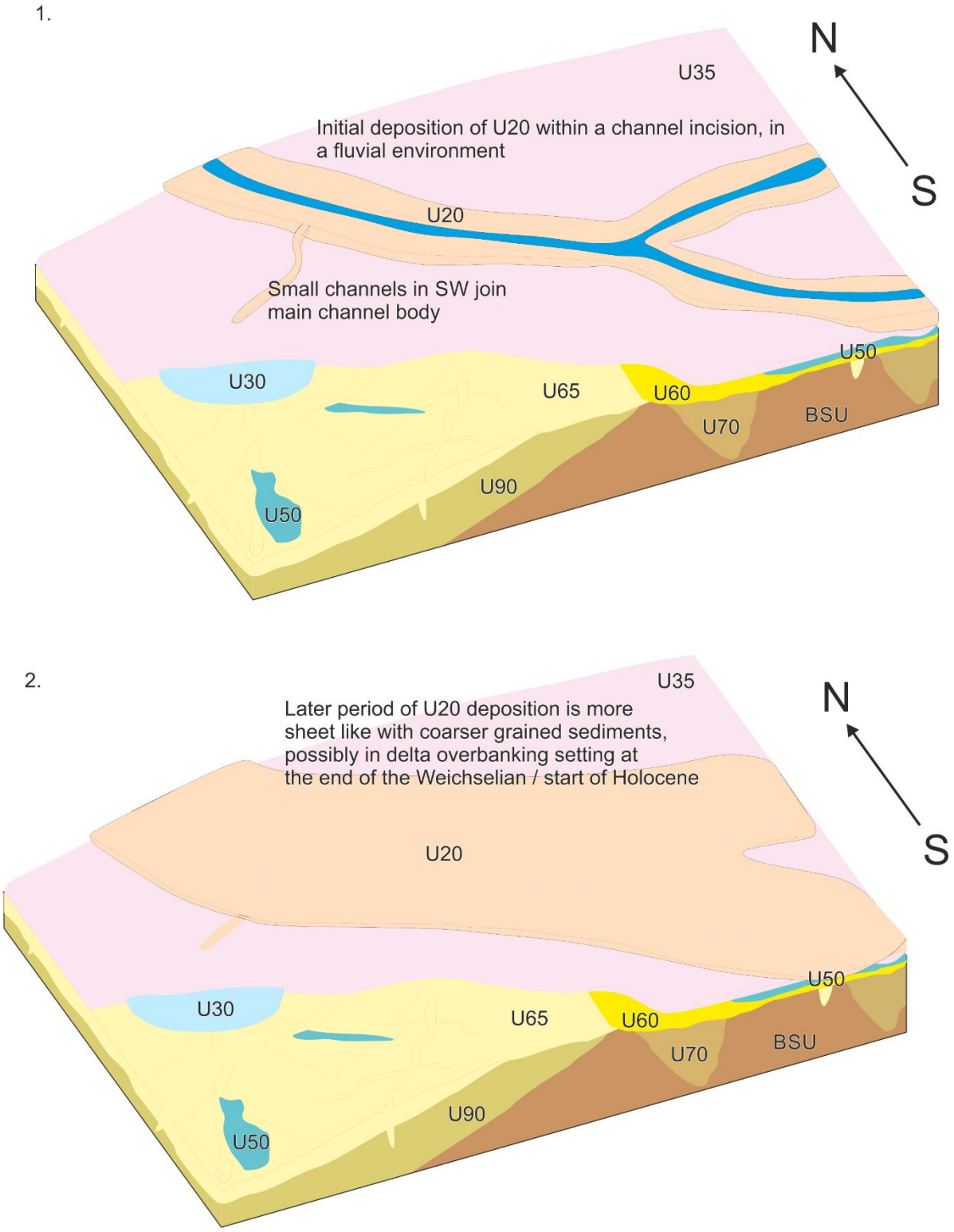

Figure 6.12: Depositional processes associated with U20. 1) Initial sediments are predicted to have been deposited in a fluvial delta with low energy material observed in spatially limited channels. 2) As the early Holocene marine transgression continued the site was likely drowned and higher energy sand sediments are observed.

Sampling and CPT data within geological unit U20 show a gradation from coarser sediments in the upper section to finer grained cohesive sediments (Section 6.15.2) in the lower sections, particularly in the channelised areas. The geotechnical unitisation reflects this by

aiding the definition of two geological subunits; U20a and U20b. These subunits could not be identified in the geophysical data, so data integration is not currently possible.

Figure 6.13 and Figure 6.14 show the correlation between the thickness of geological unit U20 in the seismic data and the geotechnical locations of geological subunits U20a and U20b. Geological subunit U20b is largely confined to the channel incision areas, whereas geological subunit U20a is present across the area. There are some differences in the thickness of the U20 subunits between the CPT and borehole data, this is likely due to difference in unitisation of the subunit split at those locations. This is from previous reporting stages where geological unit U20 was not split at the original CPT integration phase. Not all areas of geological unit U20 were sampled and variability in the observed thicknesses may exist. Table 5.2 presents the differences in soil type between these two subunits. This difference is also reflected in the thickness of geological subunit U20a, with greatest thickness of the geological unit U20a present in the channel areas, but thinner in the more downstream areas. The base of geological unit U20 in geophysical and geotechnical data shows very good correlation coefficients, suggesting high confidence in extrapolation using geophysical datasets.

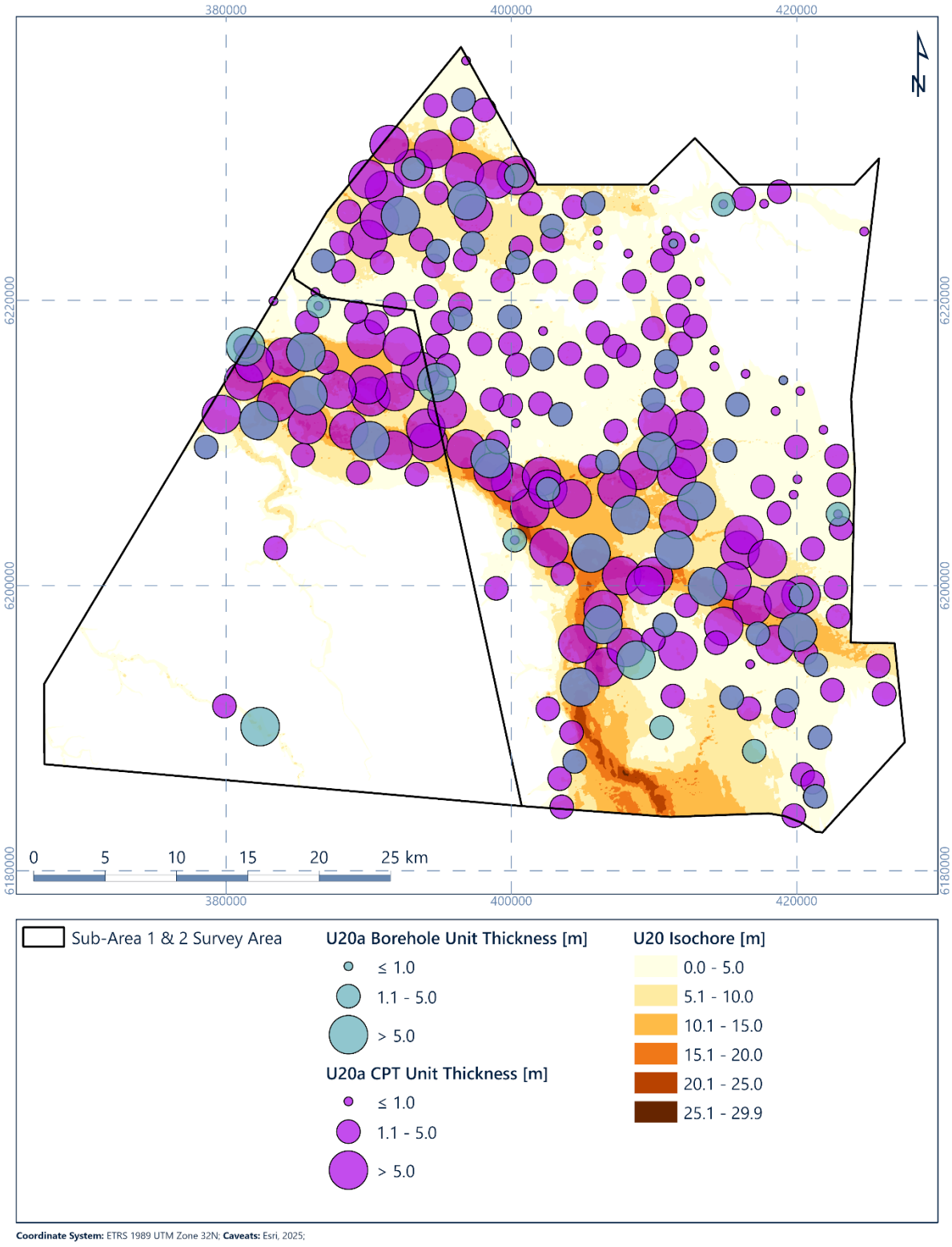

Figure 6.13: Isochore for geological unit U20a correlated with geotechnical data recoveries

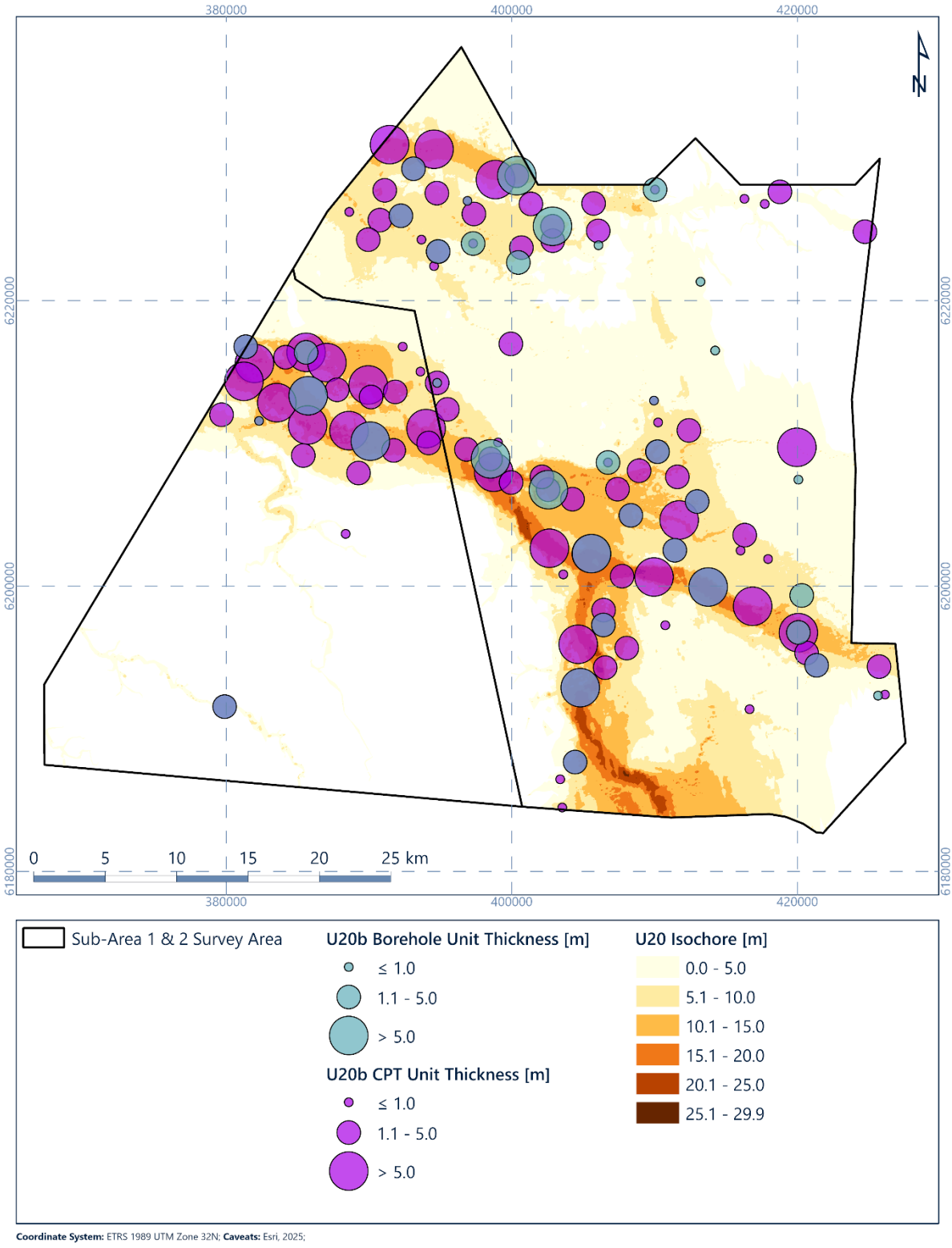

Figure 6.14: Isochore for geological unit U20b correlated with geotechnical data recoveries

The presence of peat or organic-rich clay (Figure 6.10 and Figure 6.11) is represented by a seismic anomaly with a negative polarity in the 2D UHR seismic data, and observed in geotechnical sample data with decreased CPT cone resistances and increased friction ratio. The peat at the base of geological unit U20 is evidence for subaerial deposition following the

deposition of geological units U30 and U35 during the Weichselian glacial period. Geological unit U20 is interpreted to be the Holocene infill of the Weichselian incised channels (Figure 6.12). The normally consolidated clay (geological subunit U20b) is evidence of a low energy marine environment. The combination of clinoforms and the coarsening upward successions of clay to the sand of geological subunit U20a indicate coastline progradation and decreasing water depths.

The orientation of the primary and secondary channels indicates that geological unit U20 is a buried extension of the modern river systems that drain western Jutland (western Denmark) to the North Sea (Figure 3.7; Konradi et al., 2005; Friborg, 1996).

At the base of the unit, high amplitude areas often correspond to organic deposits, as observed in borehole data. Figure 6.15 shows an example of the peat deposits associated with a small tributary system in the north of the study area. Due to the localised nature of the channel and amplitude anomalies, this area is not included in the mapped amplitude anomalies presented in Section 6.15.1.

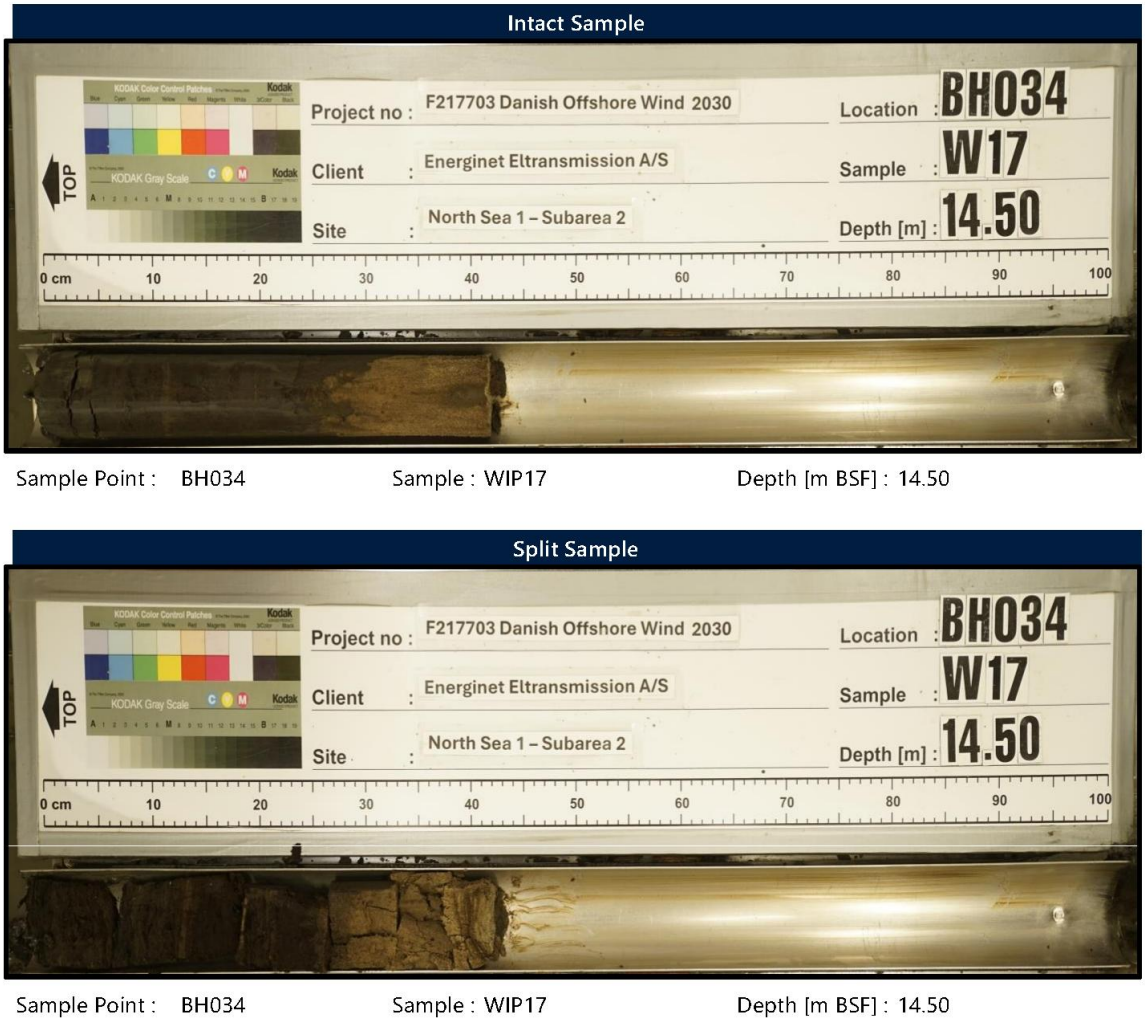

Figure 6.15: Example of peat deposits in geological unit U20 at BH034

Note that observed instances of geological subunit U20b are present in mapped channel thalwegs, including both large channel features, and localised tributary channels observed in the site.

Geological subunit U20a materials are observed to be almost entirely sands in sampling geotechnical datasets, with a variable secondary component of silt sediments. Organic matter is frequently observed in these sediments, highlighting their likely connection to terrestrial sediment source inputs despite the interpretation of gradual sea level transgression during this period.

Geological subunit U20b sediments are observed to be more variable, with an approximate split between sand and clay in sampling data highlighting the variable environment in which these sediments were deposited.

6.5 Geological Unit – Unit U30

6.5.1 Seismic Character

Geological unit U30 is present in small areas, mainly in the north-west and south-west of the Sub-Area 1 site and very locally in Sub-Area 2, reaching a maximum thickness of 12 m (Figure 6.16, Figure 6.17 and Figure 6.18).

This unit has a sheet-like geometry with a horizontal to undulating base marked by horizon H30, a low to medium amplitude positive polarity reflector. Internally, the unit is acoustically complex, or acoustically transparent to locally stratified with medium amplitude parallel reflectors (Figure 6.19).

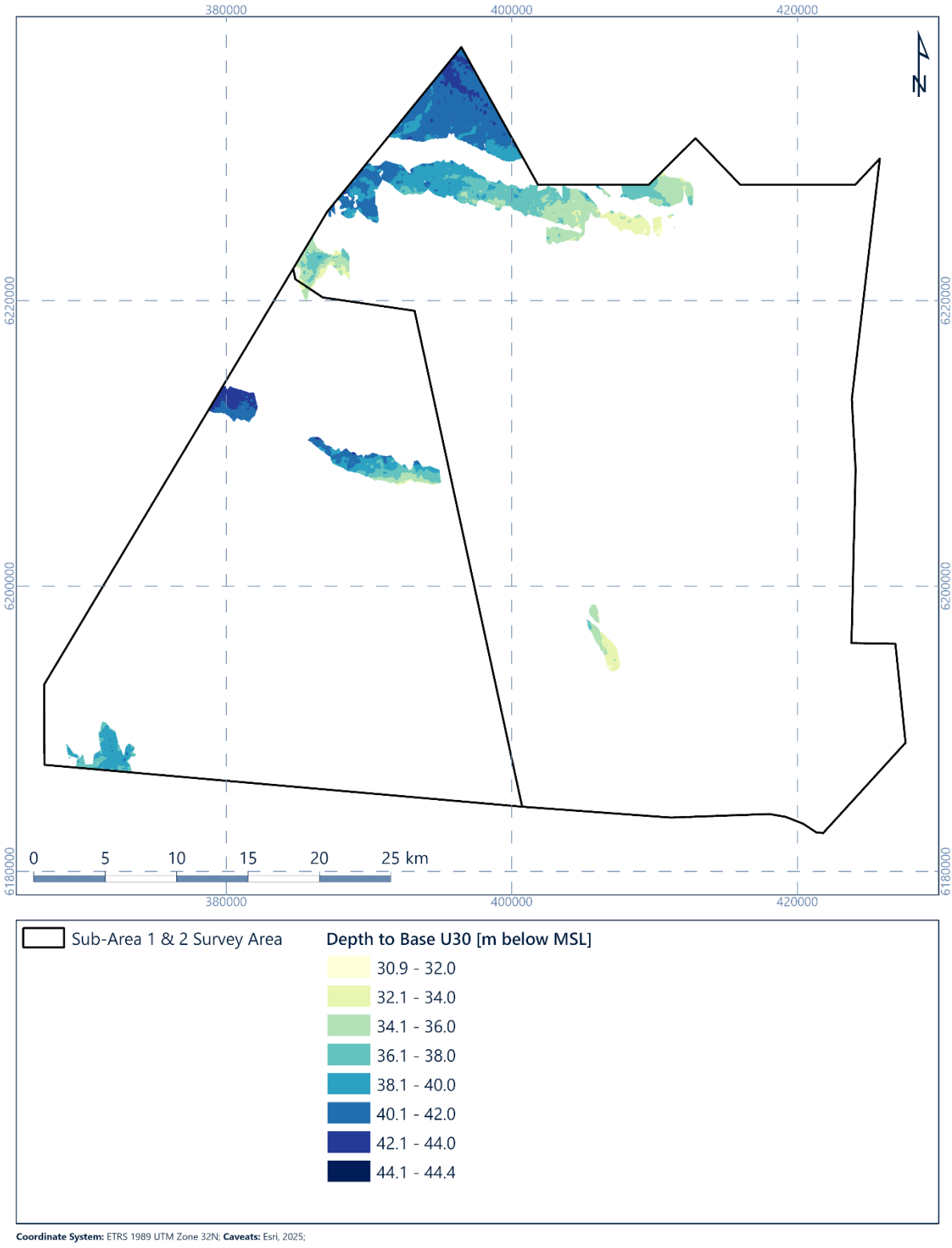

Figure 6.16: Depth [m below MSL] to horizon H30 (base of geological unit U30)

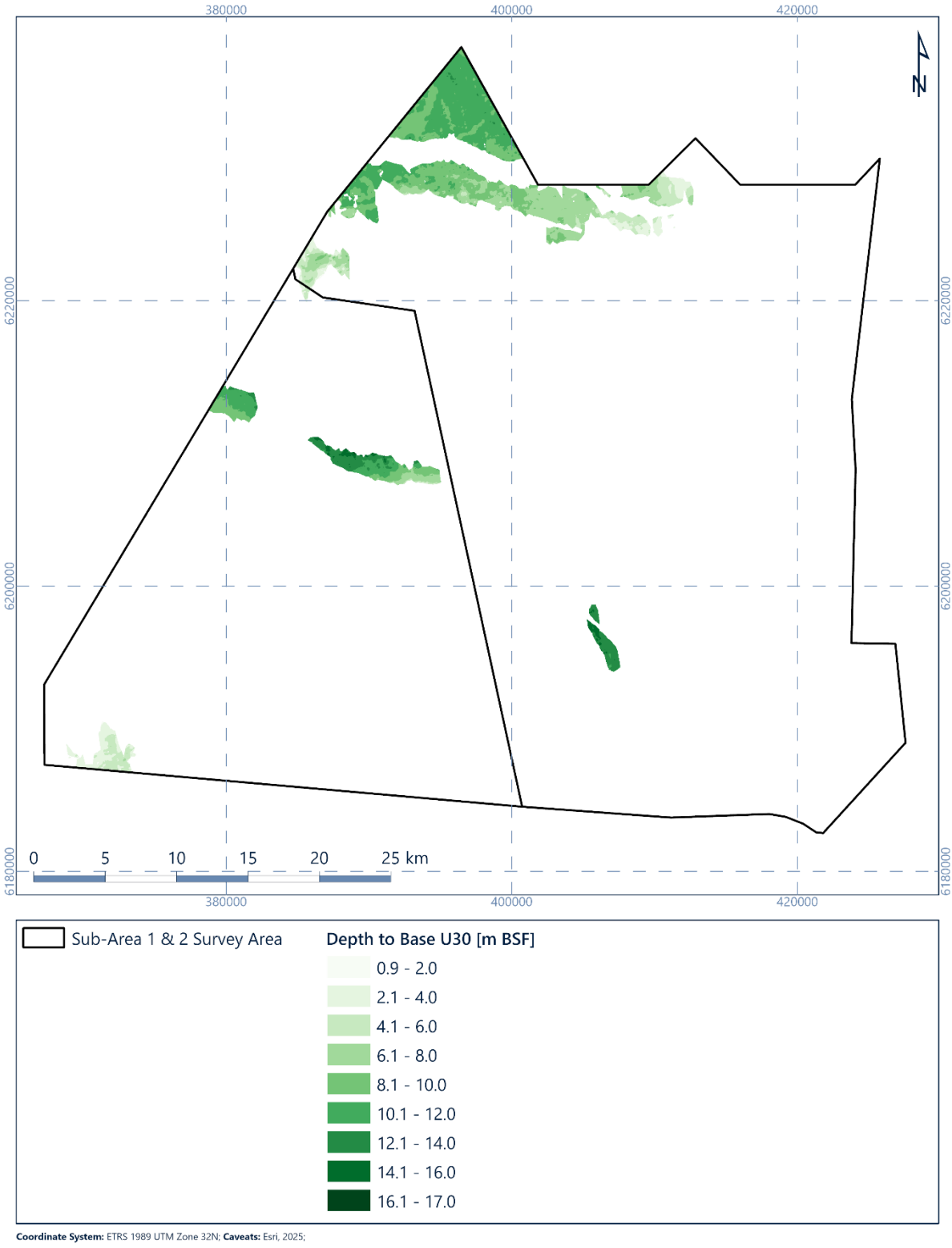

Figure 6.17: Depth [m BSF] to horizon H30 (base of geological unit U30)

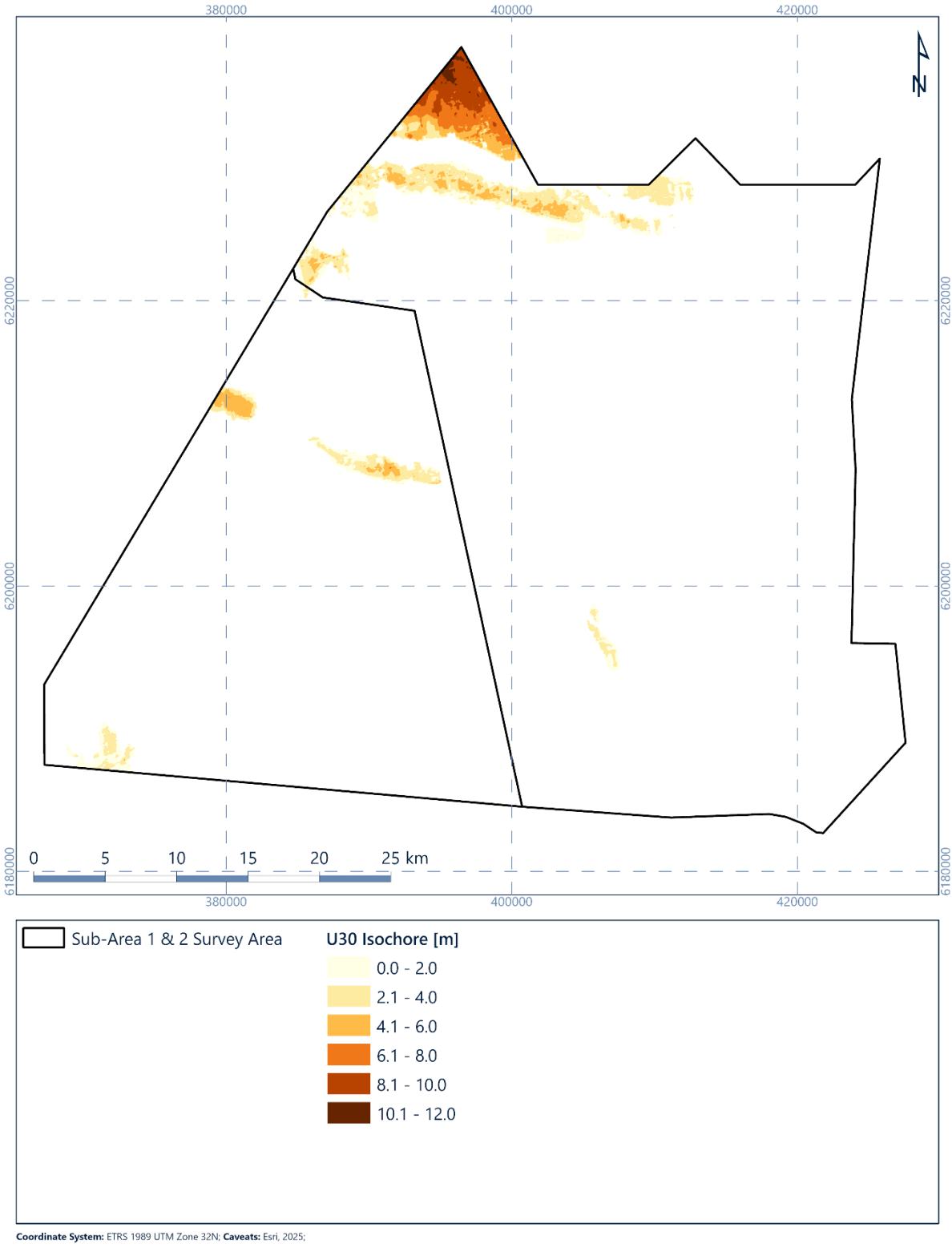

Figure 6.18: Isochore of geological unit U30 [m]

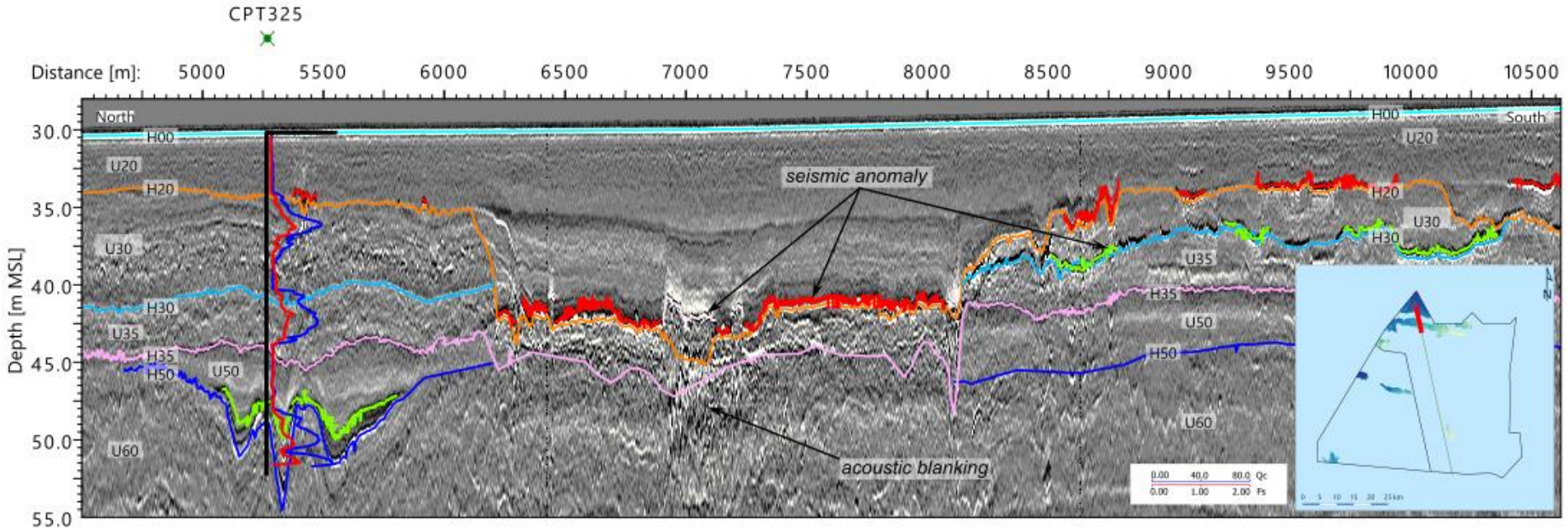

Figure 6.19: 2D UHR seismic data example of Unit U30. Line EAAN253, CPT325

6.5.2 Integration and Interpretation

Geological unit U30 is interpreted to have been deposited in a meltwater (glacio-fluvial) environment based on the acoustically complex seismic character and the silty and clayey sand-dominated soil type. The sand sediments may represent a series of abandoned channels associated with glacio-fluvial output and a continuation of the northernmost channel area, as observed in the underlying geological unit U35 sediments. Sands within the geological unit are observed to be of variable sorting and generally fine. Figure 6.20 displays the correlation between the geological unit U30 geophysical and geotechnical locations. Correlation between datasets is generally suitable. One location is outside mapped horizons, but the thickness is less than 2 m and reflects the challenge of differentiating between geological unit U30 and the underlying geological unit U35 in some areas.

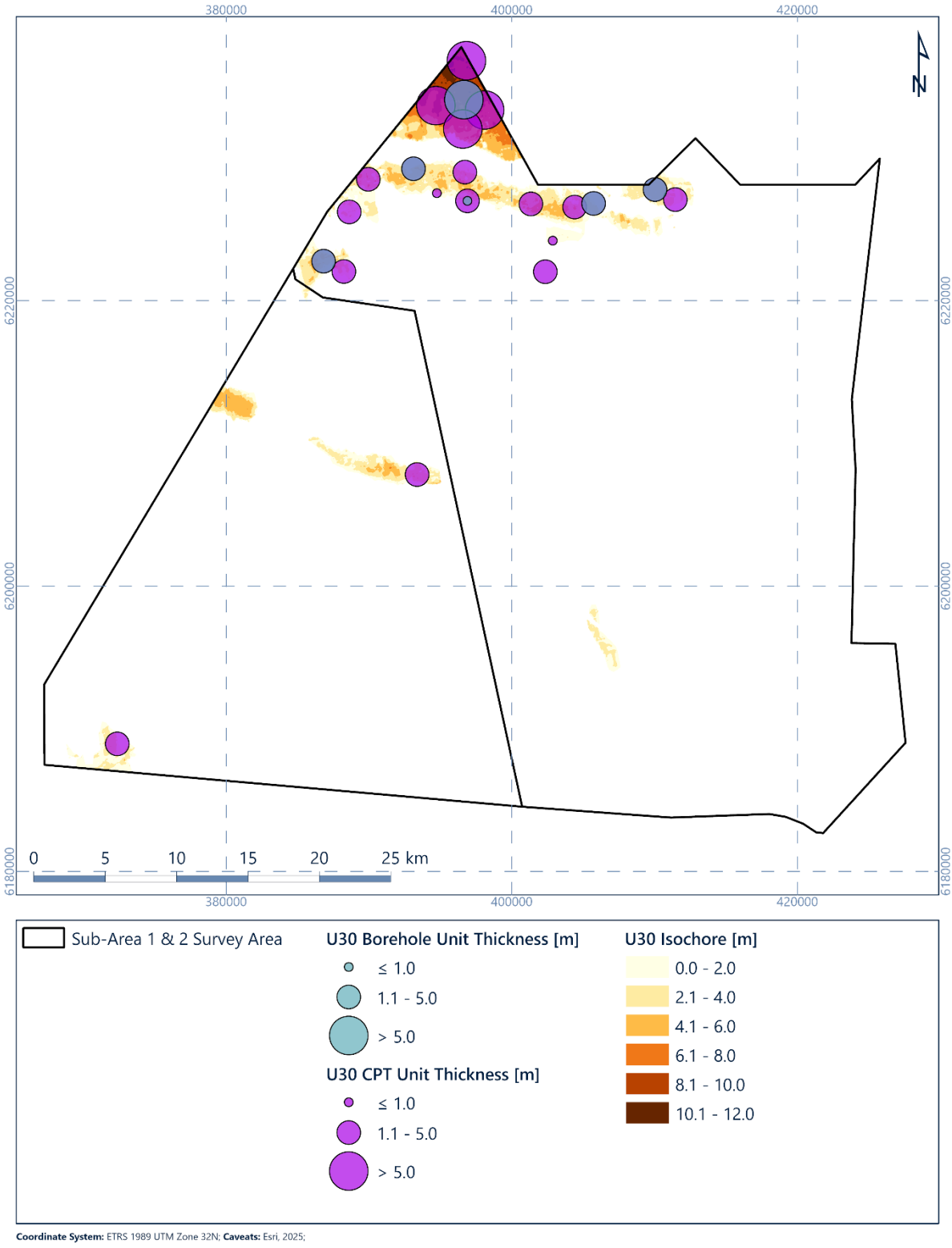

Figure 6.20: Isochore for geological unit U30 correlated with geotechnical data recoveries

The clay bed at the base of geological unit U30, which accumulates over kilometres to tens of kilometres, is interpreted to be a freshwater (pro-glacial lacustrine) clay. The presence of peats and organic rich clays, interpreted to be deposited in a lacustrine environment, supports this interpretation (Section 6.15.1). Clays and possibly peats are observed on both

sides of the mapped geological unit U30 sediments. The stratigraphic position of this geological unit between deposits interpreted as Weichselian (geological unit U35) and late Weichselian to Holocene (geological unit U20) indicates a glacial (Late Weichselian) age. The presence of peat deposits may allow future dating of the geological unit.

6.6 Geological Unit – Unit U35

6.6.1 Seismic Character

Geological unit U35 is present in the north, east, and south-west of the site, and has a sheet-like to channelised geometry (Figure 6.21 and Figure 6.22). Its average thickness is approximately 5 m, and it locally reaches a maximum thickness of approximately 24 m (Figure 6.23).

In the north and east of the site, geological unit U35 usually overlies geological units U50 and U60 (Figure 6.24), and in Sub-Area 2 overlying geological unit U65. The basal horizon H35 is flat to undulating and locally forms a channelised base. Where geological unit U35 is channelised, it is generally associated with geological unit U20 (Figure 6.10). However, some of the channels visible in horizon H35 are orientated in different directions to the geological unit U20 channel areas, suggesting changes in channel orientation over the depositional period associated with geological unit U35.

Internally, this unit is characterised by chaotic seismic facies to locally horizontal and inclined stratification and internal erosion surfaces (Figure 6.24). In the lower part of geological unit U35, high amplitude positive reflectors are locally present and may represent gravel beds (Section 6.15.4).

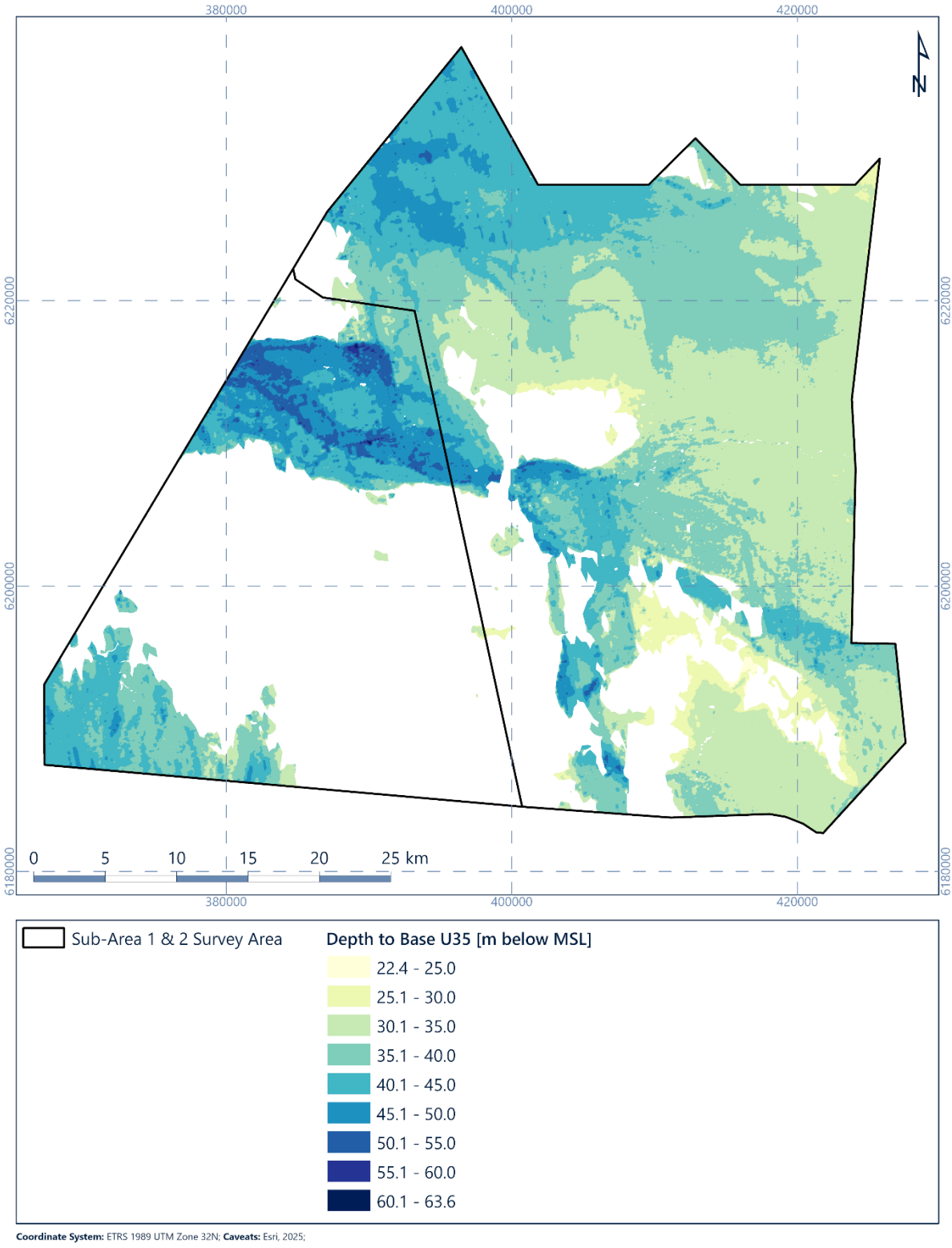

Figure 6.21: Depth [m below MSL] to horizon H35 (base of geological unit U35)

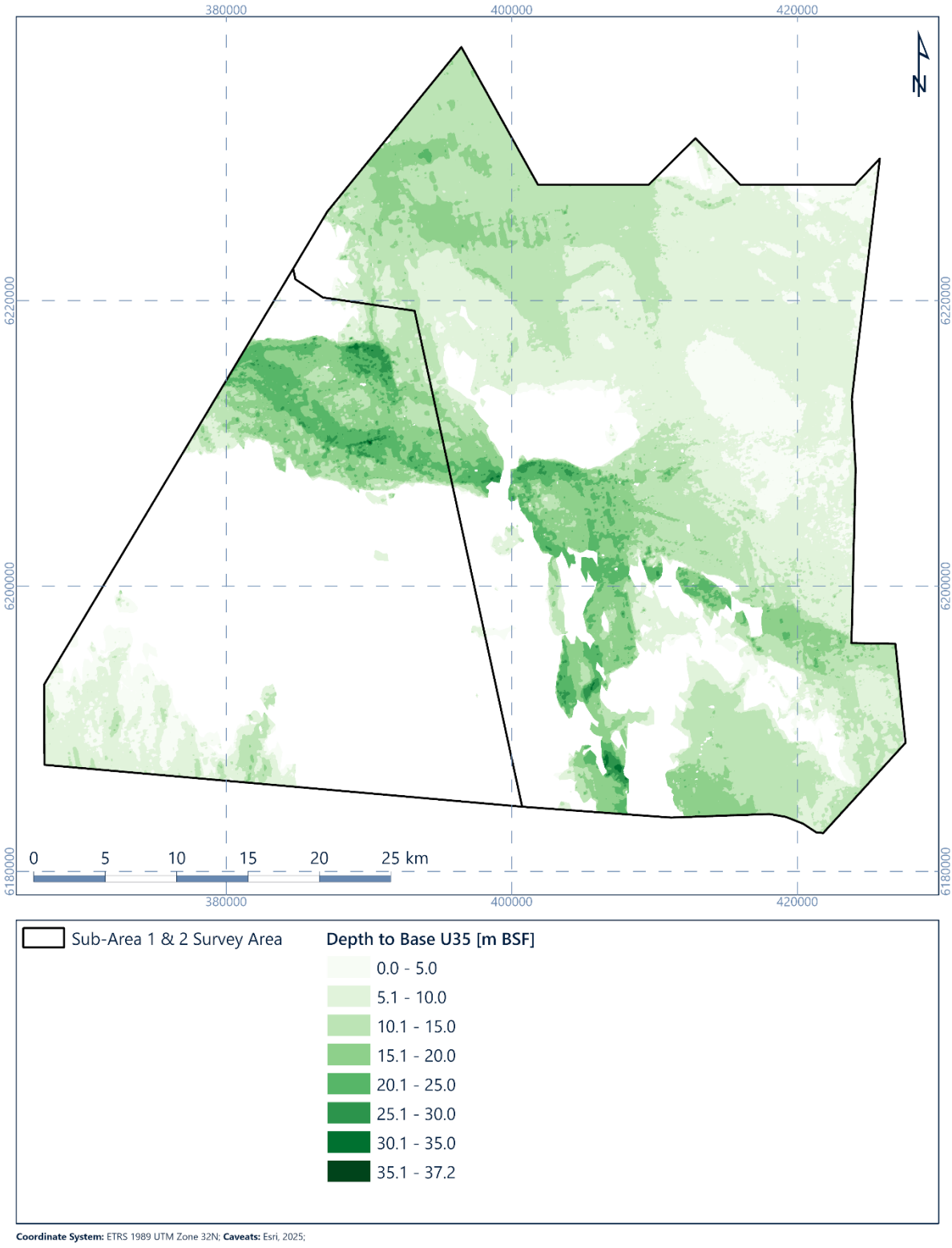

Figure 6.22: Depth [m BSF] to horizon H35 (base of geological unit U35)

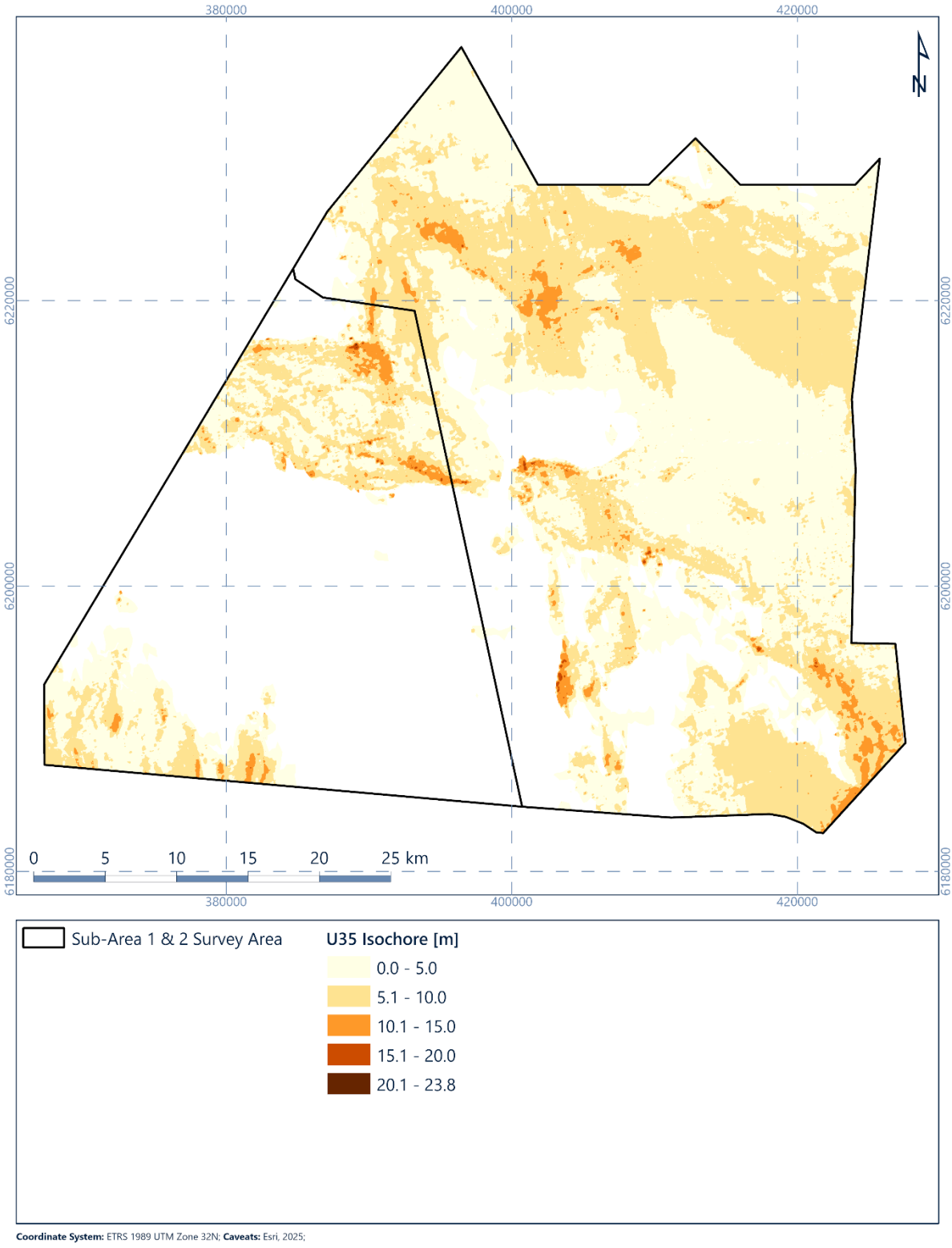

Figure 6.23: Isochore of geological unit U35 [m]

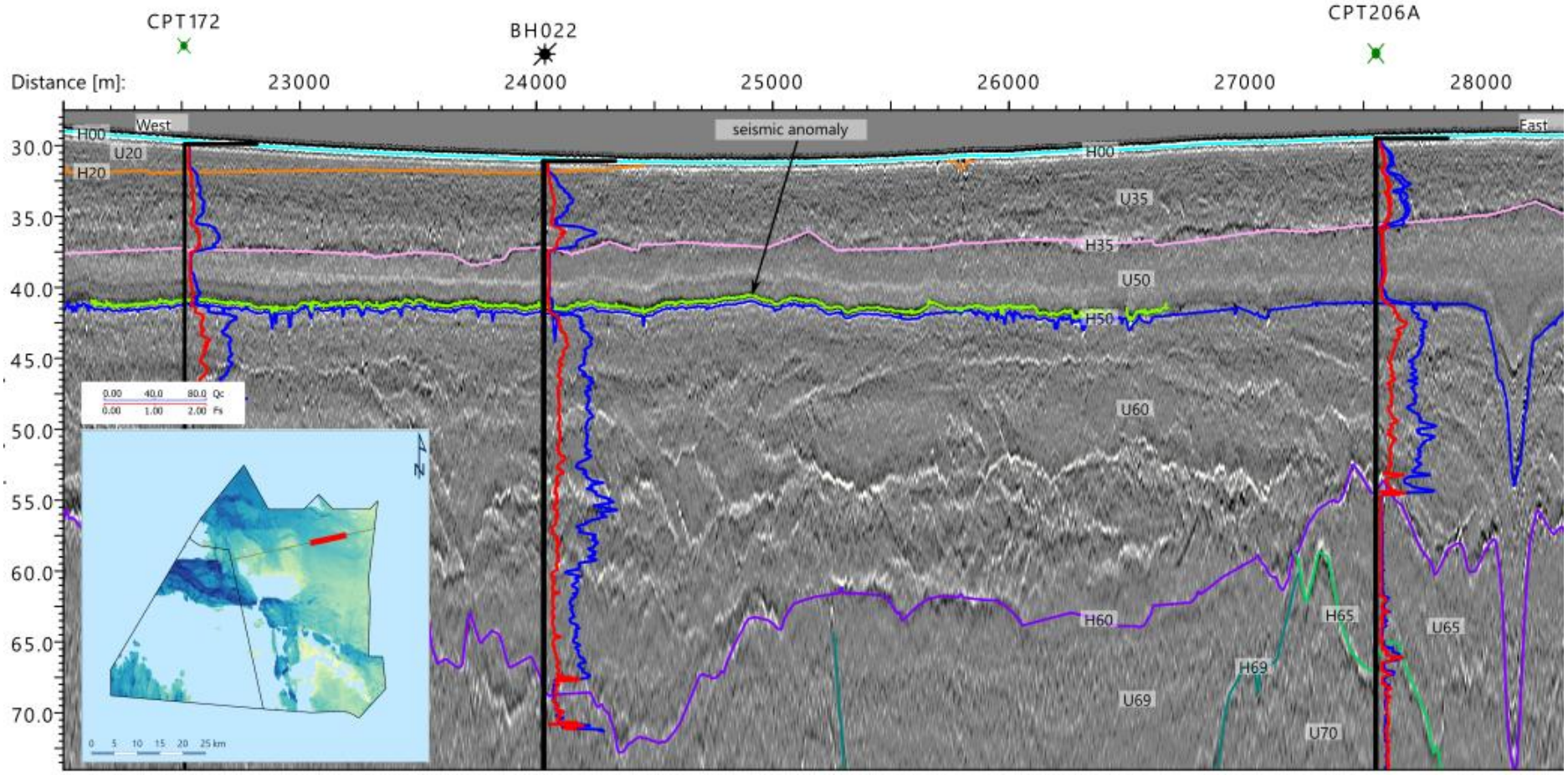

Figure 6.24: 2D UHR seismic data example of Unit U35

6.6.2 Integration and Interpretation

This Weichselian period is defined by the deposition of sediment that has not been subsequently ice loaded and overconsolidated at the NS1 site. The Weichselian ice sheet is interpreted to have been present to the north and to the east of NS1 during the Weichselian glacial period. As a result, the deposited sediments are interpreted to have formed within a glacio-fluvial setting (e.g. braided river systems). Possible fluvial and outwash sediments have been identified (U35) with a coarse base present in geotechnical datasets. In addition, geological unit U30 sediments were predicted to have been deposited during a similar time period and may represent slightly lower energy environments on the periphery of the main geological unit U35 sediment body. Figure 6.25 presents a schematic figure example of this interpreted environment.

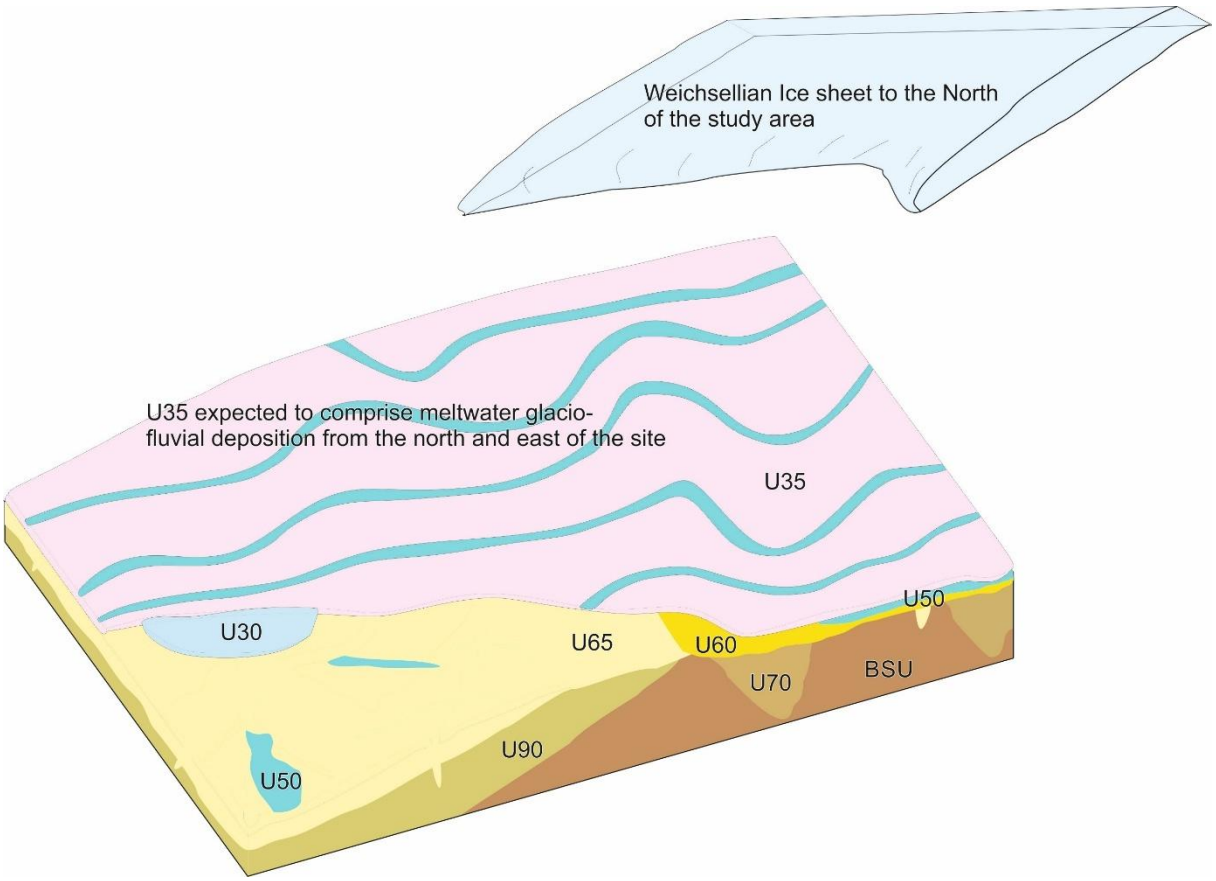

Figure 6.25: Deposition of U35 sediments in a glacio-fluvial environment

Geological unit U35 overlies geological unit U50 in Sub-Area 1, which is of Eemian age (Konradi et al., 2005; Larsen & Andersen, 2005). In Sub-Area 2, geological unit U35 overlies geological unit U65, which is a glacial unit interpreted to be of Saalian age (Fiborg, 1996; Kondradi et al, 2005); indicating a large gap in depositional ages.

Figure 6.26 shows the correlation between the thickness of geological unit U35 in the geophysical data and the geotechnical locations. The thickness of units is consistent with the geophysical data. Channel areas also seen in geological unit U20 represent the greatest

thickness, highlighting the continuity between this and the overlying units despite the changes in channel orientations. Correlation between geotechnical datasets and geophysical horizons is suitable, with high correlation coefficient values. The greatest discrepancy is seen in areas where the unit has an incised base, leading to variations over short distances.

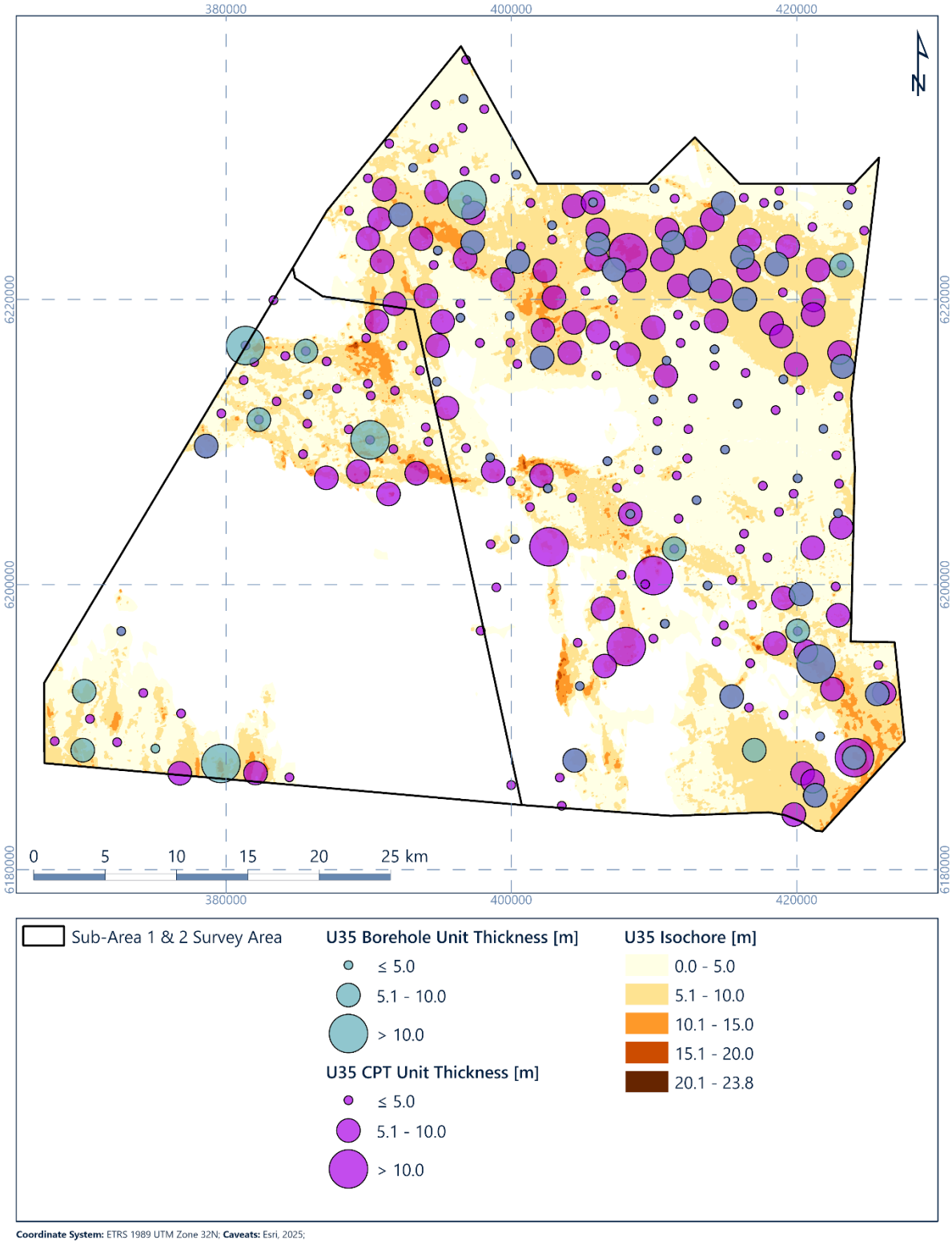

Figure 6.26: Isochore for geological unit U35 correlated with geotechnical data recoveries

6.7 Geological Unit – Unit U36

6.7.1 Seismic Character

Geological unit U36 is present locally in the east of the site (Figure 6.27 Figure 6.28). It has an average thickness of approximately 5 m, locally reaching a maximum thickness of approximately 24 m (Figure 6.29). Geological unit U36 gradually overlies geological unit U50 and is often overlain by geological unit U35. Originally part of U50 in previous interpretation, It was split out as it was primarily sandy and well defined in comparison to the more variable lithology of geological unit U50.

Geological unit U36 is characterised by stratified seismic facies with parallel to subparallel, dipping to subhorizontal, reflectors (Figure 6.30). Reflectors in the north dip towards the south, and those in the south dip towards the north. The stratification becomes more horizontal and its amplitude decreases towards the west of the unit (Figure 6.30).

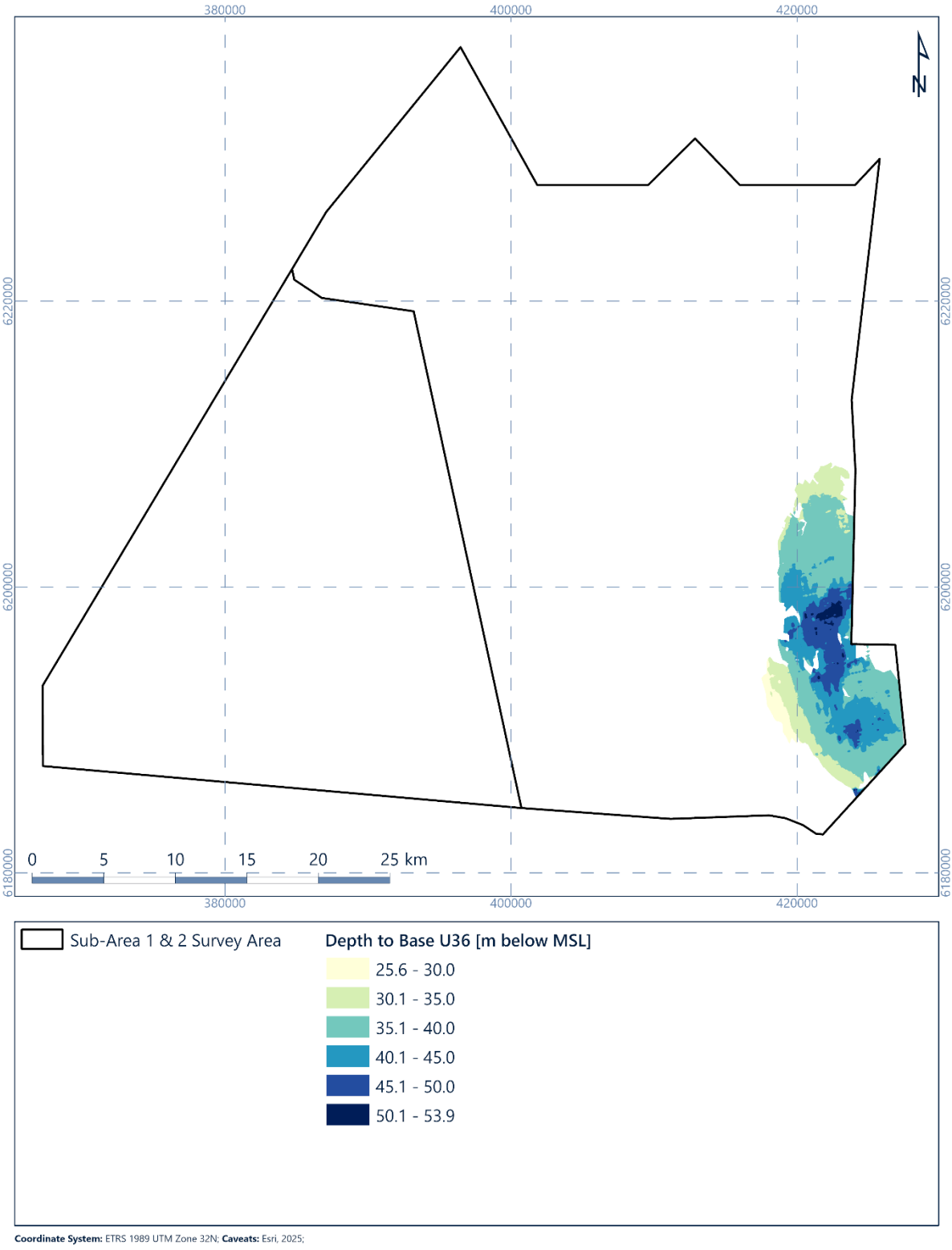

Figure 6.27: Depth [m below MSL] to horizon H36 (base of geological unit U36)

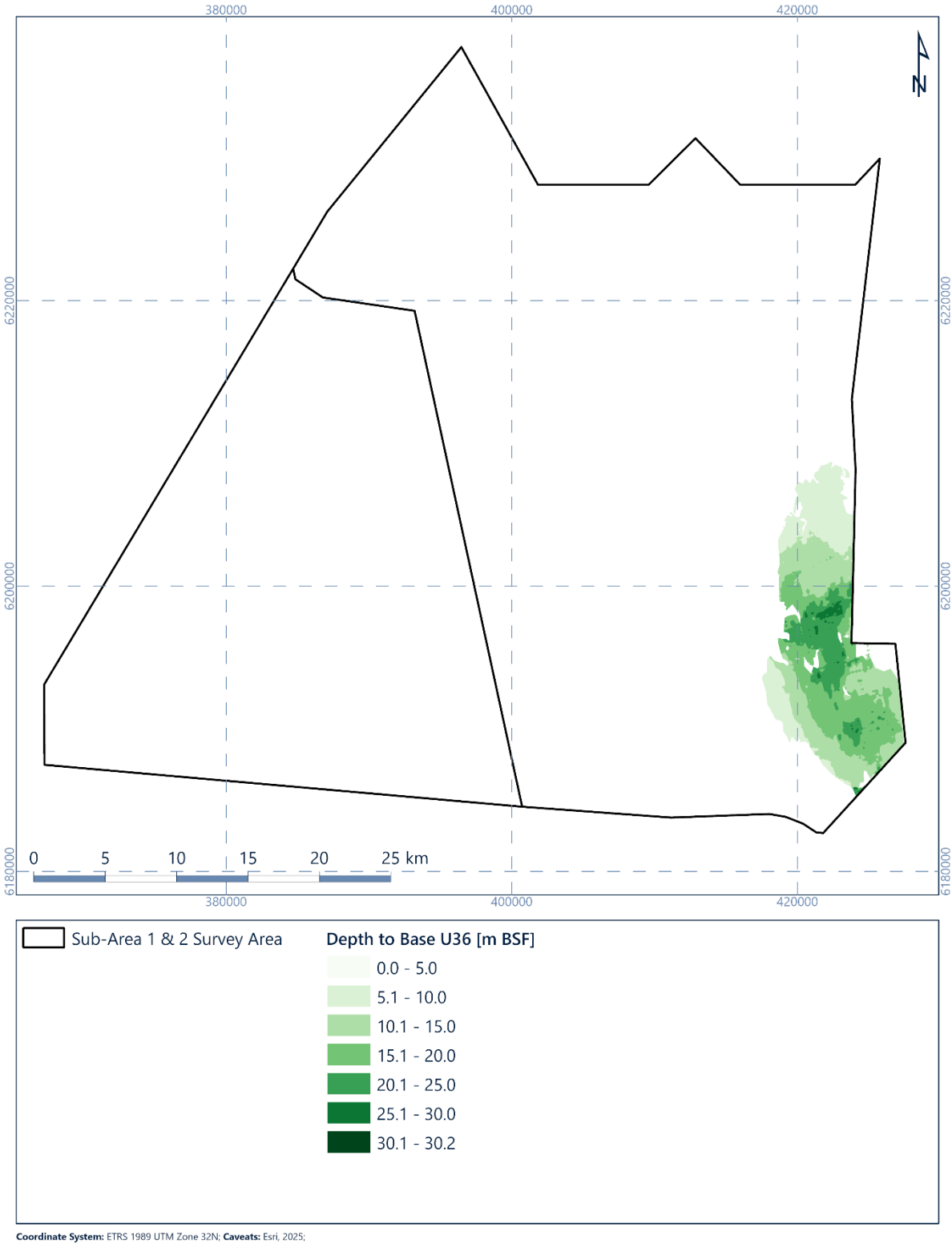

Figure 6.28: Depth [m BSF] to horizon H36 (base of geological unit U36)

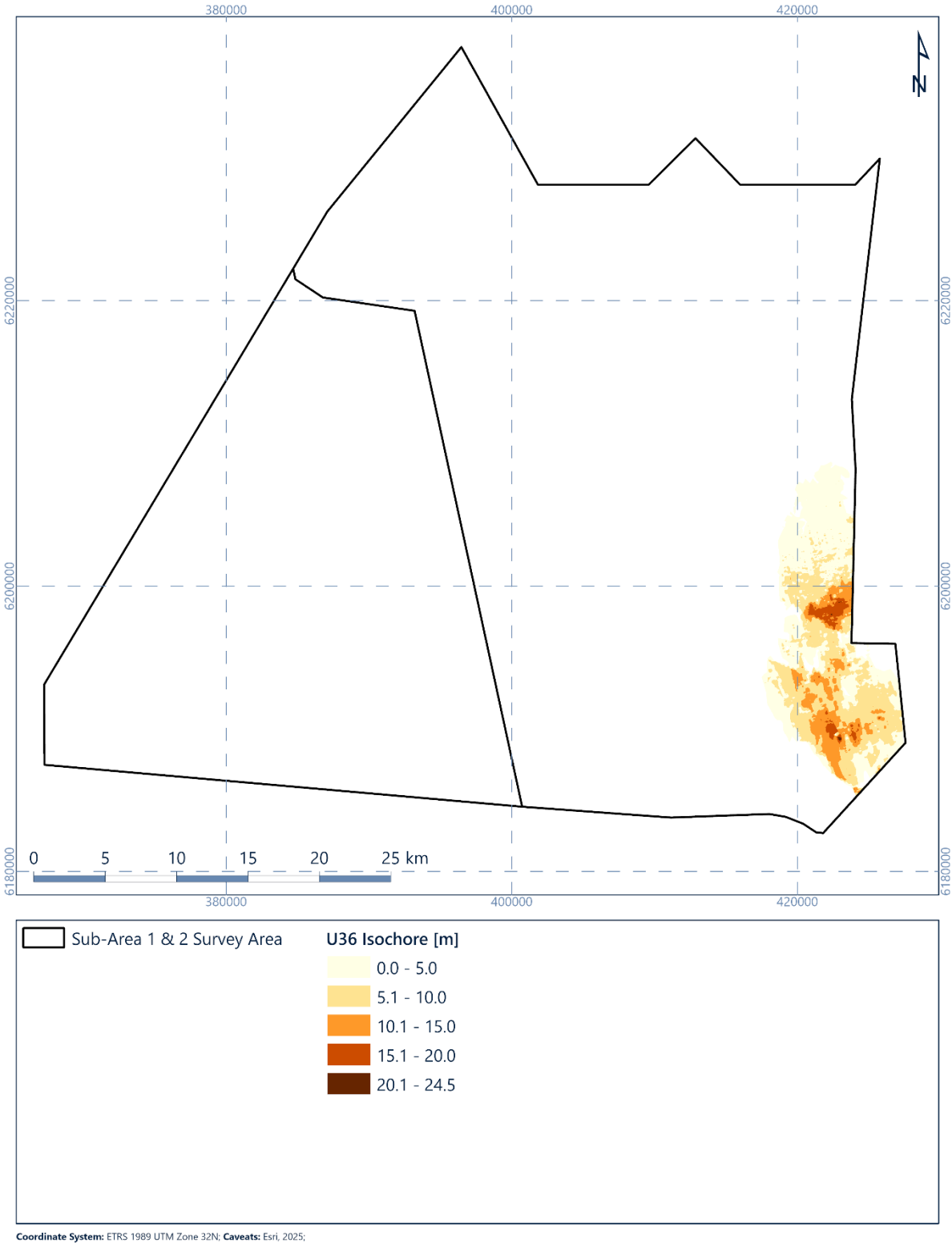

Figure 6.29: Isochore of geological unit U36 [m]

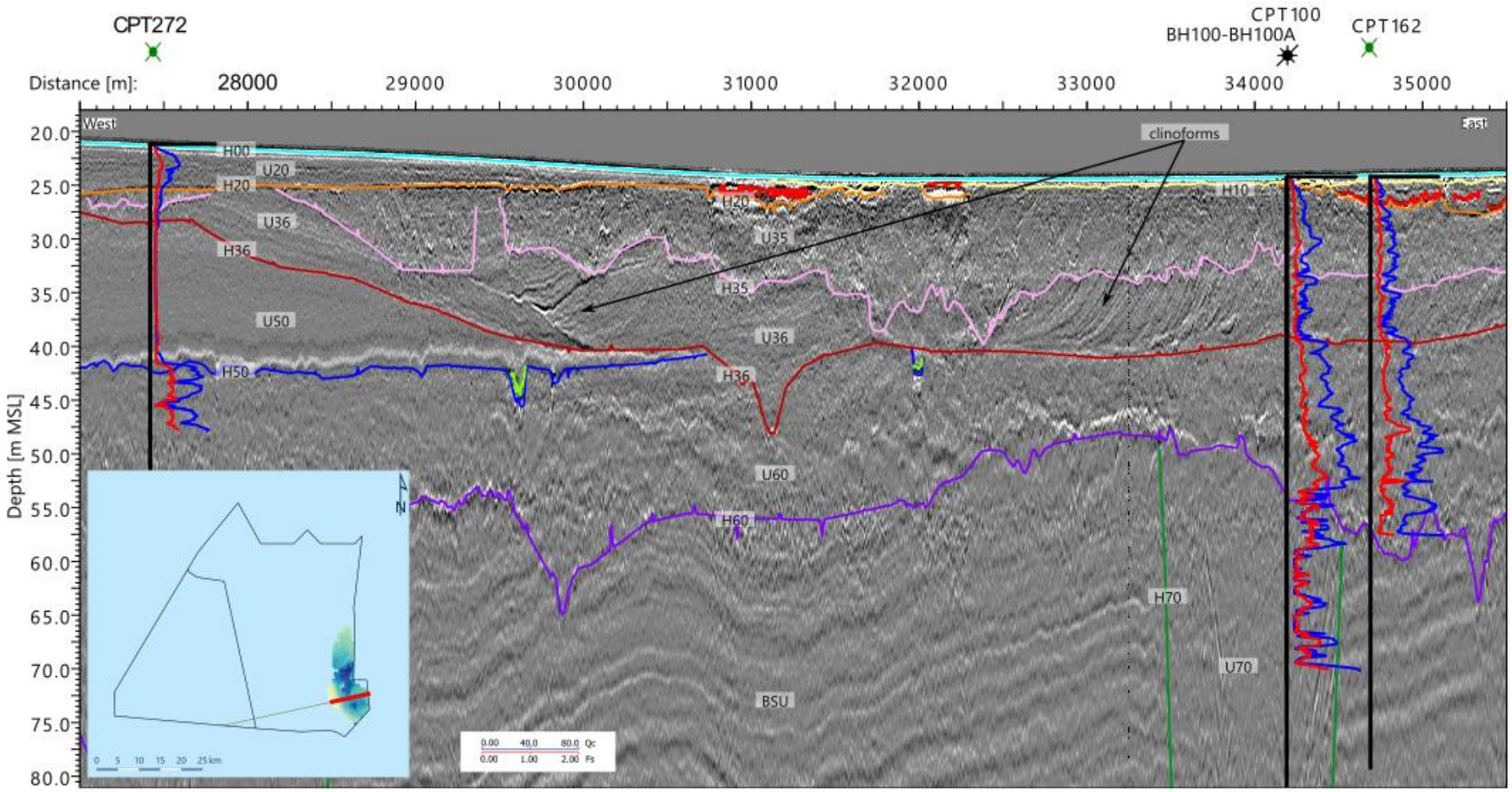

Figure 6.30: 2D UHR seismic data example of Unit U36

6.7.2 Integration and Interpretation

At the end of the Eemian interglacial period, deposition of geological unit U36 is interpreted to overlay the U50 sediments in the east of Sub-Area 1, as sea levels fell, sediments from geological unit U36 were deposited in a deltaic marine environment.

The presence of clinoforms and the coarsening upward succession of geological units U50, U36 and U35 may indicate that geological unit U36 was deposited in a deltaic marine environment. The variable dip direction of the stratification in geological unit U36 can be explained by the presence of multiple delta lobes, which prograded in different directions.

Figure 3.6 shows channels from post-Eemian periods that may be associated with the delta-like deposits of geological unit U36.

Figure 6.31 displays the correlation between the thickness of geological unit U36 in the geophysical and geotechnical locations. Some inconsistencies between the geophysical and geotechnical datasets are seen in the north of the unit, due to the gradation of sediment types from the sands of geological unit U36 to the laterally equivalent clays of geological unit U50, making integration more challenging in this area. Suitable correlation is observed in the center of the unit.

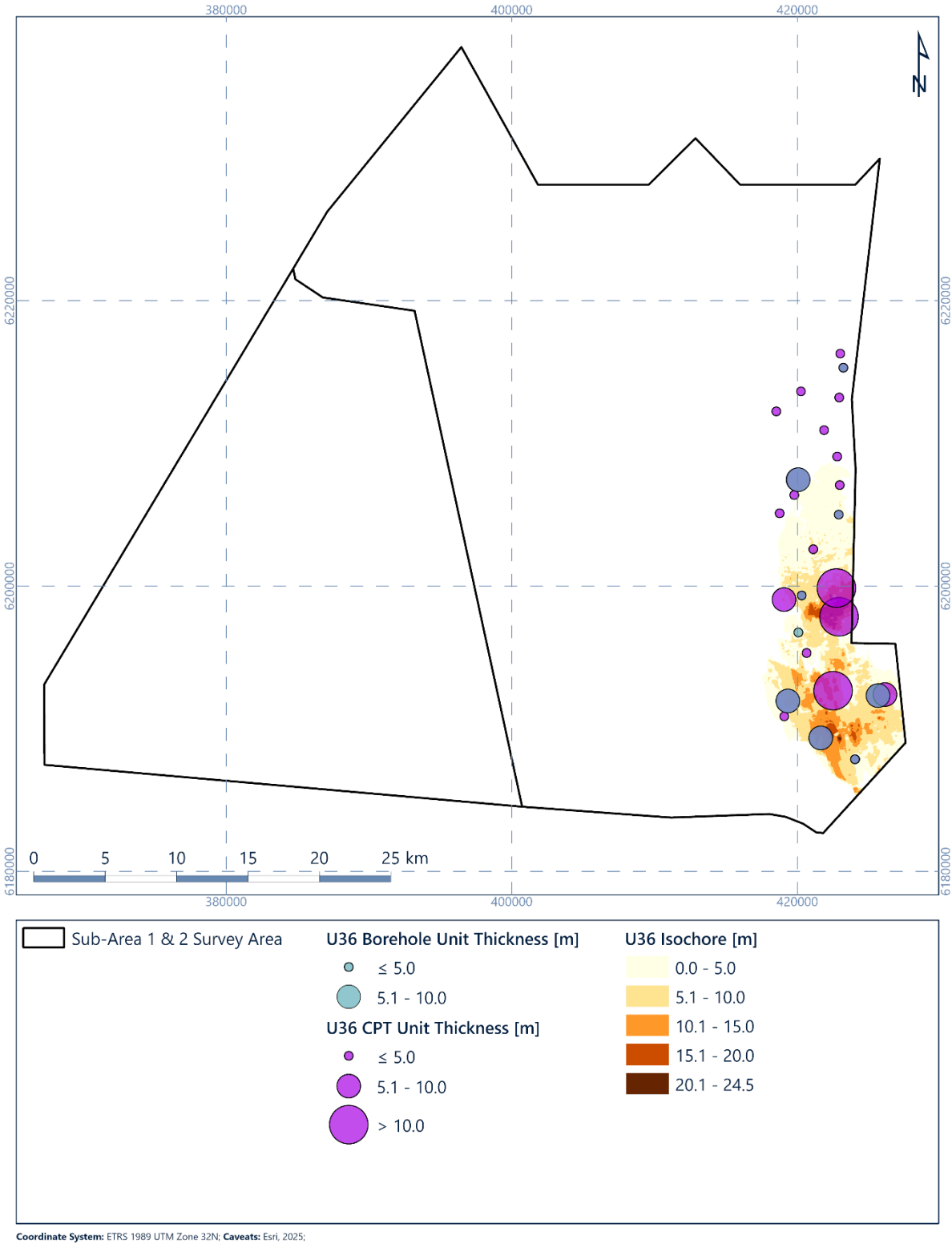

Figure 6.31: Isochore for geological unit U36 correlated with geotechnical data recoveries

6.8 Geological Unit – Unit U50

6.8.1 Seismic Character

Geological unit U50 is mainly present in the eastern half of the site, and has a sheet-like geometry (Figure 6.32, Figure 6.33 and Figure 6.34). It is locally present across the rest of the site and forms channel infills (Figure 6.35). The average thickness of this unit is approximately 8 m, very locally reaching approximately 50 m (Figure 6.34). Where geological unit U50 forms a channel infill, it is often associated with the tunnel valleys of geological unit U65 (Figure 6.35).

Internally, geological unit U50 is acoustically transparent to weakly stratified in the east of the site Where it forms a channel infill, it is well stratified (Figure 6.35). In the east, the basal horizon H50 is often overlain by a flat low amplitude positive reflector (Figure 6.35).

A seismic anomaly with a high amplitude negative polarity is regularly present at the base of geological unit 50 (Section 6.15.1). Acoustic blanking is locally associated with channels at the base of this geological unit (Section 6.15.3).

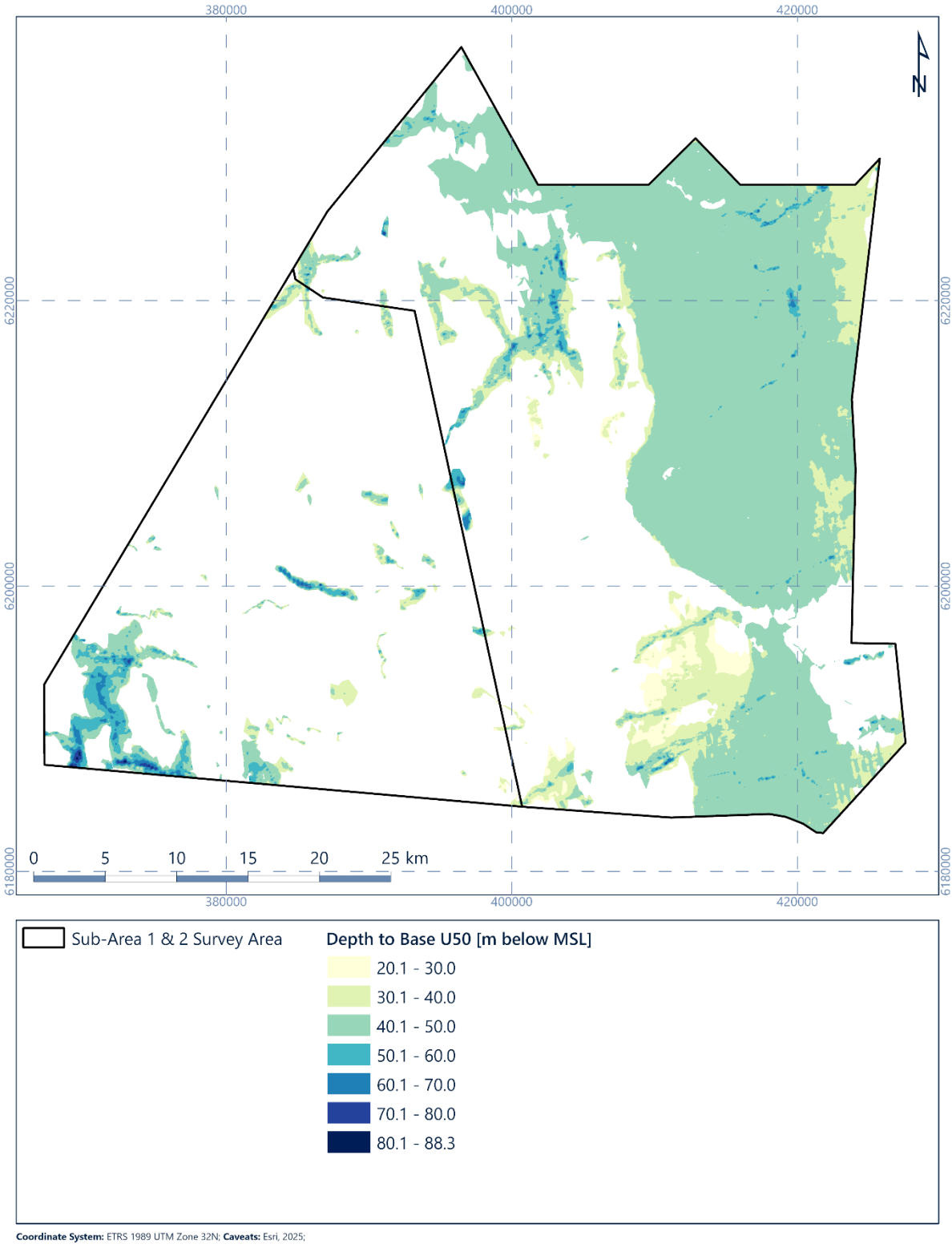

Figure 6.32: Depth [m below MSL] to horizon H50 (base of geological unit U50)

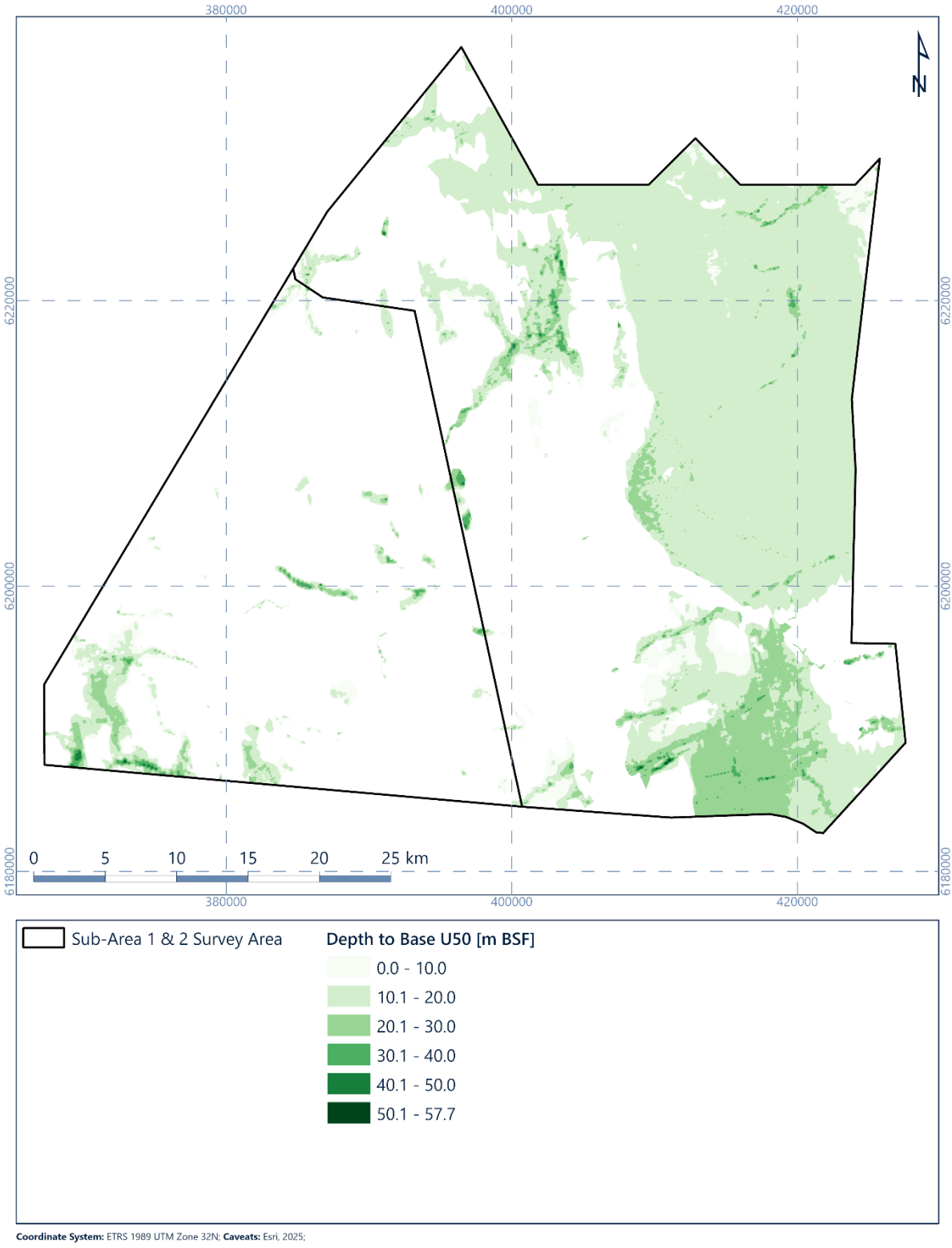

Figure 6.33: Depth [m BSF] to horizon H50 (base of geological unit U50)

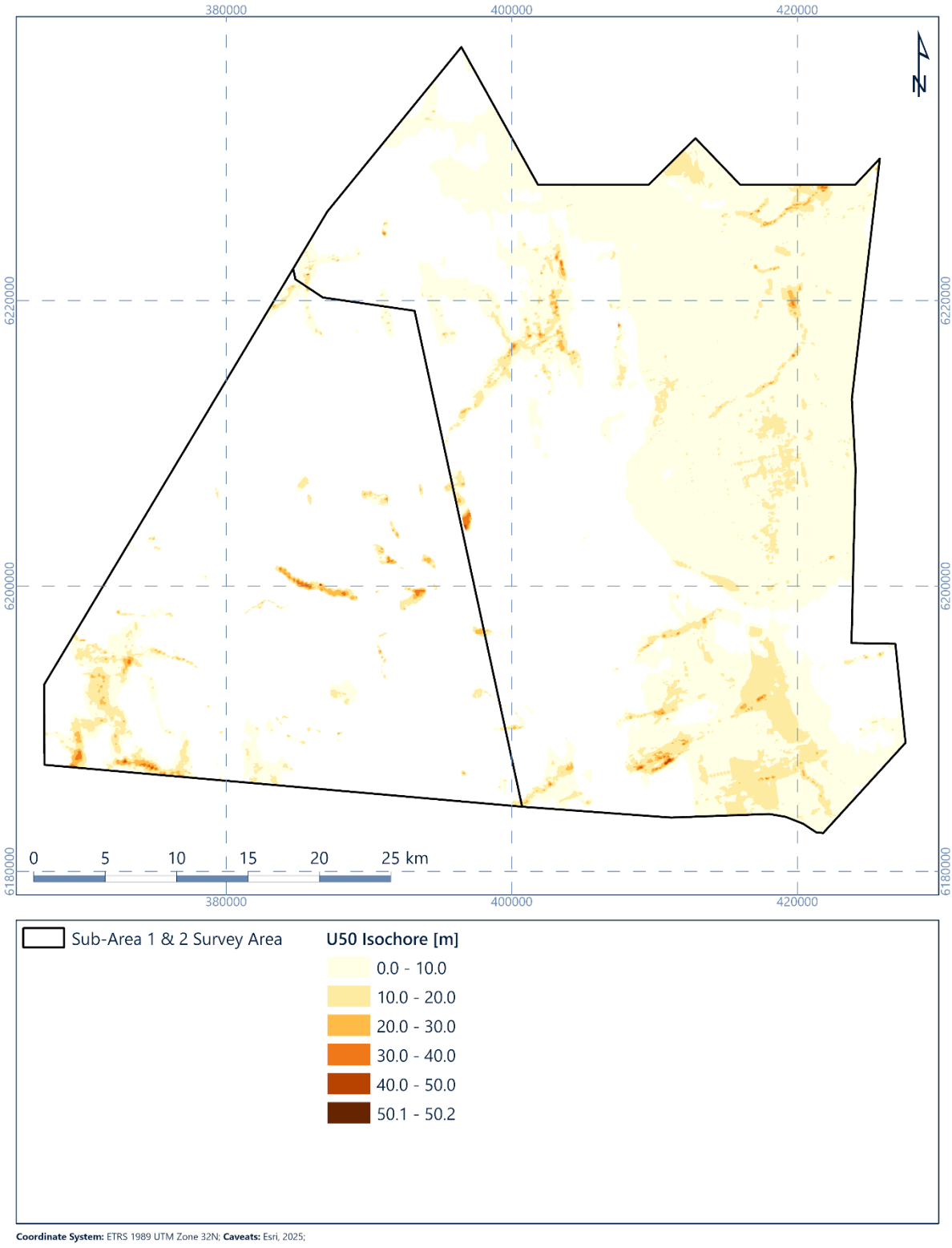

Figure 6.34: Isochore of geological unit U50 [m]

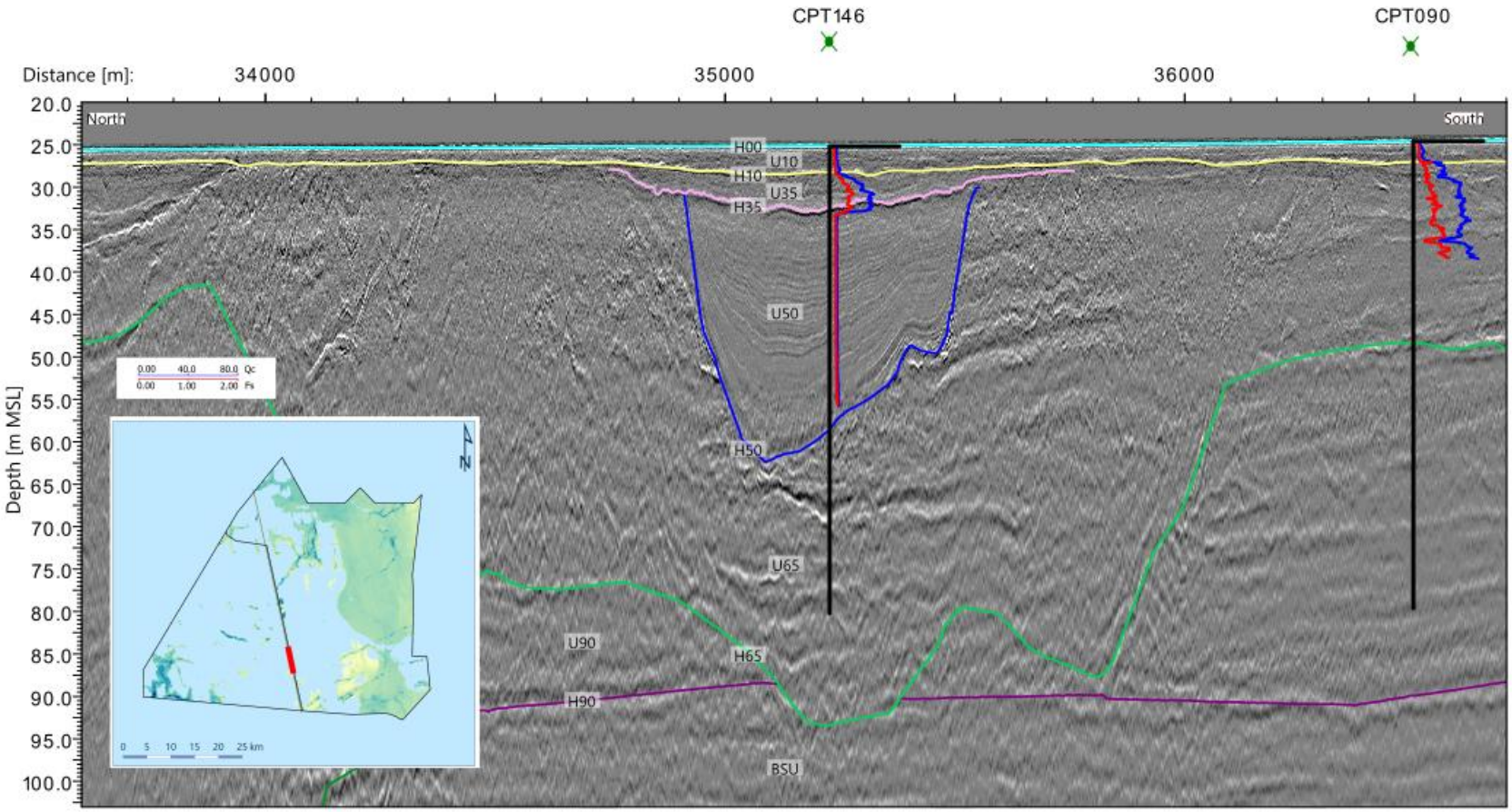

Figure 6.35: 2D UHR seismic data example of Unit U50. Line EAAH228P1, CPT146 and CPT090

6.8.2 Integration and Interpretation

Following the end of the Saalian, the site was exposed to the Eemian interglacial period (Section 3.3.4). During this period, marine deposition is predicted to have occurred in the east of the NS1 site, where the presence of marine clays are observed in geotechnical datasets as geological unit U50. In the west of the site, limited Eemian sediments are predicted to have been deposited in localised depressions within valley incision from the preceding Saalian period, in a similar fashion to the depositional environments seen associated with geological unit U69. Figure 6.36 presents a schematic diagram of this process.

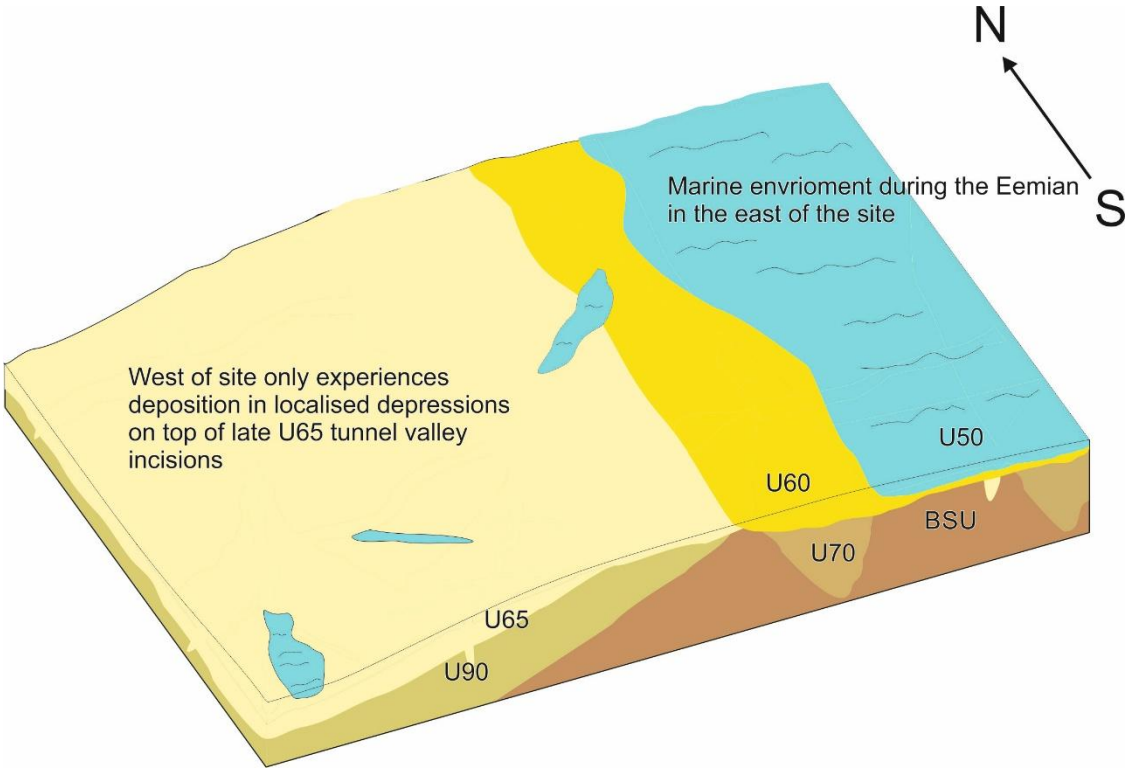

Figure 6.36: Deposition of U50 marine sediments from the Eemian interglacial period in the east of the study area and associated with limited depositions

The mapped extents within the channelised areas in the west of the site are more uncertain, as only limited mapping of the complex geometries between seismic inlines was possible. The infill of depressions observed in areas of geological unit U50 to the west of the site may indicate depositional processes similar to those observed in geological unit U69, with these sediments and the marine deposits observed at the west of the site possibly being deposited at different times. Figure 6.37 shows the correlation in the thickness of geological unit U50 between the geophysical data and geotechnical locations. Suitable correlation between datasets is observed across the site.

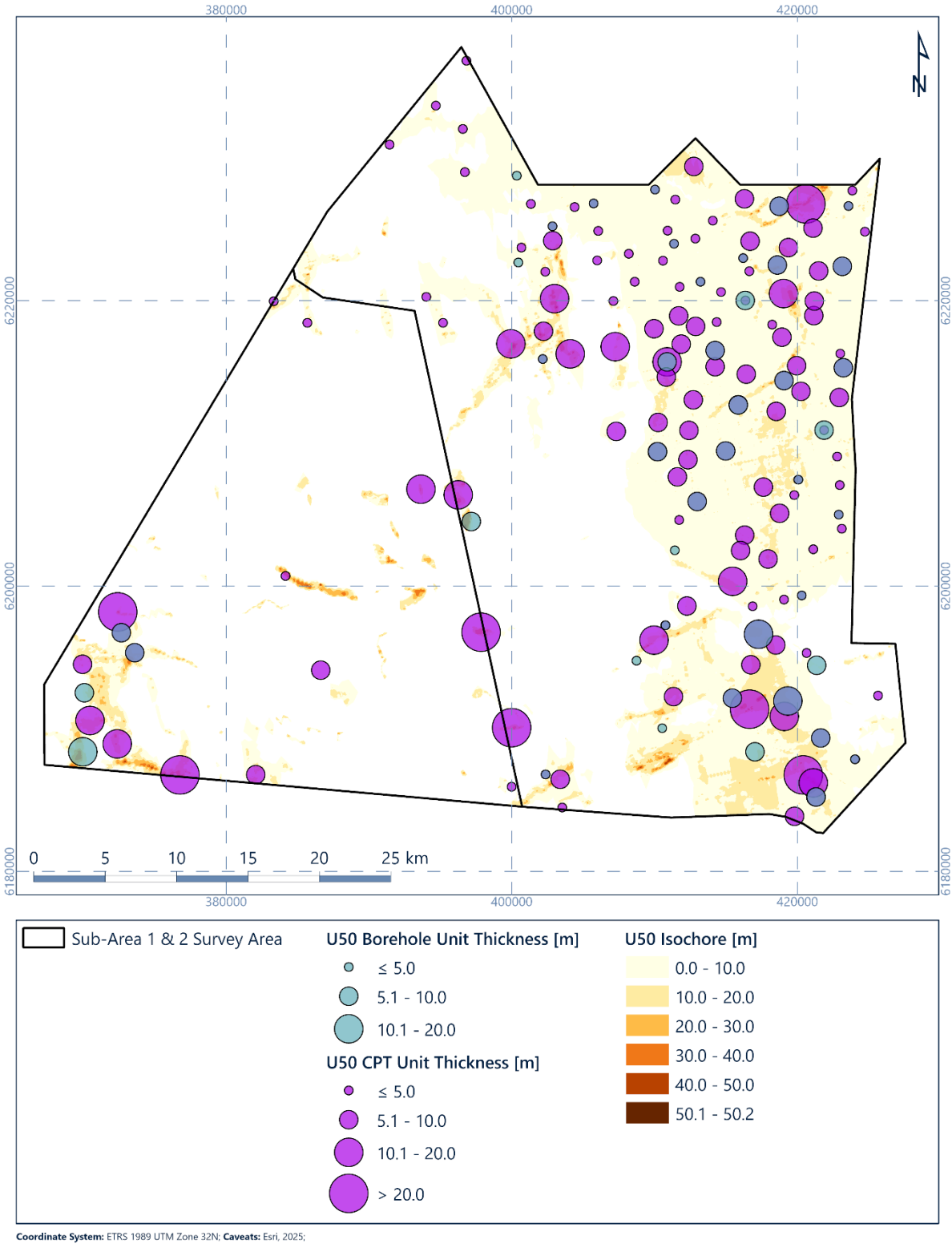

Figure 6.37: Isochore for geological unit U50 correlated with geotechnical data recoveries

6.9 Geological Unit – Unit U60

6.9.1 Seismic Character

Geological unit U60 is present in the north and east of the site (Figures Figure 6.38 and Figure 6.39) but absent in the south-west. It forms the sheet-like infill of a wide (approximately 20 km) but shallow (approximately 30 m) valley (Figure 6.40). This valley has steep margins, which have a sinuous-shape in planform (Figure 6.41). Geological unit U60 locally increases in thickness close to the margins of the valley (Figure 6.39). The basal horizon H60 is flat to undulating (Figures Figure 6.38 and Figure 6.39). Where the base of this unit is channelised, it reaches a maximum thickness locally of approximately 80 m (Figure 6.40).

Internally, geological unit U60 has a complex seismic character, including chaotic seismic facies to horizontal and inclined stratification and internal erosion surfaces. High amplitude positive reflectors are locally present and may represent gravel beds (Section 6.15.4).

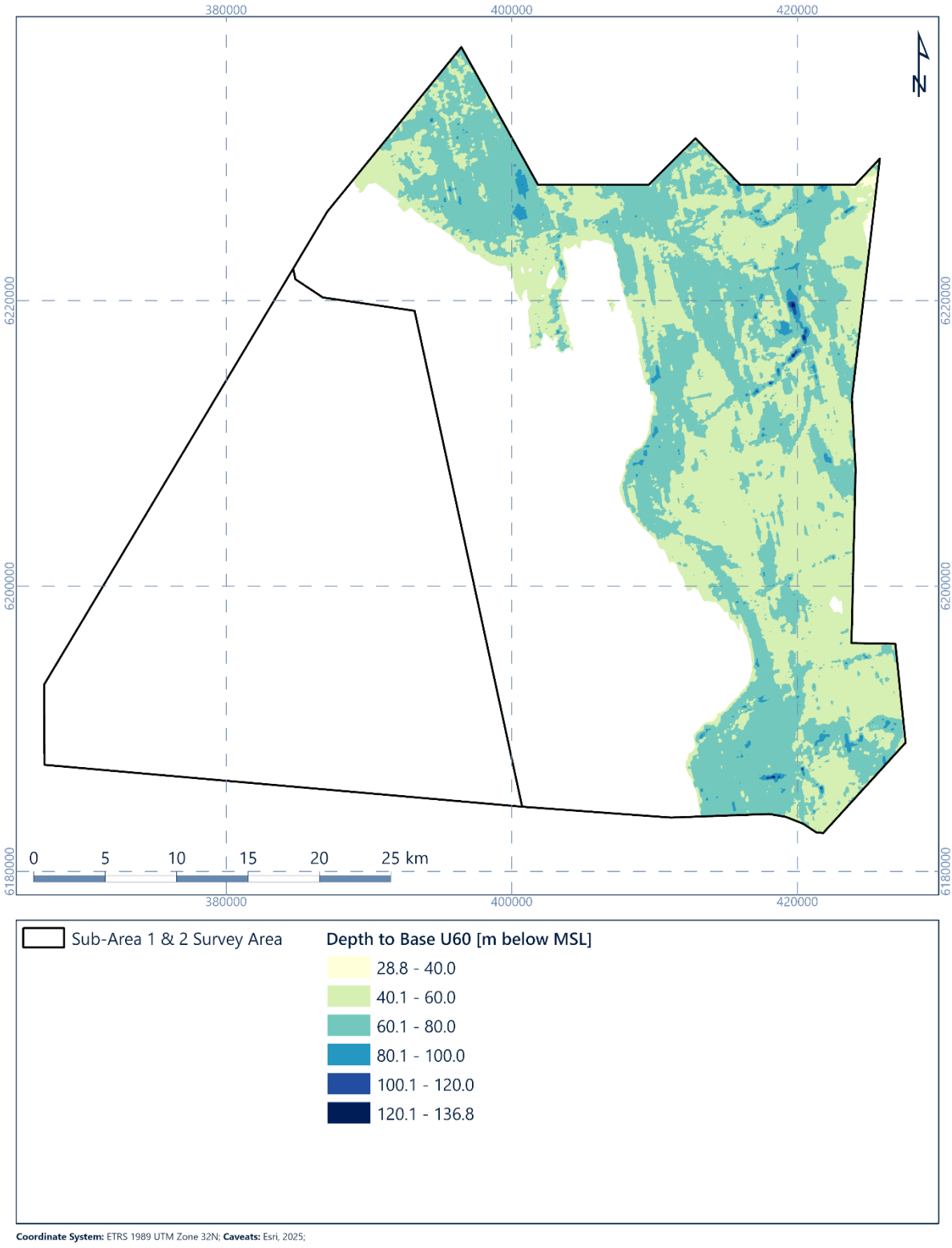

Figure 6.38: Depth [m below MSL] to horizon H60 (base of geological unit U60)

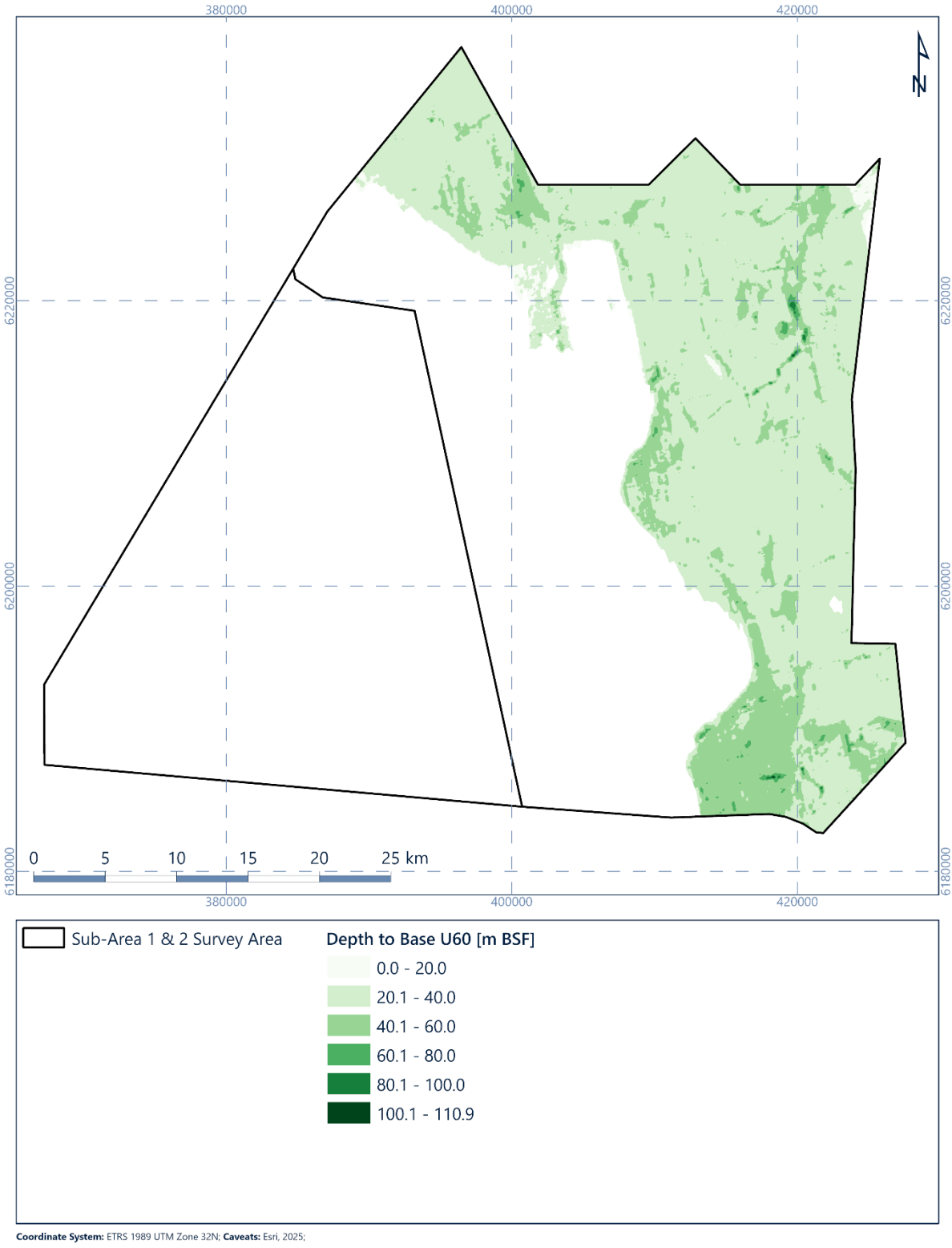

Figure 6.39: Depth [m BSF] to horizon H60 (base of geological unit U60)

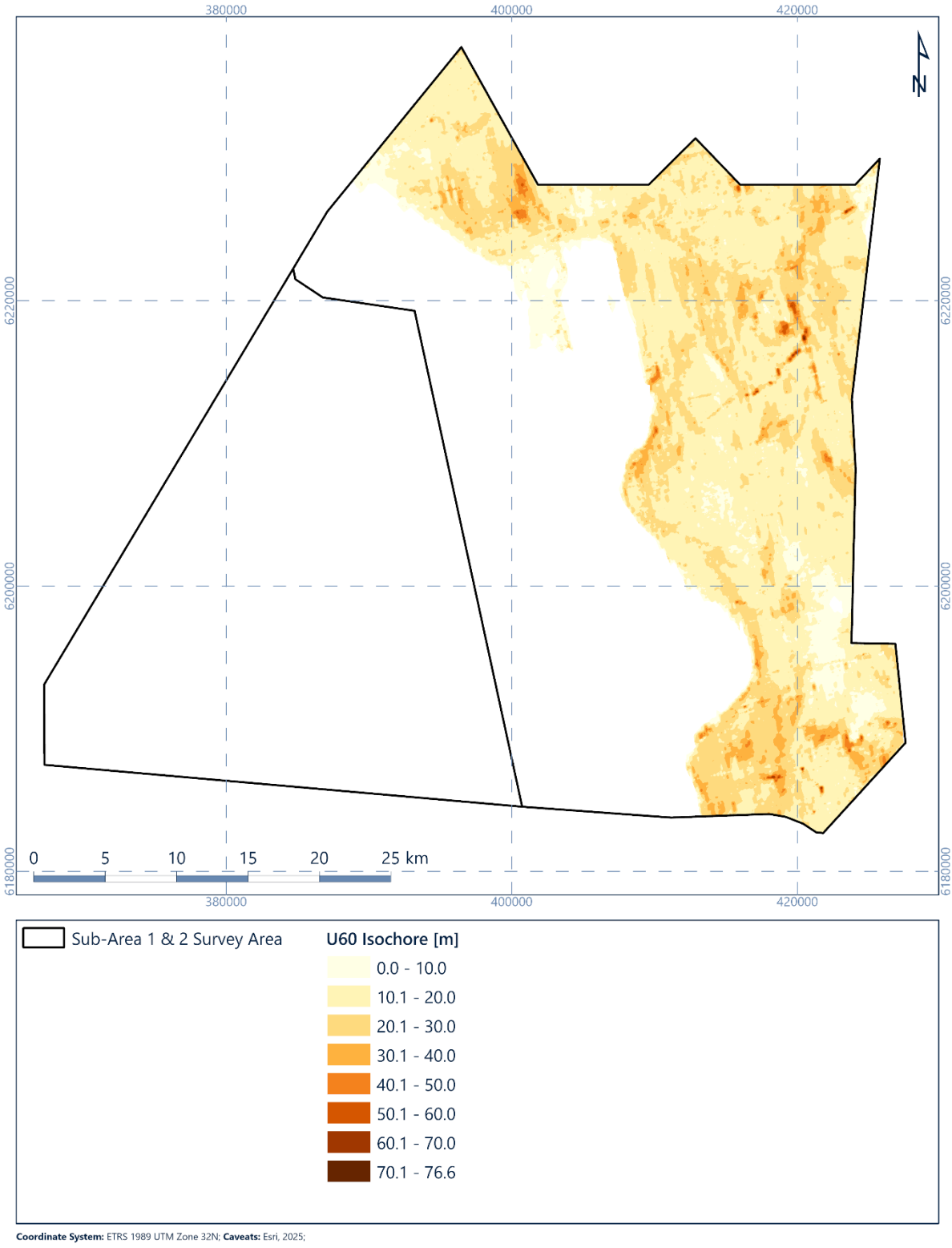

Figure 6.40: Isochore of geological unit U60 [m]

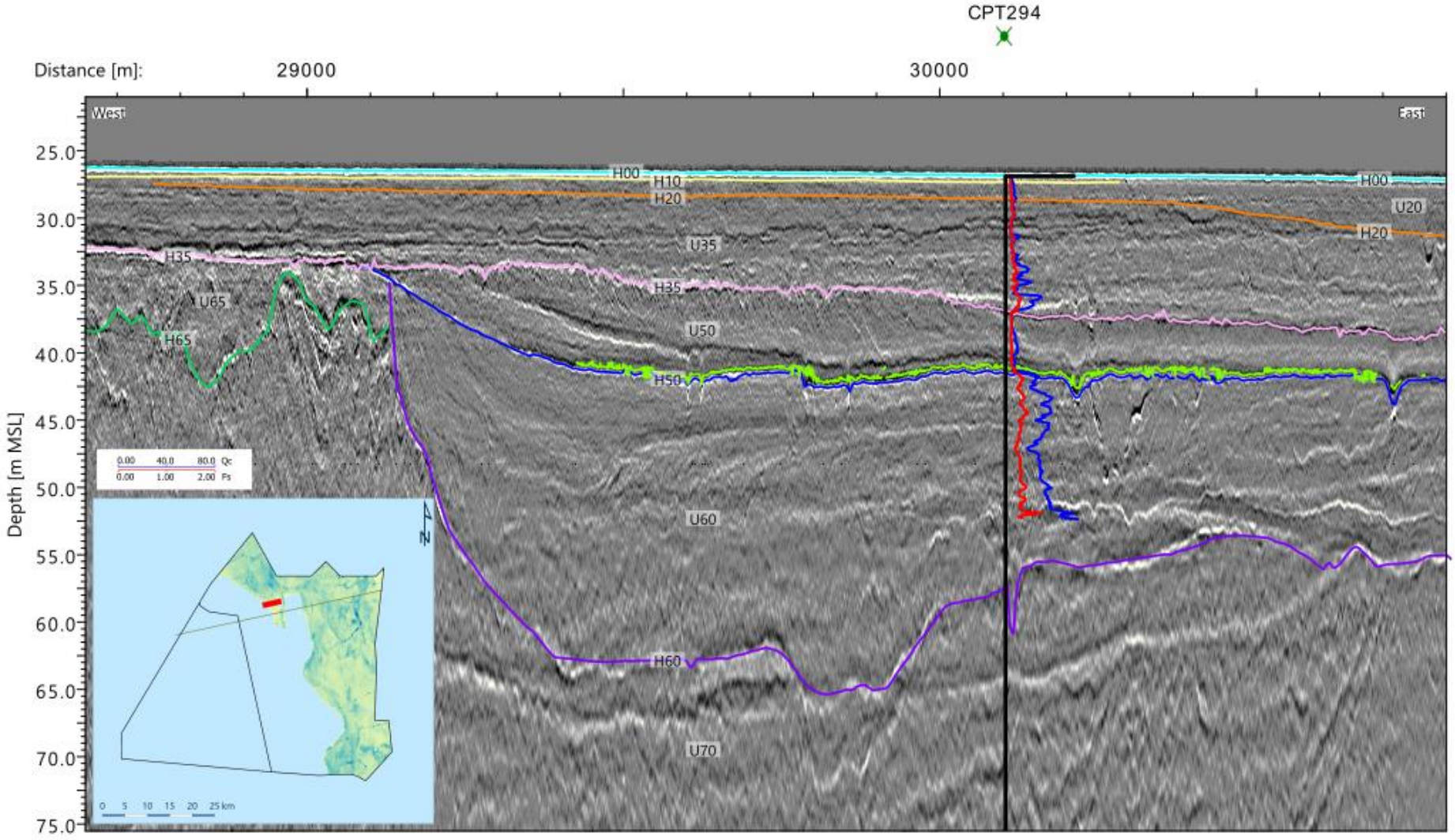

Figure 6.41: 2D UHR seismic data example of the Unit U60. Line EAXA384P1, CPT294

6.9.2 Integration and Interpretation

Following the retreat of the ice sheet at the end of the Saalian period, meltwater deposition was interpreted to continue at the site, particularly in the east of the NS1 site, which may have been further eroded by ice sheet retreat at the end of the Saalian (Section 3.3.3). This is observed at the site as sand dominated sediments from geological unit U60. Figure 6.42 presents a schematic diagram of this process. Sediments from U60 are interpreted in infill an eroded area from the last period of ice sheet advance in the Saalian period.

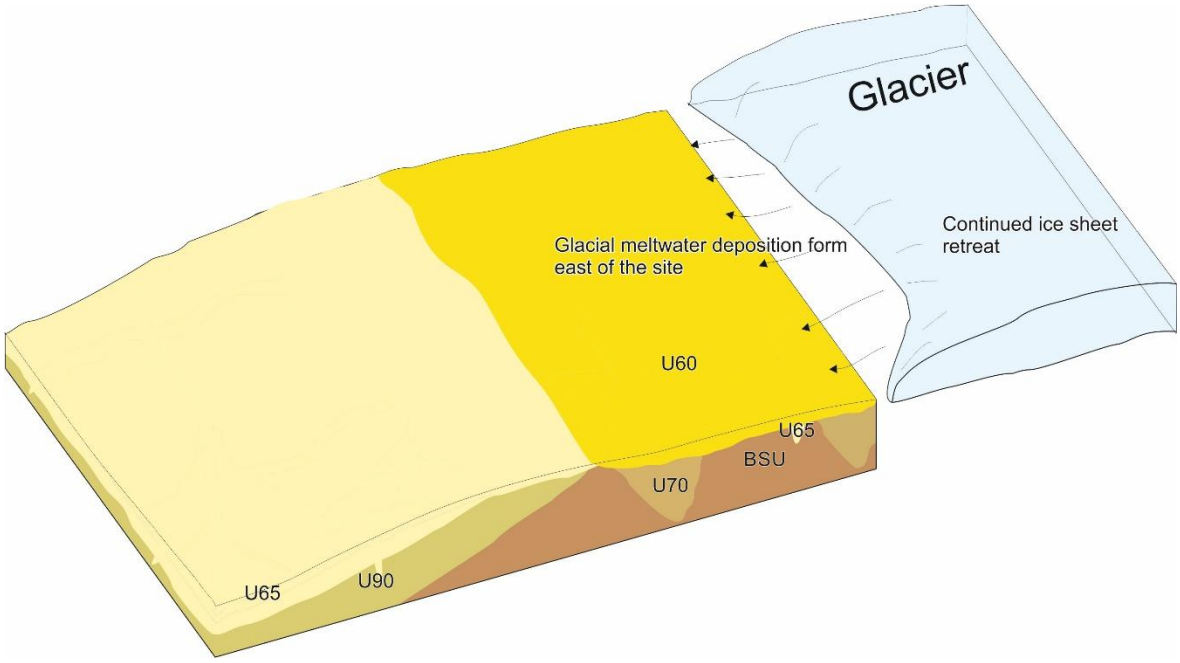

Figure 6.42: Deposition of U60 glacial outwash sediments in the east of the study area

Sediments sampled within boreholes in geological unit U60 are predominantly sands with some gravel and organic material, supporting the interpretation of a fluvial environment. There is also a basal gravel bed in some areas, highlighting the erosive nature of the unit.

Figure 6.43 shows the correlation between the thickness of geological unit U60 within the geophysical and geotechnical locations.

Its stratigraphic position between geological units U65 (interpreted as Saalian age) and U50 (interpreted as Eemian age) suggests that geological unit U60 was deposited in the latest stage of the Saalian glacial period, when the ice sheets had already retreated from the site and been replaced by a fluvial outwash plain (Friborg, 1996; Konradi et al., 2005). Correlation between datasets is generally suitable. Limited outliers are identified, however, associated with the infilling of depressions in geological unit U70 by geological unit U60 sediments. In addition, the boundary between sands in these two units can be challenging to identify in the geotechnical data, for example at location BH075.

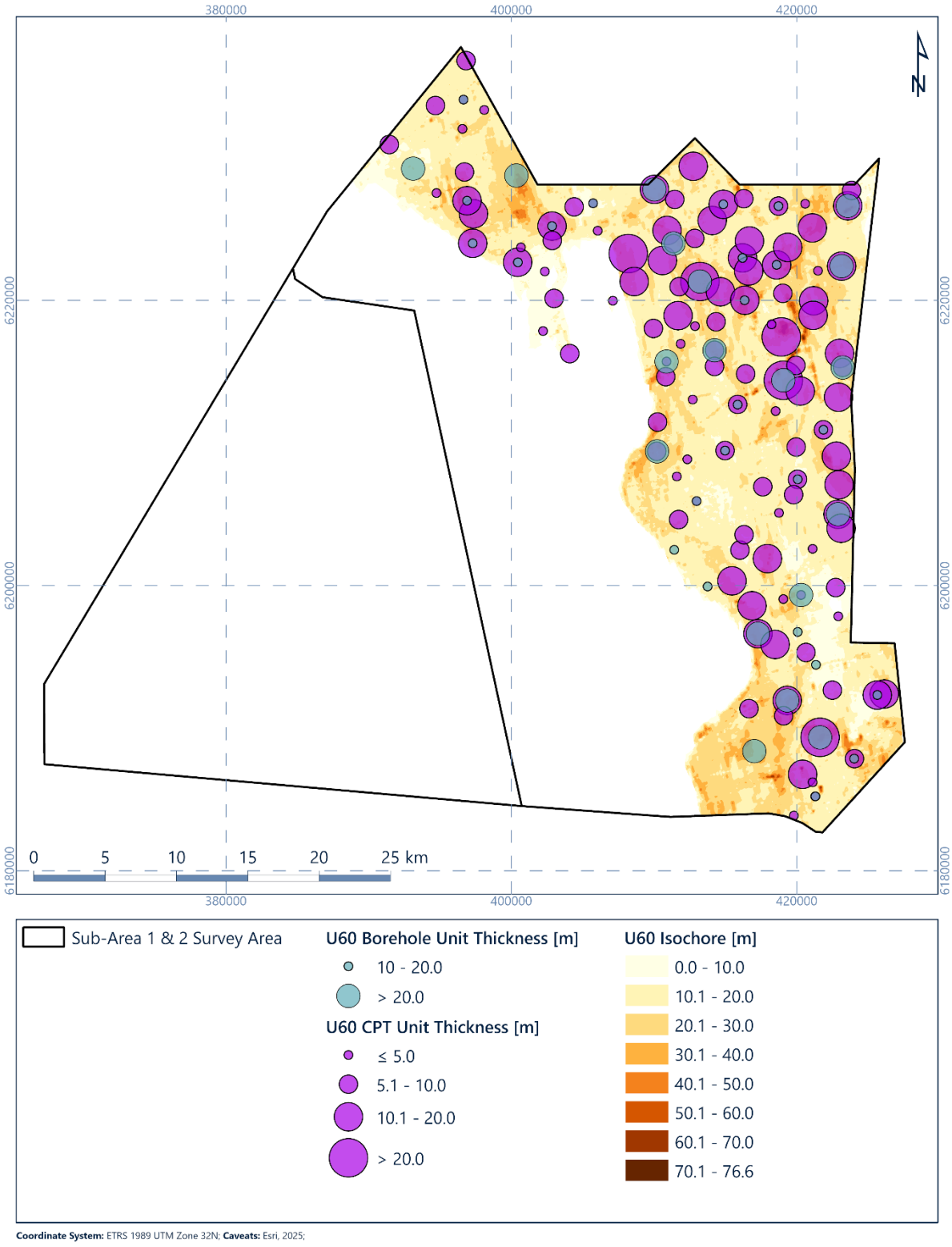

Figure 6.43: Isochore for geological unit U60 correlated with geotechnical data recoveries

6.10 Geological Unit – Unit U65

6.10.1 Seismic Character

Geological unit U65 is present mainly in the south-west of the site, becoming more intermittent towards the north-east (Figures Figure 6.44 and Figure 6.45). This unit forms the infill of tunnel valleys, deep incisions, and a layer with sheet-like geometry that gradually overlies geological unit U90 on the western edge of the study area. The boundary between geological units U65 and U90 is picked such that the stratified and lateral continuous seismic character is included in geological unit U90, and internal erosion surfaces with a laterally variable seismic character are part of Unit 65. However, the pick of this boundary is locally uncertain as the transition between these two units is gradual. The thickness of geological unit U65 is generally around 30 m to 50 m in inter-valley areas, reaching a maximum of nearly 200 m in tunnel valleys (Figure 6.46). These tunnel valleys are 500 m to 2000 m wide.

Geological unit U65 has a variable and complex seismic character, including chaotic seismic facies, horizontal and inclined stratification, internal erosion surfaces and facies that are acoustically transparent (Figures Figure 6.35, Figure 6.41 and Figure 6.47). This variable seismic character is reflected in the variable sediment characteristics.

Tunnel valleys in the study area filled with geological unit U65 have an overall west-south-west to east-north-east orientation (Figures Figure 6.44 and Figure 6.47). The infill has a variable seismic character, exhibiting horizontal and inclined stratification, acoustically transparent to chaotic seismic facies (Figure 6.47).

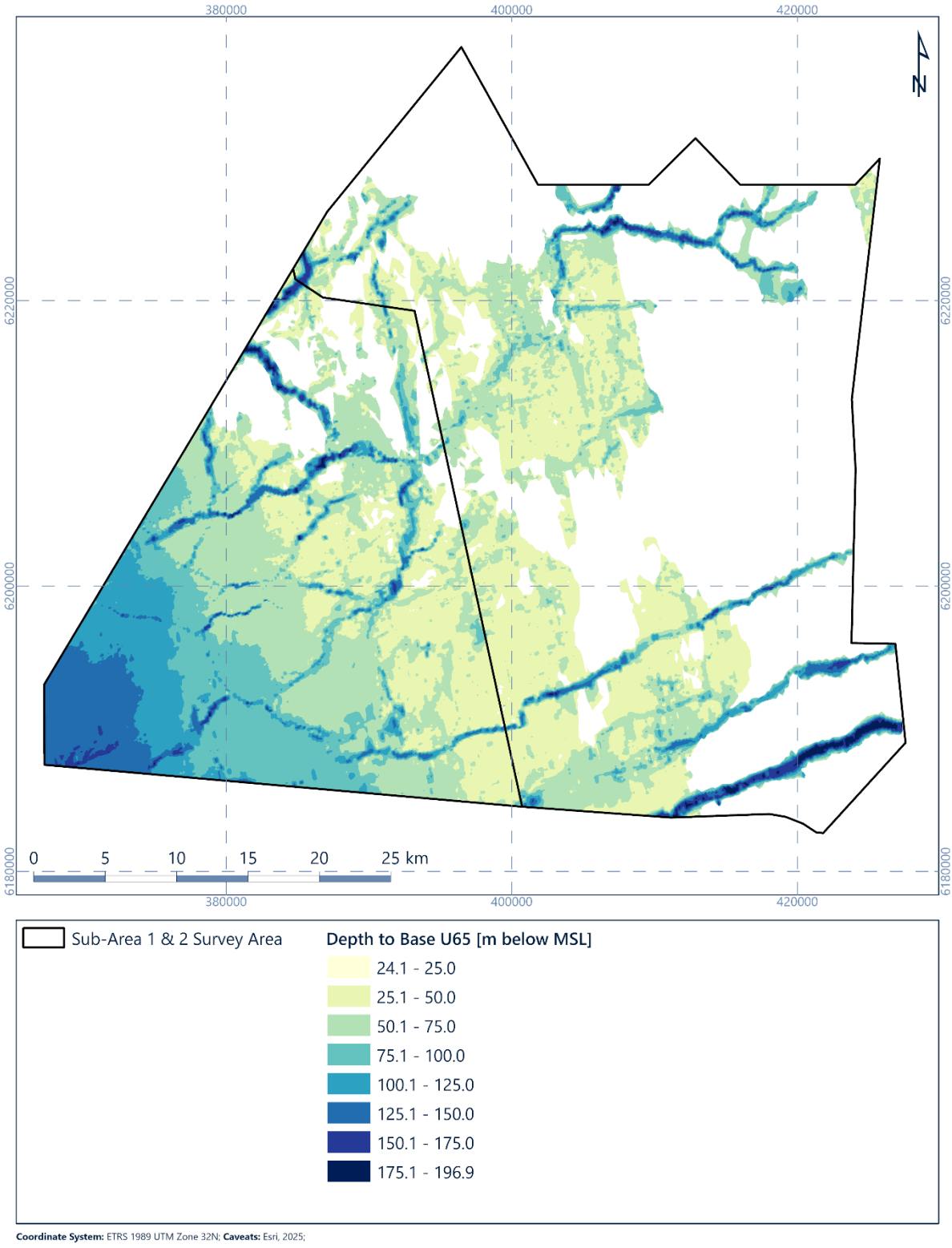

Figure 6.44: Depth [m below MSL] to horizon H65 (base of geological unit U65)

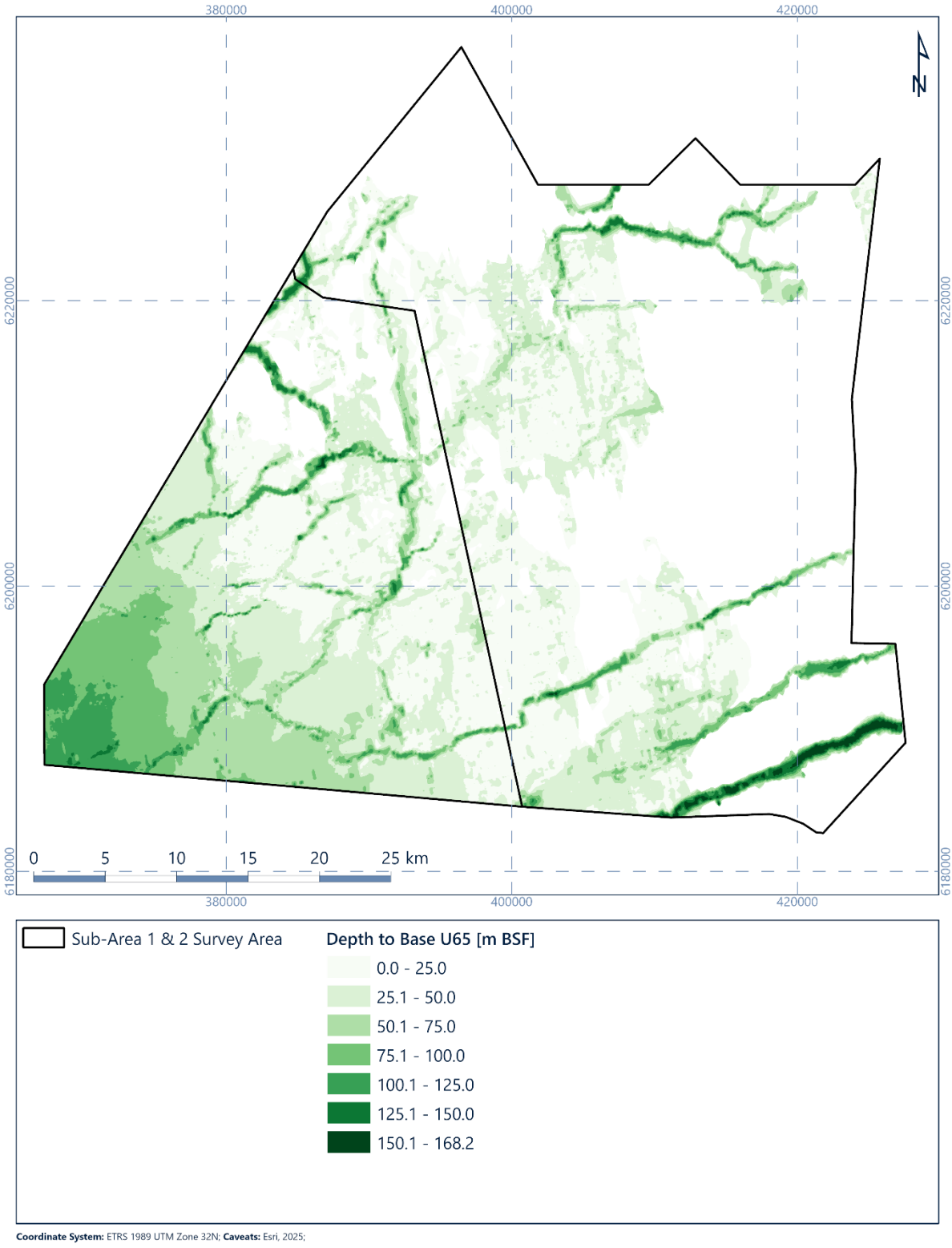

Figure 6.45: Depth [m BSF] to horizon H65 (base of geological unit U65)

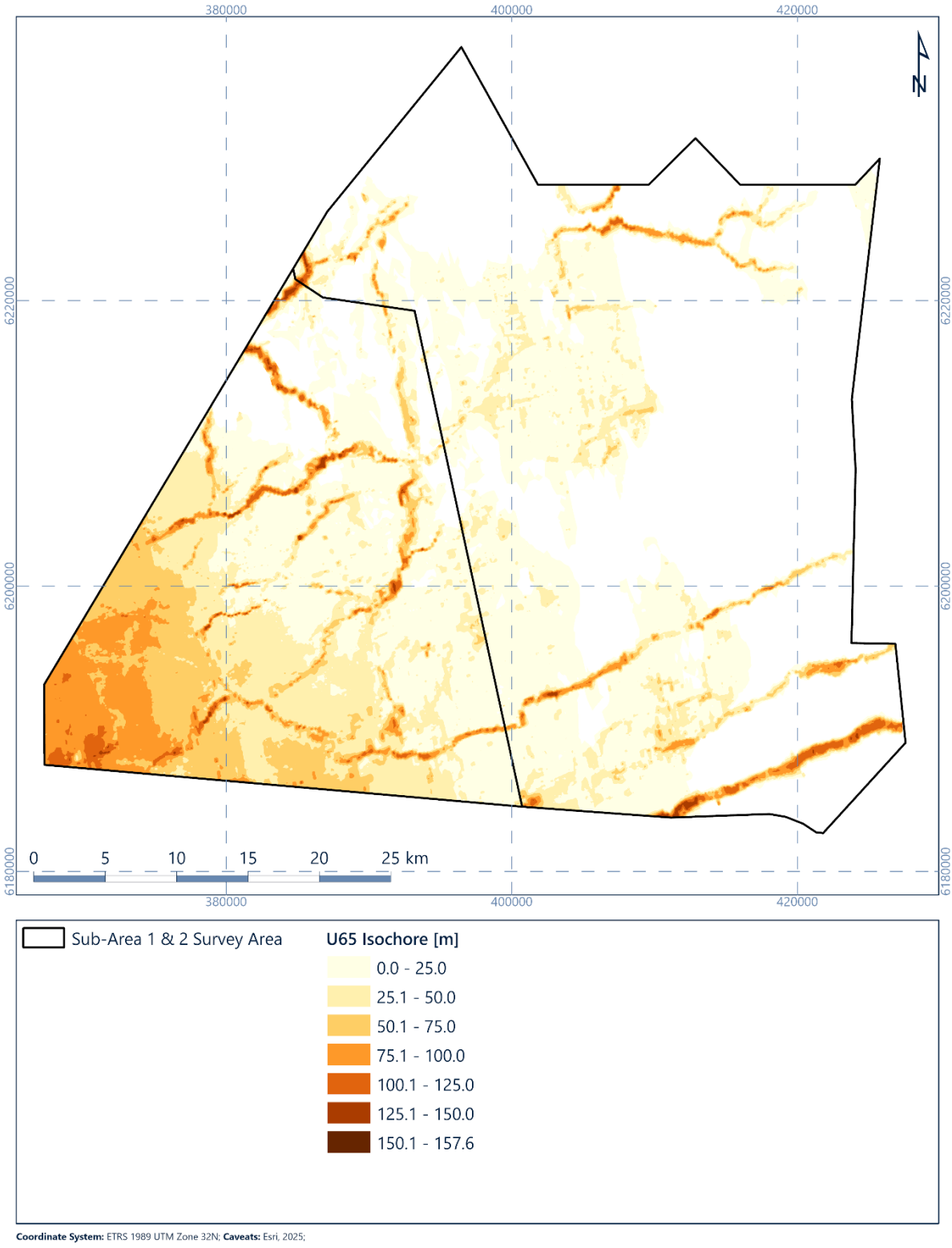

Figure 6.46: Isochore of geological unit U65 [m]

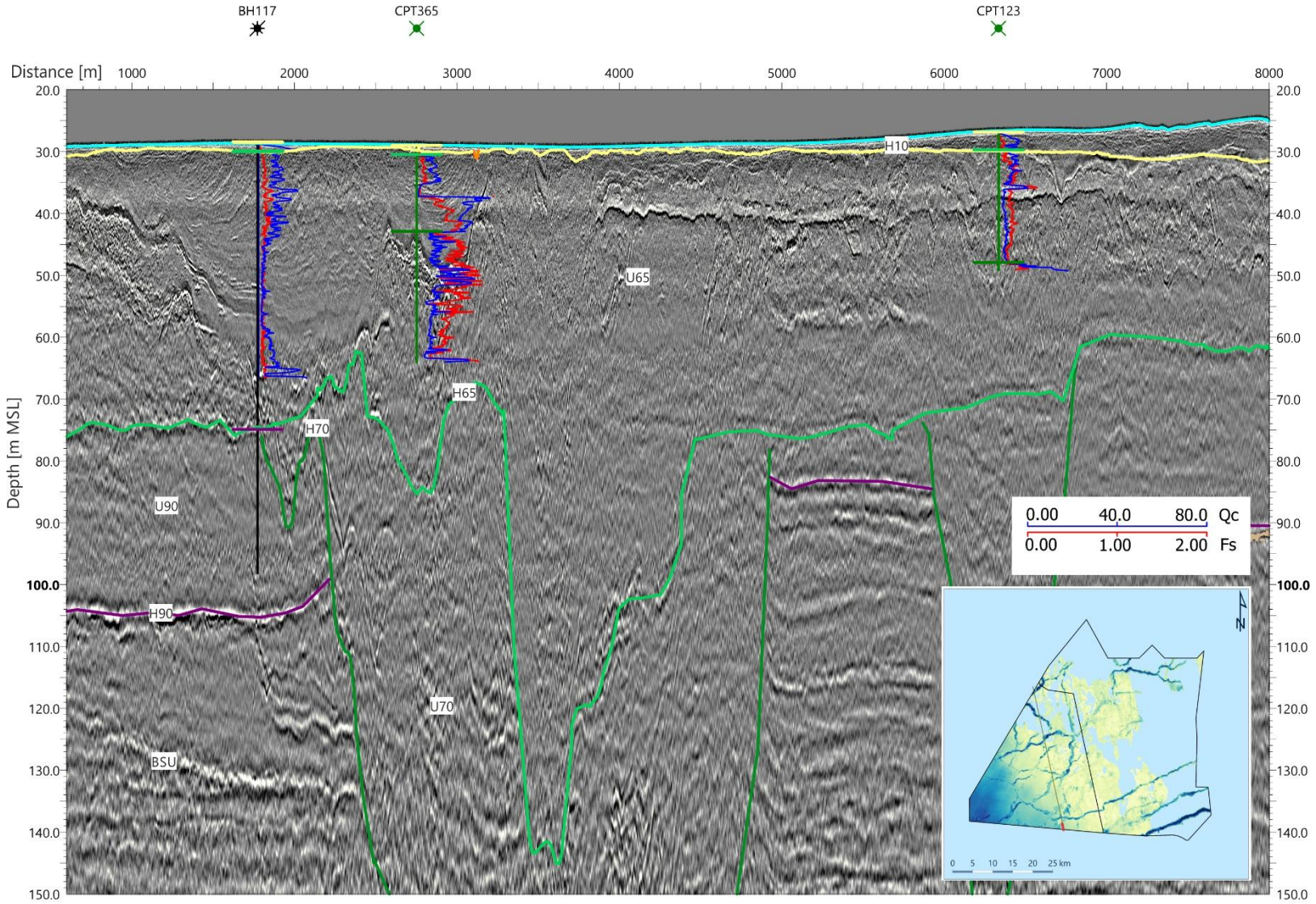

Figure 6.47: 2D UHR seismic data example of Unit U65. Line EAAE191, BH117.

6.10.2 Integration and Interpretation

Following the end of the Holstenian interglacial period, the site underwent the most recent period of glacial advance that resulted in ice coverage across the site (again, the NS1 site was not covered by ice during the more recent Weichselian glacial period (Section 3.3.5)). The Saalian glacial period was expected to have had several periods of ice sheet advance and retreat that led to multiple phases of tunnel valleys incision and associated infills. The exact timing of each of these advance and retreat cycles is not currently resolved and in the absence of age dating data, it is not possible to assign precise ages to the tunnel valley formation or sediments. However, it is important to consider that this period represents multiple phases of glacial activity, with a highly complex interplay of different depositional environments leading to highly variable sediment conditions. Within the geological model, this period is represented by geological unit U65. Figure 6.48 presents a simplified schematic diagram of how these periods of ice sheet advance and retreats may have led to the conditions we see in the sample data at the site today.

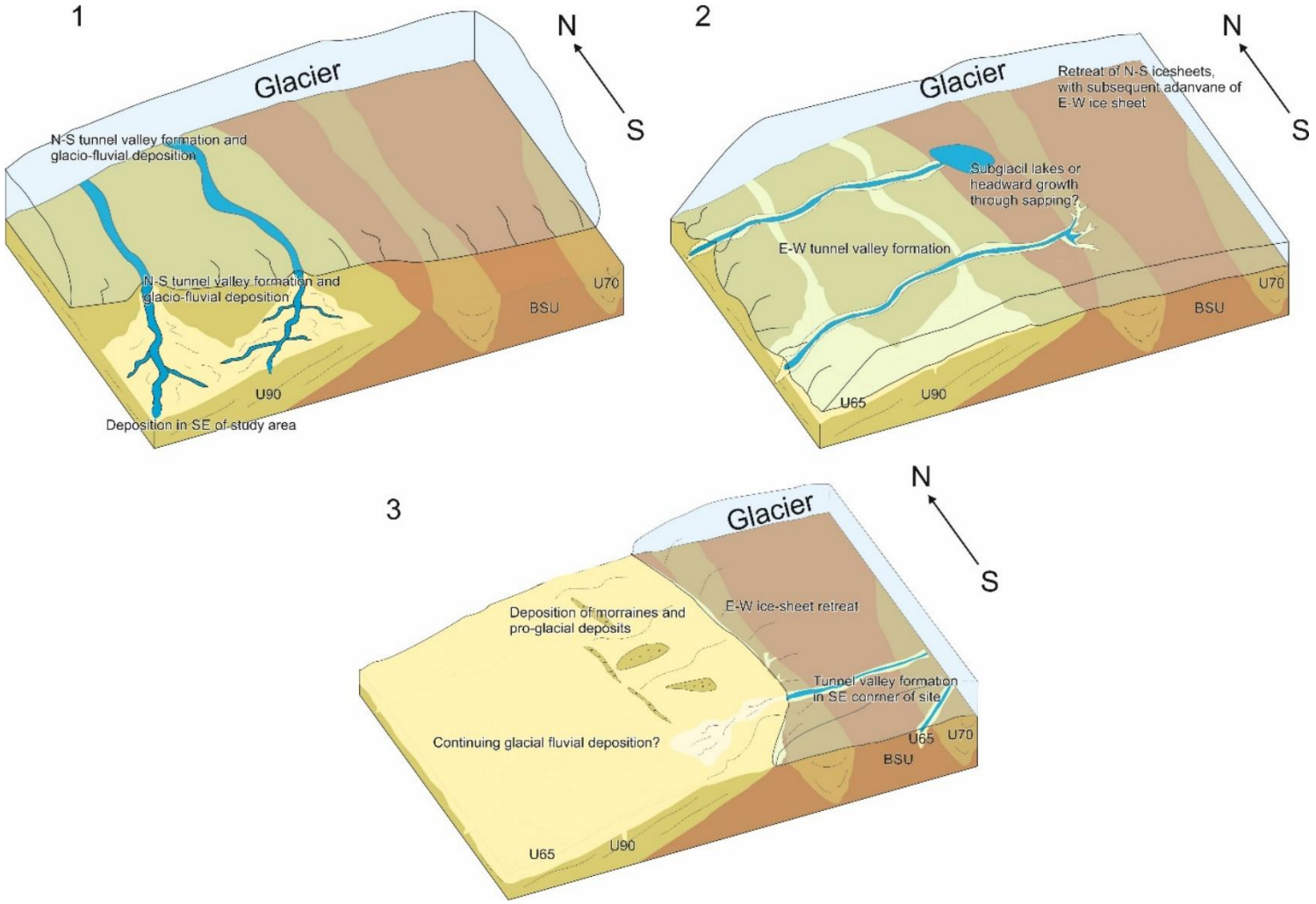

Figure 6.48: Schematic diagram presenting the process of deposition of U65 across the west of the NS1 site. 1) Initial ice advance from a North to South direction, leading to more north-south orientated tunnel valleys. 2) A second period of ice sheet advance, in this case from the East, likely causing period of tunnel valley incision in a east-west orientation. 3) Final ice sheet retreat, with deposition of till and moraine deposits in addition to further most recent tunnel valley features observed in the southeast corner of the site

Seismic anomalies in these deposits are interpreted to be a result of the presence of overbank peat beds (Section 6.15.1).

Clay deposits are interpreted to represent deposition in a low energy freshwater (glacio-lacustrine) or (glacio-)marine setting. These deposits have an acoustically transparent to well stratified seismic character.

Tunnel valley features are also observed within the geological unit U65 package, and have a chaotic seismic character. These areas have variable soil types including till, and are interpreted to be glacial deposits. The tunnel valley features are orientated in a north-east to south-west direction, suggesting ice advance from the east. This may represent late Drenthe or Warthe 1 ice advance phases (Winsemann et al., 2020).

Geological unit U65 can be correlated with variable glacier deposits in south-west Jutland (onshore Denmark), which are Saalian in age. Onshore Jutland, the Saalian glacier deposits form Saalian glacial landscapes called hill islands (bakkø) (Figure 3.6; Friborg, 1996; Konradi et al., 2005). The Saalian glacial period includes several stadials and interstadials (Figure 3.3). The complexity of geological unit U65 can be attributed to this long period of deposition in variable environment. Overconsolidation and possible higher strength clays near the top of the unit suggest direct ice loading.

Correlation between datasets is generally good. Due to the variability found in the geotechnical locations, leading to greater uncertainty regarding the nature of the infill.

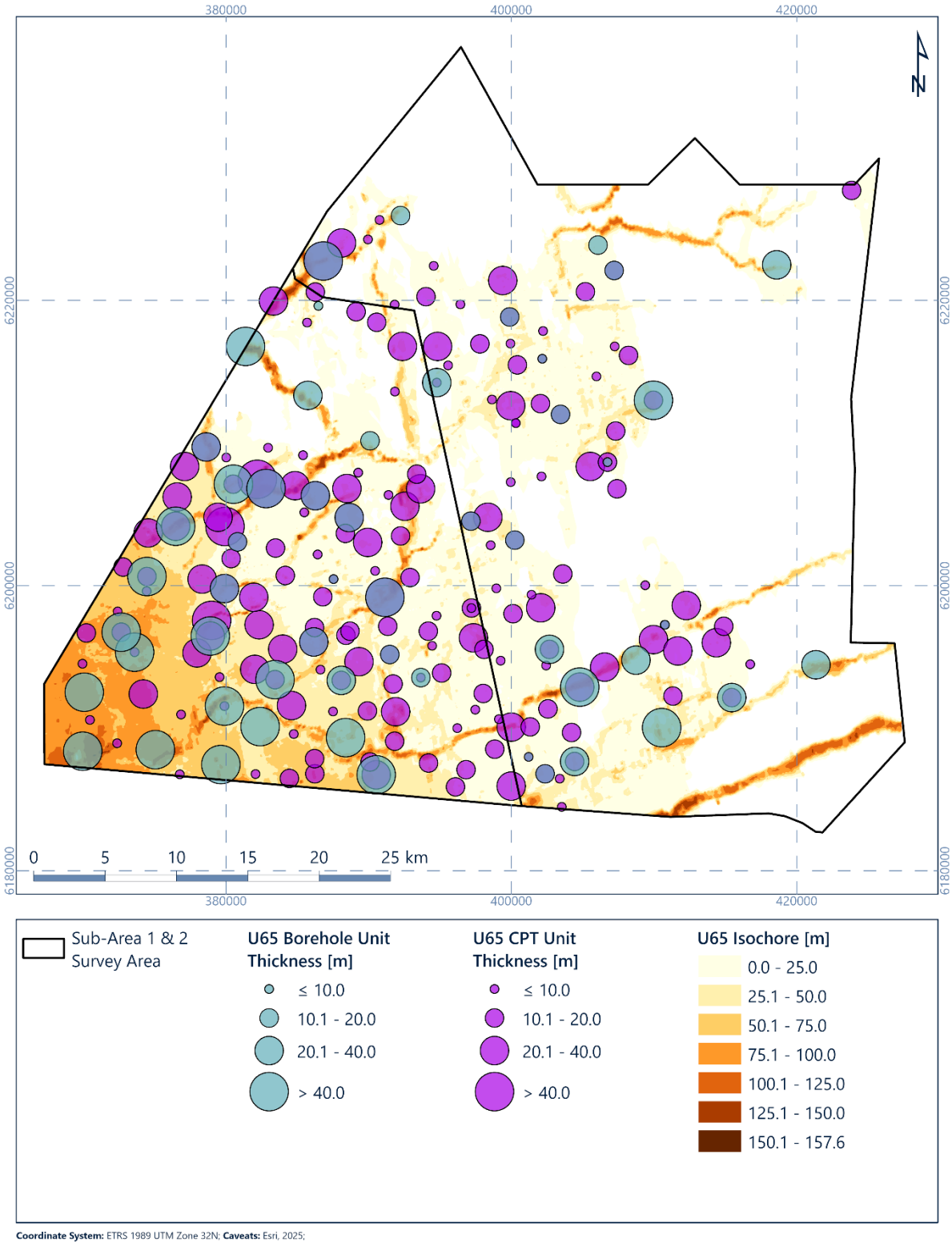

Figure 6.49: Isochore for geological unit U65 correlated with geotechnical data recoveries

6.11 Geological Unit – Unit U69

6.11.1 Seismic Character

Geological unit U69 forms the upper part of the infill of deep tunnel valleys with a north to south orientation (Figure 6.50 and Figure 6.51). This unit lies within the larger tunnel valley formations delineated by geological unit U70 (Figure 6.65) and represents the upper portion of these sediments. The base is marked by horizon H69, which is characterised by the onlap of reflectors onto the horizon. The seismic character of the unit is defined by stratified or acoustically transparent seismic data. In some areas it can be up to approximately 105 m thick (Figure 6.52).

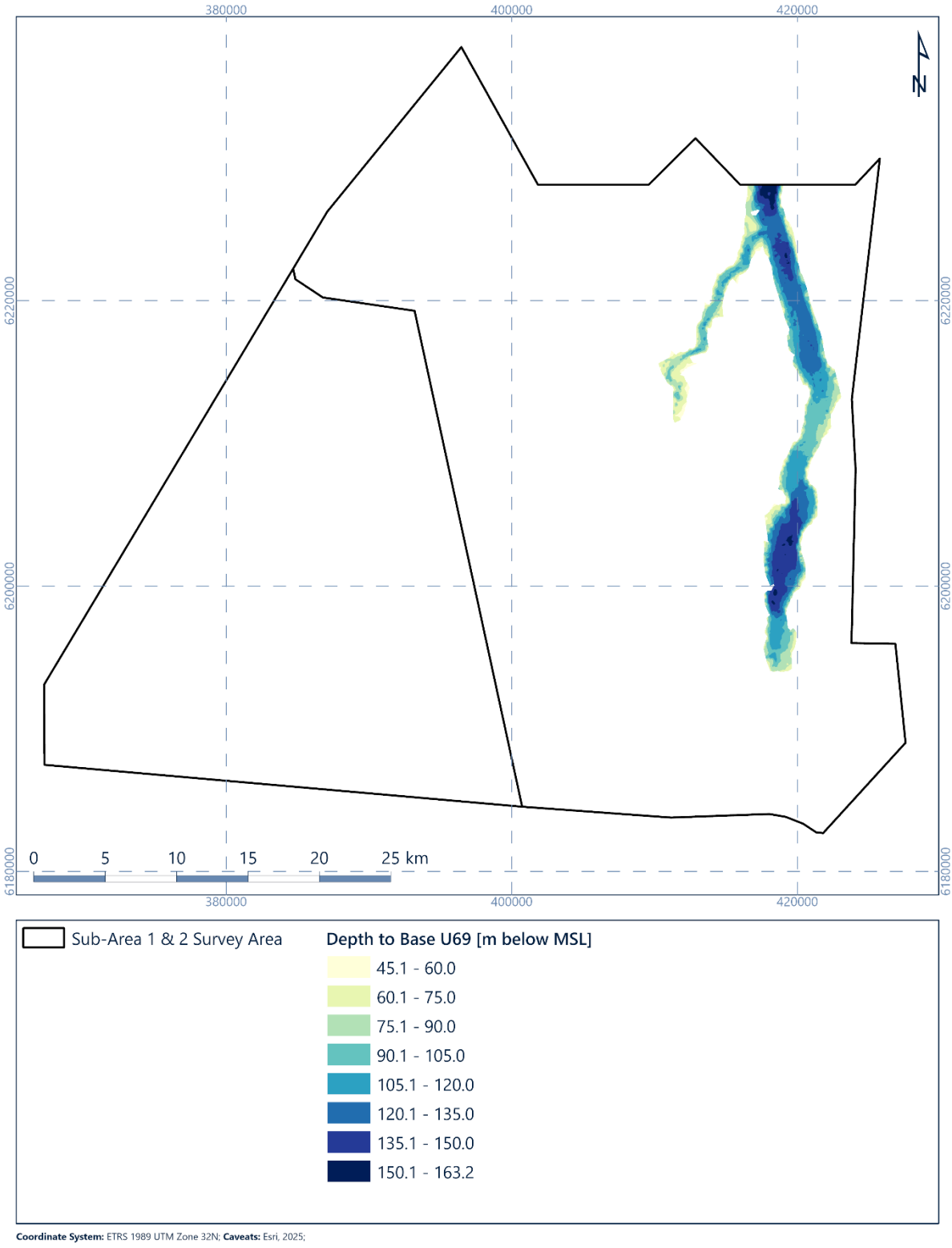

Figure 6.50: Depth [m below MSL] to horizon H69 (base of geological unit U69)

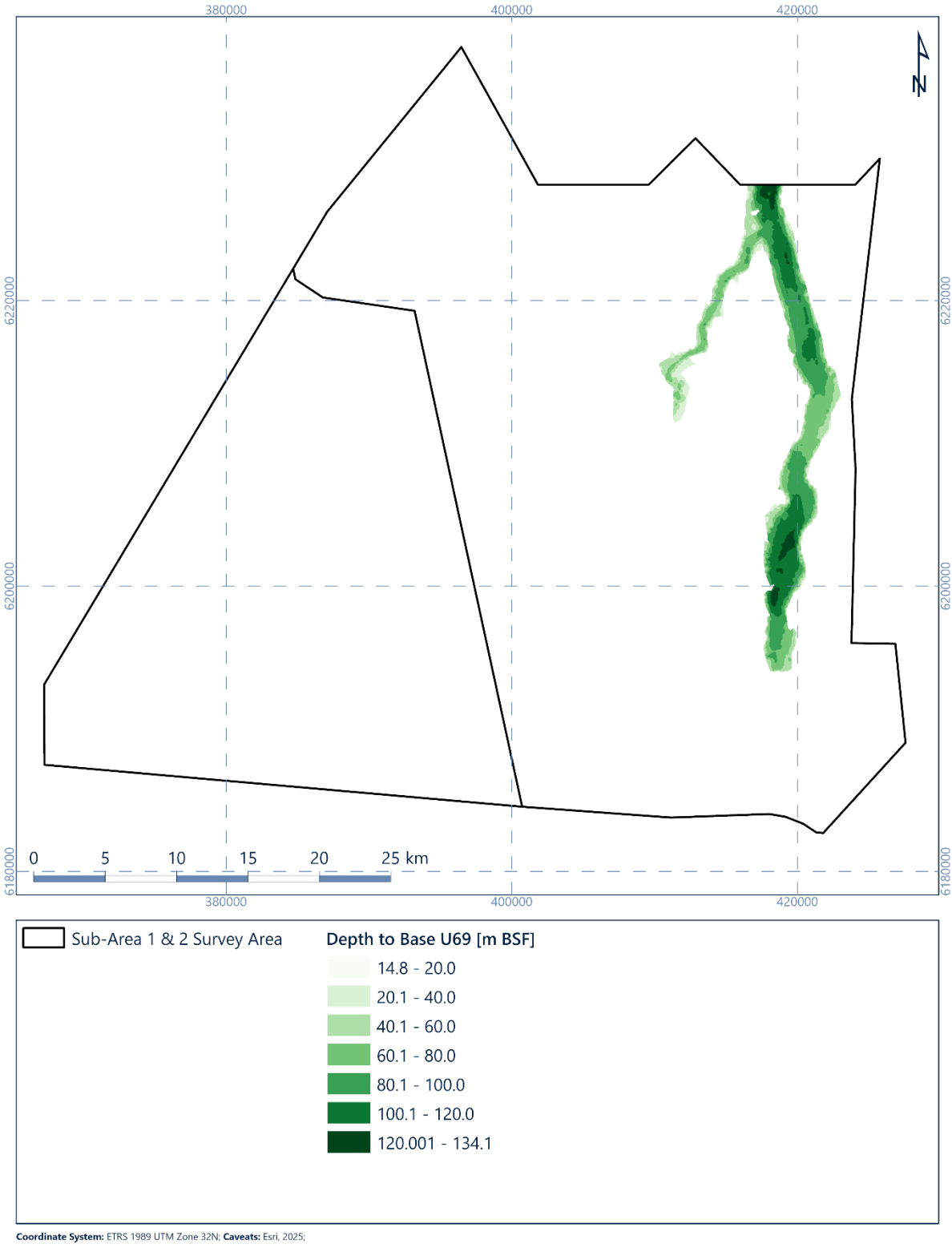

Figure 6.51: Depth [m BSF] to horizon H69 (base of geological unit U69)

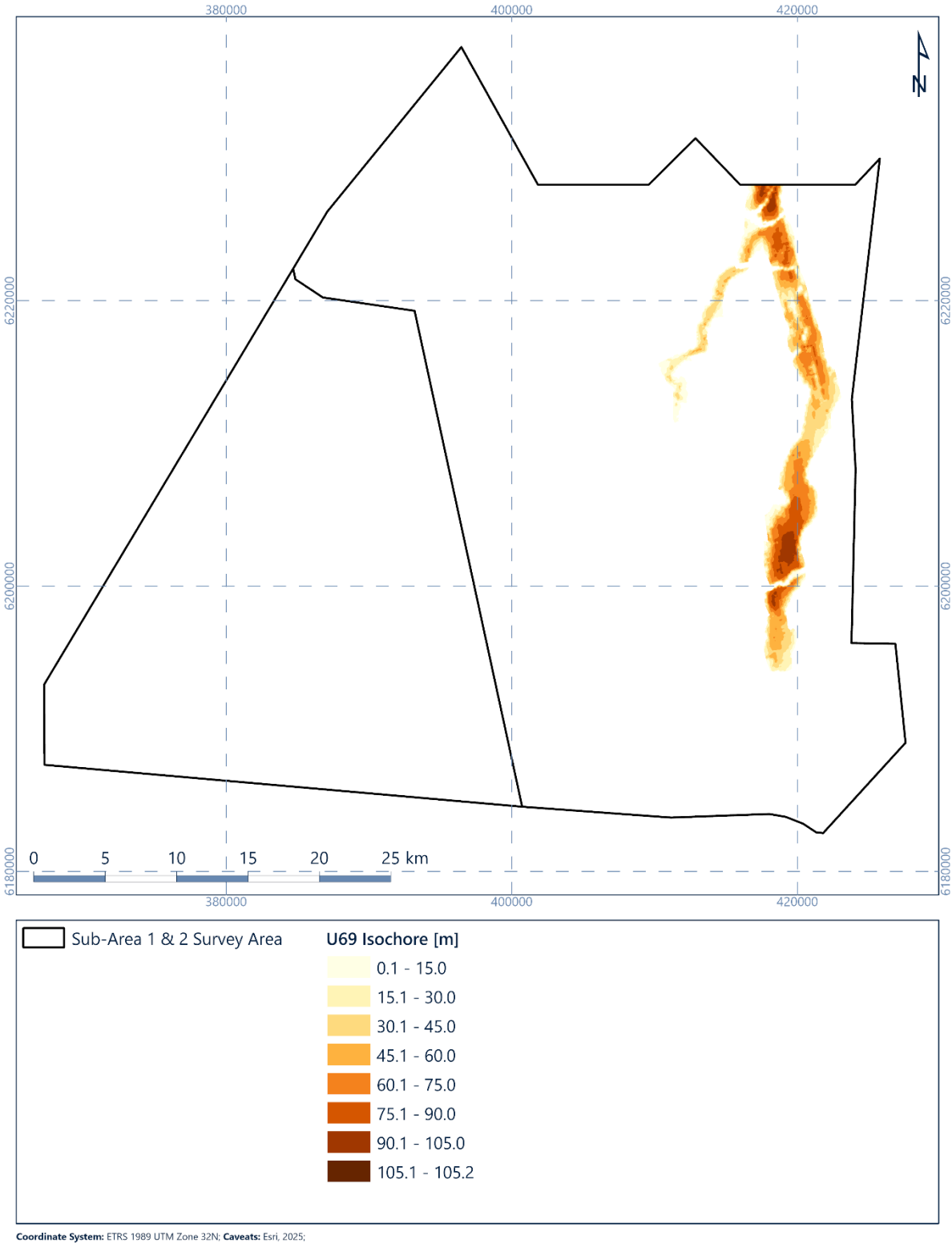

Figure 6.52: Isochore of geological unit U69 [m]

6.11.2 Integration and Interpretation

Associated with the valley features from the Elsterian period, a specific infill unit is identified. This is geological unit U69. It is interpreted to represent a period of glacial lacustrine deposition that followed the incision of the valleys during the Elsterian glacial period (Section 3.3.1). A topographic low is interpreted to have formed during the period of erosion associated with the tunnel valley formation, which was subsequently infilled with geological unit U69 material. Sampling of these units show sediments deposited in a low energy environment. It is interpreted that these sediments represent deposition during the Holstenian interglacial period.

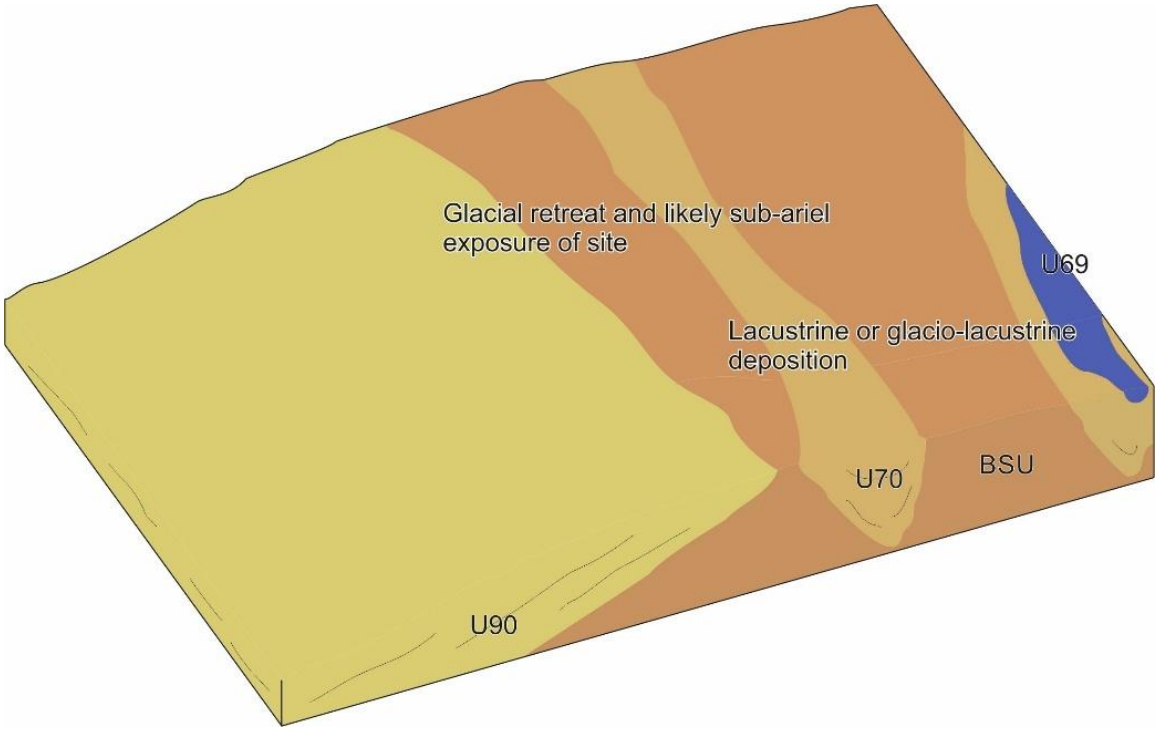

Figure 6.53: Schematic diagram of site conditions during the Holstenian period (U69 deposition)

The geological unit is geotechnically consistent, comprising clay sediments with variable secondary components. The presence of shell fragments may suggest connection to a marine environment. Figure 6.54 shows an example of the clay sediments in geological U69 at BH009.

Figure 6.54: Example of U69 clay sediments at BH009

Figure 6.55 shows the correlation between the thickness of geological unit U69 in the geophysical and geotechnical locations. Suitable correlation between the top of the unit in the geotechnical and geophysical datasets is observed. Horizon H69 was penetrated at very few locations, so it is difficult to comment on integration quality at the base of the unit. Where penetration did capture the base of geological unit U69, the datasets do correlate well.

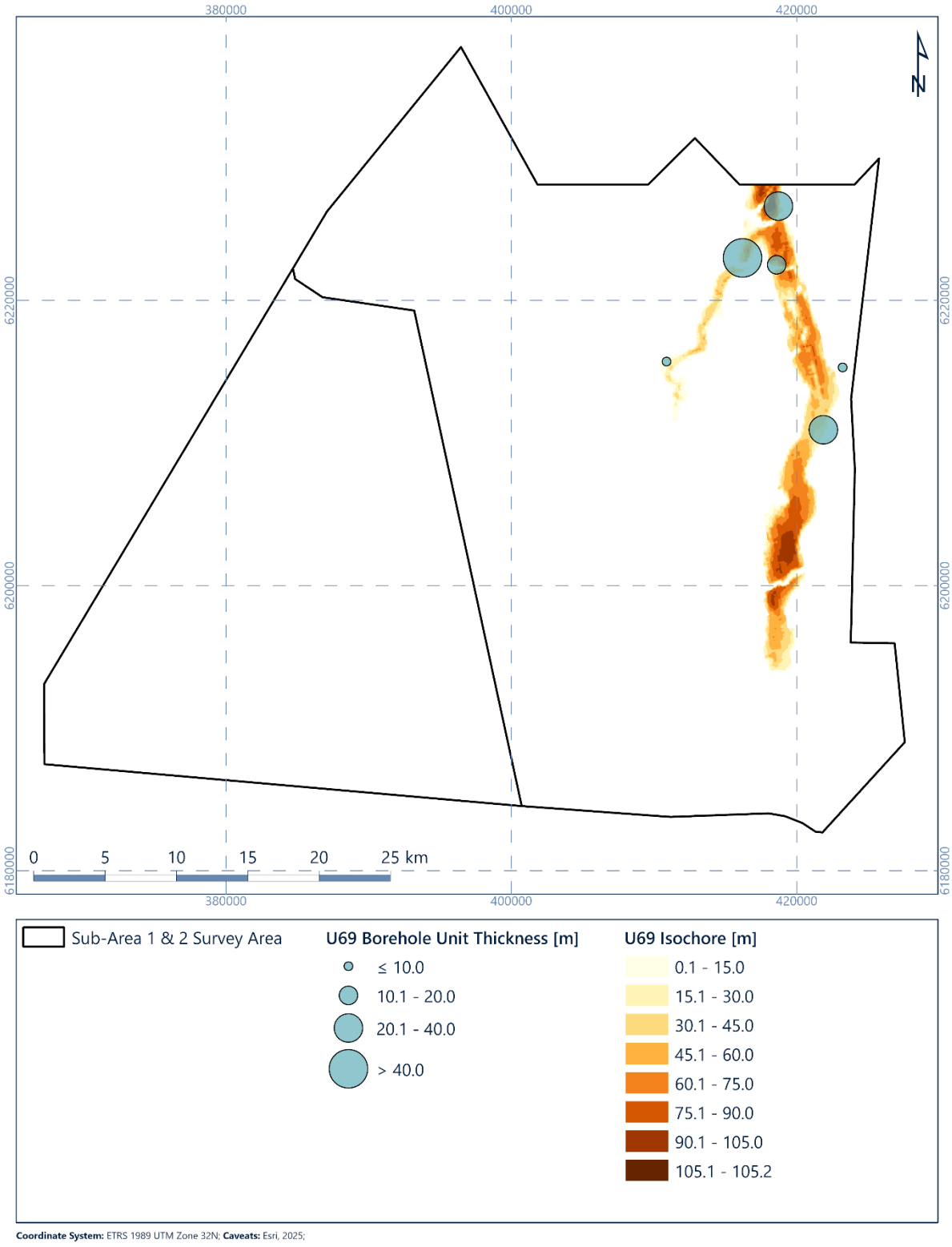

Figure 6.55: Isochore for geological unit U69 correlated with geotechnical data recoveries

6.12 Geological Unit – Unit U70

6.12.1 Seismic Character

Geological unit U70 forms the infill of deep tunnel valleys with a generally north to south orientation (Figure 6.56, Figure 6.57 and Figure 6.58). The base is marked by horizon H70, which often lies deeper than the maximum penetration of the 2D UHR seismic data (approximately 200 m below MSL). The tunnel valleys form a complex spatial network, with different generations intersecting (Figure 6.56).

Multiple seismic facies are observed in geological unit U70 (Figure 6.59), with seismic character varying from semi-transparent to chaotic areas. Deeper seismic packages are frequently associated with the geological unit U69 sediments, with characteristics similar to the overlying units. These are not delineated in the current model due to their depth.

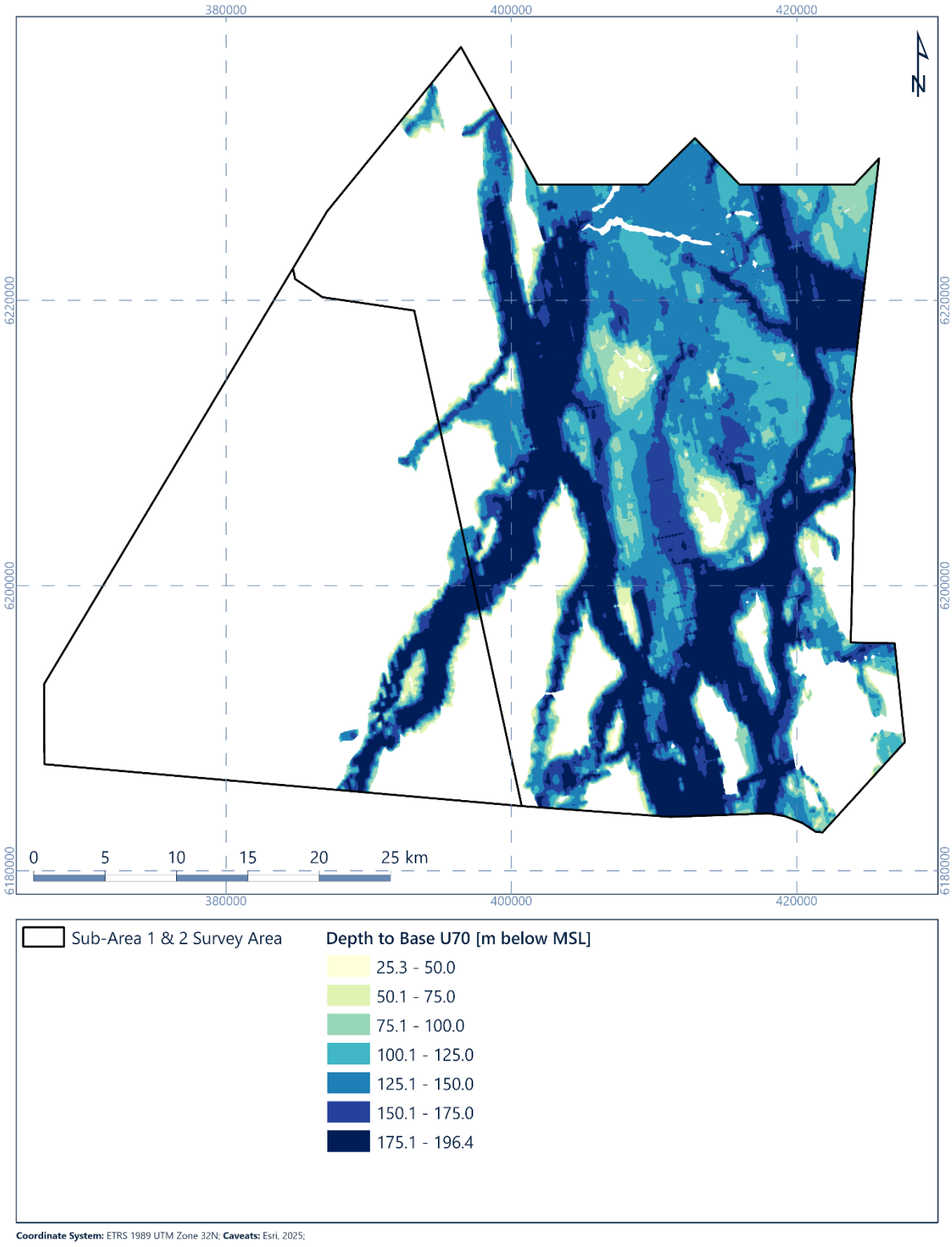

Figure 6.56: Depth [m below MSL] to horizon H70 (base of geological unit U70)

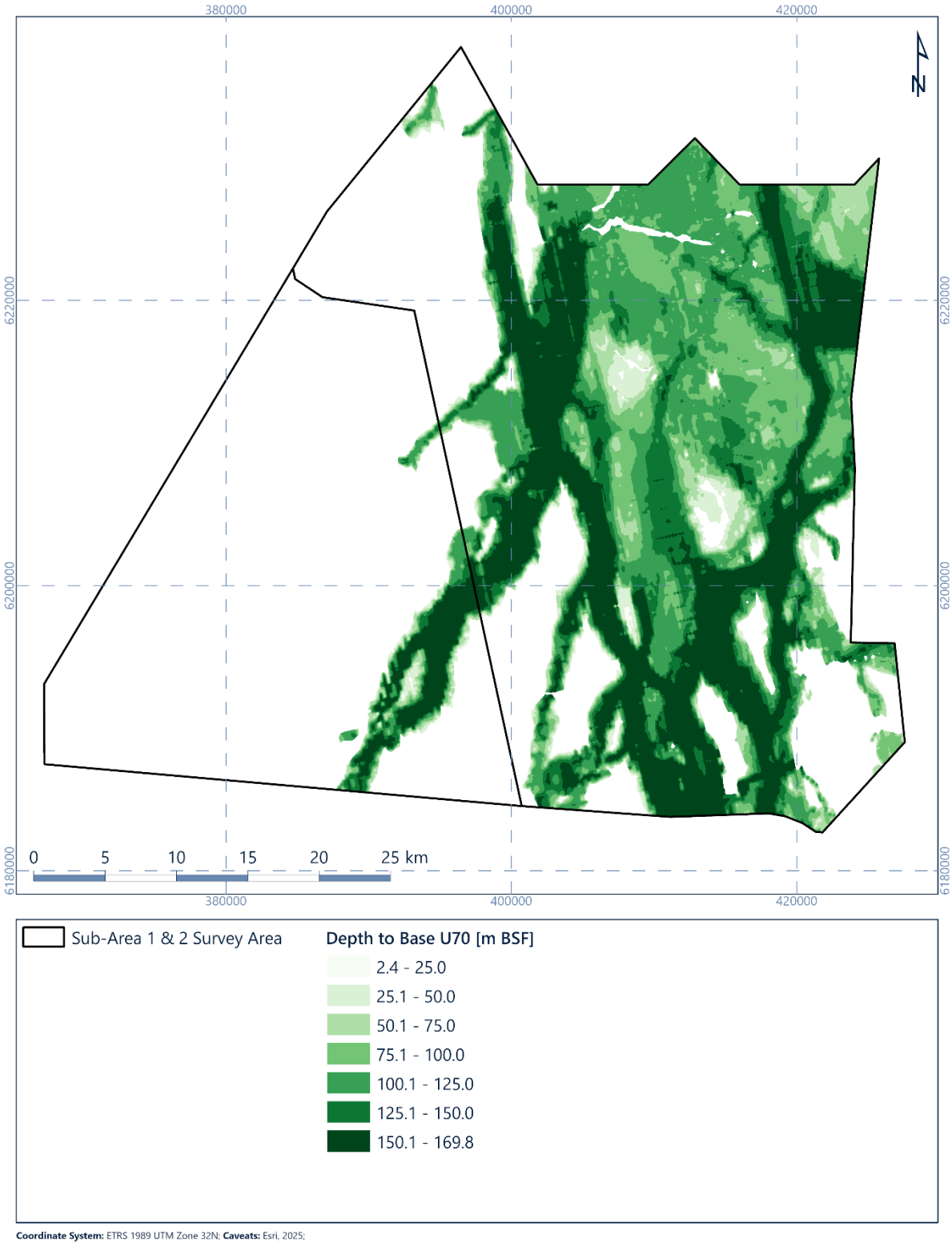

Figure 6.57: Depth [m BSF] to horizon H70 (base of geological unit U70)

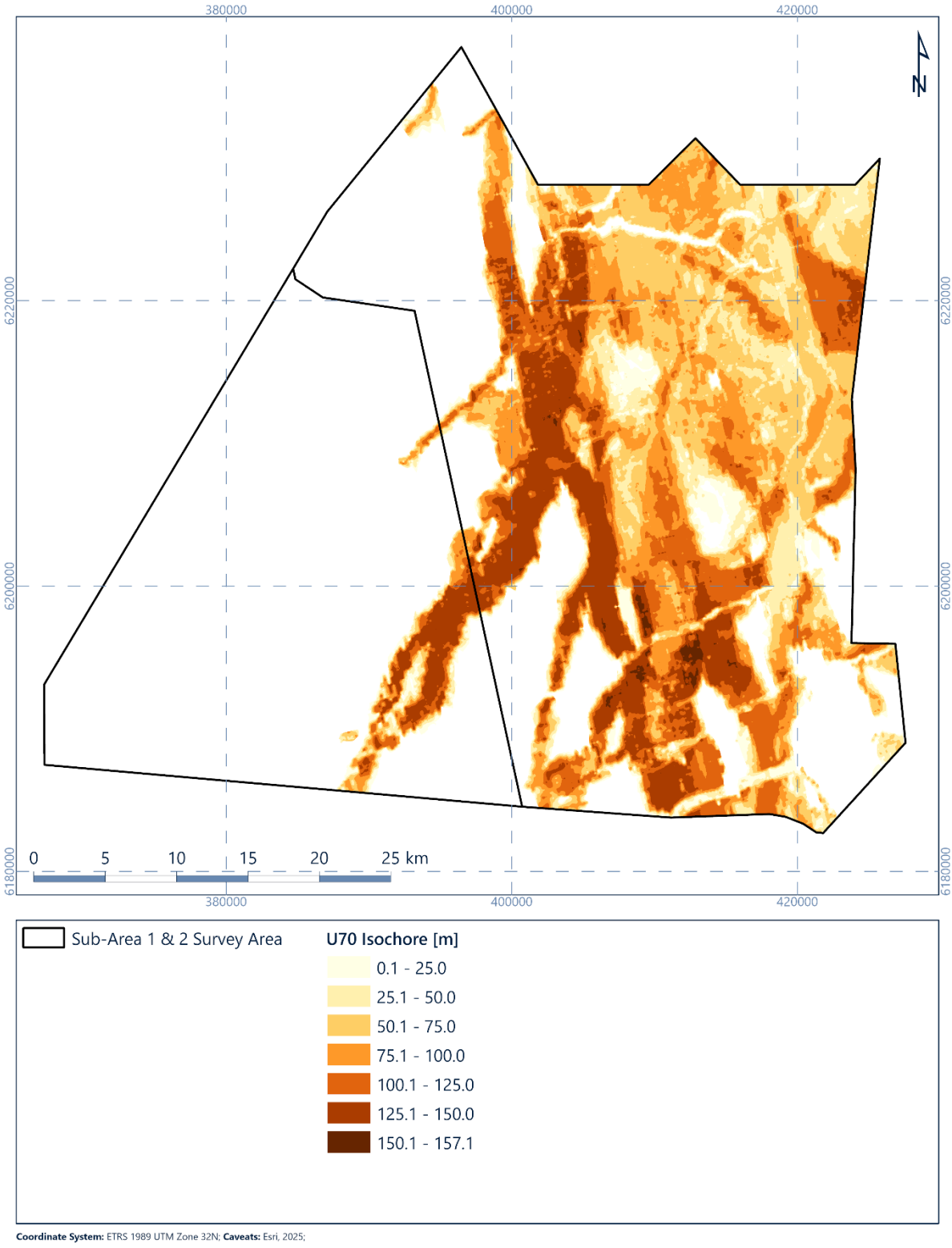

Figure 6.58: Isochore of geological unit U70 [m]

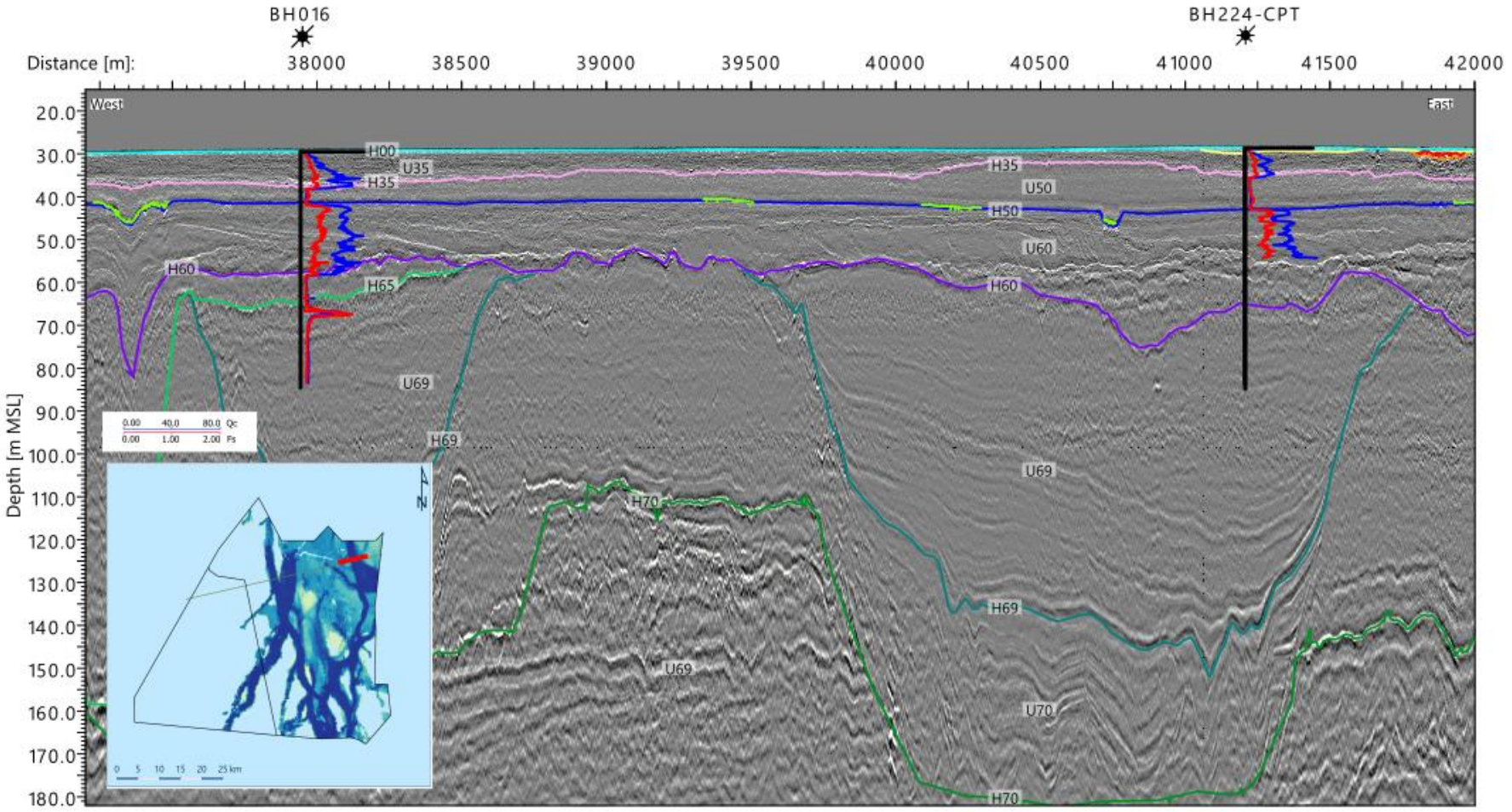

Figure 6.59: 2D UHR seismic data example of Unit U69 and U70. Line EAXA384P1, CPT016, CPT224

6.12.2 Integration and Interpretation

The oldest observed glacial deposition within the site is associated with material from geological unit U70, which has been interpreted to represent sediment from the Elsterian glaciation and ice advance. Associated with the geological unit U70 sediments in the site are a series of tunnel valley features which are focused in the east of the site and have a strong N-S orientation (Section 6.15.5). The valley features are observed to cross-cut one another suggesting multiple phases of ice sheet advance and retreat, each with separate tunnel valley incision and infill. Figure 6.60 presents a schematic diagram of the site during this period. The exact nature of the infill of the valleys is expected to be highly complex, with the current single unit infill likely a simplification of the unit. In addition, areas of overbanking associated with subglacial deposition is also observed associated with this period and the geological unit U70 material.

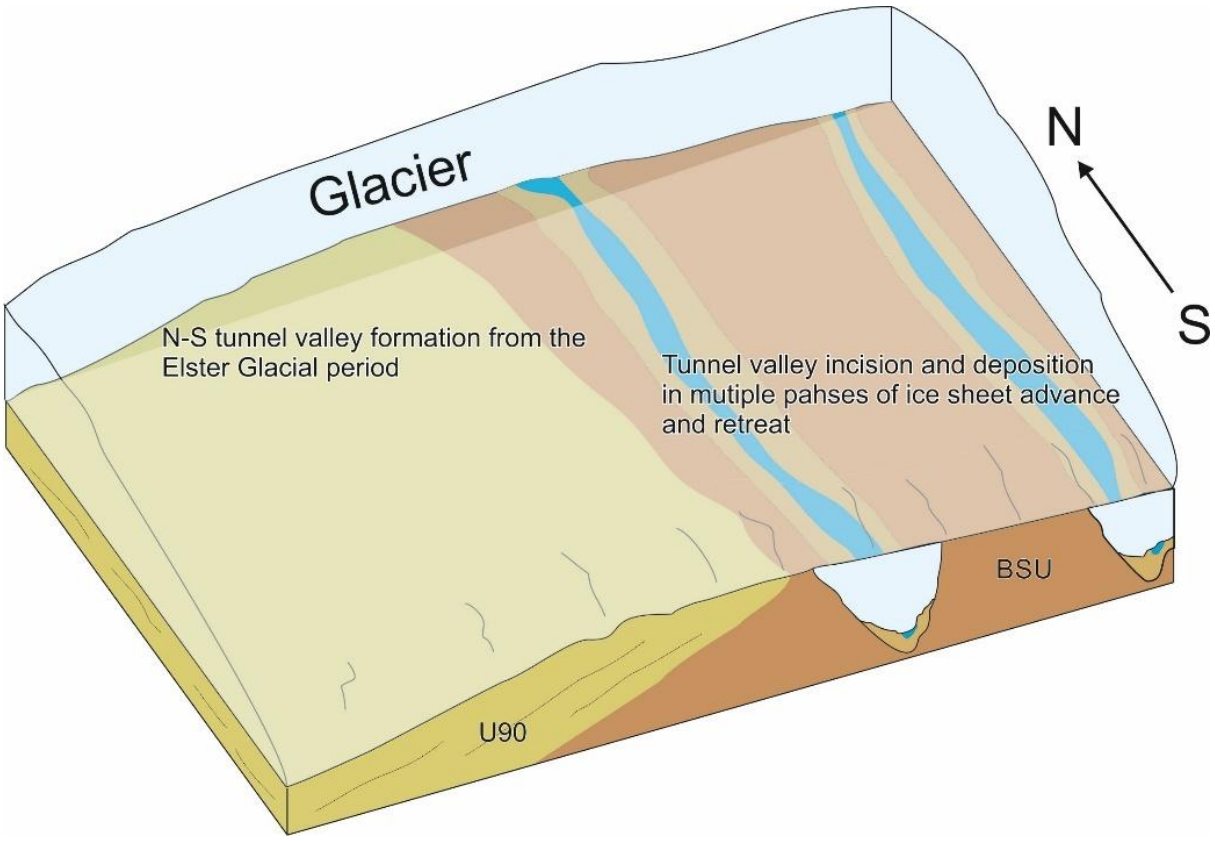

Figure 6.60: Schematic diagram of site conditions during Elsterian glacial period (U70 deposition)

Geotechnical data are highly variable, reflecting the deposition environment (Section 7). Some inconsistency in the integration of geotechnical data with geophysical horizons is observed in the south-east corner of the site. Geological unit U60 sediments overlie possible intervalley areas of geological unit U70, their similar seismic character and geotechnical properties make seismic picking challenging.

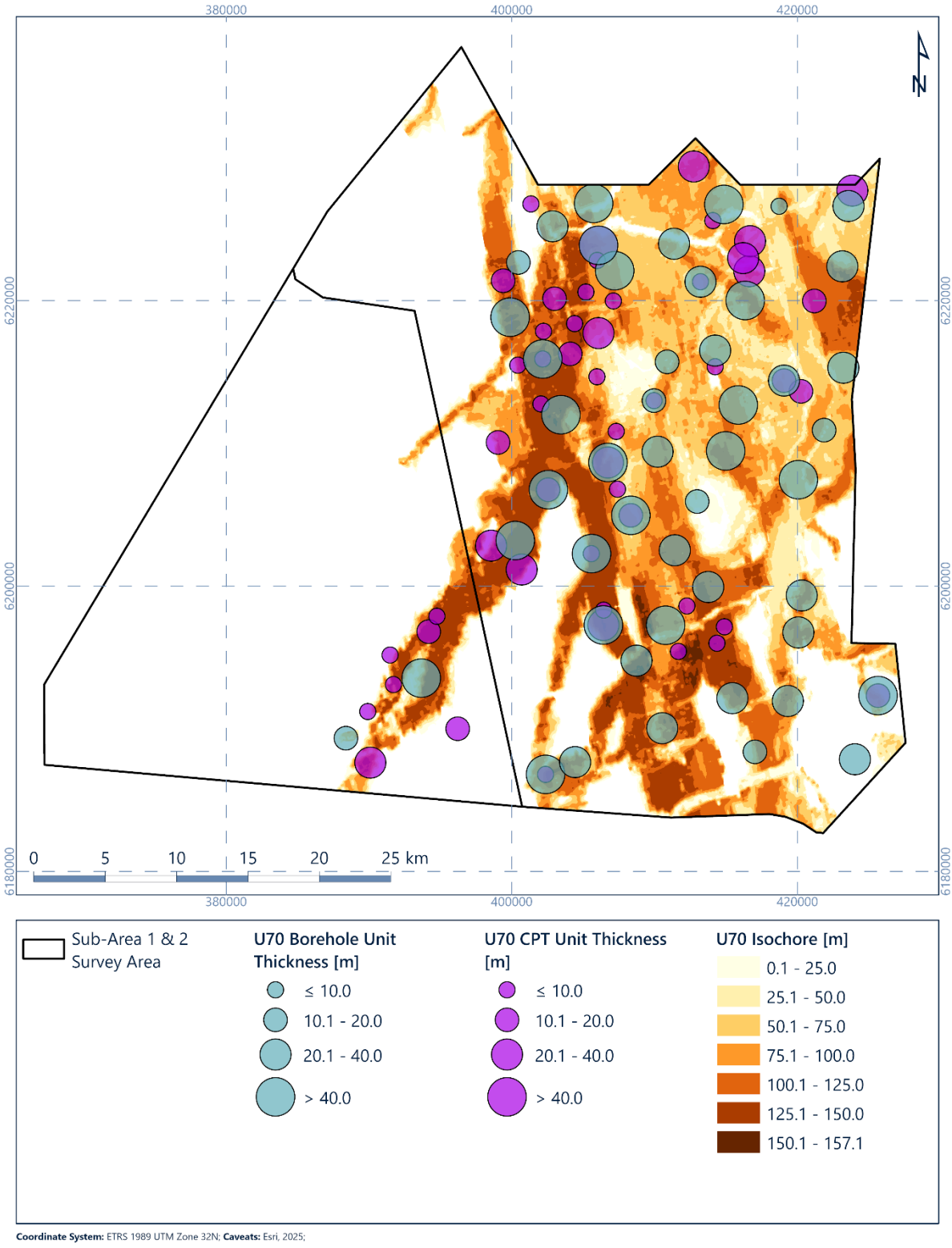

Figure 6.61: Isochore for geological unit U70 correlated with geotechnical data recoveries

6.13 Geological Unit – Unit U90

6.13.1 Seismic Character

Geological unit U90 is present in the south-west of the site (Figures Figure 6.62, Figure 6.63 and Figure 6.64) and has a sheet-like geometry. The base dips towards the south-west, lying below the maximum penetration of the 2D UHR seismic data in the most south-westerly part of the site (Figure 6.65).

Internally, this unit has a stratified to complex seismic character. The stratification is formed by discontinuous reflectors with variable amplitudes. The upper section is generally transparent with point like anomalies. The lower section shows greater number of discontinuous reflectors.

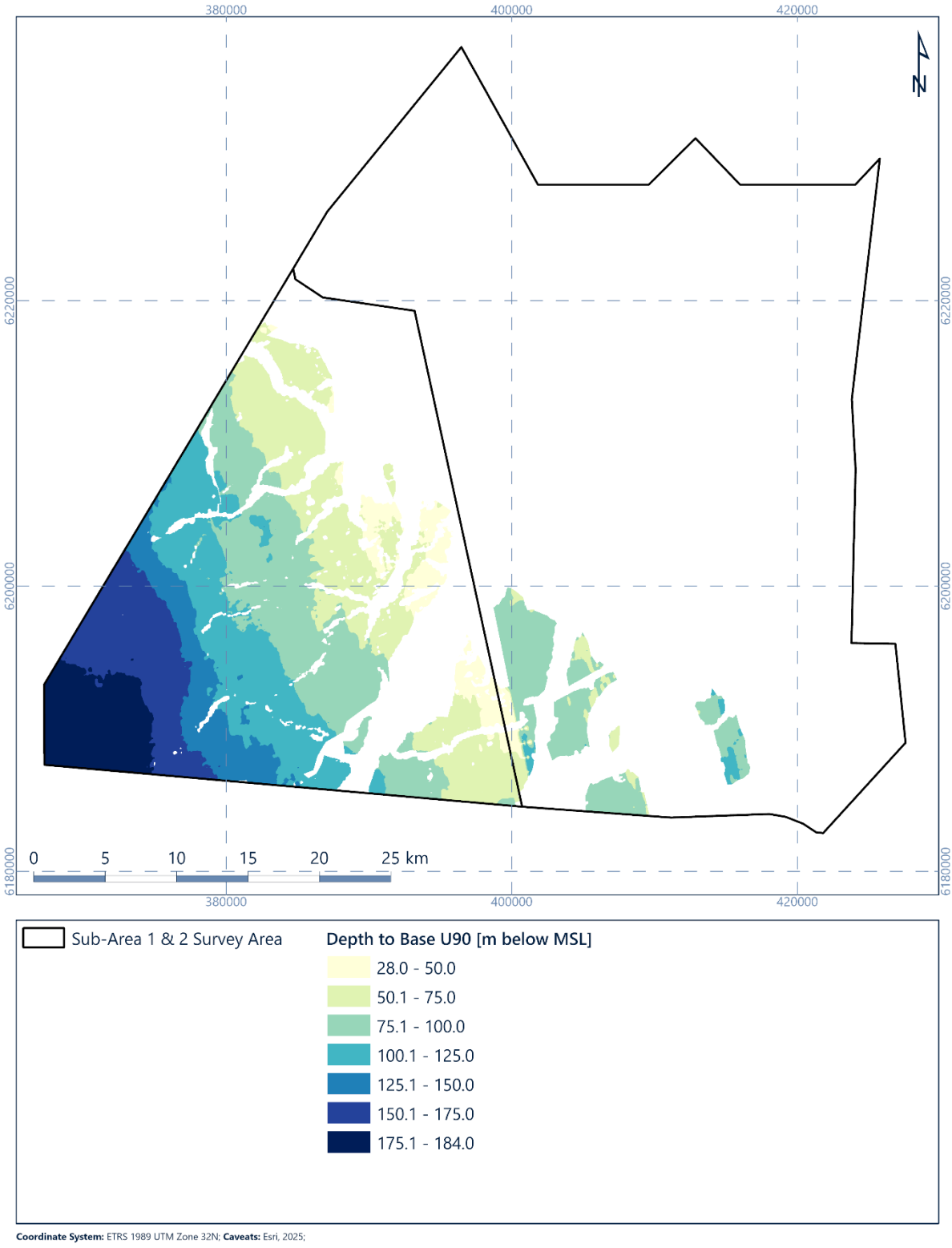

Figure 6.62: Depth [m below MSL] to horizon H90 (base of geological unit U90)

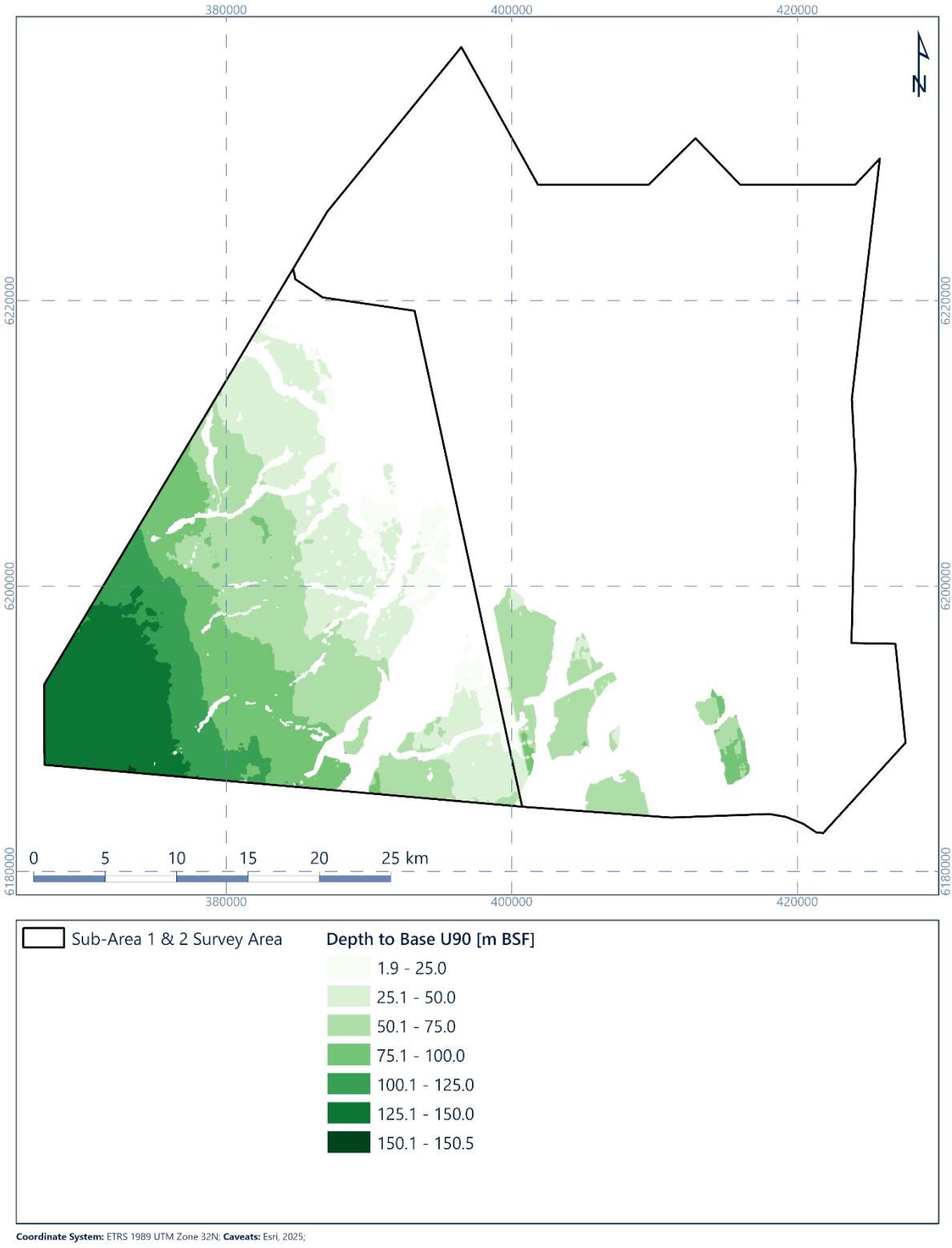

Figure 6.63: Depth [m BSF] to horizon H90 (base of geological unit U90)

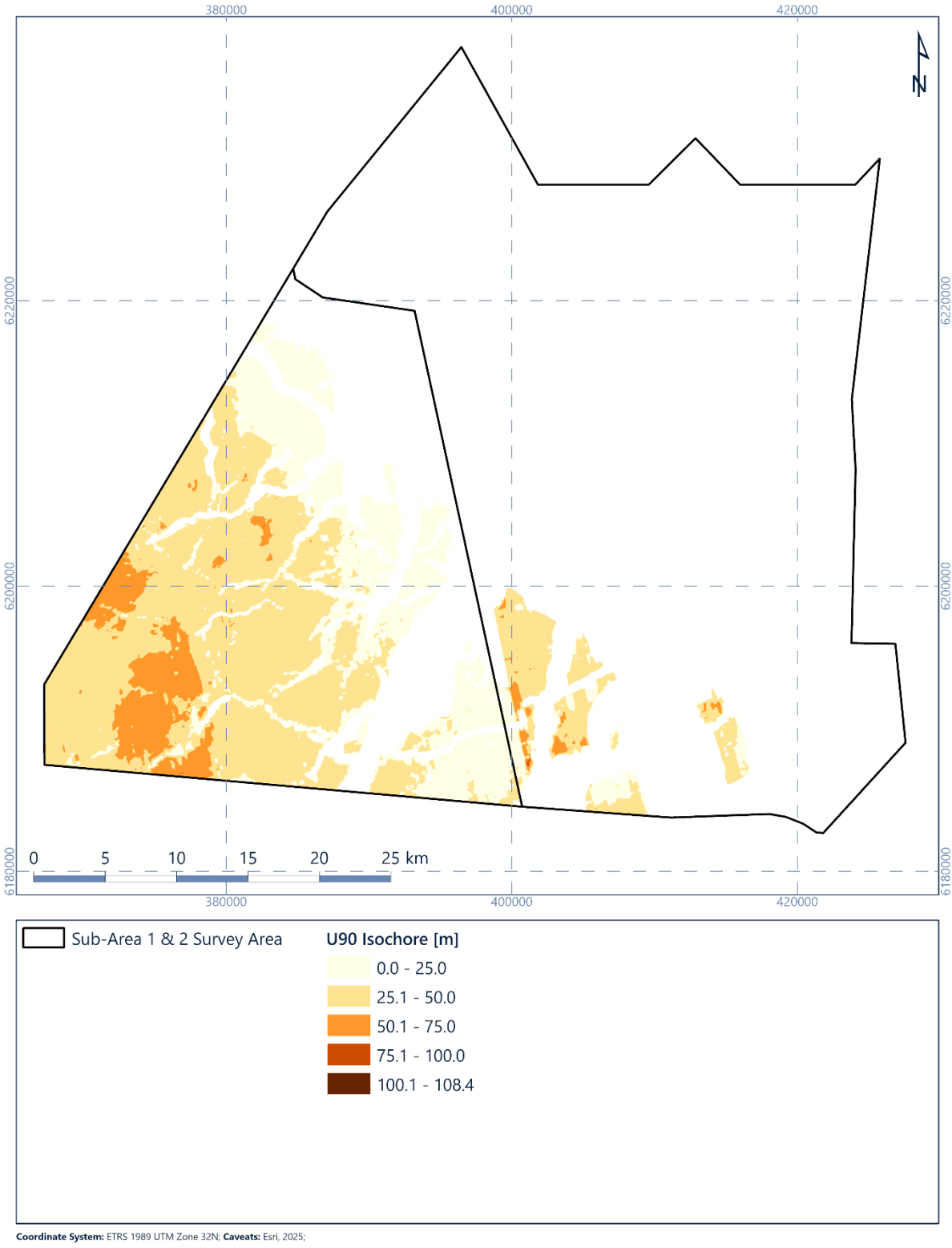

Figure 6.64: Isochore of geological unit U90 [m]

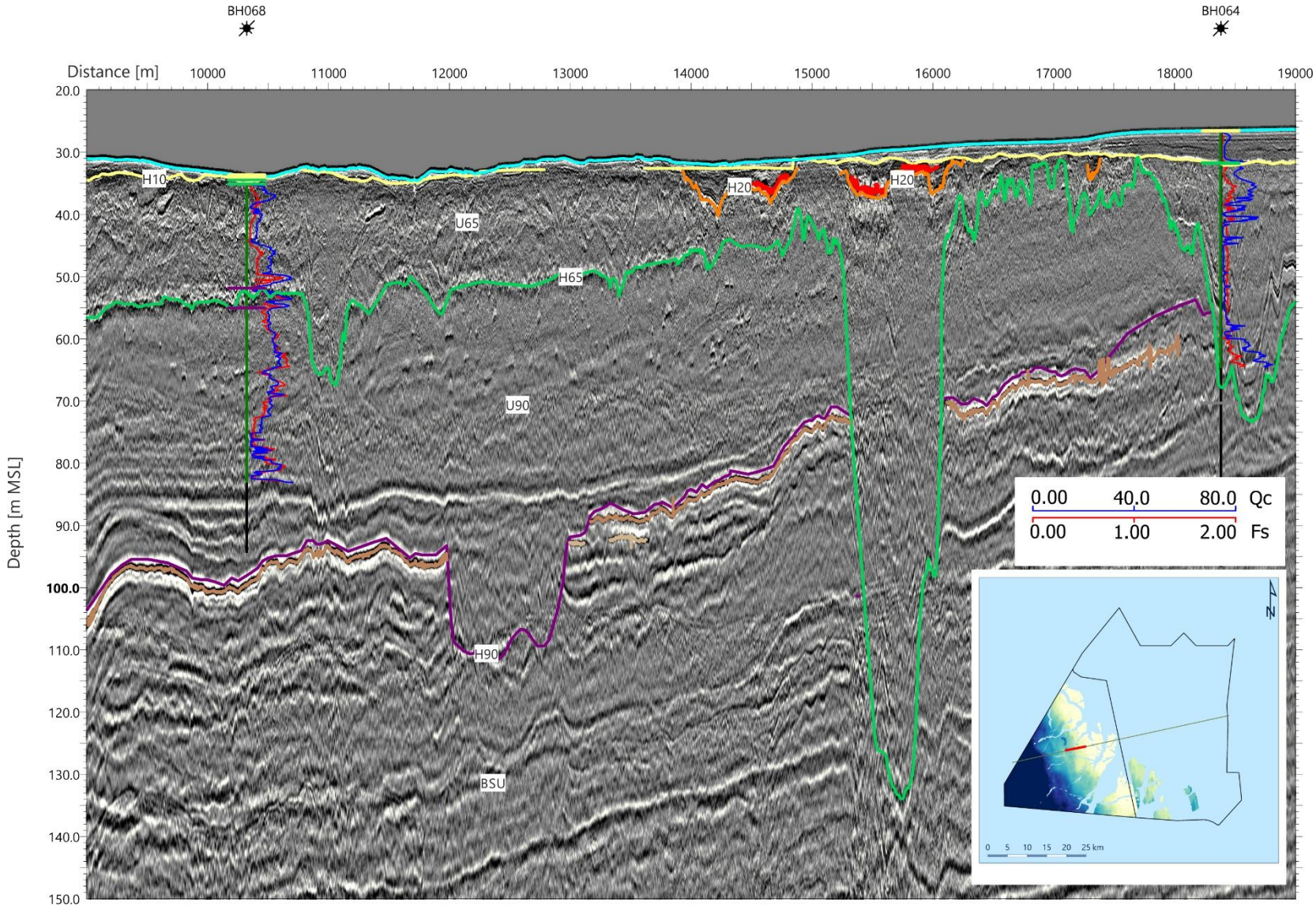

Figure 6.65: 2D UHR seismic data example of Unit U90. Line EAXB396P1, BH64 and BH068

6.13.2 Integration and Interpretation

The gradual expansion of the delta of the Eridanos river from the east of the site into the west of the site resulted in a transition from open marine sediments to fluvial sediments being deposited. The boundary between these Pre-Quaternary sediments and the earliest Quaternary material is observed as a regional deposit of organic rich peat and clay. Geological unit U90 material above this boundary characterises deposition in the early Pleistocene, with sediments within the study area suggesting a fluvial depositional environment that continued for the duration of the geological unit U90 deposition. The exact age of these sediments cannot be determined using currently available data, but are thought to represent early and middle Pleistocene deposition.

The geometry of the unit and the dominant soil type, comprising mostly sand with possible local peat beds, indicates that geological unit U90 was deposited in a meltwater (braided river in an outwash plain) depositional environment. Geological unit U90 is interpreted to form fluvial delta-top deposits of the Cenozoic delta system of the Eridanos river (Figures 3.1 and 3.2), suggesting a Miocene to Middle Pleistocene age. Available geotechnical data in geological unit U90 does not show significant variability compared with the other geological units across the site. Figure 6.66 displays the correlation of the H90 geophysical horizon with the geotechnical data recovered.

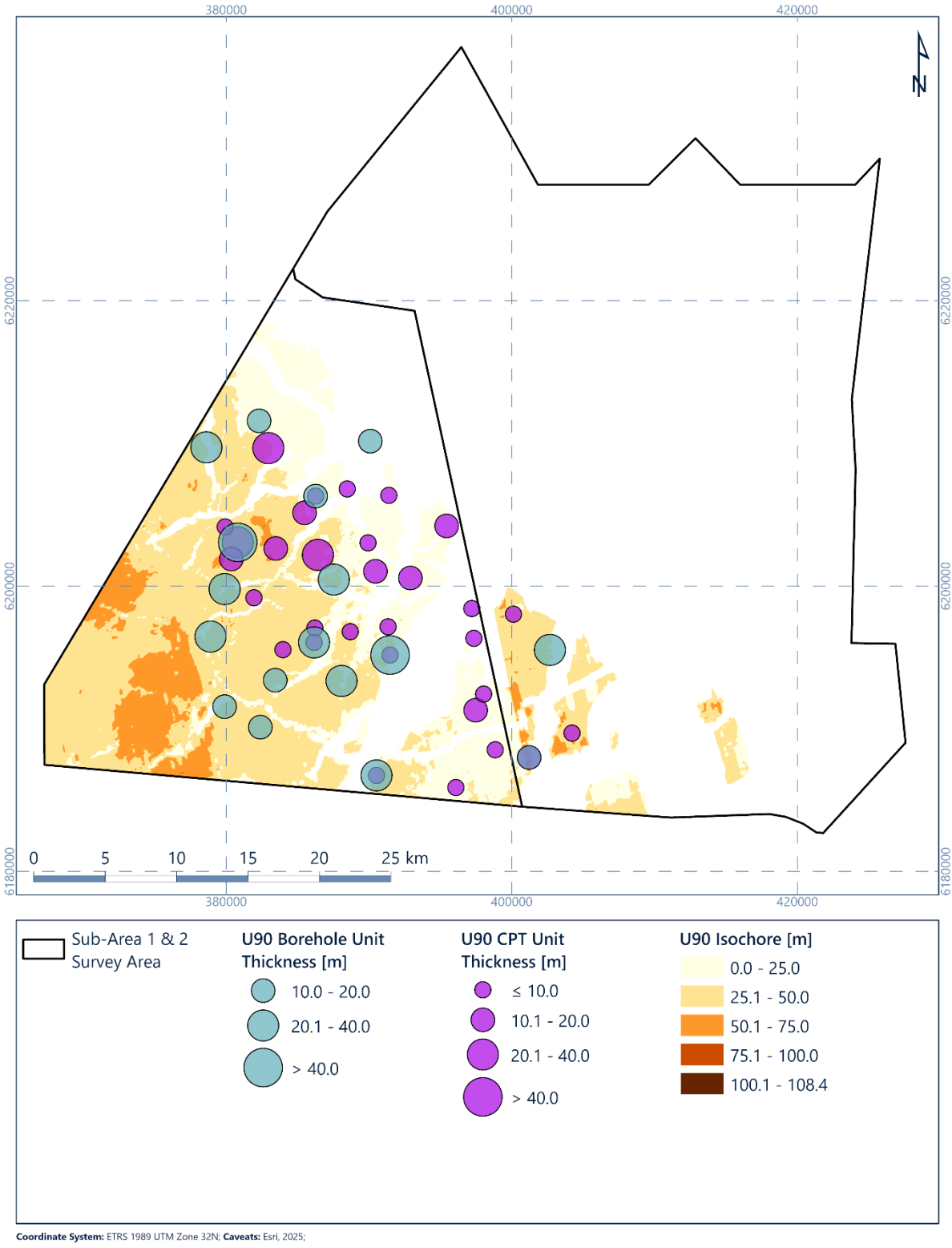

Figure 6.66: Isochore for geological unit U90 correlated with geotechnical data recoveries

6.14 Geological Unit – Base Seismic Unit

6.14.1 Seismic Character

The BSU is the deepest interpreted unit within the depth of penetration of the 2D UHR seismic data. Its top is locally very close to the seafloor in areas where it was thrust upwards by glacio-tectonic deformation.

The BSU is internally stratified. The parallel reflectors are horizontal to gently dipping towards the south-west (Figure 6.65 and Figure 6.67). The boundary between the BSU and the overlaying geological unit U90 is not marked by a clear reflector but is depicted by the change in seismic character between the two units. A negative polarity high amplitude reflector is present in the BSU in the south-east of the site. Other local internal erosion surfaces and high amplitude seismic anomalies with negative polarity are observed in BSU (Section 6.15.1).

The BSU is deformed by thrust faults that generally dip towards the east and north in the north, centre, and south-east of the site (Section 6.15.7). It contains locally steep normal faults in the east of the site (Section 6.15.8).

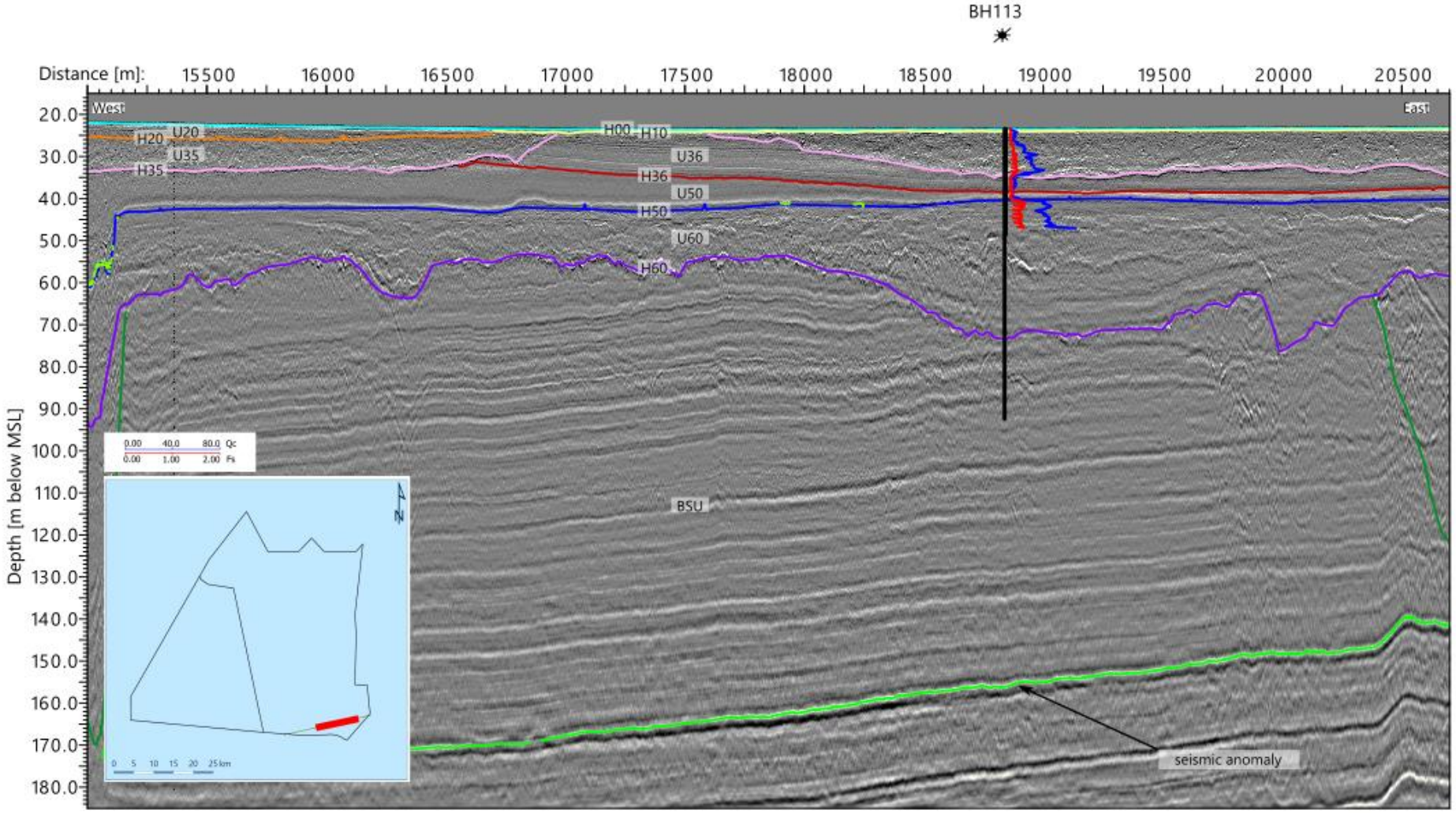

Figure 6.67: 2D UHR seismic data example of the BSU. EAAXD420P1, SCPT113

6.14.2 Integration and Interpretation

The oldest sediments at the site are predicted to belong to the Pre-Quaternary, likely from the Miocene (Section 3.2). These sediments, as outlined in the regional geological setting, were largely deposited in a fluvial deltaic environment with a marine regression occurring during this period. This period of deposition is represented by the Base Seismic Unit (BSU), which comprises both sands and clay, with a gradual increase in the coarse-grained component in the upper and younger sections of the unit.

The westward dip of the strata may be a structural dip or delta clinoforms (Overeem et al., 2001; Gibbard & Lewin, 2016). Geotechnical data show this unit is not lithified within the sampled depth ranges, but is instead represented by high strength clay sediments. Although no locations reached the base of the unit, the top shows consistency between datasets.

6.15 Geological Features and Geohazards

This section describes sub-seafloor geological features and geohazards identified in both geophysical data (including the SBP and 2D UHR seismic data) and geotechnical data in the survey area. Table 6.1 provides an overview. It is important to note that these geohazards are typical of the North Sea offshore environment, and windfarms have been developed to the north and south of this site. Detailed site characterisation should mitigate many of the impacts these geohazards.

Table 6.1: Overview of geological features and geohazards

Feature or Geohazard	Associated Geological Units	Possible Impact
Peat and/or organic clay	U20, U30, U50, BSU	High compressibility due to being very low strength may result in uneven and non-uniform support. It may cause a chemical reaction between the soil and steel. It also may affect cable performance due to limited thermal conductivity
Low strength clays	U20	Can only give limited and potentially uneven support to structures. May also affect cable performance due to limited thermal conductivity
Shallow gas	U20, U50	Soils with shallow gas have the potential for high compressibility, low and laterally variable soil strength and reduced bearing capacity. Gas may migrate into skirted foundations. Potential risk for blow out or gas release during drilling and piling operations
Coarse material	U10, U30, U35, U60, U65, U70, U90	May form an obstruction and result in insufficient or non-uniform support and/or penetration of foundations. May also form an obstruction for cable trenching
Buried channels and tunnel valleys	U20, U30, U35, U50, U60, U65, U69, U70	Likely to be associated with high lateral and horizontal variability in soil conditions, as well as uneven support for foundations. Lag deposits often exist at the base of each succession, comprising gravels, cobbles and possible boulders
Geological unit U65 variability	U65	Soils with high variability both vertically and laterally, with chaotic glacial soils and cross-cutting tunnel valleys, could provide non-uniform support to foundations. Presence of

Feature or Geohazard	Associated Geological Units	Possible Impact
		extremely high strength and low strength material gives contrasting bearing limits
Glacial deformation	U65, U70, BSU	May be associated with variability in soil conditions and lower lateral resistance due to deformation from glacial processes. This may result in non-uniform foundation support
Faults	U70, BSU	Soil properties may vary vertically and laterally resulting in non-uniform support of foundations. Faults may be re-activated due to human interference. Active faults may be associated with critical stress and possible failure of structures
Notes BSU = Base seismic unit		

6.15.1 Peat and/or Organic Clay

Peat is an organic-rich fibrous sediment formed following partial decomposition of plant and organic material. Peat is likely to have been deposited in a terrestrial setting when sea level was lower, such as in a deltaic environment.

Peat and organic clay typically forms a very low strength soil that is highly compressible, resulting in uneven or non-uniform support which may require consideration for foundation design and installation, as well as cable installation due to its limited thermal conductivity. The presence of peat can also cause a chemical reaction between the soil and steel that could locally increase corrosion rates.

Seismic anomalies with high amplitude and negative polarity were observed in several units; these are interpreted as potential accumulations and layers of peat and/or organic clay.

High amplitude, negative polarity reflectors are present in geological units U20 (Section 6.4), U30 and U50 (Sections 6.5 and 6.8) with a length of up to 3 km. Locally, signal attenuation is observed below. These seismic anomalies are typically at or near the base of these units and can be associated with buried channels. These high amplitude reflectors are mapped as '*2DUUHR_seismic_anomalies_U20*' and '*2DUUHR_seismic_anomalies_U30U50*' in Figure 6.68 and Figure 6.70. These anomalies were tested by CPTs and boreholes at several locations and have a high friction ratio as well as peat and organic-rich sediments. Figure 6.69, Figure 6.71 and Figure 6.72 show examples of this sampled peat and organic-rich sediments in geological units U20, U30 and U50.

In the BSU, continuous high amplitude, negative polarity reflectors are present in the south-west of the site, with a length of up to 20 km. This high amplitude reflector is mapped as '*2DUUHR_seismic_anmolies_BSU (a, b or c)*' (Figure 6.73). These anomalies were tested by geotechnical locations and may represent beds of peat and/or organic-rich clay, with some correlation between them and these deposits, but also the boundary between geological unit U90 and BSU. Figure 6.74 presents one example of

peat within BSU that correlates to this seismic anomaly in BSU and to the boundary between geological unit U90 and BSU at BH059.

There is also a continuous positive high amplitude reflector is present at a depth of 100 m to 170 m BSF, and locally as shallow as 10 m BSF, with a length of up to 15 km (Figure 6.73 and Figure 6.74). This high amplitude reflector is mapped as '*2DUUHR_seismic_anomalies_BSU*'. It may indicate a bed with a different soil type within the BSU such as organic clay and/or peat. Alternatively, this reflector may indicate a soil boundary from clay above to sand below the reflector. The thrust faults detach more or less at the same depth as this seismic anomaly. This observation confirms the likelihood of a change in material properties, such as at a boundary of sand and clay.

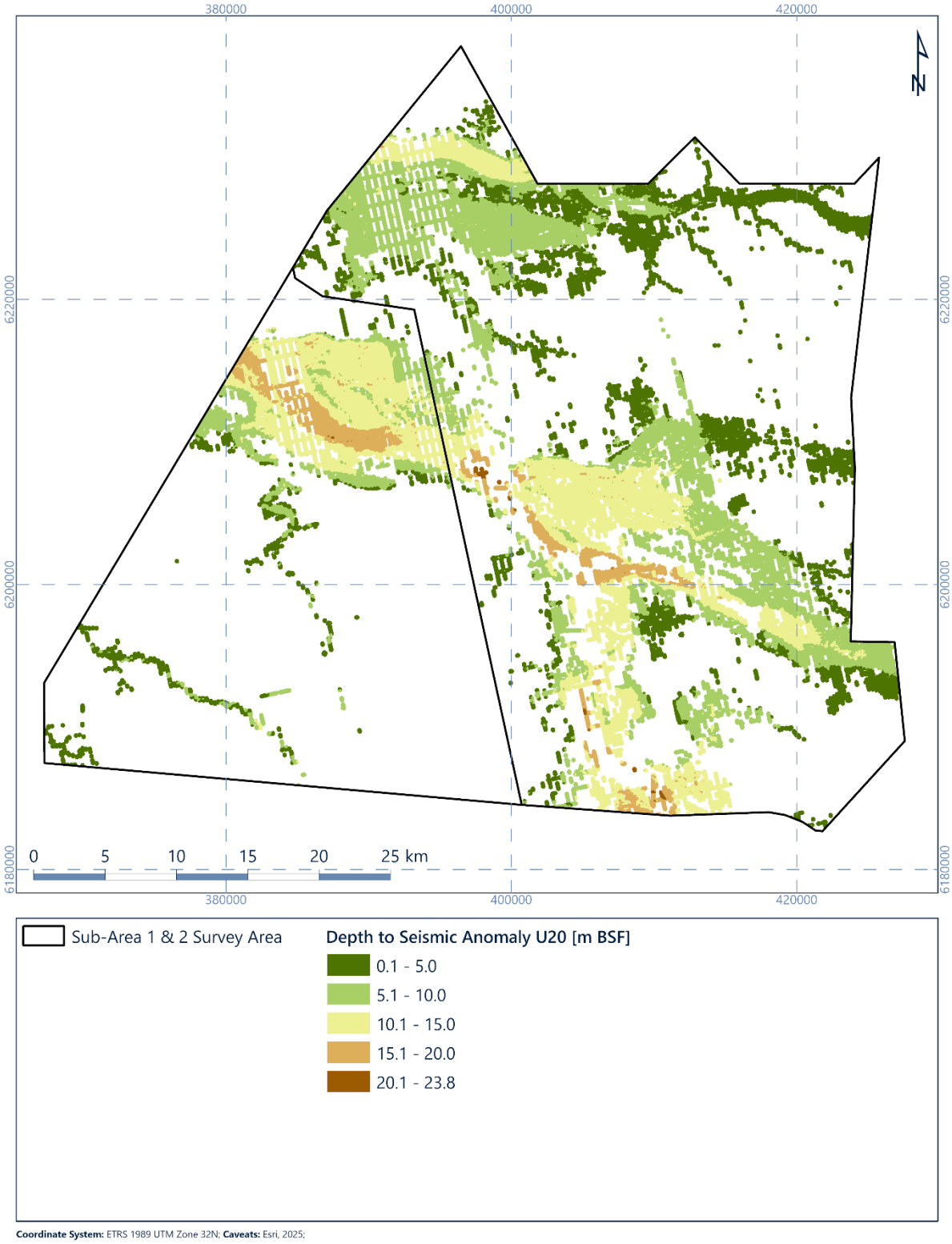

Figure 6.68: Map of seismic anomalies in geological unit U20 [m BSF]

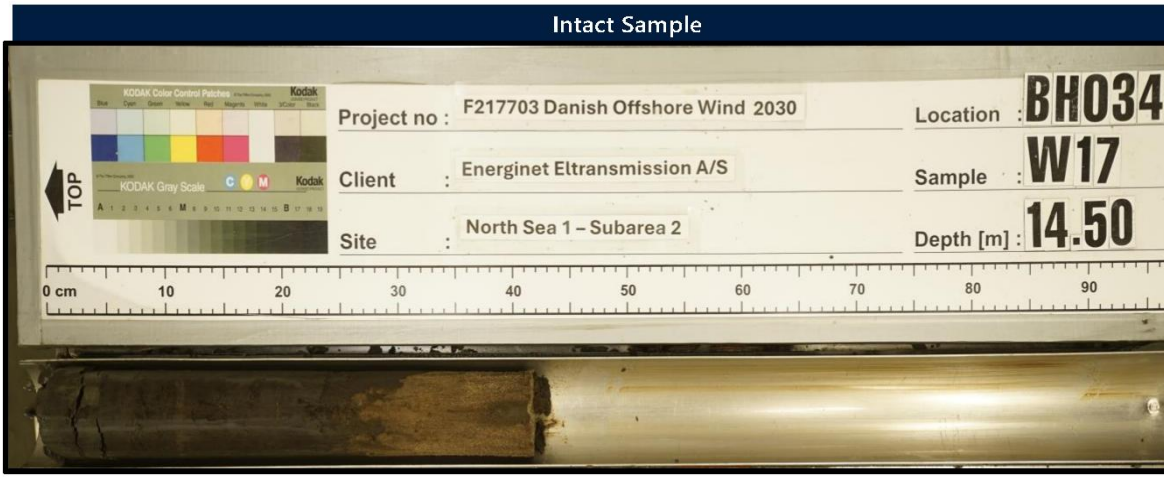

Sample Point : BH034 Sample : WIP17 Depth [m BSF] : 14.50

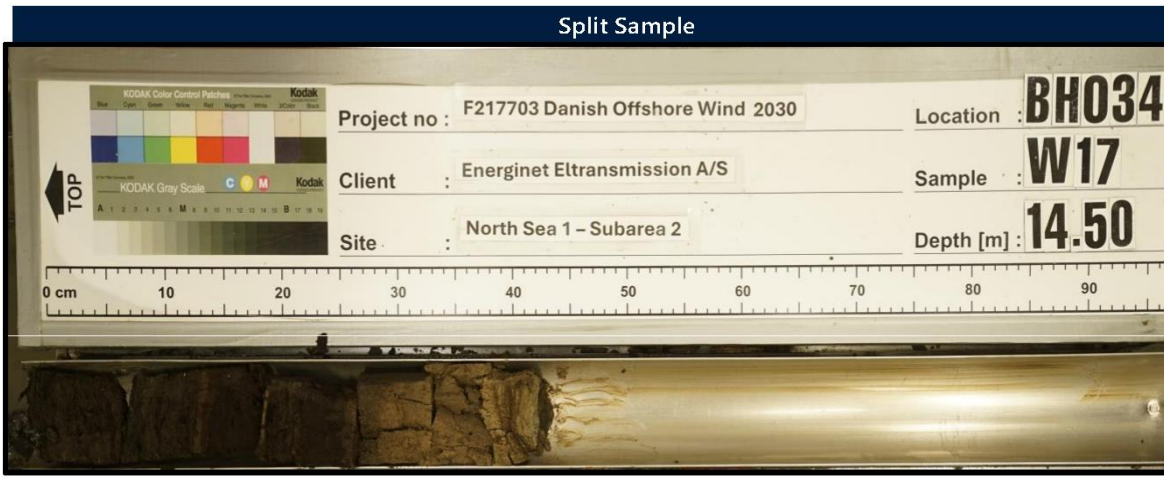

Sample Point : BH034 Sample : WIP17 Depth [m BSF] : 14.50

Figure 6.69: Geotechnical example of peat/organic clay in geological unit U20 at BH034

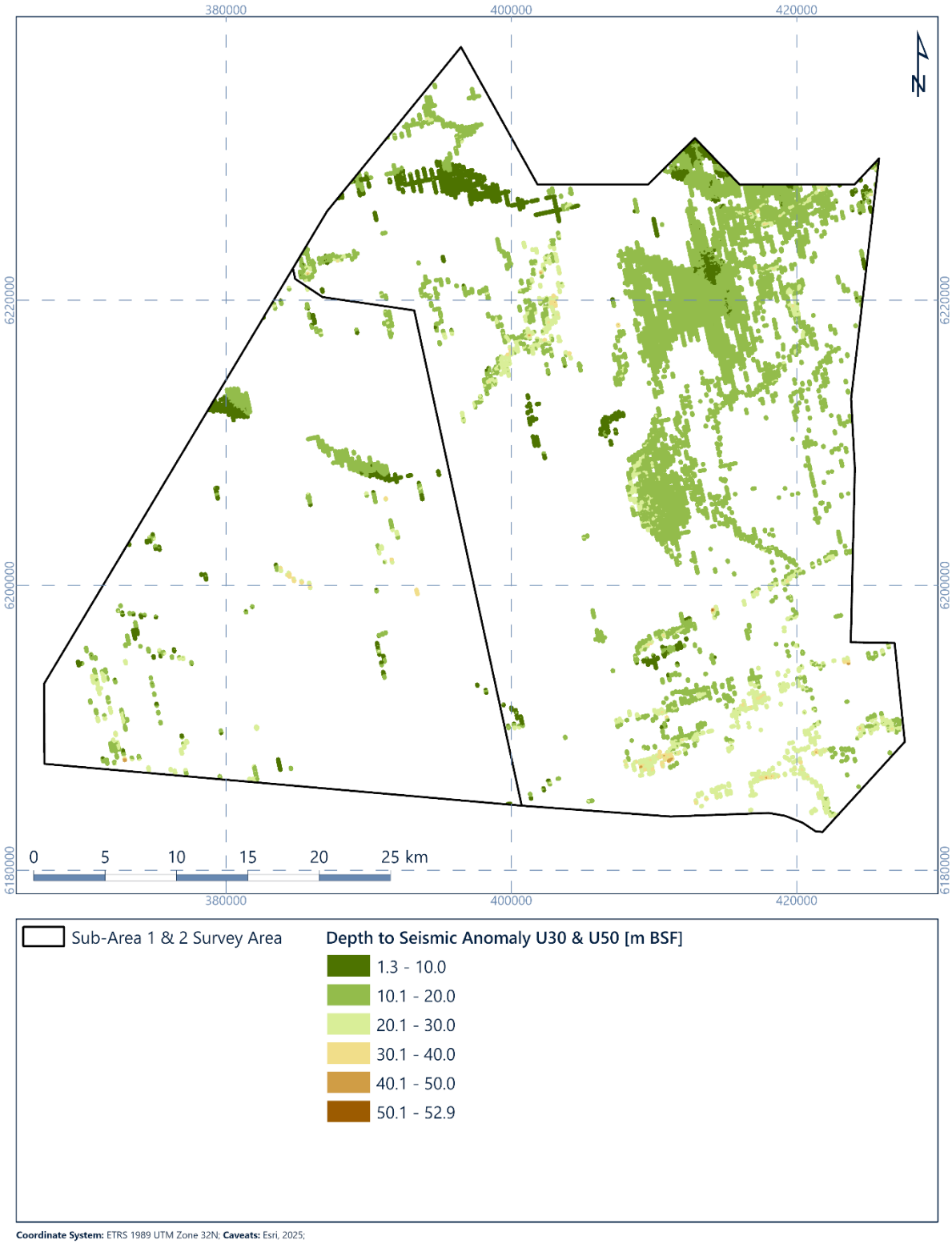

Figure 6.70: Map of seismic anomalies in geological units U30 and U50 [m BSF]

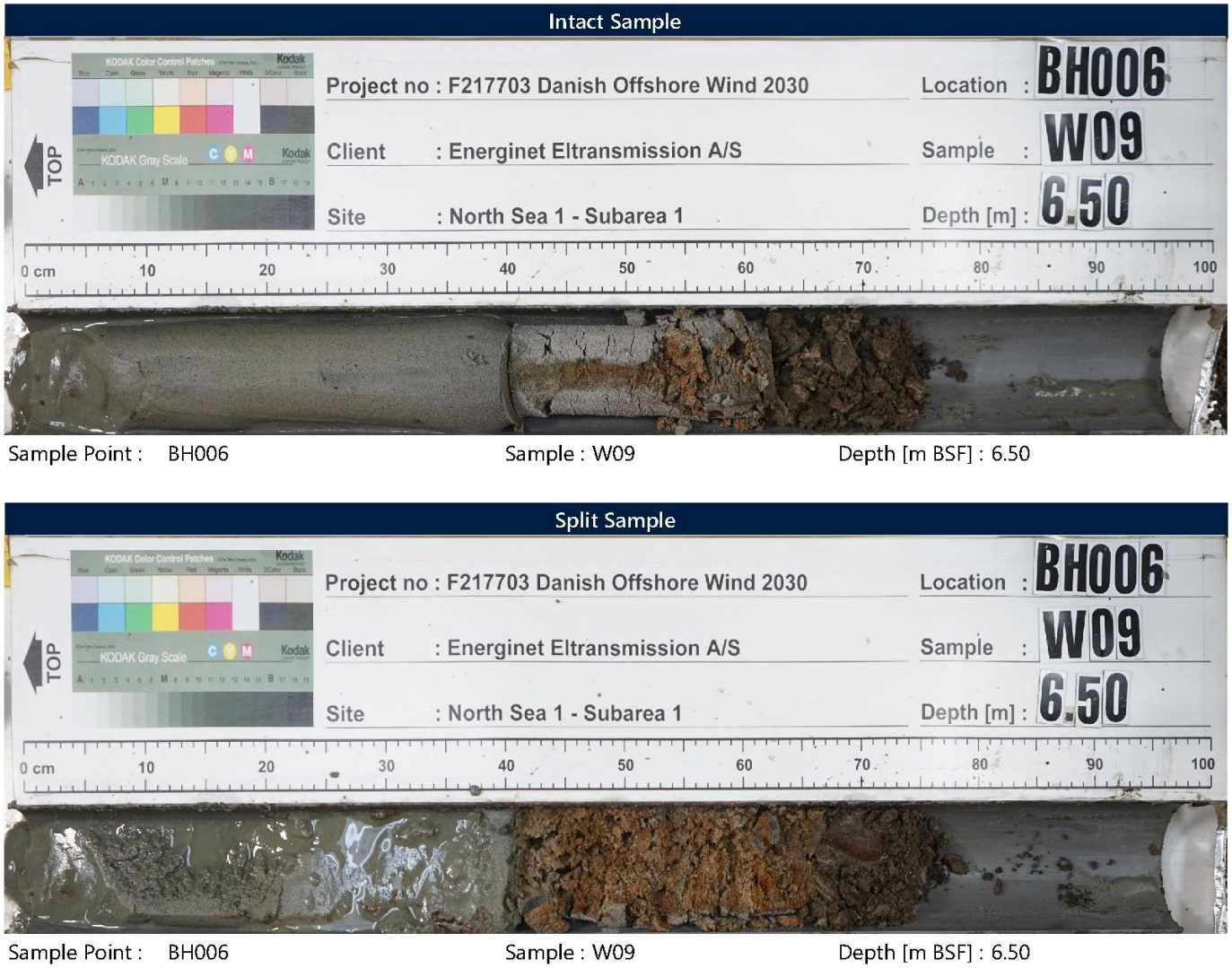

Figure 6.71: Geotechnical example of peat or organic clay in geological unit U30 at BH006

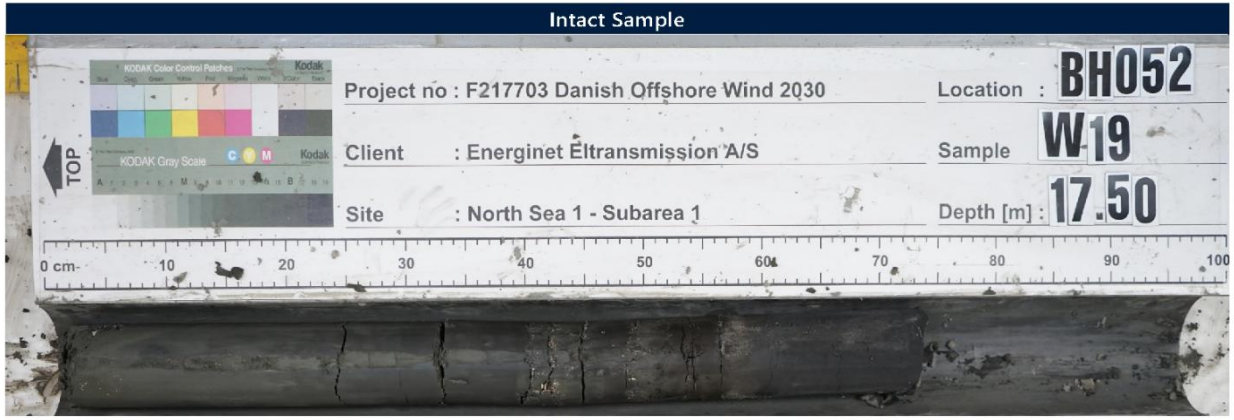

Sample Point : BH052 Sample : W19 Depth [m BSF] : 17.50

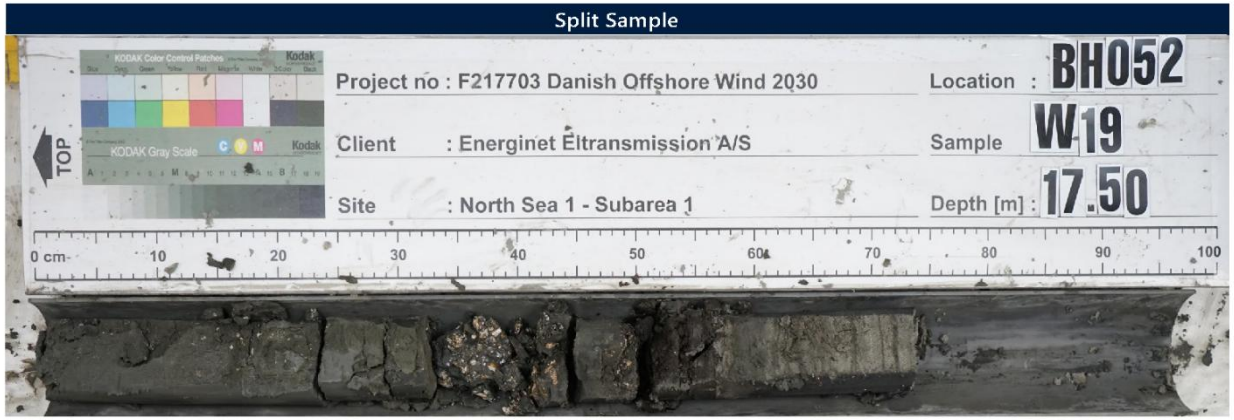

Sample Point : BH052 Sample : W19 Depth [m BSF] : 17.50

Figure 6.72: Geotechnical example of peat or organic clay in geological unit U50 at BH052

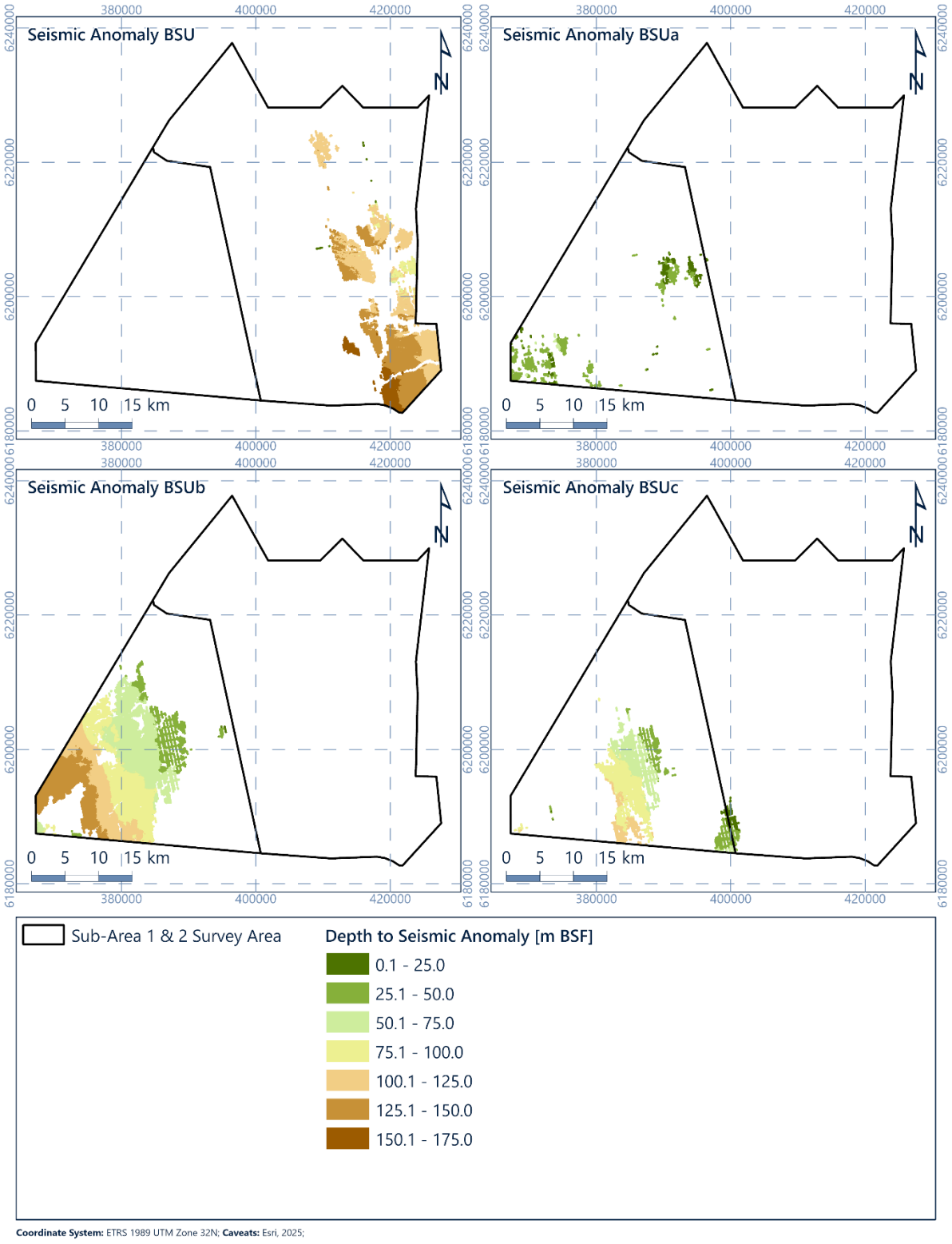

Figure 6.73: Map of seismic anomalies in geological unit BSU [m BSF]

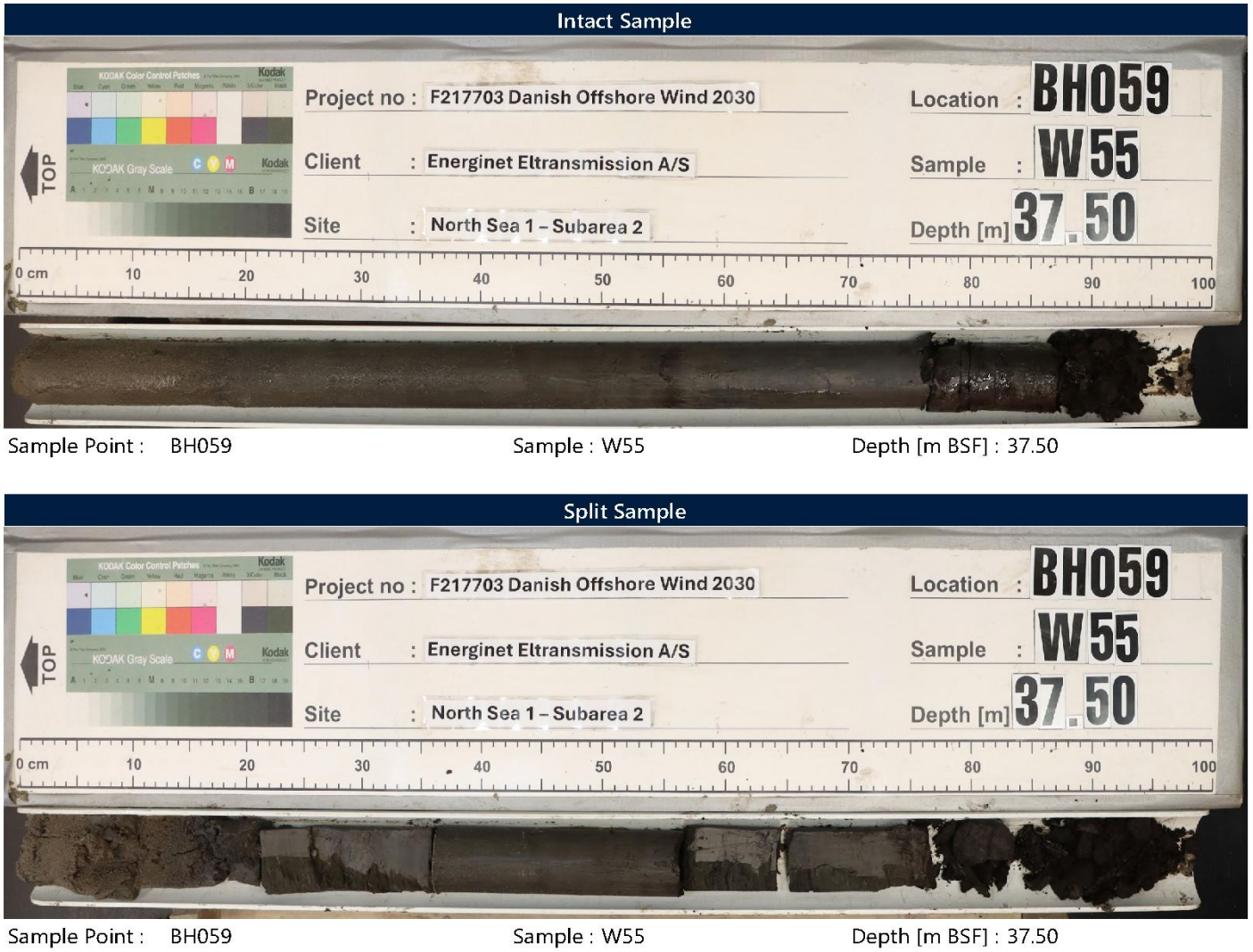

Figure 6.74: Geotechnical example of peat or organic clay in geological unit BSU at BH059

6.15.2 Low Strength Clay

Geological unit U20, particularly subunit U20b, contains low strength clay sediments that may represent a challenge for foundation engineering as it may give limited and potentially uneven support to structures and may also affect cable performance due to limited thermal conductivity. These clay units were likely to be deposited in post-LGM lacustrine or enclosed estuarine marine depositional environments prior to the Holocene transgression.

Figure 6.14 show the spatial extent and locations where geological unit U20b is present in the geotechnical data. For further details of the geotechnical characteristics of these sediments, see Section 7.

6.15.3 Shallow Gas

Accumulations of shallow gas can be caused by biogenic production of methane, and subsequent migration, and accumulation in the subsurface. Due to the nature and possible presence of organic matter, free gas is likely to be generated and trapped in the Upper Pre-Quaternary (Miocene) deltaic environments that correlate to geological unit BSU and/or within Quaternary palaeo-channel or tunnel valley deposits.

The presence of shallow gas within the foundation depth of interest may degrade the strength of the soils, reducing pile capacity. The chemistry of the related pore fluids may also result in accelerated corrosion. The presence of shallow gas in soils can also lead to high compressibility, with low and laterally variable soil strength. Gas can also migrate into skirted foundations. The occurrence of shallow gas poses a potential risk for blow out or gas release during drilling or piling operations.

The 2D UHR seismic data shows evidence for the presence of shallow gas in the form of acoustic blanking and signal attenuation often, but not always, associated with a high amplitude, negative polarity reflector. Acoustic blanking is present in geological Units U20 and, to a much lesser extent, U50.

In geological unit U20, seismic anomalies with associated acoustic blanking or signal attenuation are present at a depth of approximately 5 m and 15 m BSF (Figure 6.75 and Figure 6.77). Acoustic blanking is present where geological unit U20 is thick enough to develop free gas, which causes the acoustic blanking (Tóth et al., 2014). Correlation with organic-rich materials in geological subunit U20b and the blanking area is possible.

During the Sub-Area 2 borehole campaign, H2S was encountered at BH046, this was odour was noticed from 1 m BSF; correlating the beginning of geological unit U20.

In geological unit U50, seismic anomalies (Figure 6.76 and Figure 6.78) with associated acoustic blanking and signal attenuation are only locally present, often where the base of geological unit U50 is channelised. These anomalies are associated with velocity pull-downs. Velocity pull-downs, acoustic blanking and signal attenuation indicate the presence of gas in the soil.

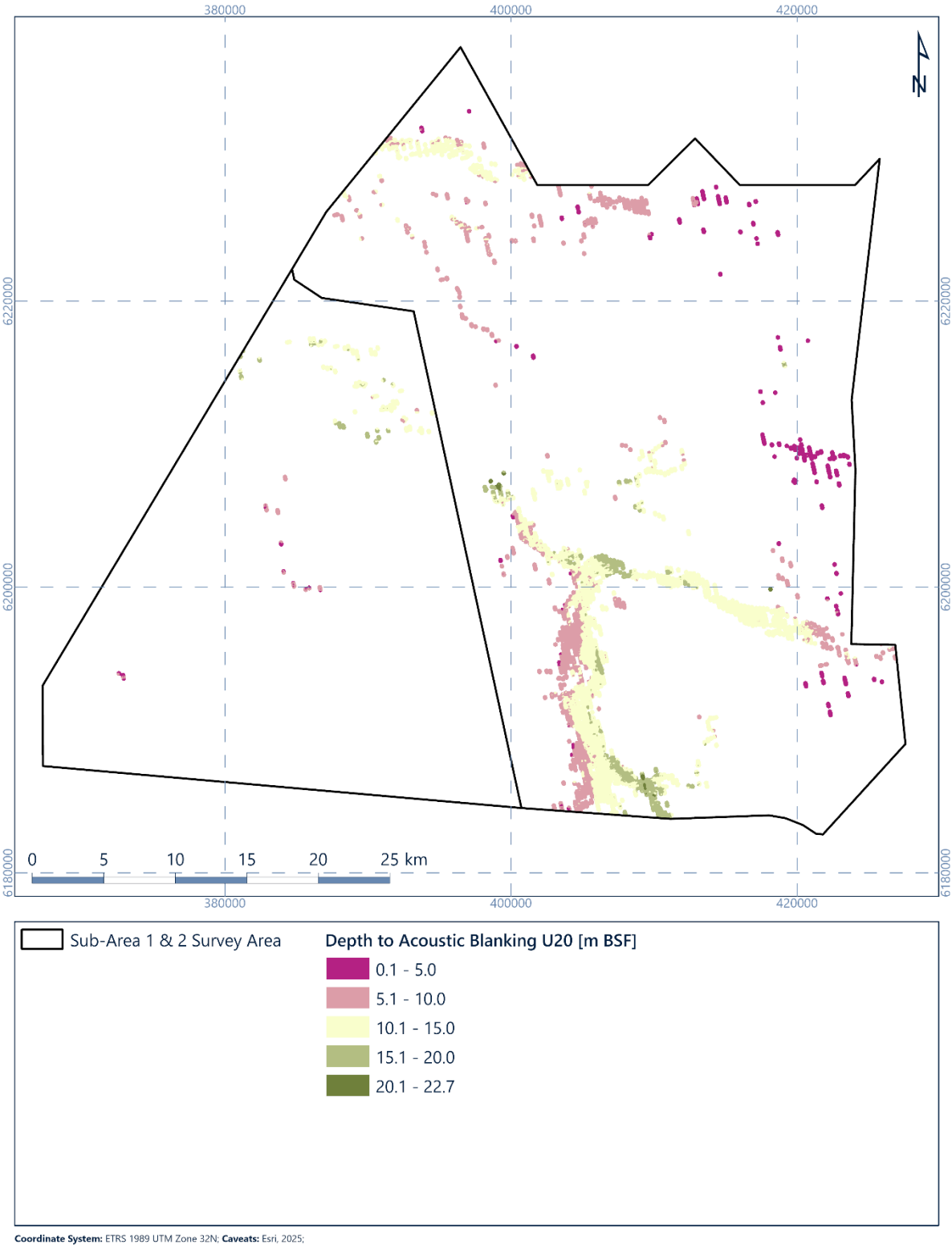

Figure 6.75: Depth (m BSF) to top of acoustic blanking in geological unit U20

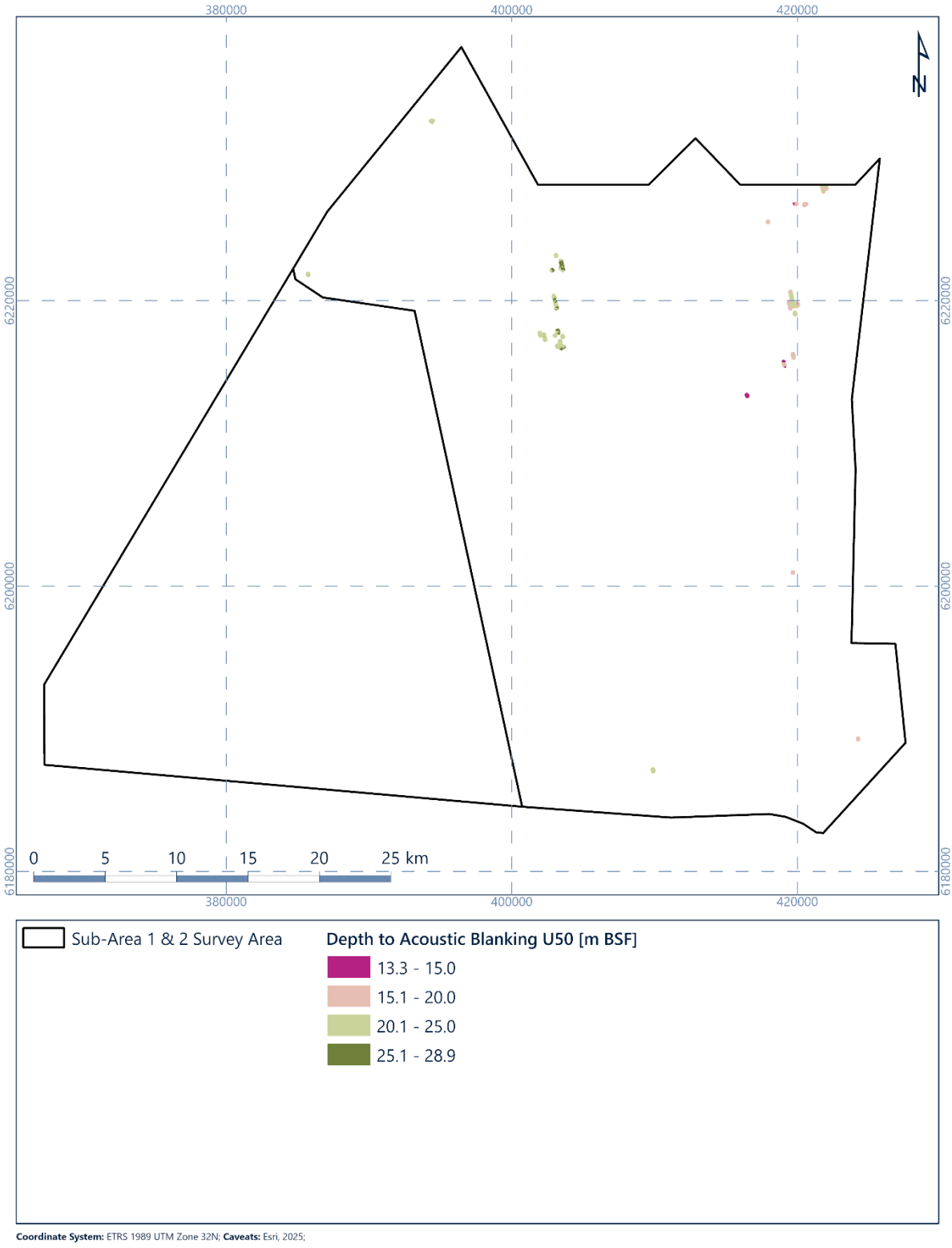

Figure 6.76: Depth (m BSF) to top of acoustic blanking in geological unit U50

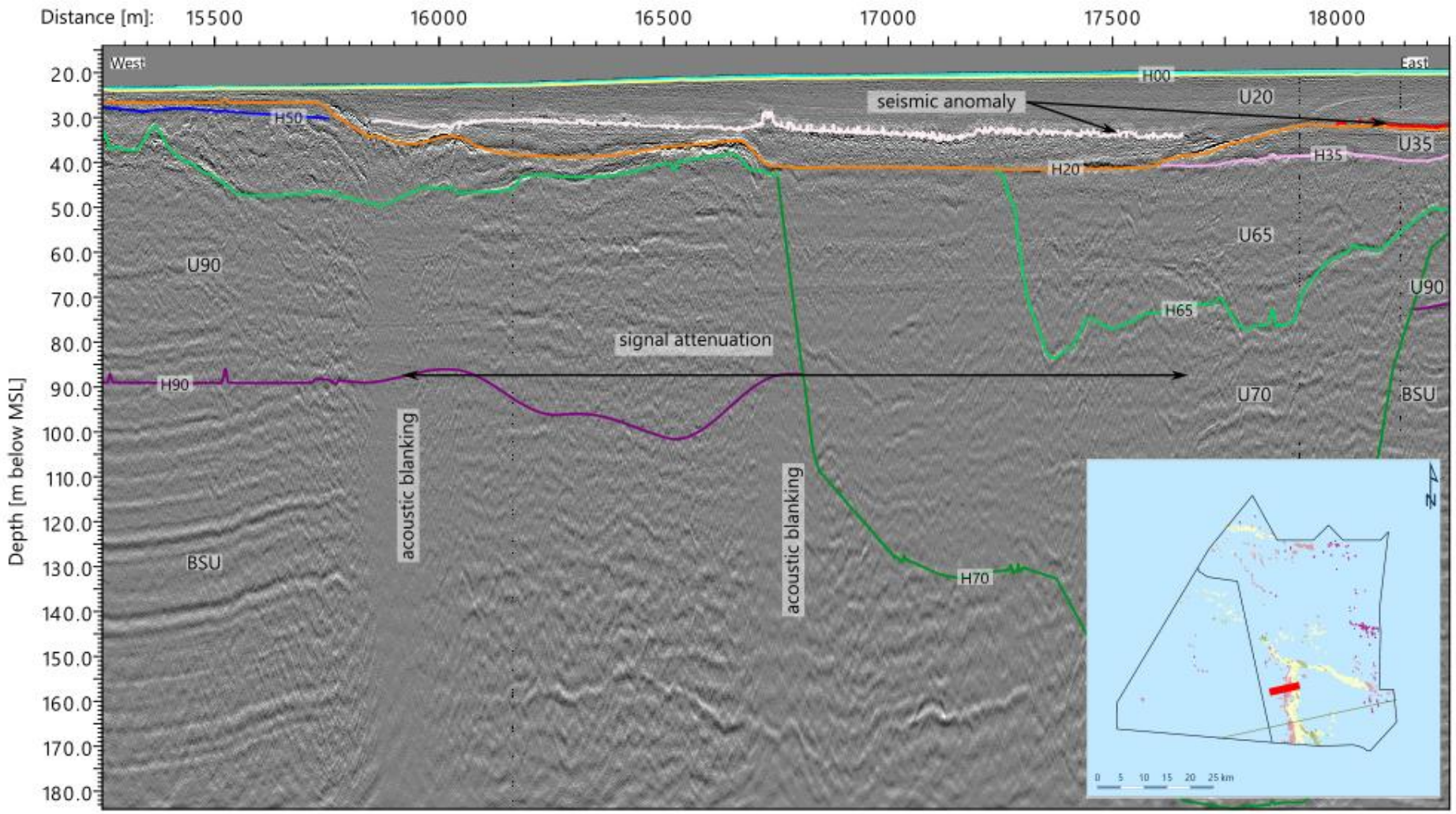

Figure 6.77: 2D UHR seismic data example of acoustic blanking and signal attenuation in geological unit U20. Line EAXD415P1

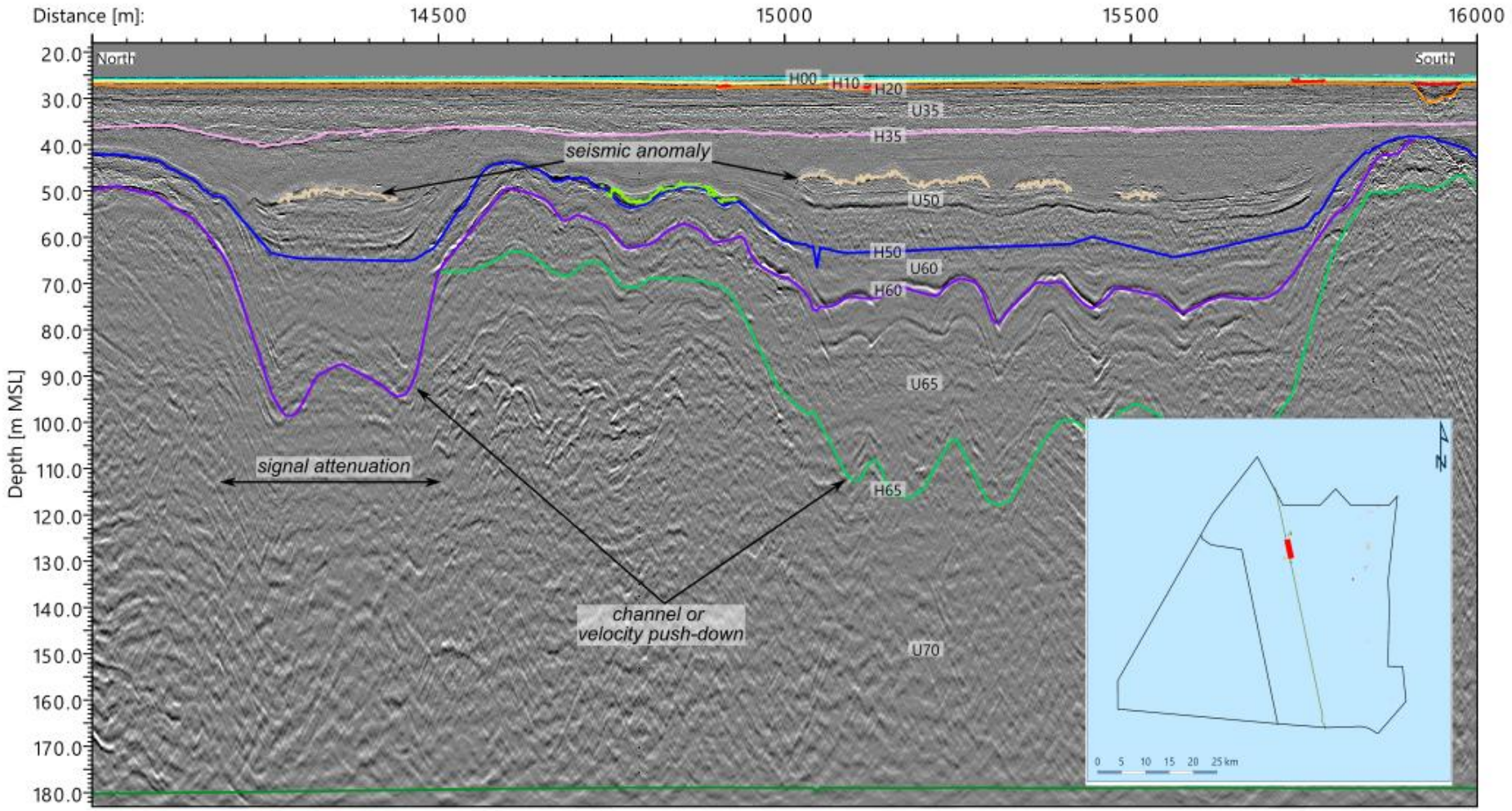

Figure 6.78: 2D UHR seismic data example of signal attenuation in geological unit U50. Line EAAS267P1

6.15.4 Coarse Material

6.15.4.1 Coarse Material – Gravel and Cobbles

As described throughout this report, a wide range of depositional environments have existed across the NS1 site, leading to the presence of variable soils across the region. These include glacial and deltaic sediments, which in Fugro's experience, are likely to contain coarse material such as accumulations of gravel and cobbles.

This coarse material may form obstructions and result in insufficient or non-uniform support and/or penetration for foundations, but may also impact trenching abilities for cables.

Reworking of glacial soils during flood events across the Danish North Sea during the Holocene transgression (Section 3.4) shows shallow coarse material within Holocene sediments. Shallow coarse material is predominantly expected within the Holocene Post-LGM to recent sediments, for example geological unit U10. This unit has formed large sand banks that are observed at seafloor that are visible in Sub-Area 2 where geological unit U10 is significantly thicker. There is more presence of gravel within the geotechnical data higher energy shallow marine environments.

Geological units U30, U35, U60, U65 and U90 comprise sediments interpreted to have been deposited in a braided river environment. Gravel and cobbles are associated with braided river environments. In geological units U35 and U60, positive, relatively high amplitude internal reflectors may represent gravel beds or accumulations. Furthermore, gravel is sampled within units in the borehole data at many locations, especially where geological unit U65 is present.

Cobbles were found at several locations where it impacted the drilling capability. For example, at BH072A and BH091, a drill-out was needed for the removal of a cobble in geological unit U65. In total, 11 locations in Sub-Area 1 and 10 locations in Sub-Area 2 encountered gravel layers or cobbles that required a drill-out for sampling to continue.

6.15.4.2 Boulders

Boulders (greater than 200 mm in diameter) are known to be a common feature within glacially derived sediments across the North Sea. In particular, boulders are deposited within glacial melt-out sediments and as a direct result of ice action, either at the front or at the base of ice sheets. Less frequently, they are deposited within the glacio-marine and glacial-lacustrine environments as dropstones from icebergs. Post-depositional reworking and erosion of glacial sediments may lead to boulders being present within non-glacial geophysical units. Regional Fugro experience shows that where glacial tills are present at, or near, seafloor, an increase in the density of boulders is observed.

Boulders may represent a constraint and a potential hazard for installation. An irregular seafloor morphology related to presence of boulders may lead to operational issues and

positioning uncertainties during installation operations. Early refusal or tip damage of driven pile foundations may occur where boulders are encountered.

Micro-siting of infrastructure may be required where boulders are identified both at seafloor and in the sub-surface. We expect the sub-seafloor conditions will be consistent with the Thor site (COWI, 2021) that is currently being installed.

Geological units U65 and U70 are interpreted as deposited in glacial depositional environments. Glacial deposits are often poorly sorted and may contain gravel, cobbles, and boulders.

Two geotechnical locations in Sub-area 1 where an obstruction was encountered are BH040 within geological unit U65 and BH013 within non-glacial geological unit U60. Although not confirmed as boulders, due to the geological units that these occurred in, these obstructions could be caused by the presence of boulders.

6.15.5 Buried Channels and Tunnel Valleys

6.15.5.1 Buried Channels

A buried channel is an erosive surface consequently flooded and infilled by multiple and variable sequences of fluvial and marine sediments (clay, sand and gravel). Lag deposits often exist at the base of each succession, comprising gravels, cobbles and possible boulders (Section 6.15.4). Compared to tunnel valleys, buried channels are smaller in size (depth and width) and occur shallower in the subsurface (Section 6.15.5.2), these can be formed in both glacial and post-glacial environments.

Buried channels are likely to be associated with high lateral and vertical variability in soil conditions and can potentially provide uneven support for foundations.

Geological units U20, U35, U50 and U60 locally form channel fills (Table 6.2). Some form relatively narrow channels with a low width-to-depth ratio. Others, especially in the east of the site, form relatively wide channels with a high width-to-depth ratio.

Geological units U30, U35 and U60 are interpreted to partially be deposits of braided river systems and contain internal channels and erosion surfaces.

Table 6.2: Occurrence of buried channels

Unit	Channelised Base [Y/N]	Internal Channels and Erosion Surfaces [Y/N]
U10	N	N
U20	Y (locally)	N
U30	N	Y
U35	Y (locally)	Y
U36	N	N

Unit	Channelised Base [Y/N]	Internal Channels and Erosion Surfaces [Y/N]
U50	Y (locally)	N
U60	Y (locally)	Y

6.15.5.2 Tunnel Valleys

Tunnel valleys are formed from sub-glacial processes during the Elsterian and Saalian (Section 3). These are much larger, and typically occur deeper, than buried channels (Section 6.15.5.1). Fugro experience shows tunnel valley infill typically comprise successions of sands and clay of variable density and strength and often contain coarse material, including boulders (Section 6.15.4).

Tunnel channels are likely to be associated with high lateral and vertical variability in soil conditions, including high strength material and can potentially provide uneven support for foundations.

Geological units U65, U69 and U70 form the infill of tunnel valleys. Geological unit U65 is also interpreted to partially be a deposit from a braided river system with internal and cross cutting valleys (Table 6.3).

Table 6.3: Occurrence of tunnel valleys

Geological Unit	Channelised Base [Y/N]	Internal Channels and Erosion Surfaces [Y/N]
U65	Y (locally)	Y
U69	Y	N
U70	Y	Y (similar to overlying Unit 69 but in deeper areas)
U90	N	N
BSU	N	N
Notes BSU = Base seismic unit		

6.15.6 U65 Variability

Borehole and geophysical data have revealed a complex subsurface sedimentary sequence within geological unit U65, with high lithological, spatial and geotechnical variability. Sections 6.10, 6.15.5.1 and 6.15.6.2 outline some of the characteristics of this geological unit, its inferred glacial origin, and the challenges it poses for subsurface mapping and hazard assessment.

The variability in this unit can cause high vertical and lateral changes, providing non-uniform support for foundation. The presence of extremely high strength and low strength materials will give contrasting bearing limits within a small area.

6.15.6.1 Internal Till Sediment

Within geological unit U65 there is a shallow interval associated with the unit predominantly located in the south-west of Sub-Area 2, the extent of which is presented in Figure 6.79 This was identified based on integration of geotechnical and geophysical data. This area was identified in BH data as representing an interval of more chaotic till sediment, characterised by a variable mixture of clay, sand, silt, and gravel.

This interval was corelated with geophysical data which highlighted a reflector associated with the base of this interval (Figure 6.80). Below this horizon, the lithology transitions into a coarser assemblage dominated by sand with subordinate gravel and silt, and a reduction in fine-grained material. Despite correlation between the datasets, the chaotic nature of the unit meant it is not possible to fully integrate these datasets and extrapolate a gridded depth horizon across the site. With further data acquisition at a future stage, this may be possible. It is interpreted that the observed variability within this unit may reflect deposition during a more recent glaciation event.

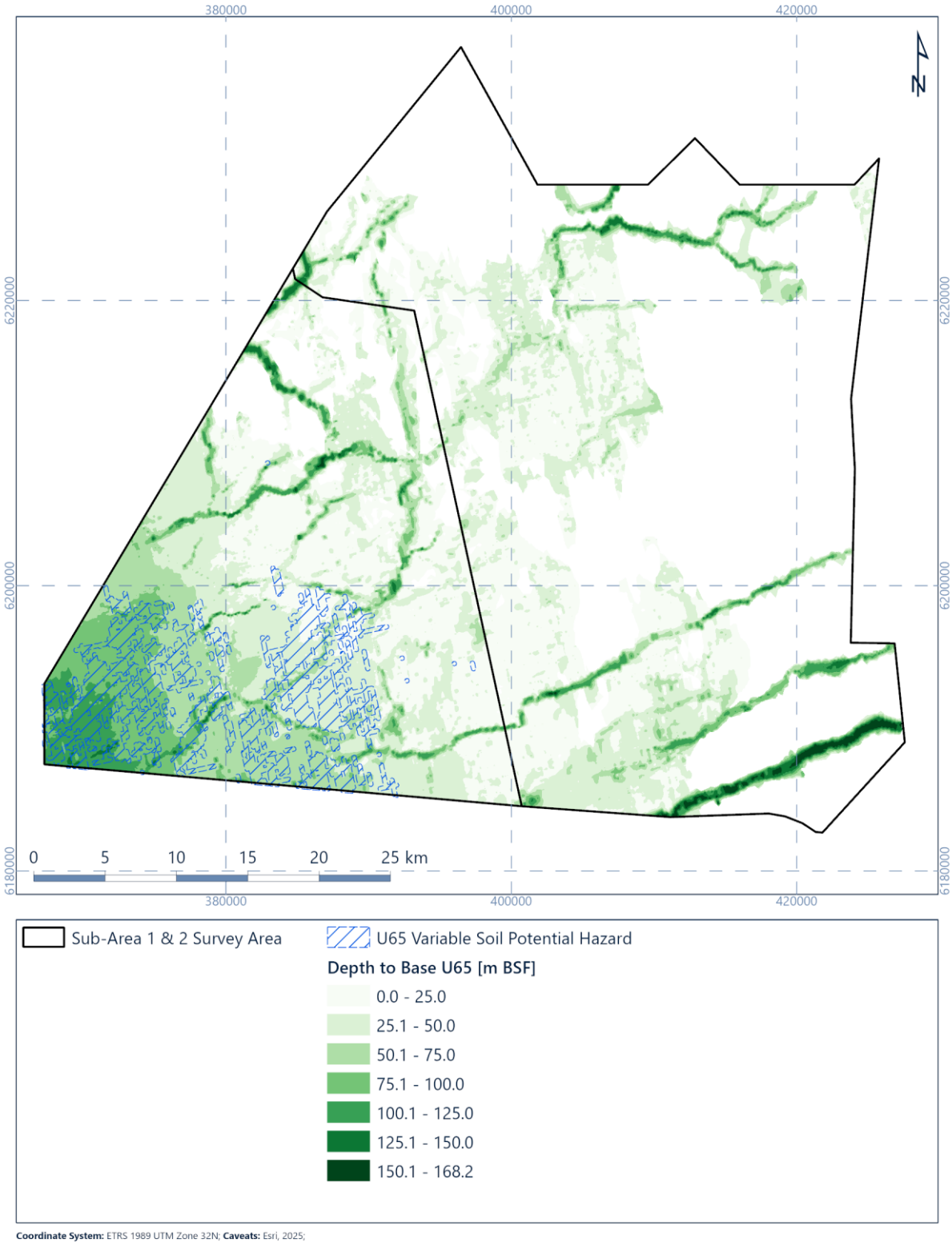

Figure 6.79: Geological Unit U65 variability

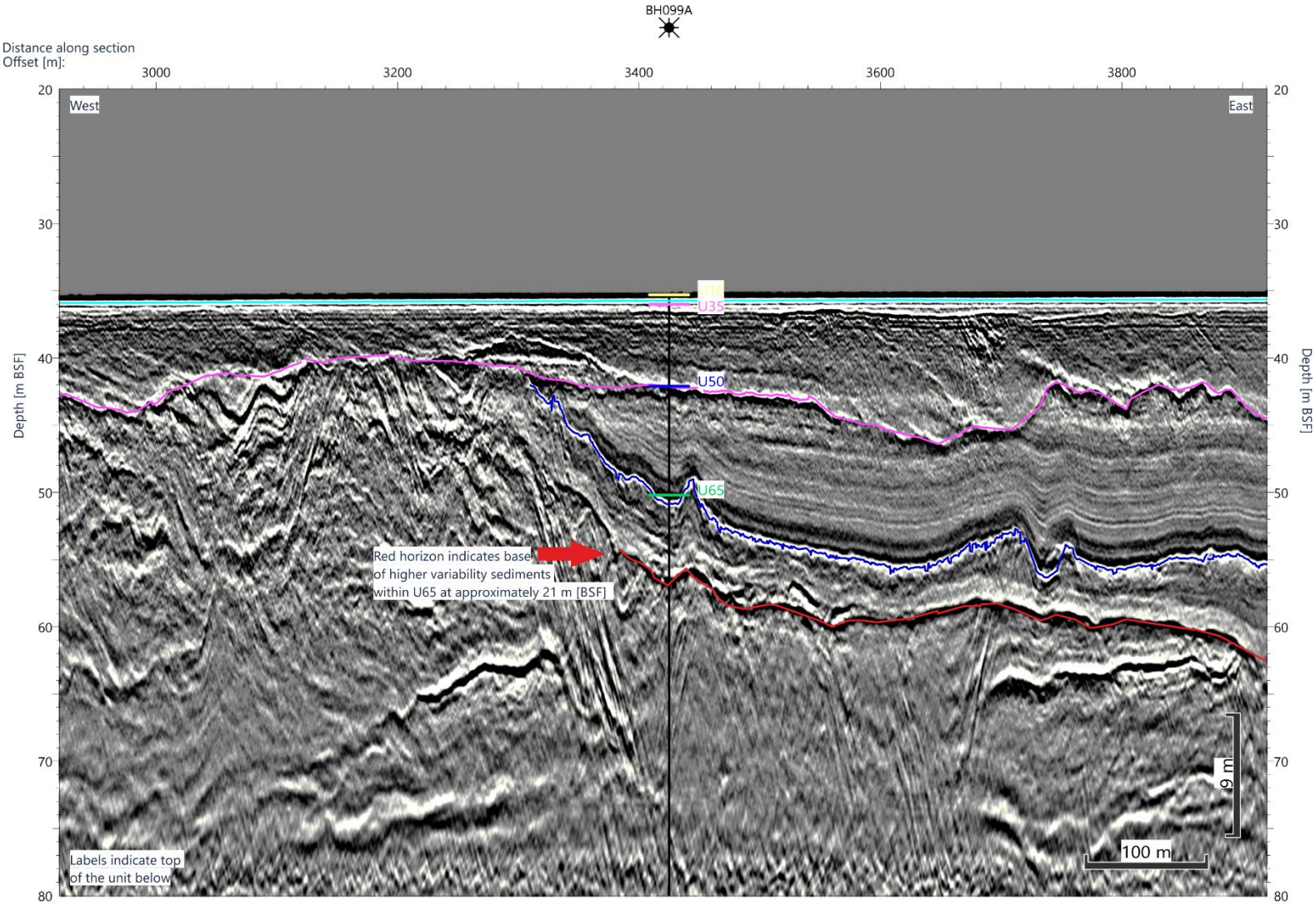

Figure 6.80: Higher variability sediments mapped within U65. Seismic line name (EAXC404P1) adjacent to BH099

6.15.6.2 Channels

Figure 6.81 illustrates the presence of glacial channels within geological unit U65, where two distinct sets have been identified. The first, likely to be older, trends north–south aligning with the inferred direction of the former ice sheet (Section 3.3). These channels exhibit deeper incision, suggesting prolonged meltwater flow and greater erosive power, consistent with an earlier phase of glaciation.

The second, likely younger, trends north-east–south-west and is generally shallower. These channels appear to crosscut the older north–south features, particularly within Sub-Area 2, indicating a later phase of glacial activity. Fugro interpret these to have formed through repeated episodes of subglacial meltwater erosion and ice scouring during glacial recession.

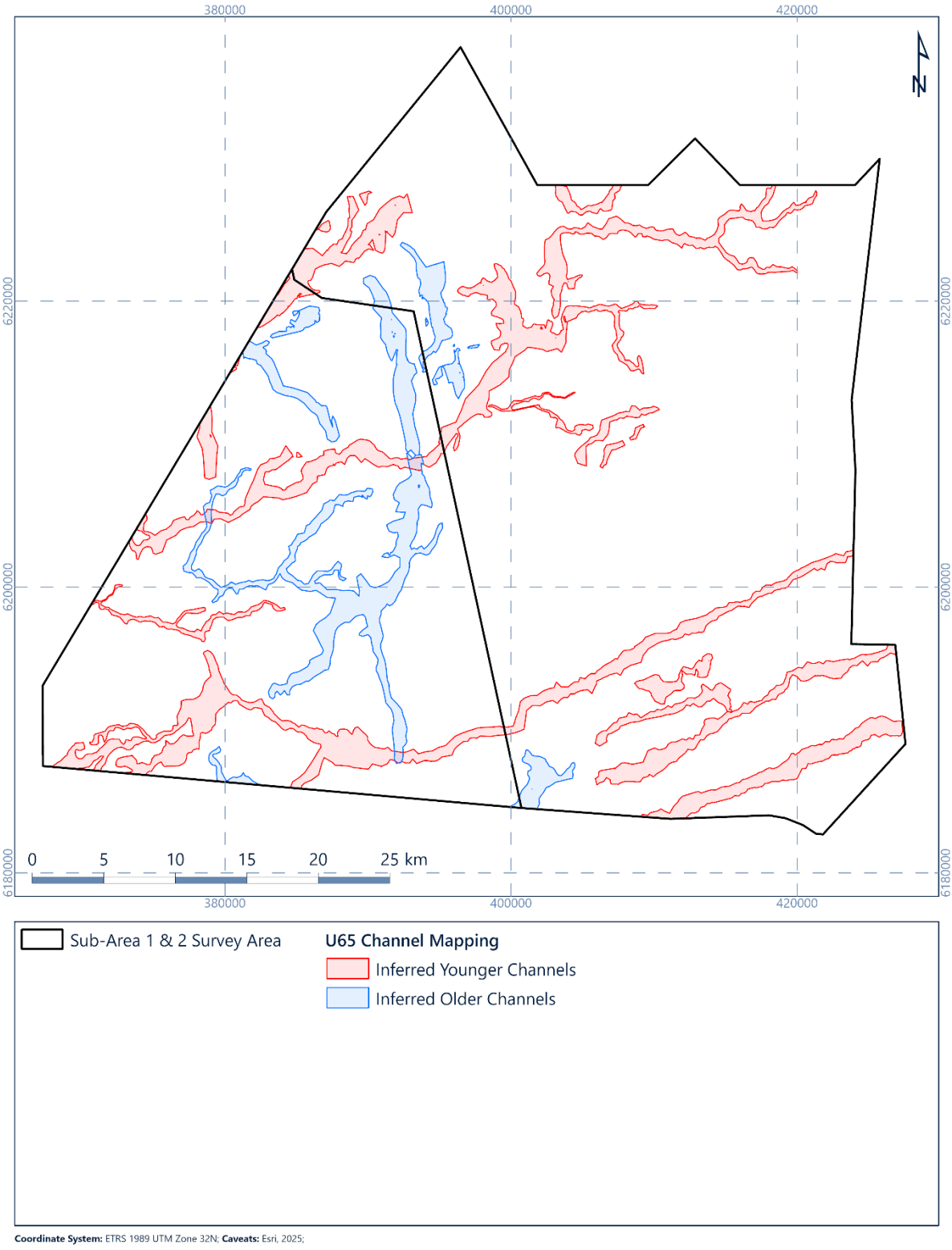

Figure 6.81: Combined U65 channel mapping extent

6.15.7 Glacial Deformation

Well-defined thrust faults are widespread within the BSU in the north, centre and south-east of the site (Figure 6.82 and Figure 6.83). They generally dip towards the east and north and are interpreted to be the result of ice-sediment interaction at the base of advancing ice sheets (Huuse & Lykke-Andersen, 2000a; Larsen & Andersen, 2005; Winsemann et al., 2020; Cartelle et al., 2021). Their orientation indicates that the ice advance came from the north-east.

This deformation can cause variability within the soil and have lower lateral resistance, resulting in non-uniform foundation support.

The chaotic seismic character and presence of localised folding and thrust-faults within geological units U65 and U70 suggests these glacial units are likely to have been deformed by glacial processes. It is recommended that clay fabric logging is considered for future geotechnical data collection in this interval.

6.15.8 Faults

Normal faults were observed locally in geological unit U70 and in BSU (Figure 6.82). These may be of tectonic origin, caused by the collapse of tunnel valley margins within geological unit U70 or as a result of the extension of sediments as ice sheets retreated across the region.

Soil conditions may vary vertically and laterally resulting in non-uniform support of foundations. Faults could be re-activated due to human interference and therefore active faults may be associated with critical stress and possible failure of structures.

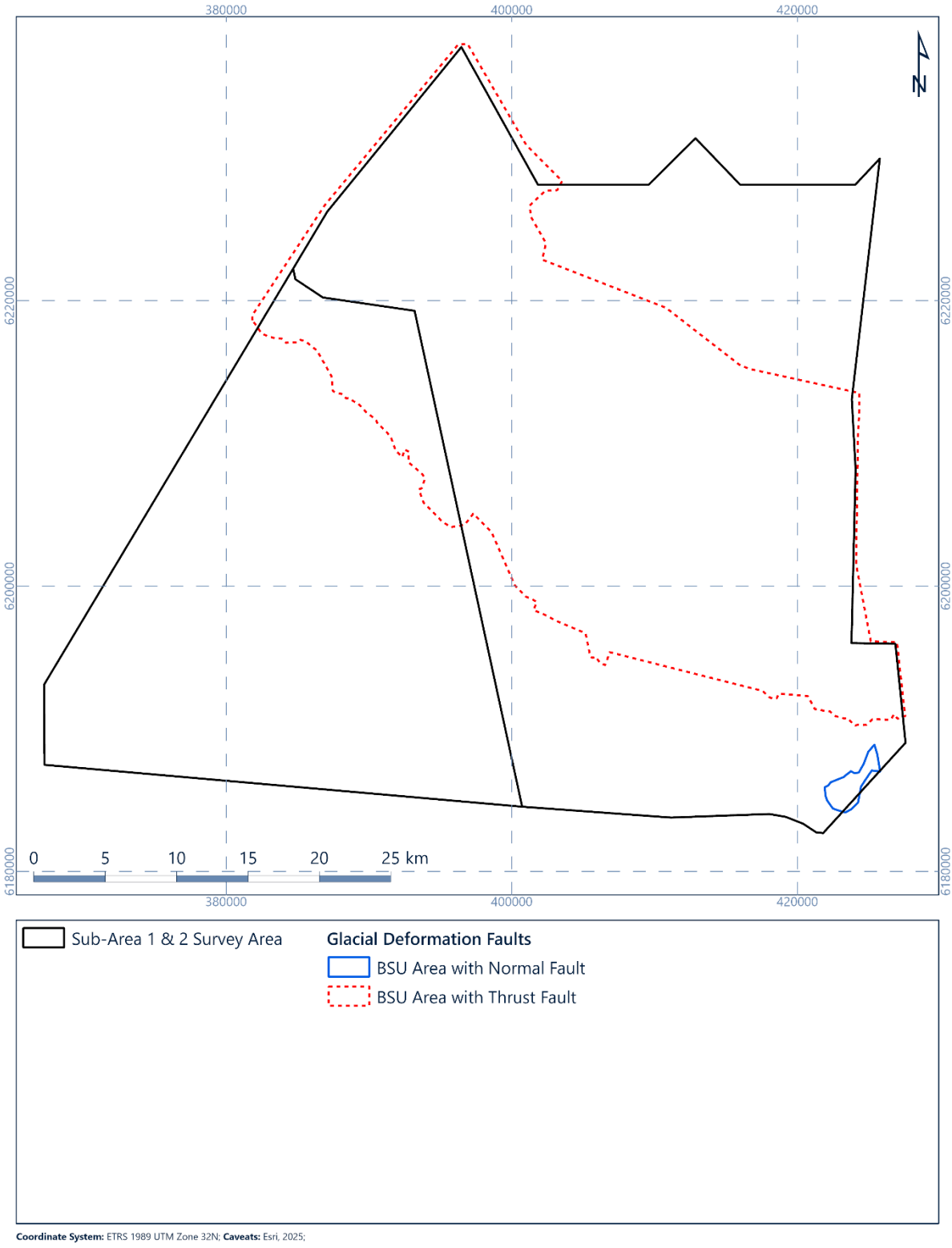

Figure 6.82: Mapped extent of glacial deformation (thrust faults) and normal faults in the BSU across the NS1 site

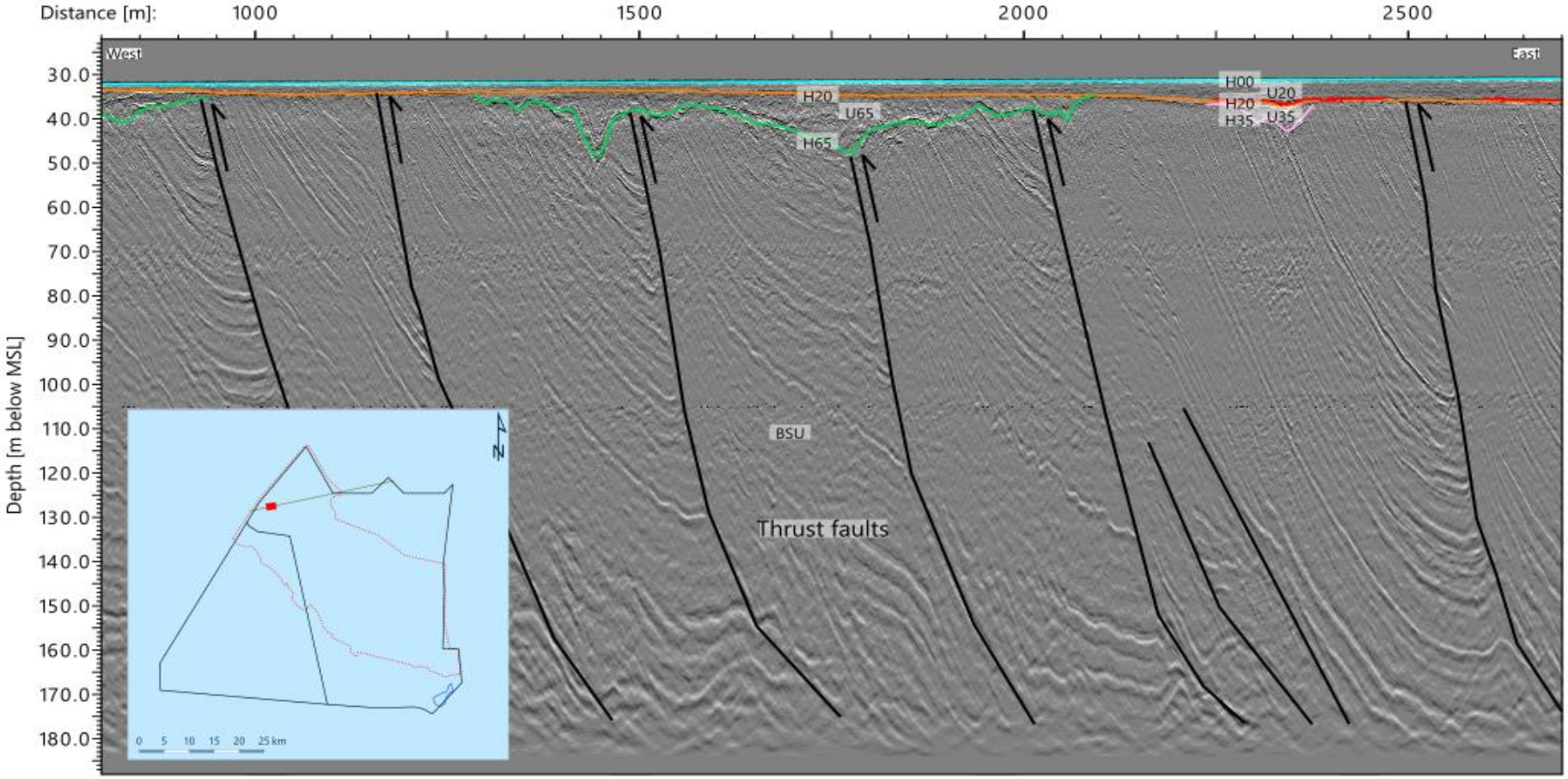

Figure 6.83: 2D UHR seismic data example of thrust faulting in BSU. Line EAXA376P1

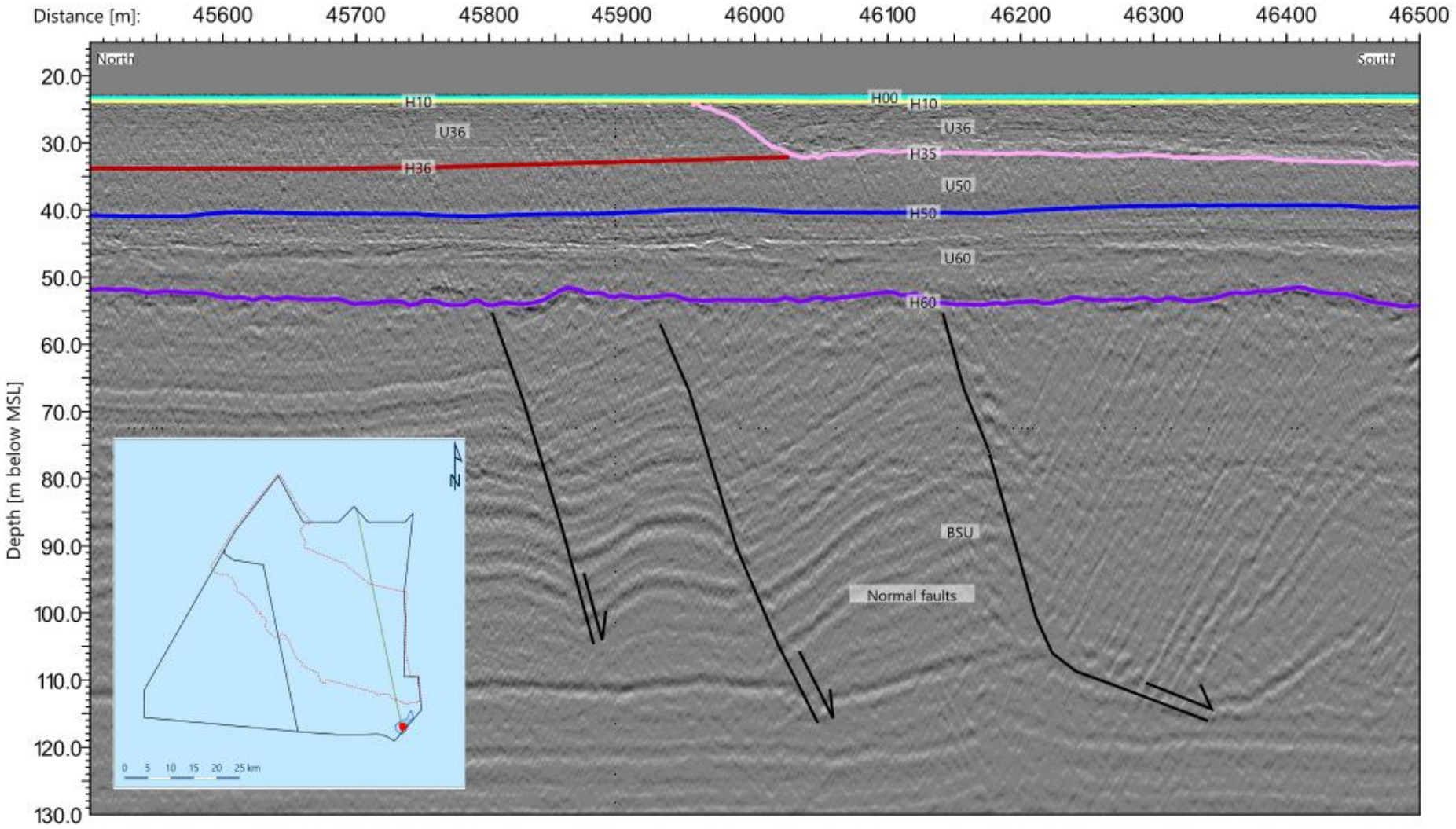

Figure 6.84: 2D UHR seismic data example of normal faulting in BSU. Line EAAZ318P1

7. Geotechnical Interpretation

7.1 Overview

Geotechnical characteristics for each of the geological units were derived from the available geotechnical data. Unitisation for geotechnical data is detailed in Section 6.

The ground conditions anticipated at the NS1 site are comparable to other OWF developments (COWI, 2021) in the vicinity that have foundation and cable infrastructure in place. This indicates that foundations can successfully be designed for the general geotechnical characteristics of the shallow geology anticipated at the NS1 site, provided the hazards associated with these depositional environments (Section 6) are considered, fully characterised and mitigated, where possible.

7.2 Geotechnical Characteristics

This section outlines the general geotechnical characteristics of each geological unit. The supporting unit-based geotechnical characteristic values are presented in Section 7.3.

Table 7.1 presents the geological units alongside their minimum and maximum depths. Fugro's description of each unit, based on the offshore sampling, can be found in Table 5.2.

Table 7.1: Synthetic geotechnical unit descriptions

Geological Unit	Minimum Top Depth [m BSF]*	Maximum Bottom Depth [m BSF]*
U10	0.0	10
U20a	0.0	19.9
U20b	0.0	18.7
U30	2.0	10.7
U35	0.0	31.4
U36	4.0	24.5
U50	0.2	50
U60	9.3	60.0
U65	0.0	> 70.0
U69	27	> 70.0
U70	0.0	> 70.0
U90	8.85	> 70.0
BSU	6.8	> 70.0

Notes
BSF = Below seafloor
BSU = Base seismic unit
* = Depth extracted from geotechnical data, greater depth ranges may be observed on site and in integrated geophysical datasets

Fugro also assessed variability in the descriptions of borehole samples. Table 7.2 presents the primary lithologies as outlined by Larsen et al. (1995). These are based on field descriptions of the primary lithologies, and do not consider secondary descriptions. Refer to particle size distribution carried out via dynamic image analysis (DIA) during the offshore work (Fugro, 2024g) for further information on the primary and secondary constituents of the sediments.

Table 7.2: Summary of primary lithologies

Unit	Primary Lithology (Larsen et al., 1995)							
	CLAY [%]	CLAY TILL [%]	GRAVEL [%]	PEAT [%]	SAND [%]	SILT [%]	SILT TILL [%]	STONES [%]
U10	< 0.5		0.5		99			
U20a	2			< 0.5	98			
U20b	54			5	36	5		
U30	20			3	71	6		
U35	5		< 0.5		94	1		
U36	25				71	4		
U50	88				8	4		
U60	6		1		93	< 0.5		< 0.5
U65	36	< 0.5	< 0.5	< 0.5	60	4		
U69	99				1			
U70	53	2	< 0.5		40	2	3	
U90	6			1	93			
BSU	67		< 0.5	< 0.5	32	1		

Notes
Percentage values are from recovered sample intervals only, therefore total lithology values may vary
BSU = Base seismic unit

7.3 Geotechnical Characteristic Values

7.3.1 General

This section presents the derived geotechnical characteristic values for each of the geotechnical units predicted at the Energinet 2030 NS1 site, with details of the methodology followed and associated uncertainties. The derived values are summarised in Table 7.4.

7.3.2 Methodology

Geotechnical characteristic values were derived based on the unitised geotechnical data from the offshore site investigation (Section 2.2.2). Fugro statistically assessed the values presented in Table 7.3 using the offshore datasets.

These values were derived using available offshore laboratory data, CPT and borehole data (Section 2), unitisation (Section 6) and an understanding of the regional geological setting (Section 3).

Table 7.3: Presented characteristic values

Symbol	Parameter	Unit	Notes
Basic Physical Properties			
γ^{l}	Submerged unit weight	kN/m^3	Submerged unit weight values were derived for each unit based on offshore geotechnical data test data. Unit weight values were from volume mass calculation, and water content test values
WC	Water content	%	Water content values were derived for each unit based on offshore geotechnical data test data
wP wL IP	Atterberg limits: liquid limit, plastic limit, and plasticity index	%	Atterberg limit test values derived based on offshore test data.
D_{min} D_{max}	Minimum and maximum dry density	Mg/m^3	Minimum and maximum dry density values derived based on offshore data
Cone Penetration Test Parameters			
q_c	Cone resistance	MPa	Based on downhole and seafloor CPT data collected across site
Strength Parameters			
s_u	Undrained shear strength (of clay)	kPa	Fugro defined Su values based on field geotechnical test data, derived from PP, TV and UU testing Separate presentation of CPT derived SU values from downhole and seafloor geotechnical data (Section 7.3.3.2)
D_r	Relative density (of sand)	%	Based on downhole and seafloor CPT data collected across site (Section 7.3.3.3)

Notes
CPT = Cone penetration test
PP = Pocket penetrometer
TV = Torvane
UU = Unconsolidated undrained triaxial

Minimum, maximum and average (mean) values are presented for each unit alongside the characteristic values.

In addition to the simple statistical analysis, Fugro derived further statistical analysis of the testing values. Where measured offshore laboratory data were available, the statistical approach recommended by DNV GL (2019) was followed. Recommended representative BE values were derived based on a corrected mean, calculated by establishing the average (X_{av}) and standard deviation (σ) of the dataset. Values exceeding the limits of (X_{av}) plus or minus two times standard deviation ($\pm 2\sigma$) were considered outliers, due to the variability in the dataset. The recommended representative BE values were then evaluated by a recalculation of the X_{av} with these outliers removed.

The threshold for this assessment was set at 30 tests. This was due to instances of where there were too few datapoints for a full statistical analysis to be practical.

Further site-specific geotechnical data acquisition and appropriate laboratory testing are required to constrain these ranges and parameters.

Derivation methods for each geotechnical value are discussed in Section 7.3.3.

7.3.3 Geotechnical Characteristics: Cone Penetration Test

This section outlines the approach for the derivation of the values from in-situ testing. Refer to Fugro (2024b, 2024c) for further information.

7.3.3.1 Net Cone Resistance

Net cone resistance was derived using Equation 7.1.

$$q_n = q_t - \sigma_{v0}$$

Equation 7.1

Where:

q_n = Net cone resistance [MPa]
q_t = Total cone resistance [MPa]
σ_{v0} = Overburden pressure [kPa]

This value was calculated using Equation 7.2 to derive the total cone resistance.

$$q_t = q_c + (1 - a)u_0$$

Equation 7.2

Where:

q_t = Total cone resistance [MPa]
q_c = Cone resistance [MPa]
a = Net area ratio of probe [-]
u_2 = Pore pressure [kPa]

7.3.3.2 Undrained Shear Strength

Values of undrained shear strength (s_u) for clay derived based on CPT data were calculated using Equation 7.3 (Rad & Lunne., 1988).

$$s_u = 1000 \frac{q_n}{N_{kt}}$$

Equation 7.3

Where:

s_u = Undrained shear strength [kPa]
q_n = Net cone resistance [MPa]
N_{kt} = Empirical factor relating cone resistance to undrained shear strength [-]

N_{kt} ranges between 15 and 20 for typical clays. No site-specific N_{kt} review was performed for this report. For the derivation of geotechnical characteristic values, CPT-derived s_u values are presented. The values calculated are based on N_{kt} values of 15 and 20, with no specific N_{kt} values per unit. Fugro recommend that specific values are derived when the appropriate laboratory data are available.

7.3.3.3 Relative Density

Values of relative density (D_r) for sand were derived based on available geotechnical data (CPTs). D_r was calculated from CPT data using the formula shown in Equation 7.4 (Jamiolkowski et al., 2003).

$$D_r = \frac{1}{0.0296} \cdot ln\left(\frac{q_c}{2.494\left(\frac{\sigma'_{v0}\left(\frac{1+2\cdot K_0}{3}\right)}{100}\right)^{0.46}}\right)$$

Equation 7.4

Where:

D_r = Estimated dry relative density [%]
q_c = Cone resistance [MPa]
σ'_{v0} = Vertical effective overburden stress [kPa]
K_0 = Coefficient of lateral earth pressure at rest (taken equal at 1)

K_0 values of 0.5 and 2.0 were used in the datasets.

7.3.3.4 Statistical Values

Unlike the laboratory test data that follow the approach outlined in DNV GL (2019), values for CPT information are more variable. Therefore, only BE values derived using the approach outlined in Section 7.3.2 are presented.

7.4 Geotechnical Characteristic Values – Considerations

Geotechnical characteristics for each unit were assessed based on the offshore dataset, following the integration approach outlined in this report. It is expected that the characteristic values presented will be refined when laboratory testing is complete. Further considerations for the values are outlined in Sections 7.4.1 and 7.4.2.

7.4.1 Parameter Variability with Depth

A relationship between depth and parameter values may be expected for some units. Characteristic values derived from the datasets do not currently consider trends with depth. Examples of this are the undrained shear strength values in Unit 50, where strength appear to increase with depth. Further assessment of parameters is recommended when the full laboratory dataset are available.

7.4.2 Complex Unit Lithologies

High internal variability may be expected in some units, based on the associated geological processes. Section 7.2 includes examples of the variability associated with lithologies in the units; these can result in very high variability in values (Section 7.5). Units 65 and 70 are associated with the deposition of till sediments. High local variability is expected, and therefore caution should be exercised when using values based on these units.

7.5 Characteristic Value Table

The derived geotechnical values are presented in Table 7.4, Table 7.5, Table 7.6 and Table 7.7. Characteristic values presented for the sampled interval of each geotechnical unit do not detail any anticipated change in the geotechnical conditions with depth.

Table 7.4: Derived parameters table: classification characteristics

Unit	Depth* [m]	γI [kN/m³] Number	Min	Max	Mean	LE	BE	HE	WC [%] Number	Min	Max	Mean	LE	BE	HE
U10	0.0 2.6	221	17.2	22.3	**19.7**	18.9	19.6	20.4	95	11.3	32.3	**23.4**	18.0	23.8	29.5
U20a	0.1 10.0	946	9.7	21.9	**19.3**	18.6	19.4	20.3	404	15.8	116.7	**27.1**	20.5	26.4	32.4
U20b	0.1 18.6	452	12.1	20.7	**17.9**	16.2	18.1	20.1	170	17.1	167.9	**41.7**	18.8	38.4	58.0
U30	2.3 10.6	111	18.7	21.6	**19.9**	19.3	19.9	20.4	51	19.0	41.0	**24.6**	19.9	24.3	28.6
U35	0.2 29.5	1257	9.7	22.3	**19.9**	19.1	20.0	20.8	748	7.1	73.8	**22.6**	17.5	22.3	27.0
U36	4.3 19.7	195	17.3	20.7	**18.9**	17.8	18.8	19.9	98	19.6	38.7	**29.0**	21.3	29.0	36.7
U50	0.3 40.0	1146	14.2	24.6	**19.8**	18.7	19.8	20.8	537	8.7	80.4	**24.9**	18.9	24.6	30.3
U60	9.5 59.9	2837	17.0	35.3	**20.0**	19.3	20.0	20.7	2066	8.3	35.6	**21.7**	18.5	21.8	25.1
U65	1.8 70.8	2434	13.6	32.5	**20.9**	18.8	20.9	23.0	1610	7.8	99.6	**19.9**	10.5	19.6	28.7
U69	29.2 70.1	936	16.7	24.0	**19.2**	18.0	19.2	20.3	332	9.9	48.4	**28.9**	21.4	28.9	36.4
U70	8.2 70.8	6993	12.2	40.0	**20.4**	18.5	20.3	22.0	3518	4.5	131.3	**22.1**	14.1	22.2	30.4
U90	9.0 45.7	114	13.6	21.3	**18.6**	16.2	18.7	21.3	81	12.5	30.4	**21.2**	15.9	20.9	25.8
BSU	6.8 70.6	3256	4.9	25.0	**20.0**	19.1	19.9	20.7	1424	7.5	41.0	**23.7**	19.9	24.3	28.7

Notes:
Statistical approach to define LE BE and HE presented in Section 7.3.2
Test data is based on offshore work phase only therefore may be revised once laboratory testing is complete
No split between sediment lithology and test values has currently been performed. Caution should be exercised when using datasets
* Depth range values present the range of depths that geotechnical test data is available within. For full range of thickness please see spatial geological model

Table 7.5: Derived parameters table: Atterberg limits

Unit	Depth*	Liquid Limit							Atterberg Limit Plastic Limit							Plasticity Index						
	[m]	Number	Min	Max	Mean	LE	BE	HE	Number	Min	Max	Mean	LE	BE	HE	Number	Min	Max	Mean	LE	BE	HE
U10	No Tests																					
U20a	No Tests																					
U20b	3.0 9.2	6	34	70	**51**	Insufficient Data			6	20	50	**31**	Insufficient Data			6	14	25	**19**	Insufficient Data		
U30	No Tests																					
U35	8.0	1	33	33	**33**	Insufficient Data			1	17	17	**17**	Insufficient Data			1	16	16	**16**	Insufficient Data		
U36	No Tests																					
U50	4.0 18.8	38	22	51	**37**	26	37	48	38	6	28	**19**	15	20	24	38	7	32	**17**	8	17	26
U60	40.7	1	43	43	**43**	Insufficient Data			1	22	22	**22**	Insufficient Data			1	21	21	**21**	Insufficient Data		
U65	7.0 63.0	19	32	112	**50**	Insufficient Data			19	15	80	**27**	Insufficient Data			19	12	44	**23**	Insufficient Data		
U69	28.3 68.7	12	31	51	**44**	Insufficient Data			12	17	34	**25**	Insufficient Data			12	14	26	**19**	Insufficient Data		
U70	15.5 69.3	103	21	87	**50**	32	51	70	103	12	38	**24**	16	23	29	103	8	53	**26**	11	25	40
U90	No Tests																					
BSU	11.4 70.5	73	32	74	**52**	37	54	71	73	19	41	**28**	22	28	33	73	10	45	**24**	12	23	34

Notes:

Statistical approach to define LE BE and HE presented in Section 7.3.2

Test data is based on offshore work phase only therefore may be revised once laboratory testing is complete

No split between sediment lithology and test values has currently been performed. Caution should be exercised when using datasets. SU values represent clay layers within sand sediments in predominantly sand units. For split material please see Table 7.2

* Depth range values present the range of depths that geotechnical test data is available within. For full range of thickness please see spatial geological model

Table 7.6: Derived parameters table: minimum and maximum characteristics

Unit	Depth [m]	Min index dry density [kN/m3]							Max index dry density						
		Number	Min	Max	Mean	LE	BE	HE	Number	Min	Max	Mean	LE	BE	HE
U10	0.0 2.0	17	1.31	1.56	**1.44**	Insufficient Data			17	1.65	1.86	**1.75**	Insufficient Data		
U20a	0.1 7.0	29	1.20	1.46	**1.33**	Insufficient Data			29	1.56	1.79	**1.65**	Insufficient Data		
U20b	0.5 9.1	4	1.20	1.45	**1.29**	Insufficient Data			4	1.54	1.79	**1.64**	Insufficient Data		
U30	5.2 7.0	3	1.38	1.52	**1.45**	Insufficient Data			3	1.70	1.83	**1.77**	Insufficient Data		
U35	0.3 31.4	57	1.26	1.64	**1.45**	1.33	1.45	1.57	57	1.57	1.92	**1.76**	1.61	1.76	1.90
U36	11.5 17.6	2	1.37	1.38	**1.38**	Insufficient Data			2	1.70	1.70	**1.70**	Insufficient Data		
U50	12.3 18.5	2	1.43	1.53	**1.48**	Insufficient Data			1	1.72	1.84	**1.78**	Insufficient Data		
U60	11.4 52.5	113	1.32	1.62	**1.45**	1.36	1.44	1.53	113	1.62	1.99	**1.77**	1.68	1.77	1.86
U65	2.3 37.0	14	1.32	1.58	**1.45**	Insufficient Data			14	1.68	1.94	**1.81**	Insufficient Data		
U69	30.3	1	1.52			Insufficient Data			1	1.85			Insufficient Data		
U70	17.4 69.5	57	1.09	1.49	**1.36**	1.29	1.37	1.45	57	1.32	1.93	**1.69**	1.60	1.70	1.80
U90	11.0 41.5	5	1.17	1.42	**1.30**	Insufficient Data			5	1.54	1.73	**1.66**	Insufficient Data		
BSU	19.0 63.5	10	1.23	1.57	**1.36**	Insufficient Data			10	1.60	1.85	**1.71**	Insufficient Data		

Notes:

Statistical approach to define LE BE and HE presented in Section 7.3.2

Test data is based on offshore work phase only therefore may be revised once laboratory testing is complete

No split between sediment lithology and test values has currently been performed. Caution should be exercised when using datasets. SU values represent clay layers within sand sediments in predominantly sand units. For split material please see Table 7.2

* Depth range values present the range of depths that geotechnical test data is available within. For full range of thickness please see spatial geological model

Table 7.7: Derived parameters table: strength characteristics laboratory test data

Unit	Depth^ [m]	Su [kPa] Number	Min	Max	Mean	LE	BE	HE
U10	0.2	1	29	29	**29**	N/A		
U20a	4.7 8.6	12	11	30	**19**	Insufficient Data		
U20b	4.7 17.2	90	5	195	**32**	7*	29*	50*
U30	6.4 10.6	7	67	200	**144**	Insufficient Data		
U35	2.6 16.0	29	10	258	**62**	Insufficient Data		
U36	11.6 12.9	6	6	22	**11**	Insufficient Data		
U50	1.5 22.6	446	4	358	**115**	40	110	179
U60	13.2 49.7	21	80	735	**393**	Insufficient Data		
U65	1.7 69.8	471	8	1121	**357**	0.0#	331	683
U69	29.2 70.1	379	55	613	**213**	81	196	312
U70	17.3 70.6	1565	32	1368	**449**	80	429	778
U90	No Tests							
BSU	7.8 70.8	923	37	917	**412**	189	413	637

Notes:
Statistical approach to define LE BE and HE presented in Section 7.3.2
Test data is based on offshore work phase only therefore may be revised once laboratory testing is completed
No split between sediment lithology and test values has currently been performed. Caution should be exercised when using datasets. SU values represent clay layers within sand sediments in predominantly sand units. For split of material please see Table 7.2
* Plot of data suggests relationship with depth, which is not currently captured in the dataset. Caution should be exercised when considering values
^ Depth range values present the range of depths that geotechnical test data is available within. For full range of thickness please see spatial geological model
# Statistical value is not considered valid. This is due to the high variability and large standard deviation within test data

Table 7.8: Derived parameters table: strength characteristics

Unit	Depth~ [m]	Cone Resistance qc [MPa]							Su from CPT Data					Dr From CPT Data				
		Number	Min	Max	Mean	LE	BE	HE	Number	Min	Max	Mean	BE	Number	Min	Max	Mean	BE
U10	0.0 7.2	53785	0.0	44.6	**8.6**	0.0#	7.3	17.3	96	3.7	119.0	**24.2**	19.6	46411	<5	>100	**90.1**	93.2
U20a*	0.0 13.3	94604	0.0	49.0	**6.7**	0.0#	5.2	12.2	2547	6.8	358.1	**40.9**	35.9	89345	<5	>100	**56.4**	54.8
U20b*	1.0 19.9	34304	0.1	32.7	**1.3**	0.0#	1.0	2.2	29914	3.4	358.7	**34.5**	29.4	3905	<5	>100	**24.9**	22.0
U30	0.9 10.7	7687	0.6	58.9	**13.4**	1.5	12.7	23.9	1057	28.8	244.3	**114.3**	118.6	6630	<5	>100	**83.1**	86.6
U35	0.0 30.5	117652	0.0	92.3	**21.8**	1.6	20.2	38.9	2106	3.3	586.2	**109.0**	96.4	114418	<5	>100	**90.3**	93.3
U36	3.3 24.0	10521	1.0	46.9	**15.8**	0.0#	15.4	32.9	642	42.0	245.3	**103.9**	102.0	9879	<5	>100	**62.3**	63.7
U50	0.2 50.0	110541	0.1	56.8	**3.7**	0.0	3.0	6.0	73379	12.8	755.5	**107.2**	99.7	36792	<5	>100	**30.8**	26.2
U60	7.4 55.5	140766	0.2	118.7	**42.1**	26.4	43.0	59.8	1210	81.7	>1000	**460.1**	453.9	136053	<5	>100	**93.8**	96.4
U65	0.0 57.0	344993	0.0	132.2	**24.4**	0.0#^	22.8	47.4	94378	12.0	>1000	**310.3**	265.5	246544	<5	>100	**86.5**	89.3
U69	25.4 56.5	11729	0.4	50.9	**5.7**	1.7	4.8	7.9	10532	24.9	>1000	**195.8**	181.0	833	14.8	88.8	**48.0**	46.9
U70	0.6 57.5	83287	0.2	126.0	**22.1**	0.0#	20.6	42.4	39437	40.0	>1000	**463.6**	425.7	39383	<5	>100	**77.2**	78.1
U90	2.0 56.5	38257	0.1	128.3	**42.1**	14.6	39.8	64.9	1828	101.2	>1000	**558.1**	514.8	32958	<5	>100	**87.3**	88.7
BSU	3.2 57.5	60129	0.2	128.1	**19.4**	0.0#	16.8	39.3	35113	52.2	>1000	**347.5**	318.5	23868	<5	>100	**83.2**	85.1

Notes:
Statistical approach to define LE BE and HE presented in section 7.3.2
Test data is based on offshore work phase only, therefore may be revised once laboratory testing is completed
Cone resistance values show build up which may affect values
No split between sediment lithology and test values has currently been performed. Caution should be exercised when using datasets. SU values represent clay layers within sand sediments in predominantly sand units. For split material please see Table 7.2
* Values from locations with BH data only, which is used to split datasets
BE only provided for derived values due to variability of CPT data and values
^ Values from both clay and sand member, results should be approached with caution and may not reflect conditions
~ Depth range values present the range of depths that geotechnical test data is available within. For full range of thickness please see spatial geological model
# Statistical value is not considered valid. This is due to the high variability and large standard deviation in the test data

8. Geotechnical Soil Zonation

8.1 Overview

This section presents the geotechnical soil zonation mapping and indicative profiles. The zonation is based on the mapped geological units presented in Section 6, across both Sub-Area 1 and 2 at the NS1 site.

The soil zonation, profiles and associated geotechnical locations per zone have been updated from Report 3 (Fugro, 2024) and integrated based on the additional data collected for Sub-Area 2.

8.2 Zonation

A soil zonation allows better understanding of the lateral variability between geological units (Section 6). A soil zonation was generated for the study area to depict the spatial extent of several key factors that divide the site, based on the geometry of the spatial geological model.

The following units, determined with Energinet (meeting, 2 May 2024), were the primary drivers in the defined soil zonation as they are expected to significantly impact foundation design due to horizontal and vertical variations and require greater consideration:

1. Geological unit U20 is a channelised Holocene sediment that is expected to produce areas of lower strength material to greater depth than otherwise is the case in other units across the site;
2. Glacial geological units U65 and U70 represent a change in the depositional environment at the site and are expected to be associated with an increase in soil strength, as well as greater variability in the ground conditions. This grouping excludes sediments from geological unit U69, although they were deposited in glacial periods, due to their relative consistency in geotechnical data.

The detail of soil condition factors for each of these elements are summarised in Table 8.1 and Table 8.2, and Figure 8.1 to Figure 8.3.

Table 8.1: Geological unit U20: soil thickness (spatial extent shown in Figure 8.1)

Soil Condition Factor	Soil Zonation Naming Convention	Engineering Implication
Geological unit U20 absent	a	Shallow depth to intermediate strength units or high strength units
Geological unit U20 present, thickness between 0.1 m and 6 m	b	Shallow depth to intermediate strength units or high strength units, geological unit U20 likely to largely comprise sand sediments from geological subunit U20a

Soil Condition Factor	Soil Zonation Naming Convention	Engineering Implication
Geological unit U20 present, thickness between 6 m and 10 m	c	Geological unit U20 likely to comprise sand (geotechnical subunit U20a) and low to very low strength clay (geological subunit U20b) sediments
Geological unit U20 present, thickness greater than 10 m	d	Thick areas of geological unit U20 with extensive geological subunit U20b low to very low strength sediments

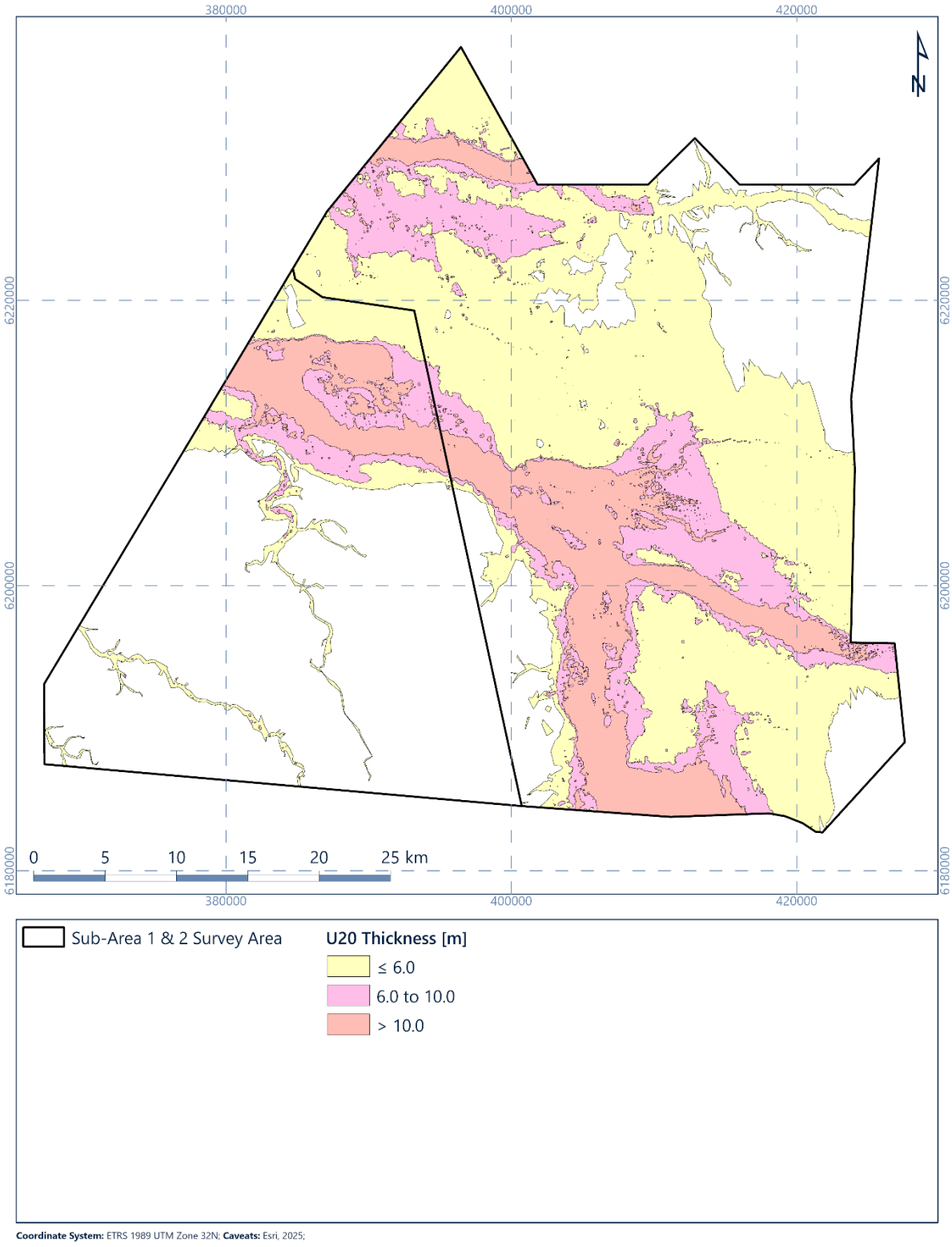

Figure 8.1: Thickness categories for geological unit U20 zonation , blank areas where no geological unit U20 is present (Category a in Table 8.1)

Depth to base of geological unit U20 was appraised as part of the zonation work, as lower strength units are expected to be present at greater depths in areas where geological unit U20 is thicker. This may affect foundation capacity.

The second factor is based on the depth to the top of glacial geological units U65 and U70. These reflect the shallowest and youngest units that are associated with a period when direct glacial action is expected to affect the geotechnical properties of the soils, creating greater variability in sediment properties. Depth intervals associated with the top of this unit were selected based on their relevance for different foundation concepts and are summarised in Table 8.2. Extents associated with these zones are presented in Figure 8.2

Table 8.2: Geological units U65 and U70: top of glacial till units across site

Soil Condition Factor	Soil Zonation Naming Convention	Engineering Implication
Geological units U65 and U70 not present	1	Sediments comprise variable thickness of post Saalian sediments on top of geological units U90 or BSU. Geological units 90 or BSU may be encountered in depth of interest
Top of geological units U65 and U70 present < 10 m BSF	2	High strength and variable units expected at less than 10 m BSF, affecting most foundation types
Top of geological units U65 and U70 present between 10 m and 40 m BSF	3	High strength and variable units expected within typical depth range for foundations, likely to affect deeper pile and monopile foundations
Top of geological units U65 and U70 present > 40 m BSF	4	High strength and variable units may not be present within typical depth range for foundations, would only affect the base of very deep foundations
Notes BSU = Base seismic unit BSF = Below seafloor		

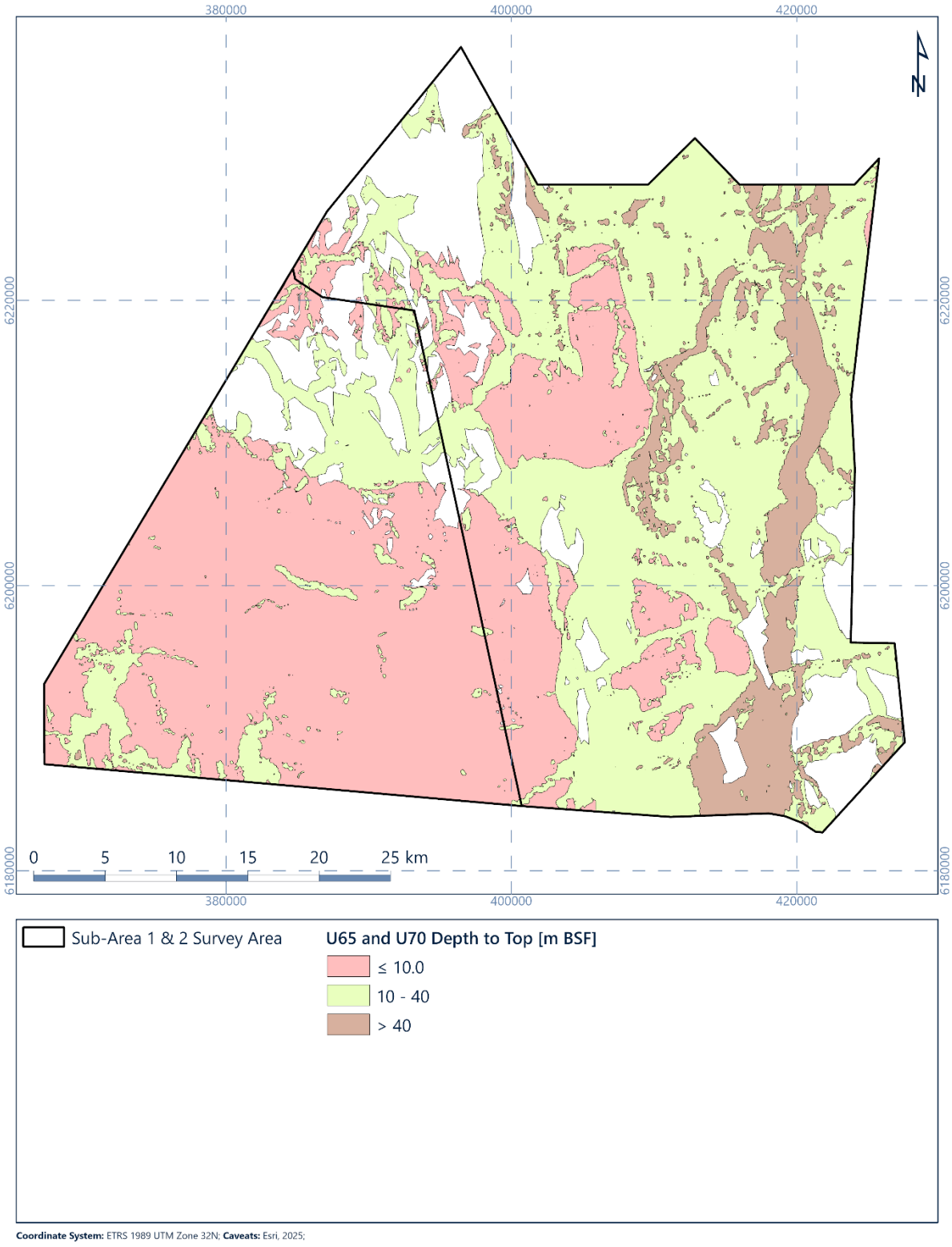

Figure 8.2: Depth to top of geological glacial units U65 and U70. Blank areas where these units are not present (Category a in Table 8.2)

Using the approach detailed above, Fugro defined 16 zones across the NS1 site. These are detailed in Table 8.3. A zonation map highlighting the spatial distribution of each zone is presented in Figure 8.3.

Table 8.3: Combined zonation naming convention

Condition Factors	Geological Units U65 and U70 Absent	Top of Geological Units U65 and U70 Present < 10 m BSF	Top of Geological Units U65 and U70 Present 10 m– 40 m BSF	Top of Geological Units U65 and U70 Present > 40 m BSF
Geological Unit U20 Absent	1a	2a	3a	4a
Geological Unit U20 Thickness 0.1 m–6 m	1b	2b	3b	4b
Geological Unit U20 Thickness 6 m–10 m	1c	2c	3c	4c
Geological Unit U20 Thickness > 10 m	1d	-	3d	4d

Notes
BSF = Below seafloor
- = Zone 2d is not possible due to conflicting factors. Geological unit U20 cannot be > 10 m thick if geological units U65 or U70 are present within 10 m BSF

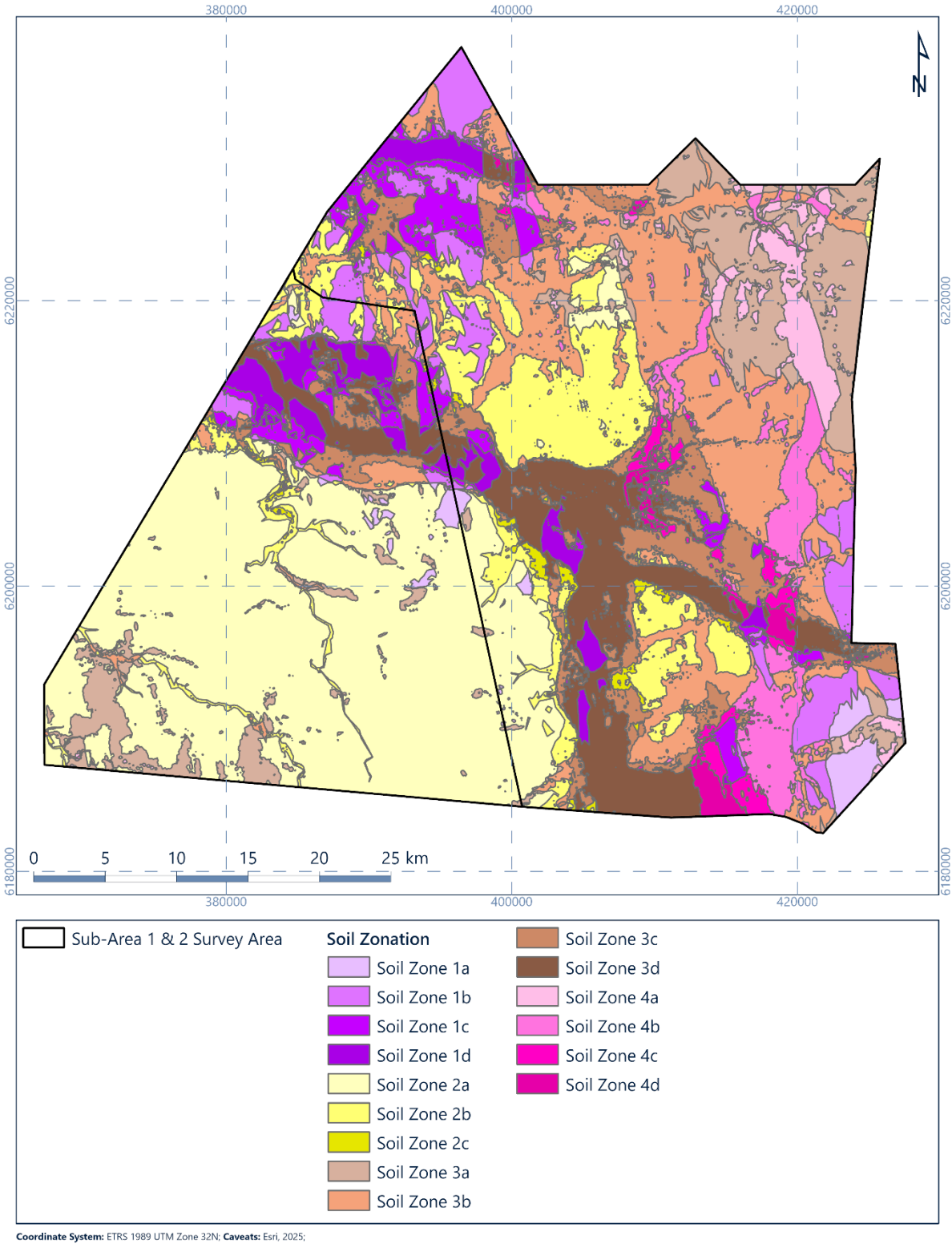

Figure 8.3: Map of defined zones across the NS1 site

The percentage coverage of each zone across the NS1 site is presented in Table 8.4.

Table 8.4: Percentage coverage associated with soil zones in NS1

Soil Zone	Area [km^2]	Site Coverage [%]
1a	29.2	1
1b	123.5	6
1c	83.7	4
1d	73.0	3
2a	608.9	28
2b	208.9	10
2c	18.7	1
3a	188.0	9
3b	322.2	15
3c	155.2	7
3d	182.2	8
4a	51.2	2
4b	89.1	4
4c	30.6	1
4d	21.2	1

8.2.1 Considerations

Some minor inconsistencies were observed at the top of geological units U65 and U70. These were largely constrained to areas with more limited UHRS line coverage, and were caused by gridding between seismic lines. They were adjusted in the zonation process.

Another consideration for the soil zonation is the resolution of the zonation is constrained by the resolution of the gridding of the units used. For more details on gridding, refer to Section 3.1.1.

Given lack of base geophysical horizon for BSU, percentage coverage for this unit cannot be derived. The percentages given in Table 8.5 to Table 8.19 are based primarily on the spatial distribution of the geophysical horizons; therefore it is assumed that any unit below the defined horizons is classed as BSU.

8.3 Typical Soil Profiles

For each soil zone, Fugro defined a typical soil profile to highlight the expected geological units within the depth of interest. The mean depth to base of each unit is presented in the soil profiles, which was determined using the geophysical horizons. Each soil profile is described in Sections 8.4.1 to 8.4.15. Figure 8.4 presents the predicted soil profiles. Within each profile, a geological unit is only presented in the profile when present in greater than 40% of a zone.

Alongside each soil profile through Sections 8.4.1 to 8.4.15, Fugro also present a soil profile from selected, representative geotechnical locations within each zone. The aim of this is to show the likely occurrence and thickness of geological units within a soil zone based on sample data and to best represent the expected ground conditions within the depth of interest. In some instances, these vary from the predicted soil profiles present in Figure 8.4 as these are site-specific and based on sample data.

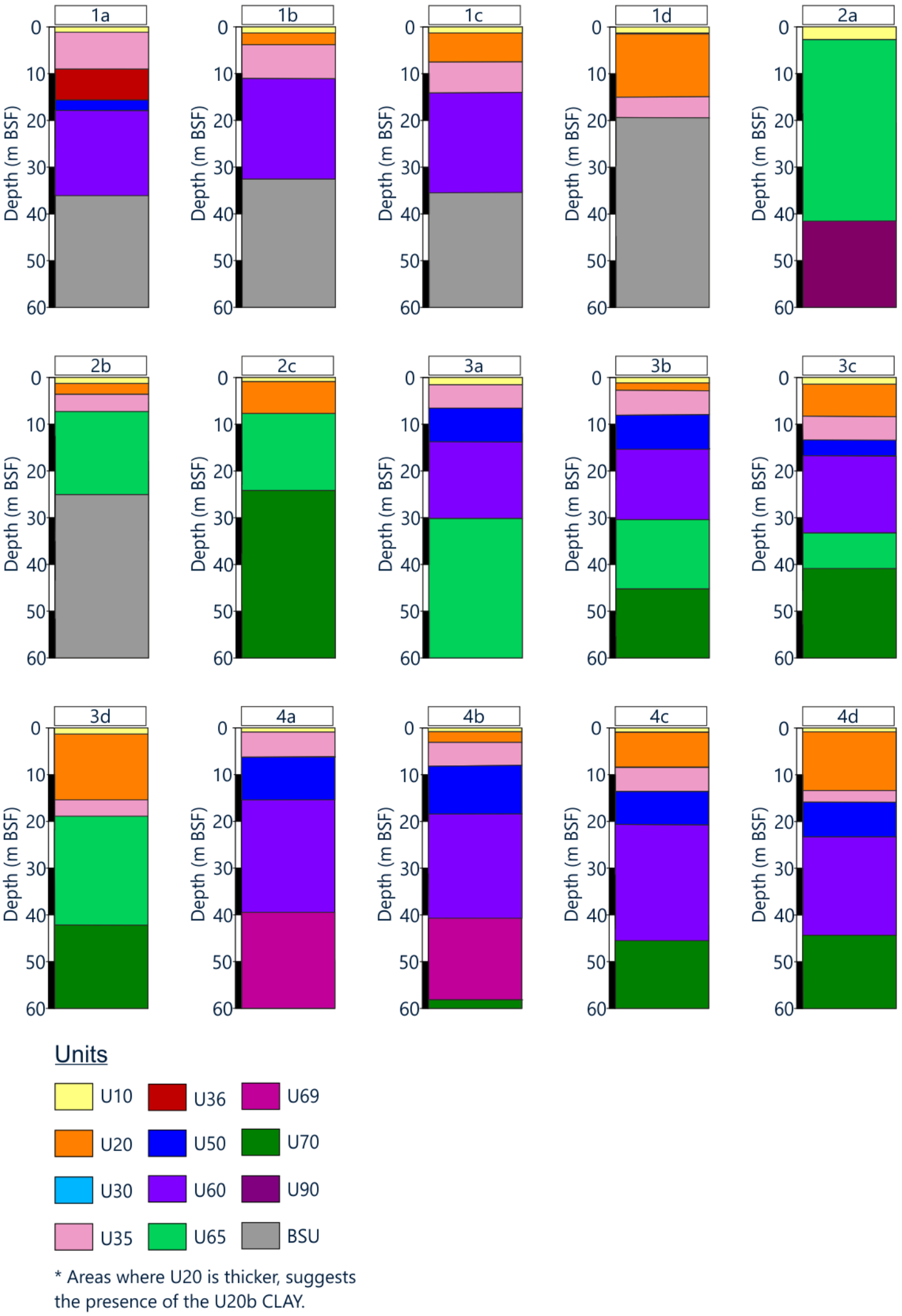

Figure 8.4: Typical soil profile where geological units cover >40% of the soil province.

8.3.1 Soil Zone 1a

Geological unit thicknesses within Soil Zone 1a were derived from the geological model layers defined within the Soil Zone 1a area. The mean depth to base of unit and percentage coverage of each unit in Soil Zone 1a are presented in Table 8.5.

Table 8.5: Average soil unit depth to base and percentage coverage: Soil Zone 1a

Geological Unit	Mean Base Unit Depth [m]	Coverage of Zone [%]*
10	1.3	93
20	Absent	0
30	4.8	<1
35	9.4	60
36	15.2	51
50	16.8	42
60	35.8	63
65	Absent	0
69	Absent	0
70	Absent	0
90	20.0	16

Notes
* = Unit present in the coverage % of total area of soil zone

Soil Zone 1a is defined by the possibility of shallow BSU (absence of geological unit U20 and lack of glacial till material geological units U65 and U70), as shown on the left of Figure 8.5. BH113 is a representative example based on the characteristics and unit coverage of this soil zone (Figure 8.5).

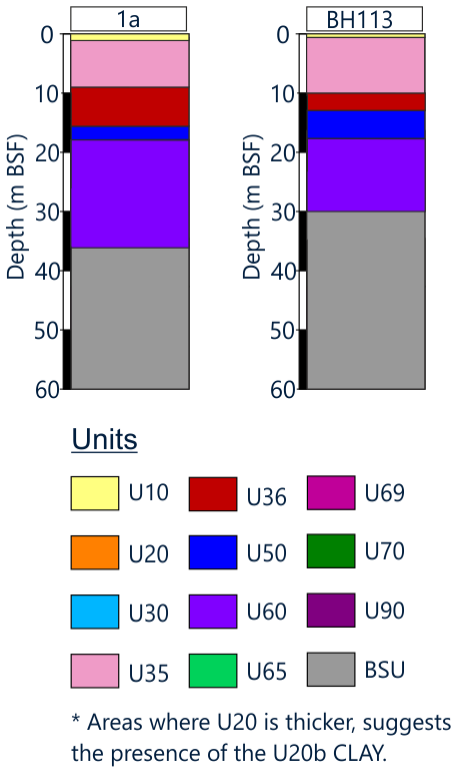

Figure 8.5: BH113 soil profile, Soil Zone 1a

8.3.2 Soil Zone 1b

Geological unit thicknesses within Soil Zone 1b were derived from the geological model layers defined within the Soil Zone 1b area. The mean depth to base of unit and percentage coverage of each unit in Soil Zone 1b are presented in Table 8.6.

Table 8.6: Average soil unit depth to base and percentage coverage: Soil Zone 1b

Geological Unit	Mean Base Unit Depth [m]	Coverage of Zone [%]*
10	1.2	46
20	3.8	100
30	9.7	26
35	10.7	86
36	14.3	26
50	16.6	31
60	32.5	58
65	Absent	0
69	Absent	0
70	Absent	0
90	41.4	5

Notes
* = Unit present in the coverage % of total area of soil zone

Soil Zone 1b is defined by the possibility of shallow BSU with a thin section of geological unit U20 in the upper profile. BH005, on the right of Figure 8.6, has a relatively thin layer of geological unit U20 with BSU at 38 m BSF. The left of the figure shows the representative soil profile.

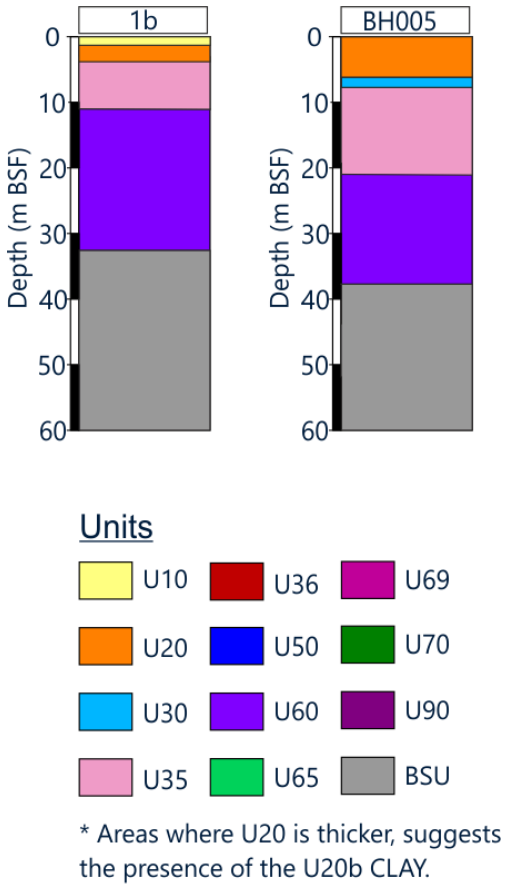

Figure 8.6: BH005 soil profile, Soil Zone 1b

8.3.3 Soil Zone 1c

Geological unit thicknesses within Soil Zone 1c were derived from the geological model layers defined within the Soil Zone 1c area. The mean depth to base of unit and percentage coverage of each unit in Soil Zone 1c are presented in Table 8.7.

Table 8.7: Average soil unit depth to base and percentage coverage: Soil Zone 1c

Geological Unit	Mean Base Unit Depth [m]	Coverage of Zone [%]*
10	1.5	55
20	8.7	100
30	10.0	19.6
35	14.5	99
36	17.7	2
50	18.9	22

Geological Unit	Mean Base Unit Depth [m]	Coverage of Zone [%]*
60	35.4	49
65	Absent	0
69	Absent	0
70	Absent	0
90	45.2	23
Notes * = Unit present in the coverage % of total area of soil zone		

Soil Zone 1c is defined by thicker geological unit U20 sediments but has no glacial till units (geological units U65 and U70). BH002 is a representative example, showing the potential stratigraphy within this soil zone (Figure 8.7).

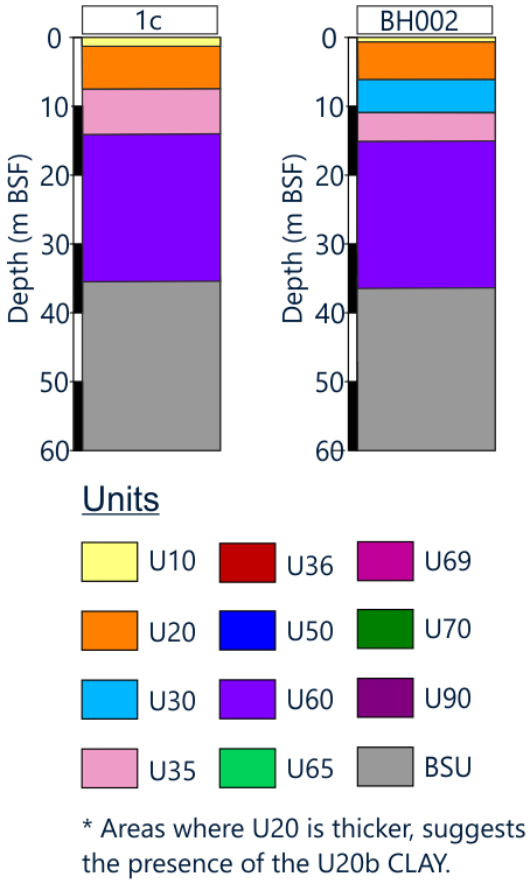

Figure 8.7: BH002 soil profile, Soil Zone 1c

8.3.4 Soil Zone 1d

Geological unit thicknesses within Soil Zone 1d were derived from the geological model layers defined within the Soil Zone 1d area. The mean depth to base of unit and percentage coverage of each unit in Soil Zone 1d are presented in Table 8.8.

Table 8.8: Average soil unit depth to base and percentage coverage: Soil Zone 1d

Geological Unit	Mean Base Unit Depth [m]	Coverage of Zone [%]*
10	1.5	82
20	14.6	100
30	13.2†	1
35	19.5	92
36	19.3	<1
50	19.1†	6
60	33.2	22
65	Absent	0
69	Absent	0
70	Absent	0
90	37.1	34

Notes
* = Unit present in the coverage % of total area of soil zone
† = Value less than younger units due to average values used and low coverage of soil unit area

Soil Zone 1d is defined by thick (more than 10 m) geological unit U20, and typically thick geological subunit U20b sediments with no till material, shown on the left of Figure 8.8. The thick geological unit U20 sediments frequently caused buckling, limiting CPT penetration. BH034A is a good example of unit coverage in Soil Zone 1d (Figure 8.8), however does have a slightly thinner geological unit U20.

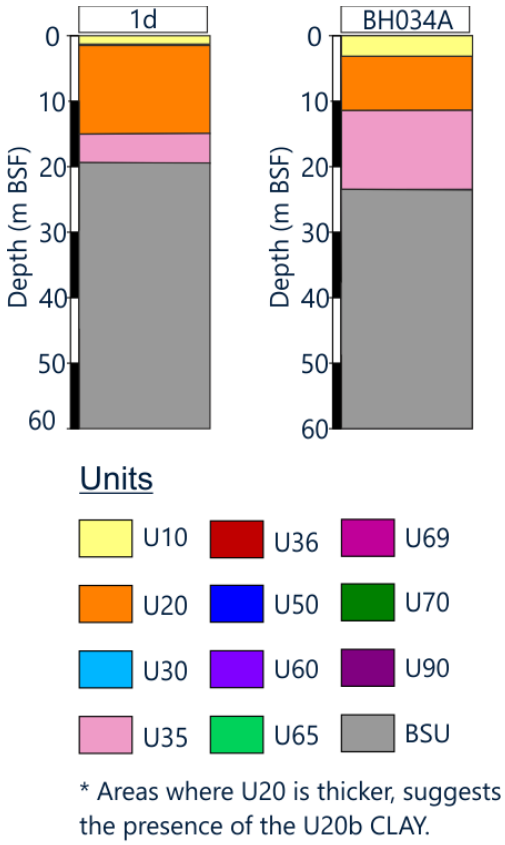

Figure 8.8: BH034A soil profile, Soil Zone 1d

8.3.5 Soil Zone 2a

Geological unit thicknesses within Soil Zone 2a were derived from the geological model layers defined within the Soil Zone 2a area. The mean depth to base of unit and percentage coverage of each unit in Soil Zone 2a are presented in Table 8.9. This zone is the most prominent across the site.

Table 8.9: Average soil unit depth to base and percentage coverage: Soil Zone 2a

Geological Unit	Mean Base Unit Depth [m]	Coverage of Zone [%]*
10	2.8	96
20	Absent	0
30	3.7	<1
35	5.4	12
36	Absent	0
50	7.0	4
60	8.7	<1
65	41.2	100
69	Absent	0
70	> 100.0	16

Geological Unit	Mean Base Unit Depth [m]	Coverage of Zone [%]*
90	75.1†	73

Notes
* = Unit present in the coverage % of total area of soil zone
† = Value less than younger units due to average values used and low coverage of soil unit area

Soil Zone 2a is defined by the shallow glacial till material of geological units U65 and U70. Location BH096 is a good example of the sediments typical of this unit, outlined by the percentage coverage in Soil Zone 2a (Figure 8.9).

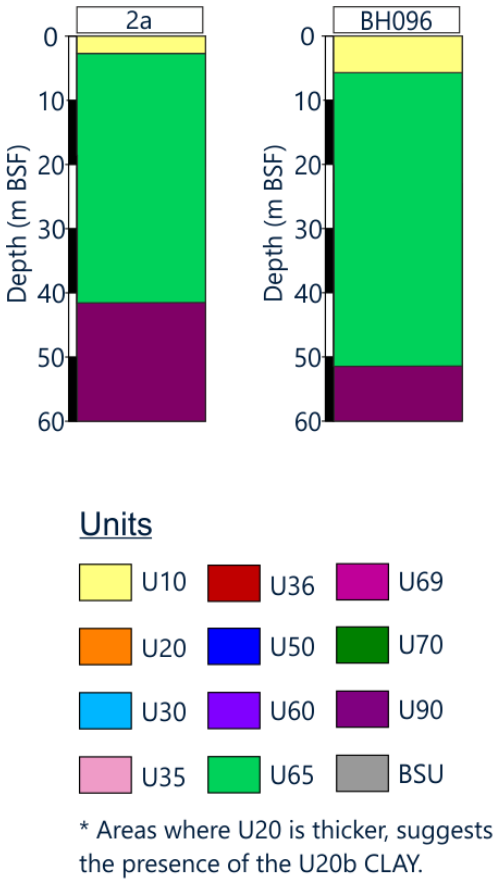

Figure 8.9: BH096 soil profile, Soil Zone 2a

8.3.6 Soil Zone 2b

Geological unit thicknesses within Soil Zone 2b were derived from the geological model layers defined within the Soil Zone 2b area. The mean depth to base of unit and percentage coverage of each unit in Soil Zone 2b are presented in Table 8.10.

Table 8.10: Average soil unit depth to base and percentage coverage: Soil Zone 2b

Geological Unit	Mean Base Unit Depth [m]	Coverage of Zone [%]*
10	1.2	80
20	3.5	100
30	4.8	2
35	6.9	41
36	Absent	0
50	7.5	17
60	9.2	< 1
65	24.6	98
69	Absent	0
70[x]	> 100	67
90	69.0	11

Notes
* = Unit present in the coverage % of total area of soil zone
[x] = Unit is not presented on predicted profile as it is greater than the depth of interest

Soil Zone 2b is defined by thin geological unit U20 sediments and shallow till material. Figure 8.10 shows the representative soil profile on the left. BH025, on the right of the figure, is an example of this soil profile. Its sediments are significantly thinner than would be expected from this zone and is missing geological unit U35, however is well representative of the shallower BSU and thin geological unit U20.

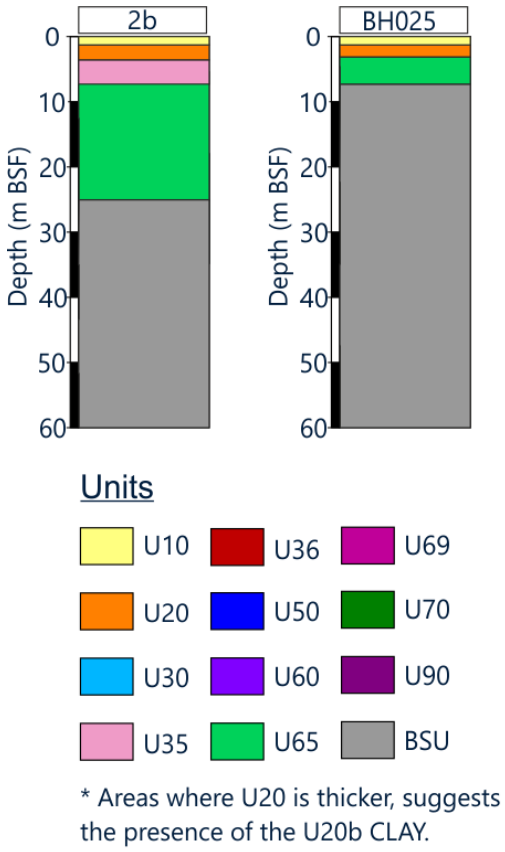

Figure 8.10: BH025 soil profile, Soil Zone 2b

8.3.7 Soil Zone 2c

Geological unit thicknesses within Soil Zone 2c were derived from the geological model layers defined within the Soil Zone 2c area. The mean depth to base of unit and percentage coverage of each unit in Soil Zone 2c are presented in Table 8.11.

Table 8.11: Average soil unit depth to base and percentage coverage: Soil Zone 2c

Geological Unit	Mean Base Unit Depth [m]	Coverage of Zone [%]*
10	1.0	80
20	8.0	100
30	8.0	1
35	9.0	30
36	Absent	0
50	9.4	3
60	Absent	0
65	23.6	96
69	Absent	0
70	> 100	57
90	56.2	15

Geological Unit	Mean Base Unit Depth [m]	Coverage of Zone [%]*
Notes * = Unit present in the coverage % of total area of soil zone † = Value more than older units due to average values used and low coverage of soil unit area		

There are no geotechnical locations that fall in this soil zone that represent the stratigraphy in the representative soil profile in Figure 8.11.

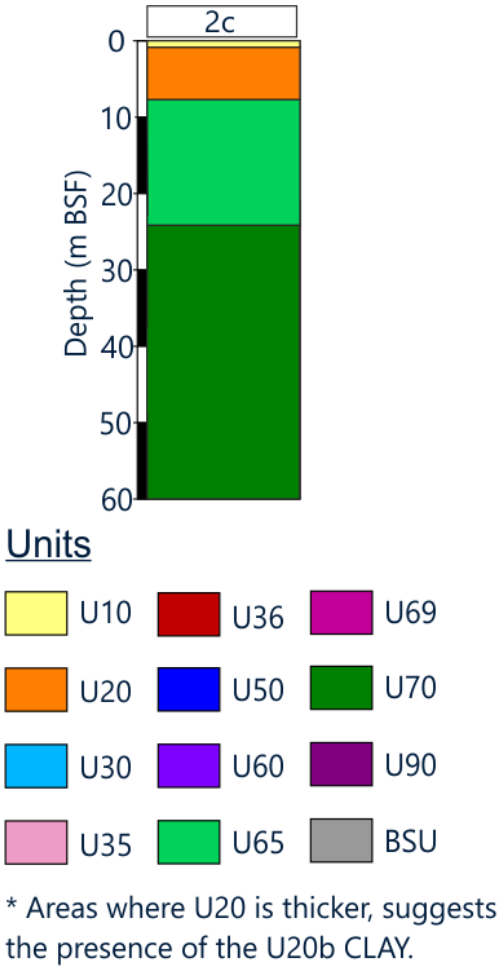

Figure 8.11: Representative soil profile, Soil Zone 2c

8.3.8 Soil Zone 3a

Geological unit thicknesses within Soil Zone 3a were derived from the geological model layers defined within the Soil Zone 3a area. The mean depth to base of unit and percentage coverage of each unit in Soil Zone 3a are presented in Table 8.12.

Table 8.12: Average soil unit depth to base and percentage coverage: Soil Zone 3a

Geological Unit	Mean Base Unit Depth [m]	Coverage of Zone [%]*
10	1.5	65

Geological Unit	Mean Base Unit Depth [m]	Coverage of Zone [%]*
20	Absent	0
30	4.0	4
35	6.8	90
36	16.8	4
50	13.9	93
60	30.3	70
65	69.5	45
69	73.4	4
70[x]	> 100	69
90	> 100	24

Notes
* = Unit present in the coverage % of total area of soil zone
[x] = Unit is not presented on predicted profile as it is greater than the depth of interest

Soil Zone 3a is defined by the absence of geological unit U20. Till material beneath an intermediate depth of Quaternary sediments indicates thicker geological unit U50 sediments. An example is BH008 (Figure 8.12), although geological unit U50 in this borehole is thinner than would normally be expected from the representative soil profile shown on the left of Figure 8.12.

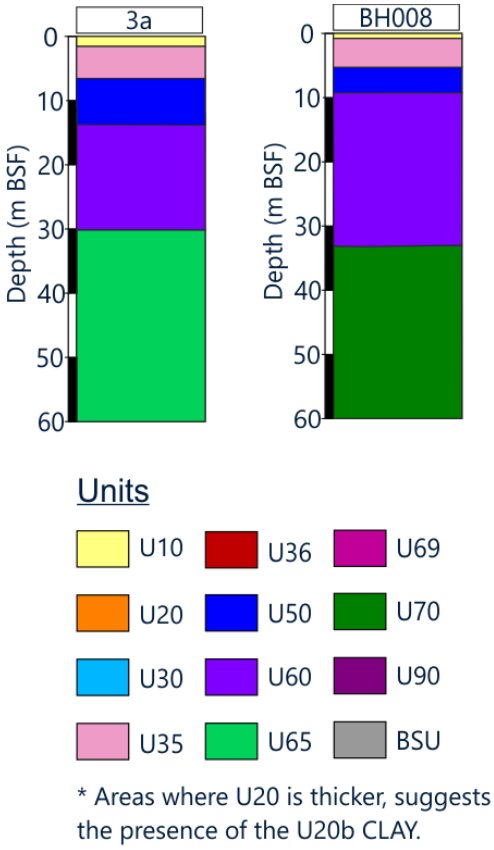

Figure 8.12: BH008 soil profile, Soil Zone 3a

8.3.9 Soil Zone 3b

Geological unit thicknesses within Soil Zone 3b were derived from the geological model layers defined within the Soil Zone 3b area. The mean depth to base of unit and percentage coverage of each unit in Soil Zone 3b are presented in Table 8.13.

Table 8.13: Average soil unit depth to base and percentage coverage: Soil Zone 3b

Geological Unit	Mean Base Unit Depth [m]	Coverage of Zone [%]*
10	1.2	52
20	3.5	100
30	8.0	11
35	8.8	91
36	13.0	8
50	15.0	85
60	30.4	97
65	43.8	43
69	64.7	1.2
70	> 100	84
90	80.4	2

Geological Unit	Mean Base Unit Depth [m]	Coverage of Zone [%]*
Notes * = Unit present in the coverage % of total area of soil zone		

Soil Zone 3b is defined by thin geological unit U20 sediments, typically of geological subunit U20a, with an intermediate package of quaternary sediments before till material. A stratigraphic type example of this is BH018, shown on the right of Figure 8.13. The representative soil profile is shown on the left of the figure.

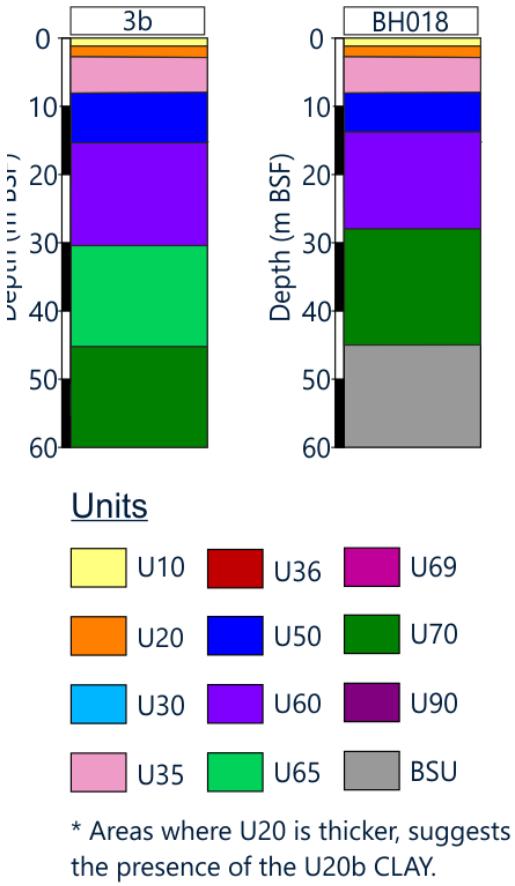

Figure 8.13: BH018 soil profile, Soil Zone 3b

8.3.10 Soil Zone 3c

Geological unit thicknesses within Soil Zone 3c were derived from the geological model layers defined within the Soil Zone 3c area. The mean depth to base of unit and percentage coverage of each unit in Soil Zone 3c are presented in Table 8.14.

Table 8.14: Average soil unit depth to base and percentage coverage: Soil Zone 3c

Geological Unit	Mean Base Unit Depth [m]	Coverage of Zone [%]*
10	1.5	60
20	9.0	100

Geological Unit	Mean Base Unit Depth [m]	Coverage of Zone [%]*
30	11.2	6
35	13.6	93
36	19.1	3
50	17.7	44
60	32.6	46
65	40.2	53
69	> 100	< 1
70	> 100	69
90	53.1	6

Notes
* = Unit present in the coverage % of total area of soil zone
† = Value more than older units due to average values used and low coverage of soil unit area

Soil Zone 3c is defined by thick geological unit U20 sediments, indicating the possible presence of geological subunit U20b clays and the presence of geological unit U65. Figure 8.14 shows a representative soil profile on the left of Soil Zone 3c. BH011 on the right of the figure is an example of this soil zone, although it has a thinner geological unit U20 sediment than would typically be expected.

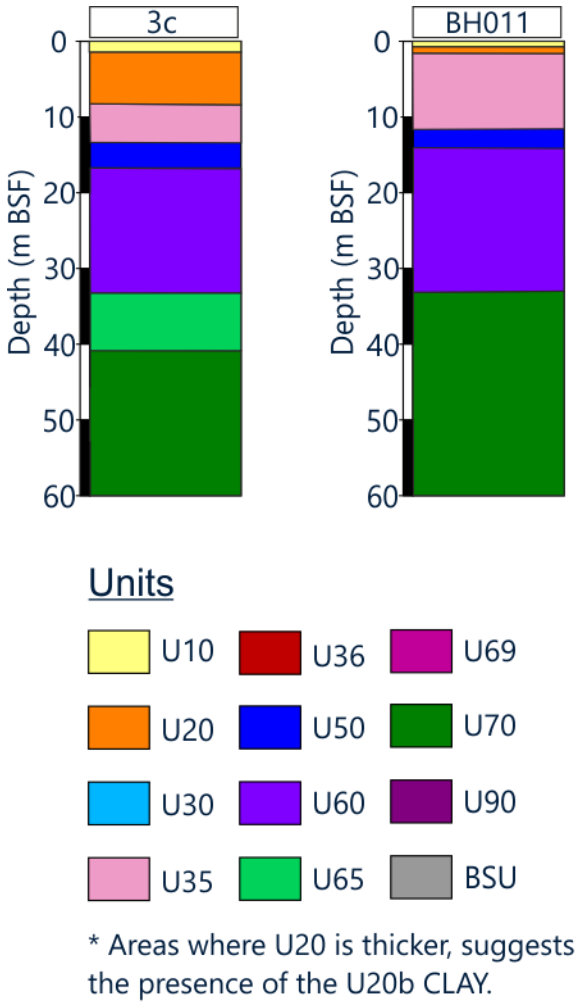

Figure 8.14: BH011 soil profile, Soil Zone 3c

8.3.11 Soil Zone 3d

Geological unit thicknesses within Soil Zone 3d were derived from the geological model layers defined within the Soil Zone 3d area. The mean depth to base of unit and percentage coverage of each unit in Soil Zone 3d are presented in Table 8.15.

Table 8.15: Average soil unit depth to base and percentage coverage: Soil Zone 3d

Geological Unit	Mean Base Unit Depth [m]	Coverage of Zone [%]*
10	1.3	90
20	14.5	100
30	13.5	1
35	18.7	81
36	21.6†	4
50	19.9	8
60	33.8	13
65	42.1	54

Geological Unit	Mean Base Unit Depth [m]	Coverage of Zone [%]*
69	Absent	0
70	> 100	69
90	55.9	10

Notes
* = Unit present in the coverage % of total area of soil zone
† = Value more than older units due to average values used and low coverage of soil unit area

Soil Zone 3d is characterised by thick geological unit U20, indicating the presence of geological subunit U20b clays, thick geological unit U65 and, within 50 m BSF, geological unit U70. Geological unit U60 is absent. This is shown in the representative soil profile on the left of Figure 8.15, and example location BH041 on the right.

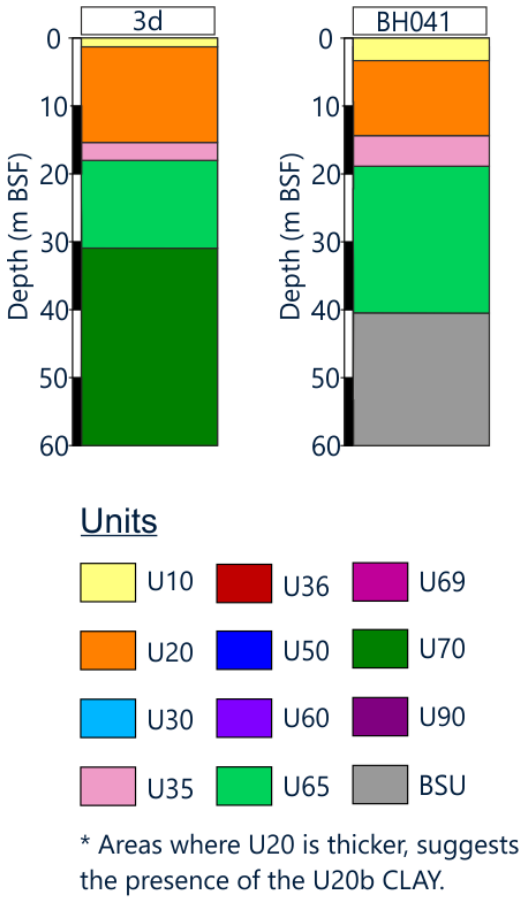

Figure 8.15: BH041 soil profile, Soil Zone 3d

8.3.12 Soil Zone 4a

Geological unit thicknesses within Soil Zone 4a were derived from the geological model layers defined within the Soil Zone 4a area. The mean depth to base of unit and percentage coverage of each unit in Soil Zone 4a are presented in Table 8.16.

Table 8.16: Average soil unit depth to base and percentage coverage: Soil Zone 4a

Geological Unit	Mean Base Unit Depth [m]	Coverage of Zone [%]*
10	0.9	39
20	Absent	0
30	4.1	1
35	6.6	99
36	16.9	9
50	15.3	98
60	39.8	99
65	93.3	16
69	83.3	60
70[x]	> 100	93
90	> 100	1

Notes
* = Unit present in the coverage % of total area of soil zone
[x] = Unit is not presented on predicted profile as it is greater than the depth of interest

Soil Zone 4a is defined by the absence of geological unit U20, the presence of geological unit U50, and a thick geological unit U60 above geological units U65 or U70 within 50 m BSF. BH009 (Figure 8.16) is a good example based on percentage coverage of the units, although this location excludes geological units U65 and U70 and includes geological unit U69 that typically sits above geological unit U70. This is shown on the left of Figure 8.16.

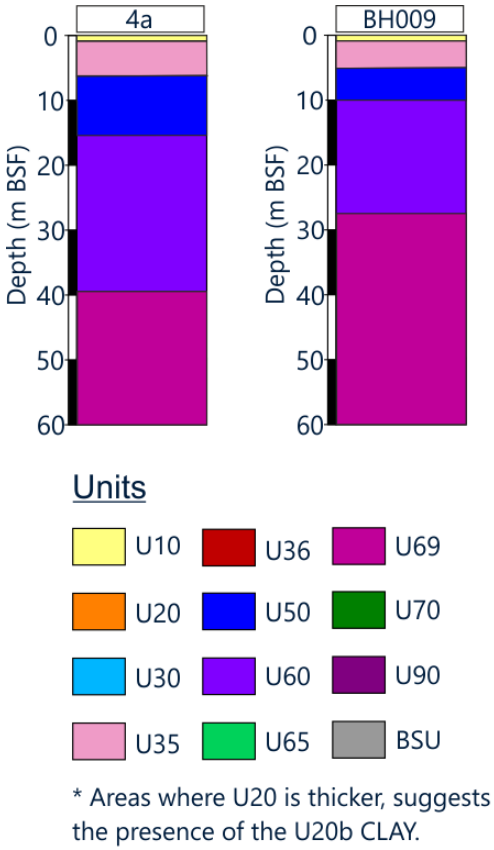

Figure 8.16: BH009 soil profile, Soil Zone 4a

8.3.13 Soil Zone 4b

Geological unit thicknesses within Soil Zone 4b were derived from the geological model layers defined within the Soil Zone 4b area. The mean depth to base of unit and percentage coverage of each unit in Soil Zone 4b are presented in Table 8.17.

Table 8.17: Average soil unit depth to base and percentage coverage: Soil Zone 4b

Geological Unit	Mean Base Unit Depth [m]	Coverage of Zone [%]*
10	0.9	41
20	3.7	100
30	7.9	5
35	8.4	90
36	10.0	23
50	18.3	99
60	40.3	100
65	96.3	13
69	79.3	40
70	> 100	97
90	85.6	1

Geological Unit	Mean Base Unit Depth [m]	Coverage of Zone [%]*
Notes * = Unit present in the coverage % of total area of soil zone		

Soil Zone 4b is defined by a thin layer of geological unit U20, indicating geological subunit U20a sands, as well as a thick layer of geological unit U60 above geological units U69 or U70. BH036 is a typical borehole in this soil zone (Figure 8.17). The representative soil profile is shown on the left.

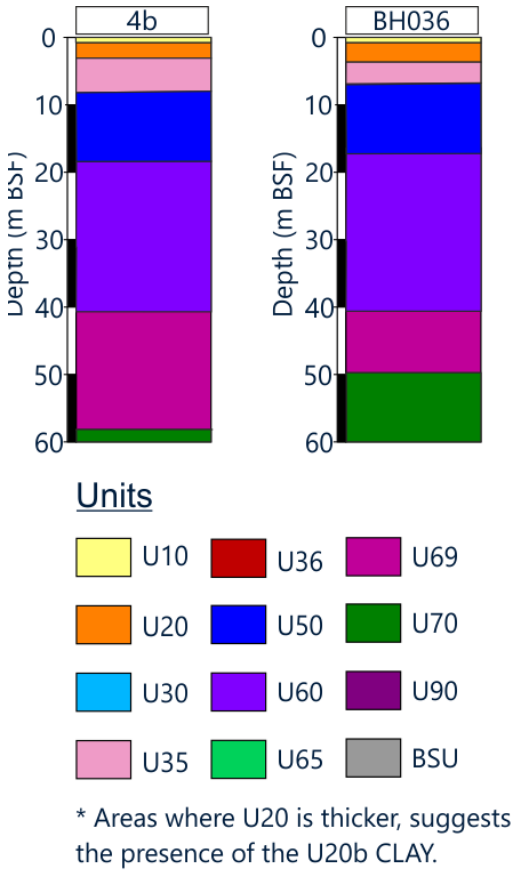

Figure 8.17: BH036 soil profile, Soil Zone 4b

8.3.14 Soil Zone 4c

Geological unit thicknesses within Soil Zone 4c were derived from the geological model layers defined within the Soil Zone 4c area. The mean depth to base of unit and percentage coverage of each unit in Soil Zone 4c are presented in Table 8.18.

Table 8.18: Average soil unit depth to base and percentage coverage: Soil Zone 4c

Geological Unit	Mean Base Unit Depth [m]	Coverage of Zone [%]*
10	0.9	50
20	8.3	100

Geological Unit	Mean Base Unit Depth [m]	Coverage of Zone [%]*
30	8.5	3
35	12.6	99
36	16.4	9
50	20.6	95
60	44.4	100
65	100.3	14
69	96.8	17
70	> 100	94
90	77.2	2

Notes
* = Unit present in the coverage % of total area of soil zone

Soil Zone 4c is similar to Soil Zone 4b, but geological unit U20 is thicker, indicating the possible presence of geological subunits U20a and U20b in channelised areas. No representative geotechnical locations penetrate this zone. Figure 8.18 displays a representative soil profile for this zone.

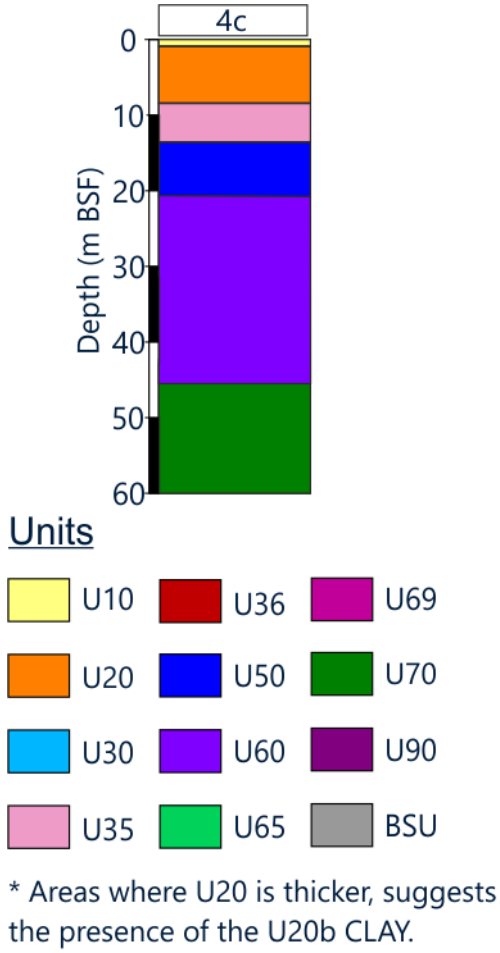

Figure 8.18: Representative soil profile, Zone 4c

8.3.15 Soil Zone 4d

Geological unit thicknesses within Soil Zone 4d were derived from the geological model layers defined within the Soil Zone 4d area. The mean depth to base of unit and percentage coverage of each unit in Soil Zone 4d are presented in Table 8.19.

Table 8.19: Average soil unit depth to base and percentage coverage: Soil Zone 4d

Geological Unit	Mean Base Unit Depth [m]	Coverage of Zone [%]*
10	0.9	64
20	13.6	100
30	Absent	0
35	16.1	94
36	19.8	7
50	22.4	83
60	45.4	100
65	106.2	14
69	8106	19

Geological Unit	Mean Base Unit Depth [m]	Coverage of Zone [%]*
70	> 100	98
90	84.0	<1

Notes
* = Unit present in the coverage % of total area of soil zone

Soil Zone 4d is comparable to zones 4b and 4c but Unit 20 is thicker, indicating the potential presence of geological subunit U20b clay. Geological unit U60 is also thicker, overlying geological unit U70 at approximately 50 m BSF. No CPTs or boreholes were available in this zone. Figure 8.19 presents the representative soil profile.

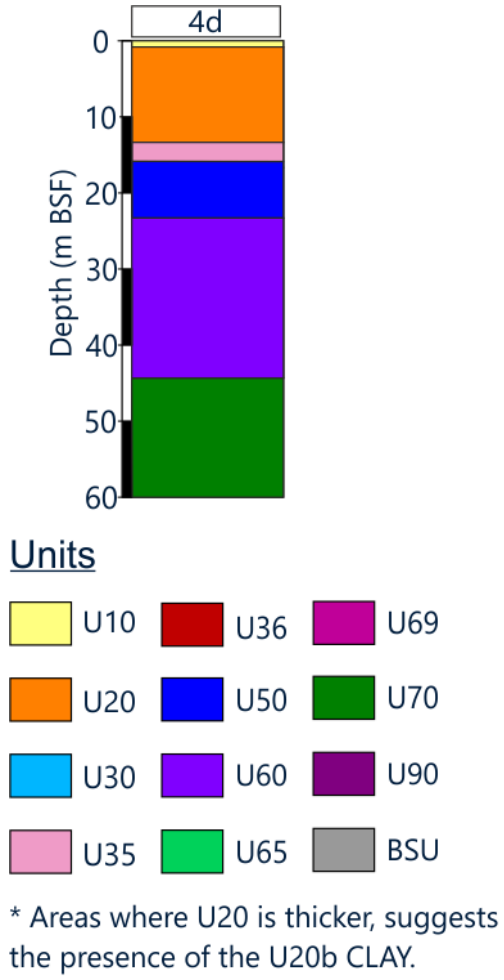

Figure 8.19: Representative soil profile, Zone 4d

9. Drawings and Data Deliverables

9.1 Drawings

Table 9.1 lists the charts provided with this report.

Table 9.1: Summary of deliverables - charts

Data Type	Chart No.	Chart Name	Description
Map chart	1	Geotechnical Locations	Locations of geotechnical and seismic data
	2	Top BSU BSB	Depth to top of BSU below seabed
	3	Base U10 MSL	Depth to base of Unit 10 below sea level
	4	Base U10 BSB	Depth to base of Unit 10 below seabed
	5	Isochore U10	Thickness of Unit 10
	6	Base U20 MSL	Depth to base of Unit 20 below sea level
	7	Base U20 BSB	Depth to base of Unit 20 below seabed
	8	Top U20 BSB	Depth to top of Unit 20 below seabed
	9	Isochore U20	Thickness of Unit 20
	10	Base U30 MSL	Depth to base of Unit 30 below sea level
	11	Base U30 BSB	Depth to base of Unit 30 below seabed
	12	Top U30 BSB	Depth to top of Unit 30 below seabed
	13	Isochore U30	Thickness of Unit 30
	14	Base U35 MSL	Depth to base of Unit 35 below sea level
	15	Base U35 BSB	Depth to base of Unit 35 below seabed
	16	Top U35 BSB	Depth to top of Unit 35 below seabed
	17	Isochore U35	Thickness of Unit 35
	18	Base U36 MSL	Depth to base of Unit 36 below sea level
	19	Base U36 BSB	Depth to base of Unit 36 below seabed
	20	Top U36 BSB	Depth to top of Unit 36 below seabed
	21	Isochore U36	Thickness of Unit 36
	22	Base U50 MSL	Depth to base of Unit 50 below sea level
	23	Base U50 BSB	Depth to base of Unit 50 below seabed
	24	Top U50 BSB	Depth to top of Unit 50 below seabed
	25	Isochore U50	Thickness of Unit 50
	26	Base U60 MSL	Depth to base of Unit 60 below sea level
	27	Base U60 BSB	Depth to base of Unit 60 below seabed
	28	Top U60 BSB	Depth to top of Unit 60 below seabed
	29	Isochore U60	Thickness of Unit 60
	30	Base U65 MSL	Depth to base of Unit 65 below sea level
	31	Base U65 BSB	Depth to base of Unit 65 below seabed

Data Type	Chart No.	Chart Name	Description
	32	Top U65 BSB	Depth to top of Unit 65 below seabed
	33	Isochore U65	Thickness of Unit 65
	34	Base U69 MSL	Depth to base of Unit 69 below sea level
	35	Base U69 BSB	Depth to base of Unit 69 below seabed
	36	Top U69 BSB	Depth to top of Unit 69 below seabed
	37	Isochore U69	Thickness of Unit 69
	38	Base U70 MSL	Depth to base of Unit 70 below sea level
	39	Base U70 BSB	Depth to base of Unit 70 below seabed
	40	Top U70 BSB	Depth to top of Unit 70 below seabed
	41	Isochore U70	Thickness of Unit 70
	42	Base U90 MSL	Depth to base of Unit 90 below sea level
	43	Base U90 BSB	Depth to base of Unit 90 below seabed
	44	Top U90 BSB	Depth to top of Unit 90 below seabed
	45	Isochore U90	Thickness of Unit 90
	46	Shallow Gas	Mapped areas of shallow gas
	47	Soil Provinces	Soil province mapping
Profile chart	48	Seismic Profile EAAG218P1	Cross section of geology
	49	Seismic Profile EAAS263P1	
	50	Seismic Profile EAAY310P1	
	51	Seismic Profile EAXA381P1	
	52	Seismic Profile EAXB390P1	
	53	Seismic Profile EAXC399P1	
	54	Seismic Profile EAXD408P1	
	55	Seismic Profile EAXD420P1	
Integration chart	56–158	BH Integration Sheets	Comparison of integration at each BH location
Notes BSU = Base seismic unit BSB = Below seabed MSL = Mean Sea Level BH = Borehole			

9.2 Digital Deliverables

Table 9.2 lists the final digital deliverables.

Table 9.2: Summary of digital deliverables

Data Type	Type	Description	Resolution [m]	Format
Grids	Grids (base)	MSL	5	ASCII XYZ and GeoTIFF

Data Type	Type	Description	Resolution [m]	Format
	Grids (top and base)	BSF	5	ASCII XYZ and GeoTIFF
	Grids	Isochore	5	ASCII XYZ and GeoTIFF
Kingdom Workspace	Kingdom project	SBP and 2D UHRS		Time (both) and depth (both)
GIS deliverable	Shallow gas	Seismic anomalies		GeoTIFF/ASCII XYZ
	Geotechnical zonation	Zonation polygon		Shapefile/GeoTIFF
	Geotechnical points	Geotechnical location points with depths		Shapefile

Notes
MSL = Mean Sea Level
BSF = Below seafloor
SBP = Sub-bottom profiler
UHRS = Ultra high resolution seismic

10. References

Arfai, J., Franke, D., Lutz, R., Reinhardt., L, Kley, J., & Gaedicke, C. (2018). Rapid Quaternary subsidence in the northwestern German North Sea. *Scientific Reports 8*, 11524. https://doi.org/10.1038/s41598-018-29638-6

Batchelor, C., Margold, M., Krapp, M., Murton, D., Dalton, A., Gibbard, P., Stokes, C., Murton, J., & Manica, A. (2019). The configuration of Northern Hemisphere ice sheets through the Quaternary. *Nature Communications, 10*, 3713. https://doi.org/10.1038/s41467-019-11601-2

Cartelle, V., Barlow, N.L.M., Hodgson, D.M., Busschers, F.S., Cohen, K.M., Meijninger, B.M.L., & van Kesteren, W.P. (2021). Sedimentary architecture and landforms of the late Saalian (MIS 6) ice sheet margin offshore of the Netherlands. *Earth Surface Dynamics, 9*, 1399–1421. https://doi.org/10.5194/esurf-9-1399-2021

Cohen, K., Gibbard, P., & Weerts, H.J.T. (2014). North Sea palaeogeographical reconstructions for the last 1 Ma. *Geologie en Mijnbouw, 93* (7–29). https://doi.org/10.1017/njg.2014.12

Cohen, K., Cartelle, V., Barnett, R., Busschers, F., & Barlow, N. (2022). Last interglacial sea-level data points from northwest Europe. *Earth System Science Data, 14*. https://doi.org/10.5194/essd-14-2895-2022

COWI. (2021). *Thor offshore wind farm – Integrated geological model* (Document No. A205839 004, issue 2, dated 1 March 2021 to Energinet Eltransmission A/S). COWI A/S.

DNV GL. (2019). *Statistical representation of soil data* (DNVGL-RP-C207). https://www.dnv.com/energy/standards-guidelines/dnv-rp-c207-statistical-representation-of-soil-data/

European Marine Observation and Data Network [EMODnet]. (2023, 15 June). *Sea-floor geology*. https://emodnet.ec.europa.eu/geonetwork/srv/eng/catalog.search#/metadata/429ef6798d5618780f9e66ff2ba8e237c852f8d6

Friborg, R. (1996). The landscape below the Tinglev outwash plain: a reconstruction. *Dansk Geologisk Forening 43*(1), 34–40. https://doi.org/10.37570/bgsd-1996-43-04

Fugro. (2023a). *Operations report – MV Arctic* (Document No. F217715-OPS-001/02). Fugro FNML.

Fugro. (2023b). *Operations report – Fugro Pioneer* (Document No. F217715-OPS-002/02). Fugro FNML.

Fugro. (2023c). *Baseline survey results report* (Document No. F217715-REP-001/02). Fugro FNML.

Fugro. (2024a). *Report no 2, 2D UHRS survey geomodel integrated with CPT data, full site* (Document No. F217715-REP-002/03). Fugro Netherlands Marine Limited.

Fugro. (2024b*). Investigation results, geotechnics. Seafloor and in situ test locations, Subarea 1* (Document No. F217703/01 03). Fugro Netherlands Marine Limited.

Fugro. (2024c*). Investigation results, geotechnics. Seafloor and in situ test locations, Subarea 2* (Document No. F217703/02 03). Fugro Netherlands Marine Limited.

Fugro. (2024d). *Preliminary geotechnical investigations for Danish offshore wind farm 2030 Lot 2 | Danish sector, North Sea – Records of operations – Excalibur* (Document No. F217703-04/02). Fugro Netherlands Marine Limited.

Fugro. (2024e). *Preliminary geotechnical investigations for Danish offshore wind farm 2030 Lot 2 – Danish sector, North Sea – Records of operations – Gargano* (Document No. F217703-03/02). Fugro Netherlands Marine Limited.

Fugro (2024f). *Preliminary geotechnical investigations for Danish offshore wind farm 2030 Lot 2 – Danish sector, North Sea – Records of operations – Voyager* (Document No. F217703-02/02). Fugro Netherlands Marine Limited.

Fugro (2024g). *Danish offshore wind 2030 – North Sea 1 – Sub area, investigation results, geotechnical borehole locations* (Document No. F217703/04-03). Fugro Netherlands Marine Limited.

Fugro (2024h). *Report no 3, 2D UHRS survey geomodel integrated with CPT and BH data, Sub-Area 1* (Document No. F217715-REP-003/02). Fugro Netherlands Marine Limited.

Fugro. (2025a). *Preliminary geotechnical investigations for Danish offshore wind farm 2030 Lot 2 – Danish sector, North Sea – Records of operations – Fugro Synergy* (Document No. F217703-05). Fugro Netherlands Marine Limited.

Fugro. (2025b). *Preliminary geotechnical investigations for Danish offshore wind farm 2030 Lot 2 – Danish sector, North Sea – Records of operations – Fugro Zenith* (Document No. F217703-06). Fugro Netherlands Marine Limited.

Fugro. (2025c). *Preliminary geotechnical investigations for Danish offshore wind farm 2030 Lot 2 – Danish sector, North Sea – Records of operations – RS Alegranza* (Document No. F217703-07). Fugro Netherlands Marine Limited.

Fugro (2026a). *Danish offshore wind 2030 – North Sea 1 – Sub area, investigation results, geotechnical borehole locations* (Document No. F217703/04). Fugro Netherlands Marine Limited. NOT IN PRINT

Gibbard, P.L., & Cohen, K.M. (2015). Quaternary evolution of the North Sea and the English Channel. *Proceedings of the Open University Geological Society 2*, 63–74. http://ougs.org/branch_matters/index.php?branchcode=ouc

Gibbard, P.L. & Lewin, J. (2016). Filling the North Sea Basin: Cenozoic sediment sources and river styles. *Geologica Belgica, 19*(3-4), 201–217. http://dx.doi.org/10.20341/gb.2015.017

Gibson, S.M., Bateman, M.D., Murton, J.B., Barrows, T.T., Fifield, L.K., & Gibbard, P.L. (2022). Timing and dynamics of Late Wolstonian Substage 'Moreton Stadial' (MIS 6) glaciation in the English West Midlands, UK. *Royal Society Open Science*, *9*. https://doi.org/10.1098/rsos.220312

Harrison, S., Smith, D.E., & Glasser, N.F. (2018). Late Quaternary meltwater pulses and sea level change. *Journal of Quaternary Science 34(1*), 1–15. https://doi.org/10.1002/jqs.3070

Houmark-Nielsen, M. (2011). Chapter 5 – Pleistocene glaciations in Denmark: A loser look at chronology, ice dynamics and landforms. *Developments in Quaternary Sciences*, *15*, 47–58. https://doi.org/10.1016/B978-0-444-53447-7.00005-2

Høyer A.-S., Jørgensen, F., Piotrowski, J.A., & Jakobsen, P.R. (2013). Deeply rooted glaciotectonism in western Denmark: geological composition, structural characteristics and the origin of Varde hill-island. *Journal of Quaternary Science, 28*(7), 683–696. https://doi.org/10.1002/jqs.2667

Hughes, A., Gyllencreutz, R., Lohne, Ø., Mangerud, J., & Svendsen, J. (2015). The last Eurasian ice sheets – a chronological database and time-slice reconstruction, DATED-1. *Boreas* (*45),* 1–45. https://doi.org/10.1111/bor.12142

Hughes, P., Gibbard, P.L., & Ehlers, J. (2020). The "missing glaciations" of the Middle Pleistocene. *Quaternary Research*, *96*, 161–183. https://doi.org/10.1017/qua.2019.76

Huuse, M., & Lykke-Andersen, H. (2000a). Large-scale glaciotectonic thrust structures in the eastern Danish North Sea. *Geological Society, London, Special Publications*, *176*, 293–305. https://doi.org/10.1144/GSL.SP.2000.176.01.22

Huuse, M., & Lykke-Andersen, H. (2000b). Overdeepened Quaternary valleys in the eastern Danish North Sea: morphology and origin. *Quaternary Science Reviews, 19*, 1233–1253. https://doi.org/10.1016/S0277-3791(99)00103-1

Jamiolkowski, M., Lo Presti, D.C.F., & Manassero, M. (2003). Evaluation of relative density and shear strength of sands from CPT and DMT. In J.T. Germaine, T.C. Sheahan, & R.V. Whitman (Eds.), *Soil behavior and soft ground construction* (pp. 201–238). ASCE. https://doi.org/10.1061/9780784406595

Jensen, J.B., Gravesen, P., & Lomholt, S. (2008). Geology of outer Horns Rev, Danish North Sea. *Geological Survey of Denmark and Greenland Bulletin, 15*, 41–44. https://doi.org/10.34194/geusb.v15.5040

Kirkham, J.D., Hogan, K.A., Larter, R.D., Self, E., Games, K., Huuse, M., Stewart, M.A., Ottesen, D., Arnold, N.S., & Dowdeswell, J.A. (2021). Tunnel valley infill and genesis revealed by high-resolution 3-D seismic data. *Geology, 49*(12), 1516–1520. https://doi.org/10.1130/G49048.1E

Knox, R.W.O.B., Bosch, J.H.A., Rasmussen, E.S., Heilmann-Clausen, C., Hiss, M., De Lugt, I.R., Kasiński, J., King, C., Köthe, A., Słodkowska, B., Standke, G., & Vandenberghe, N. (2010). Cenozoic. In J.C. Doornenbal & A.G. Stevenson (Eds.), *Petroleum geological atlas of the southern Permian basin area* (pp. 211–223). EAGE Publications.

Konradi, P., Larsen, B., & Sørensen, A. (2005). Marine Eemian in the Danish eastern North Sea. *Quaternary International*, *133–134*(1), 21–31. https://doi.org/10.1016/j.quaint.2004.10.003

Lambe, T.W., & Whitman, R.V. (1969). *Soil mechanics*. John Wiley & Sons.

Lang, J., Lauer, T., & Winsemann, J. (2018). New age constraints for the Saalian glaciation in northern central Europe: Implications for the extent of ice sheets and related pro-glacial lake systems. *Quaternary Science Reviews, 180*, 240–259. https://doi.org/10.1016/j.quascirev.2017.11.029

Lang, J., Ahlo, P., Kasvi, E., Goseberg, N., & Winsemann, J. (2019). Impact of Middle Pleistocene (Saalian) glacial lake-outburst floods on the meltwater-drainage pathways in northern central Europe: Insights from 2D numerical flood simulation. *Quaternary Science Reviews. 209*, 82–99. https://doi.org/10.1016/j.quascirev.2019.02.018

Larsen, G., Frederiksen, J., Villumsen, A., Fredericia, J., Gravesen, P., Foged, N., Knudsen, B., & Baumann, J. (1995). *A guide to engineering geological soil description*. Revision 1, Dansk Geoteknisk Forening, Aalborg Universitets trykkeri.

Larsen, B., & Andersen, L.T. (2005). Late Quaternary stratigraphy and morphogenesis in the Danish eastern North Sea and its relation to onshore geology. *Netherlands Journal of Geosciences, 84(2)*, 113–128. https://doi.org/10.1017/S0016774600023003

Möller, P., Alexandreson, H., Anjar, J., & Björck, S. (2020). MIS 3 sediment stratigraphy in southern Sweden sheds new light on the complex glacial history and dynamics across southern Scandinavia. *Boreas*, 389–416. https://doi.org/10.1111/bor.12433

Nielsen, T., Mathiesen, A., & Bryde-Auken, M. (2008). Base Quaternary in the Danish parts of the North Sea and Skagerrak. *GEUS Bulletin, 15*, 37–40. https://doi.org/10.34194/geusb.v15.5038

Ocean Infinity. (2024). *Report no 6, Geophysical Site Survey Report: Danish Offshore Wind 2030 LOT 4, Work package C, NS1* (Document No. 104287-ENN-OI-SUR-REP-LOT4WPCNS1). Ocean Infinity Group Holding AB.

Overeem, I., Weltje, G.J., Bishop-Kay, C., & Kroonenberg, S.B. (2001). The Late Cenozoic Eridanos delta system in the Southern North Sea Basin: a climate signal in sediment supply? *Basin Research, 13*, 293–312. https://doi.org/10.1046/j.1365-2117.2001.00151.x

Rad, N.S., & Lunne, T. (1988). Direct correlations between piezocone test results and undrained shear strength of clay. In J. De Ruiter (Ed.), *Penetration testing 1988: Proceedings of the first international symposium on penetration testing ISOPT-1* (Vol. 2, pp. 911–917). A.A. Balkema.

Tóth, Z., Spiess, V., Mogollón, J.M., & Jensen, J.B. (2014). Estimating the free gas content in Baltic Sea sediments using compressional wave velocity from marine seismic data. *Journal of Geophysical Research: Solid Earth, 119,* 8577–8593. https://doi:10.1002/2014JB010989

Walker, J., Gaffney, V., Fitch, S., Muru, M., Fraser, A., Bates, M., & Bates, C. (2020). A great wave: the Storegga tsunami and the end of Doggerland? *Antiquity, 94*(378), 1409–1425. https://doi.org/10.15184/aqy.2020.49

Winsemann, J., Koopmann, H., Tanner, D.C., Lutz, R., Lang, J., Brandes, C., & Gaedicke, C. (2020). Seismic interpretation and structural restoration of the Heligoland glaciotectonic thrust-fault complex: Implications for multiple deformation during (pre-)Elsterian to Warthian ice advances into the southern North Sea Basin. *Quaternary Science Reviews, 227*. https://doi.org/10.1016/j.quascirev.2019.106068

Wohlfarth, B. (2013). A review of Early Weichselian climate (MIS 5d-a) in Europe. *Technical report/Svensk kärnbränslehantering AB, 44*(50). https://archimer.ifremer.fr/doc/00499/61046/

Appendix A

Guidelines for Use of Report

This report (the "Report") was prepared as part of the services (the "Services") provided by Fugro for its client (the "Client") and in accordance with the terms of the relevant contract between the two parties (the Contract") and to the extent to which Fugro relied on Client or third-party information as was set out in the Contract.

Fugro's obligations and liabilities to the Client or any other party in respect of this Report are limited to the extent and for the time period set out in the Contract (or in the absence of any express provision in the Contract as implied by the law of the Contract) and Fugro provides no other representation or warranty whether express or implied, in relation to the use of this Report, for any purpose. Furthermore, Fugro has no obligation to update or revise this Report based on any future changes in conditions or information which emerge following issue of this Report unless expressly required by the provisions of the Contract.

This Report was formed and released by Fugro exclusively for the Client and any other party expressly identified in the Contract, and any use and/or reliance on the Report or the Services for purposes not expressly stated in the Contract, will be at the Client's sole risk. Any other party seeking to rely on this Report does so wholly at its own and sole risk and Fugro accepts no liability whatsoever for any such use and/or reliance.

Appendix B

Geotechnical Information

B.1 Geotechnical Information

This section contains all geotechnical locations collected and the depth to base for each unit.

Name	Easting [m]	Northing [m]	Total Penetration Depth [m BSF]	Water Depth [m MSL]	Vessel	U10 Depth to Base [m BSF]	U20 Depth to Base [m BSF]	U20a Depth to Base [m BSF]	U20b Depth to Base [m BSF]	U30 Depth to Base [m BSF]	U35 Depth to Base [m BSF]	U36 Depth to Base [m BSF]	U50 Depth to Base [m BSF]	U60 Depth to Base [m BSF]	U65 Depth to Base [m BSF]	U69 Depth to Base [m BSF]	U70 Depth to Base [m BSF]	U90 Depth to Base [m BSF]	BSU Depth to Top [m BSF]
BH001	396645.1	6234082.18	70	-30.6	Gargano			1.9		10.9	12.9			28.8					28.8
BH002	393120.18	6229243.71	69.7	-29.7	Fugro Voyager	0.8		4.9	6.5	10.8	14.5			37.0					37.0
BH003	400349.44	6228756.23	70	-29.8	Gargano			5.0	10.4		13.3		15.9	58.2					58.2
BH004	410030.64	6227789.33	68.4	-29.7	Gargano	2.9			4.5	6.6	10.2		14.3	35.4			70.0		
BH005	396900.24	6226991.84	69.9	-29.5	Gargano			5.4	5.9	6.8	20.9			38.8					38.8
BH006	405733.06	6226820.41	69.7	-28.7	Fugro Voyager	3.1		5.7		7.6	12.4		15.8	27.8			70.0		
BH007	414851.59	6226748.78	70.2	-30.4	Gargano	0.8		2.1			10.7			28.3			70.0		
BH008	423582.28	6226642.03	70.1	-27.1	Fugro Voyager	0.3					4.7		9.3	32.8			66.9		66.9
BH009	418728.64	6226611.65	70.7	-29.8	Gargano	1.2					4.7		10.5	28.6		66.0	70.0		
BH010	392239.51	6225952.1	70	-30.3	Fugro Voyager			5.4	8.3		13.6				23.7				23.7
BH011	402860.35	6225210.26	70.4	-28.3	Gargano	0.3		1.3	6.8		11.6		12.9	32.8			70.0		
BH012	397291.82	6224009.16	70	-28.5	Fugro Voyager	0.4		3.9	7.1		16.4			28.2					28.2
BH013	411361.85	6223986.92	70	-30.2	Gargano			0.8			9.3		12.7	34.3			70.0		
BH014	406065.76	6223876.73	70.2	-27.3	Gargano	2.9			3.4		9.7				27.6		70.0		
BH015	394848.01	6223442.73	70.0	-30.1	Fugro Voyager			2.9	5.3		9.5								9.5
BH016	416208.06	6222987.31	70.2	-29.5	Fugro Voyager	0.4					8.7		12.4	28.8	36.5	70.0			
BH017	386813.53	6222760.31	70.0	-29.3	Fugro Voyager	0.9		3.4		6.6					70.0				
BH018	400455.97	6222679.75	70.0	-27.2	Gargano			1.6	4.1		13.4		14.9	28.3			45.8		45.8
BH019	418595.36	6222491.61	70.0	-29.4	Gargano	0.2					7.5		13.2	30.5	52.3	70.0			
BH020	423140.58	6222412.59	69.7	-27.5	Fugro Voyager	0.4					5.4		13.9	40.8			70.0		
BH021	407207.32	6222100.47	70.2	-27.5	Gargano	0.9					6.4				21.3		70.0		
BH022	413223.2	6221321.01	70.0	-30.9	Gargano				0.1		5.9		10.4	36.8			70.0		
BH023	416355.52	6220006.2	69.8	-30.3	Fugro Voyager						6.2		12.7	28.3			70.0		
BH025	386473.5	6219623.0	70.2	-28.9	Fugro Zenith	2.2		3.3							6.3				6.3
BH026	399886.85	6218850.17	69.7	-25.6	Fugro Voyager	1.3		2.3			5.9				17.4		70.0		
BH027	396432.5	6218717.16	70.2	-27.9	Fugro Voyager	0.8		3.8			6.8								6.8
BH031	381363.9	6216776.4	70.5	-29.7	Fugro Synergy	1.8		9.0	11.4		23.0				70.4				
BH033	414241.41	6216497.58	70.0	-30.9	Fugro Voyager				0.7		3.5		11.2	41.3			70.0		
BH034A	385607.7	6216384.3	61.5	-26.9	Fugro Synergy	3.1		10.7	15.2		23.5								23.5
BH035	402167.56	6215906.96	69.9	-25.4	Fugro Voyager	0.5		2.2			9.3		10.5		19.7		70.0		
BH036	410871.62	6215717.73	70.0	-27	Gargano	0.8		4.6			7.8		17.8	41.2		50.0	70.0		
BH037	423222.41	6215296.91	70.3	-26.9	Gargano	0.8					6.5	8.9	14.9	40.5		48.5	70.0		
BH038	419066.22	6214396.5	69.6	-29.1	Fugro Voyager			0.3			4.5		11.9	35.3			70.0		
BH040	394772.65	6214228.87	70.8	-29	Gargano	0.2		6.4	7.2		10.2				45.5				45.5
BH041	385747.3	6213340.4	70.5	-29.2	Fugro Zenith	3.0		9.0	14.7		18.4				40.5				40.5
BH043	409952.43	6213003.27	69.9	-24.7	Fugro Voyager	0.3		3.6	4.5		7.2				54.6		70.0		
BH044	415855.05	6212694.63	70.1	-29.4	Gargano			1.9			3.8		12.9	28.8			70.0		
BH045	403450.68	6212009.97	69.7	-24.4	Gargano	0.2		2.8							16.4		70.0		
BH046	382308.4	6211580.8	69.8	-29.6	RS Alegranza	0.8		9.8	10.2		16.4							32.0	32.0
BH047	421872.19	6210918.64	70.0	-27.3	Fugro Voyager	0.4					4.3		12.2	28.8		58.1	70.0		
BH048	390094.9	6210159.9	61.9	-26.4	Fugro Synergy	4.9		12.0	18.3		33.7				59.4				59.4
BH050	378622.1	6209719.8	70.2	-33.4	Fugro Zenith	1.9		3.4			11.7				42.5			70.2	
BH051	414977.08	6209474.29	70.0	-28	Fugro Voyager			3.1			4.8		12.9	28.3			70.0		
BH052	410203.38	6209421.94	70.0	-23.8	Fugro Voyager			7.2	8.4		10.5		18.1	39.8			70.0		
BH053	398510.66	6208916.59	69.7	-23	Fugro Voyager	2.5		8.6	14.4		15.8								15.8
BH054	406745.32	6208663.86	70.3	-23.4	Fugro Voyager	0.7		4.7	6.2		9.1				17.1		70.0		
BH055	420062.76	6207457.21	69.9	-28	Fugro Voyager				0.8		4.4	10.3	14.2	26.8			70.0		
BH056	380516.7	6207120.1	71.0	-32.5	Fugro Synergy										67.5				67.5
BH057B	382811.5	6206798.2	70.5	-30.2	Fugro Zenith	3.5									70.5				
BH058	402559.57	6206750.11	70.4	-23.8	Gargano	0.5		5.3	11.6		15.6						70.4		
BH059C	386271.5	6206302.0	70.4	-28.3	Fugro Zenith	2.8									28.6			37.7	37.7
BH060	412982.79	6205921.86	70.1	-24.4	Fugro Voyager			7.9	9.1		10.9		17.5	31.3			49.3		49.3
BH062	422902.64	6205000.28	70.3	-27.3	Gargano	0.4		1.8			4.5	7.9	12.8	34.7					34.7
BH063	408344.24	6204949.16	69.9	-22.5	Gargano	0.8		5.9	10.9		14.7						69.9		
BH064	388645.8	6204769.9	70.2	-26.5	Fugro Zenith	5.3									43.8				43.8
BH065	397167.48	6204528.27	69.9	-28.5	Fugro Voyager	0.4							9.5		27.3				27.3
BH066A	376480.4	6204160.2	71.0	-34.4	RS Alegranza	1.8									70.5				
BH067	400252.02	6203190.12	70.0	-24.9	Gargano	0.3		2.3			5.9				20.4		70.0		
BH068	380807.9	6203069.7	60.8	-33.6	RS Alegranza	0.8									18.3			60.7	
BH069	411415.04	6202505.43	69.7	-22.1	Gargano	0.3		5.9	8.1		16.1		19.2	32.8			70.0		
BH071	405582.7	6202279.8	70.4	-21.7	Gargano	1.4		10.3	18.9								70.0		
BH072A	374468.8	6200642.9	70.3	-36.5	RS Alegranza	1.2									64.8				
BH073	387544.3	6200446.8	70.8	-30.2	RS Alegranza	0.8									8.6			43.0	43.0
BH075	413753.88	6199932.94	69.8	-22.1	Fugro Voyager			8.9	15.7		20.3			37.7			70.0		
BH076	379895.8	6199786.9	70.3	-30.7	RS Alegranza	2.3									31.3			66.0	66.0
BH077	420296.93	6199343.27	70.2	-25.2	Gargano			4.8	5.9		11.8	14.6	16.7	38.5			70.0		
BH078A	391138.2	6199170.3	64.5	-25.1	Fugro Zenith	5.7									64.4				
BH080	406415.37	6197278.82	70.0	-20.9	Excalibur	0.2		9.1	11.2								70.0		
BH081	410763.83	6197260.7	70.5	-20.7	Excalibur	0.5		4.4			8.6		9.0		16.1		70.0		
BH084	420071.2	6196742.04	69.8	-24.1	Fugro Voyager			9.0	11.8		16.9	20.2		34.1			70.0		
BH085	372664.5	6196737.4	70.8	-33.8	RS Alegranza	2.7					3.8		9.8		70.5				
BH086	417284.22	6196623.14	58.0	-22	Gargano			4.5					20.3	47.1					47.1
BH087	378903.7	6196469.8	70.5	-30.7	RS Alegranza	2.8									49.8			70.3	
BH088	386163.9	6196050.0	69.7	-27.6	RS Alegranza	4.0									25.9			59.0	59.0

Name	Easting [m]	Northing [m]	Total Penetration Depth [m BSF]	Water Depth [m MSL]	Vessel	U10 Depth to Base [m BSF]	U20 Depth to Base [m BSF]	U20a Depth to Base [m BSF]	U20b Depth to Base [m BSF]	U30 Depth to Base [m BSF]	U35 Depth to Base [m BSF]	U36 Depth to Base [m BSF]	U50 Depth to Base [m BSF]	U60 Depth to Base [m BSF]	U65 Depth to Base [m BSF]	U69 Depth to Base [m BSF]	U70 Depth to Base [m BSF]	U90 Depth to Base [m BSF]	BSU Depth to Top [m BSF]
BH089	402672.6	6195527.93	69.9	-24.8	Fugro Voyager	2.5									23.9			48.0	48.0
BH091	373597.7	6195320.4	70.4	-35	RS Alegranza	1.3							7.7		70.2				
BH092	391486.4	6195173.7	70.1	-26.0	Fugro Zenith	4.2									22.0			70.1	
BH093	408744.95	6194771.71	70.4	-19.6	Excalibur	2.6		8.4					12.7		36.0		70.0		
BH094	421347.88	6194443.07	69.8	-23.5	Gargano			3.4	5.4		17.5		24.4	41.1	70.0				
BH095	393658.2	6193554.7	70.2	-20.8	Fugro Zenith	6.5									22.6		70.2		
BH096	383432.6	6193400.0	70.4	-25.6	RS Alegranza	5.8									51.2			70.4	
BH097	388085.0	6193349.5	61.9	-30.7	RS Alegranza	2.8									30.9			61.9	
BH098	404802.53	6192888.01	69.9	-23.6	Fugro Voyager	0.6		5.9	11.8		15.5				70.0				
BH099A	370076.4	6192516.3	70.4	-35.3	RS Alegranza	0.7					6.8		14.9		70.2				
BH100	425652.46	6192330.37	69.8	-24.1	Gargano	0.2			0.6		9.3	15.3		29.3			70.0		
BH101	415455.88	6192139.9	70.8	-20	Excalibur	0.5		4.8			11.3		16.6		42.3		70.0		
BH102	419329.23	6191943.83	70.1	-21.6	Gargano			3.9				9.2	20.2	40.7			70.0		
BH103	379898.8	6191549.6	66.4	-31.5	Fugro Synergy	4.4			8.3						52.5			66.2	
BH105	382403.8	6190109.8	70.2	-24.8	RS Alegranza	5.8		13.3							55.8			70.2	
BH106	410539.13	6190038.81	69.8	-18.6	Excalibur	1.2		5.2					7.7		49.4		70.0		
BH107	421640.51	6189350.64	70.3	-23.3	Gargano			1.8			4.9	13.0	19.0	59.5					59.5
BH108	388393.8	6189338.9	69.8	-27.5	RS Alegranza	4.7									54.0		69.7		
BH109A	375056.8	6188486.4	70.9	-33.4	RS Alegranza	2.8					5.5				70.9				
BH110	417037.51	6188390.11	70.7	-19.5	Excalibur	1.6		6.1			13.7		21.8	51.7			70.0		
BH111	369955.4	6188379.4	70.3	-35.2	RS Alegranza	1.5					9.3		22.6		70.2				
BH112	401212.55	6187986.1	69.8	-25.2	Gargano	1.6									8.9			25.4	25.4
BH113	424036.39	6187860.66	69.8	-23.3	Fugro Voyager	0.8					10.3	14.0	16.9	29.2			49.7		49.7
BH114	404432.06	6187659.24	70.1	-22.9	Fugro Voyager	0.9		4.5	9.1		15.3				41.4		70.0		
BH115	379634.9	6187443.6	57	-28	RS Alegranza	0.8					15.8				70.4				
BH116	402374.06	6186800.28	69.9	-25.5	Fugro Voyager	0.2							1.8		20.2		70.0		
BH117	390531.6	6186729.7	69.9	-28.4	Fugro Synergy	1.6									46.4			69.8	
BH120	421307.07	6185220.58	29.9	-22.3	Gargano			1.3			10.2		18.7	37.1					37.1
BH140-CPT	417710.13	6226778.38	55.5	-29.65	Gargano	0.9			2.1		5.2		26.6	56.0					
BH160-CPT	390941.92	6222660.78	14.1	-28.57	Gargano			4.2			13.5								
BH179-CPT	418763.56	6205097.69	56.0	-27.57	Gargano			2.2			4.9	7.5	14.2	34.8		70.0			
BH185-CPT	403537.38	6184470.28	56.5	-25.23	Gargano	1.2			5.8		7.5		11.8		47.5		70.0		
BH200-CPT	402355.06	6222030.65	54.5	-27.21	Gargano	0.8		2.6			12.8		16.2	20.7	34.1		70.0		
BH224-CPT	419366.59	6223708.06	56.5	-28.8	Gargano	1.1					6.7		14.2	33.6		70.0			
BH255-CPT	400322.11	6211390.59	0.0	-24.97	Gargano	1.8		2.2							29.1		70.0		
BH283-CPT	399247.14	6194736.45	56.0	-24.76	Gargano	1.5									20.6			70.0	
BH329-CPT	419069.07	6199056.94	55.0	-24.71	Gargano			5.7			11.0	16.6	18.5	51.0		70.0			
BH357-CPT	404218.55	6189700.21	56.5	-22.33	Gargano	0.4		3.3	4.1						14.8			70.0	
BH372-CPT	404252.42	6206081.1	57.5	-22.97	Gargano	1.2		6.5	12.4		17.3						55.6		
CPT001	396643	6234080	16.2	-31.02	MV Norman Mermaid		1.9			10.7	13.4			16.2					
CPT003	400350	6228760	11.8	-29.75	MV Norman Mermaid		10.5				11.8								
CPT004	410026	6227790	32.6	-29.73	MV Norman Mermaid	2.3	4.2			6.3	9.8		13.0	32.6					
CPT005	396897	6226990	26.9	-29.51	MV Norman Mermaid		5.6			6.7	11.6			26.9					
CPT006	405730	6226820	16.9	-28.70	MV Norman Mermaid	0.9	5.7			7.3	12.8		15.6	16.9					
CPT007A	414848	6226750	27.2	-30.66	MV Norman Mermaid	0.9	1.8				11.7			27.2					
CPT008	423579	6226640	23.9	-27.15	MV Norman Mermaid	0.8					4.5		9.3	23.9					
CPT009A	418724	6226610	17.9	-29.79	MV Norman Mermaid	1.4					4.9		10.0	17.9					
CPT010	392237	6225950	13.3	-30.26	MV Norman Mermaid		8.2				13.3								
CPT011	402856	6225210	24.6	-28.33	MV Norman Mermaid	0.5	6.2				9.0		13.2	24.6					
CPT012	397289	6224010	43	-28.55	MV Norman Mermaid	1.3	7.0				16.3			28.0					
CPT013	411362	6223990	20.3	-30.19	MV Norman Mermaid		1.2				9.3		11.8	20.3					
CPT014A	406069	6223880	52.6	-27.32	MV Norman Mermaid	2.5	3.4				10.6								
CPT015	394845	6223440	52.6	-30.13	MV Norman Mermaid		6.1				8.8								
CPT016	416207	6222990	54	-29.49	MV Norman Mermaid						8.6		11.8	28.8					
CPT017	386817	6222760	53.5	-29.25	MV Norman Mermaid	1.5	4.1			6.8					54.0				
CPT018	400451	6222680	25.8	-27.22	MV Norman Mermaid		4.3				12.8			25.3					
CPT019	418594	6222490	28.3	-29.41	MV Norman Mermaid						7.6		12.8	28.8					
CPT020	423141	6222410	26	-27.47	MV Norman Mermaid	0.9					5.2		13.9	26.0					
CPT021	407203	6222100	22.2	-27.48	MV Norman Mermaid	0.6					6.2				22.2				
CPT022	413219	6221320	40.2	-30.88	MV Norman Mermaid		0.6				6.2		10.6	36.5					
CPT023A	416357	6220010	27.5	-30.27	MV Norman Mermaid						6.1		10.7	27.5					
CPT024	421184	6219980	53.4	-28.47	MV Norman Mermaid						7.7		13.6	33.4					
CPT025	386473	6219620	10.4	-28.40	MV Norman Mermaid	2.4	3.1												
CPT027A	396435	6218720	33.5	-27.93	MV Norman Mermaid	0.9	3.2				7.4								
CPT028	390561	6218460	25.9	-27.85	MV Norman Mermaid	1.4	3.9				9.2				19.3				
CPT029	404392	6218390	16.9	-25.77	MV Norman Mermaid	1.0					8.6						17.0		
CPT030	412874	6218190	14.5	-30.13	MV Norman Mermaid		1.9				6.1		11.4	15.5					
CPT032	394834	6216770	46.9	-28.14	MV Norman Mermaid		3.6				11.5				46.8				
CPT034	385608	6216380	16.9	-27.44	MV Norman Mermaid	0.5	15.0				16.9								
CPT035	402167	6215910	20.2	-25.39	MV Norman Mermaid		1.7				9.2		10.3		16.3		20.2		
CPT036	410872	6215720	22.3	-27.05	MV Norman Mermaid	0.6	3.1				8.0		18.1	22.3					
CPT037	423221	6215300	22.6	-26.88	MV Norman Mermaid						6.3	8.4	13.7	22.6					
CPT038	419067	6214400	45.2	-29.06	MV Norman Mermaid		0.9				4.8		11.4	34.2					
CPT039	381242	6214340	16.6	-30.54	MV Norman Mermaid	1.2	14.7												

Name	Easting [m]	Northing [m]	Total Penetration Depth [m BSF]	Water Depth [m MSL]	Vessel	U10 Depth to Base [m BSF]	U20 Depth to Base [m BSF]	U20a Depth to Base [m BSF]	U20b Depth to Base [m BSF]	U30 Depth to Base [m BSF]	U35 Depth to Base [m BSF]	U36 Depth to Base [m BSF]	U50 Depth to Base [m BSF]	U60 Depth to Base [m BSF]	U65 Depth to Base [m BSF]	U69 Depth to Base [m BSF]	U70 Depth to Base [m BSF]	U90 Depth to Base [m BSF]	BSU Depth to Top [m BSF]
CPT040	394769	6214230	12.4	-28.99	MV Norman Mermaid	0.7	7.3				9.3				12.4				
CPT041	385744	6213340	15.4	-29.14	MV Norman Mermaid		14.6				15.4								
CPT042	390155	6213250	13.6	-28.52	MV Norman Mermaid		8.6				13.6								
CPT044	415855	6212700	19	-29.35	MV Norman Mermaid		1.1				3.9		12.7	19.0					
CPT045	403447	6212010	14.6	-24.41	MV Norman Mermaid	0.6	2.3								14.6				
CPT046	382308	6211580	16.9	-29.93	MV Norman Mermaid		10.4				14.4								
CPT047	421869	6210920	20.4	-27.31	MV Norman Mermaid	0.5	1.4				4.7	8.8	12.9	20.4					
CPT049	394178	6210030	13.6	-29.60	MV Norman Mermaid		12.8				13.6								
CPT050	378619	6209720	43.8	-33.29	MV Norman Mermaid	1.7	3.5				11.5				43.8				
CPT051	414976	6209470	20	-28.03	MV Norman Mermaid		3.1				5.0		13.2	20.0					
CPT052	410201	6209420	26.2	-23.81	MV Norman Mermaid		8.9				10.8		18.2	26.2					
CPT054	406744	6208660	44.7	-23.36	MV Norman Mermaid	0.6	5.3				6.0				17.0				
CPT057A	382808	6206800	53.7	-30.86	MV Norman Mermaid	3.3									53.7				
CPT058	402556	6206750	32.6	-23.79	MV Norman Mermaid	0.5	11.8				16.4								
CPT059	386268	6206300	34.9	-28.25	MV Norman Mermaid	2.0									28.6				
CPT060	412980	6205920	18.6	-24.37	MV Norman Mermaid		9.5				11.1		17.4	18.6					
CPT061	392547	6205570	23.1	-26.87	MV Norman Mermaid	2.5									23.1				
CPT062	422899	6205000	28.4	-27.28	MV Norman Mermaid	0.7	1.7				5.1	8.0	12.8	28.4					
CPT063	408340	6204950	29.6	-22.50	MV Norman Mermaid	0.9	10.7				18.5								
CPT064	388643	6204770	38.1	-26.46	MV Norman Mermaid	5.1									38.0				
CPT065	397165	6204530	13.8	-28.49	MV Norman Mermaid	0.9									13.8				
CPT066	376477	6204160	28.7	-34.44	MV Norman Mermaid	1.0									28.8				
CPT067	400249	6203190	17.3	-24.92	MV Norman Mermaid	0.8	1.8				5.8				17.3				
CPT068	380808	6203070	49.1	-33.83	MV Norman Mermaid	1.1									21.0				
CPT069	411414	6202510	12.5	-22.14	MV Norman Mermaid	0.3	8.1				12.5								
CPT070	416024	6202490	26.7	-24.88	MV Norman Mermaid		7.3				11.6		16.7	26.7					
CPT071	405578	6202280	20.4	-21.66	MV Norman Mermaid	1.6	18.8												
CPT072A	374470	6200640	16.6	-37.18	MV Norman Mermaid	1.3									16.6				
CPT073	387545	6200450	16.1	-30.64	MV Norman Mermaid	1.0									8.6				
CPT074	409388	6200030	13.3	-21.34	MV Norman Mermaid	0.4	6.4				7.9				13.3				
CPT076	379898	6199790	29	-31.24	MV Norman Mermaid	2.3									29.0				
CPT077	420298	6199340	21.2	-25.19	MV Norman Mermaid		6.5				12.1	15.0	16.6	21.2					
CPT078	391142	6199170	53.7	-24.95	MV Norman Mermaid	5.8									53.7				
CPT079	402063	6198440	27.6	-25.79	MV Norman Mermaid	1.3									26.4				
CPT080	406417	6197280	41.4	-20.88	MV Norman Mermaid	0.4	11.7												
CPT081	410760	6197260	17.2	-20.69	MV Norman Mermaid	0.8	4.7				8.3		9.1		17.0				
CPT082	394190	6196800	30.9	-22.76	MV Norman Mermaid	6.6									18.1				
CPT083	388695	6196800	25.1	-30.66	MV Norman Mermaid	0.9									16.0				
CPT085	372665	6196740	21.1	-34.46	MV Norman Mermaid	1.2					3.9		10.0		21.1				
CPT086	417283	6196620	33.3	-22.01	MV Norman Mermaid		3.8						20.3	33.1					
CPT087	378904	6196470	23.3	-30.94	MV Norman Mermaid	2.5									23.3				
CPT088	386164	6196050	28.6	-27.44	MV Norman Mermaid	3.5									26.4				
CPT090	398080	6195530	13.8	-24.62	MV Norman Mermaid	2.3									13.8				
CPT091	373598	6195320	13.5	-35.61	MV Norman Mermaid	1.5							8.0		13.5				
CPT092	391487	6195170	26.3	-25.91	MV Norman Mermaid	4.1									20.4		26.4		
CPT093	408742.01	6194772.55			Excalibur														
CPT094	421349	6194440	15.4	-23.51	MV Norman Mermaid		5.3				15.4								
CPT095	393659	6193550	11.8	-21.53	MV Norman Mermaid	6.0									11.8				
CPT096	383433	6193400	23	-25.37	MV Norman Mermaid	6.0									23.0				
CPT097	388084	6193350	19.1	-31.04	MV Norman Mermaid	3.0									19.0				
CPT098	404800	6192890	50.3	-23.56	MV Norman Mermaid	0.7	11.7				15.8				50.3				
CPT100	425648	6192330	45.8	-24.13	MV Norman Mermaid	0.9					7.0	14.3	15.0	28.9					
CPT101	415453	6192140	34.2	-20.04	MV Norman Mermaid	0.6	4.6				11.1		17.2		34.1				
CPT102	419329	6191940	33	-21.58	MV Norman Mermaid		3.3					9.0	19.9	33.0					
CPT104	397470	6191300	28.3	-23.01	MV Norman Mermaid	6.8									14.9				
CPT106	410535.02	6190041.99			Excalibur														
CPT107	421637	6189350	53.4	-23.32	MV Norman Mermaid		1.5				3.9	12.8	19.9	53.4					
CPT110	417033.06	6188392.11			Excalibur														
CPT112	401214	6187990	20.1	-25.19	MV Norman Mermaid	1.6									9.2				
CPT114	404429	6187660	33.8	-22.87	MV Norman Mermaid	0.8	8.8				16.2				33.8				
CPT116	402374	6186800	20.6	-25.55	MV Norman Mermaid	0.2							1.6		19.6				
CPT118	396086	6185890	27.1	-21.17	MV Norman Mermaid	7.0									22.0				
CPT120	421303	6185220	19.3	-22.29	MV Norman Mermaid		2.2				10.3		18.0	19.3					
CPT121	369946	6194520	10	-36.89	MV Norman Mermaid	1.5							9.7		10.0				
CPT122	379932	6204140	50.3	-32.22	MV Norman Mermaid	2.4									43.6				
CPT123	389922	6191200	22.5	-26.71	MV Norman Mermaid	2.9									21.1				
CPT124	389937	6203030	31.7	-25.18	MV Norman Mermaid	4.8													
CPT125A	389950	6224270	14.3	-29.30	MV Norman Mermaid		8.2				13.5				14.3				
CPT126	389949	6228500	12.1	-30.54	MV Norman Mermaid		5.8			9.4	12.1								
CPT127	399998	6190080	52.6	-23.59	MV Norman Mermaid	3.2							25.1		52.6				
CPT128	399950	6207250	24.8	-22.86	MV Norman Mermaid	3.1	16.9				19.1				24.8				
CPT129	399954	6212610	36.9	-25.44	MV Norman Mermaid	0.8	3.5								36.9				
CPT130	399947	6216980	24	-24.87	MV Norman Mermaid	1.4	8.1				10.5		22.6		23.0				
CPT131	409953.21	6187128.3			Excalibur														

Name	Easting [m]	Northing [m]	Total Penetration Depth [m BSF]	Water Depth [m MSL]	Vessel	U10 Depth to Base [m BSF]	U20 Depth to Base [m BSF]	U20a Depth to Base [m BSF]	U20b Depth to Base [m BSF]	U30 Depth to Base [m BSF]	U35 Depth to Base [m BSF]	U36 Depth to Base [m BSF]	U50 Depth to Base [m BSF]	U60 Depth to Base [m BSF]	U65 Depth to Base [m BSF]	U69 Depth to Base [m BSF]	U70 Depth to Base [m BSF]	U90 Depth to Base [m BSF]	BSU Depth to Top [m BSF]
CPT132	409954	6196210	53.3	-20.82	MV Norman Mermaid	0.6	3.8				6.7		22.9		53.3				
CPT133	409951	6200630	30.7	-20.86	MV Norman Mermaid	1.0	18.2				30.7								
CPT134	409951	6218040	28.9	-26.04	MV Norman Mermaid		3.0				10.0		19.4	28.9					
CPT135	396830	6236810	23.3	-31.50	MV Norman Mermaid		0.9			10.5	12.1		13.3	23.2					
CPT136	420419	6186770	53.1	-22.09	MV Norman Mermaid		3.0				11.2		37.0	53.1					
CPT137	419958	6209720	22.4	-27.30	MV Norman Mermaid	0.9	14.4							22.4					
CPT138	419951	6215440	21.2	-28.69	MV Norman Mermaid						6.2		12.1	21.2					
CPT139	401348	6226770	21	-29.13	MV Norman Mermaid		5.3			7.7	12.7		13.7						
CPT140B	417706	6226780	4.4	-29.65	MV Norman Mermaid	0.9	2.0				5.2								
CPT141	420597	6226770	51.4	-29.87	MV Norman Mermaid	0.6							50.0	51.4					
CPT142	389952	6214100	17.4	-28.05	MV Norman Mermaid	2.0	17.1				17.4								
CPT143	407245	6216770	27.5	-26.10	MV Norman Mermaid		1.7				5.7		23.9		27.5				
CPT144	388483	6206800	33.2	-26.77	MV Norman Mermaid	2.9									27.8				
CPT145	393636	6206780	41.5	-28.74	MV Norman Mermaid	1.4							21.3		41.5				
CPT146	397844	6196770	30.6	-25.23	MV Norman Mermaid	3.2					7.7		30.6						
CPT147	392364	6216780	35.1	-27.70	MV Norman Mermaid	0.8	6.8				11.7				35.1				
CPT148	376767	6186770	31.7	-32.56	MV Norman Mermaid	1.9					10.3		30.6		31.6				
CPT149	382070	6186790	28.7	-31.12	MV Norman Mermaid	4.4					10.8		18.7		28.7				
CPT150	386223	6186800	19.4	-31.16	MV Norman Mermaid	1.5									19.4				
CPT152	399985	6185940	32	-23.57	MV Norman Mermaid						3.9		7.9		32.0				
CPT153	404406	6226570	22.3	-28.26	MV Norman Mermaid	1.9	3.6			7.0	12.6		14.9	22.3					
CPT154	412746	6229410	52.7	-33.17	MV Norman Mermaid	1.2							10.8	25.3					
CPT155	408203	6223280	34.8	-27.87	MV Norman Mermaid	0.2	0.4				13.5		14.2	34.8					
CPT156	407311	6210840	36.2	-24.13	MV Norman Mermaid		2.0						11.0		30.9				
CPT157	408993.5	6187641.72			Excalibur														
CPT158	387501	6191180	11.4	-26.92	MV Norman Mermaid	3.7									11.4				
CPT159	377115	6208360	28.1	-34.75	MV Norman Mermaid	0.7									28.1				
CPT160	390938	6222660	13.5	-28.66	MV Norman Mermaid		4.2				13.5								
CPT161	388623	6226220	39.2	-32.46	MV Norman Mermaid		5.2			7.4	8.6								
CPT162	426141	6192400	33.4	-23.98	MV Norman Mermaid	0.5	2.3				9.2	14.8		32.9					
CPT163	394681	6233670	20.3	-31.06	MV Norman Mermaid		2.0			10.2	13.7		14.9	20.3					
CPT164	398107	6233370	16.1	-30.88	MV Norman Mermaid		2.7			10.7	13.2			16.1					
CPT165	406051	6224880	17.4	-28.72	MV Norman Mermaid	1.2	4.7				11.5		14.0	17.4					
CPT166	396767	6222870	43.1	-28.54	MV Norman Mermaid	1.1	4.4				12.8								
CPT167	393993	6211040	14.2	-30.02	MV Norman Mermaid	0.2	13.3				14.2								
CPT168A	382198	6207460	53.7	-31.71	MV Norman Mermaid	2.3									53.7				
CPT169	398728	6207980	25.4	-22.86	MV Norman Mermaid	3.0	19.9				25.2								
CPT170	403613	6200820	39.5	-22.88	MV Norman Mermaid	0.7	6.5								18.5				
CPT171	412849	6224340	17.7	-30.87	MV Norman Mermaid		0.4				6.5		11.2	17.7					
CPT172	411754	6220970	17.9	-29.56	MV Norman Mermaid		1.7				7.5		11.4	17.9					
CPT173	411691	6218930	29.2	-28.83	MV Norman Mermaid		2.6				7.0		12.1	29.2					
CPT174	404653	6195930	16.1	-24.04	MV Norman Mermaid	0.7	13.3				>16.1								
CPT175	412338	6208860	19.3	-25.11	MV Norman Mermaid		6.7				9.4		16.4	19.3					
CPT176	412717	6213050	15.8	-27.47	MV Norman Mermaid		3.4				6.6		14.7	15.8					
CPT177	414244	6215370	22.6	-30.80	MV Norman Mermaid		0.9				3.0		10.7	18.2					
CPT178	420256	6213640	42.9	-28.29	MV Norman Mermaid		0.4				5.3	6.2	12.0	28.3					
CPT179	418761	6205100	18.6	-27.52	MV Norman Mermaid		2.2				4.9	8.5	14.2	18.6					
CPT180	423108	6204020	28	-27.04	MV Norman Mermaid		1.4				8.4		12.3	26.8					
CPT181	422911	6197850	25.6	-25.29	MV Norman Mermaid	0.3	4.1				9.6	24.0		25.6					
CPT182	409446.31	6193902.39			Excalibur														
CPT183	402215	6217860	29.3	-25.84	MV Norman Mermaid	0.9	1.6				11.2		16.2	19.8	26.1				
CPT184	396830	6187080	17.9	-21.48	MV Norman Mermaid	7.1									17.9				
CPT185	403533	6184470	12.3	-25.44	MV Norman Mermaid	1.0	5.8				7.5		11.4		12.2				
CPT187	402111	6207660	21.1	-23.83	MV Norman Mermaid	0.9	11.8				20.2				21.2				
CPT188	393608	6215020	10.8	-28.19	MV Norman Mermaid	1.0	8.5				10.8								
CPT189	387056	6215660	12.4	-30.48	MV Norman Mermaid	0.8	10.6				12.3								
CPT190B	374553	6203690	34.5	-35.43	MV Norman Mermaid	0.4									34.5				
CPT191	374437	6199610	9.5	-33.88	MV Norman Mermaid	3.9									9.5				
CPT192A	379554	6193580	6.3	-33.37	MV Norman Mermaid	0.8									5.6				
CPT193	374210	6192400	27	-35.07	MV Norman Mermaid	1.3					5.4				27.0				
CPT194	391336	6197150	21.6	-25.17	MV Norman Mermaid	5.1									17.5				
CPT195	372368	6188940	27.6	-34.72	MV Norman Mermaid	2.4				3.7	6.4		22.1		26.7				
CPT196	385713	6211290	18.4	-28.15	MV Norman Mermaid	1.8	17.9				18.4								
CPT197	390769	6225640	19.2	-29.58	MV Norman Mermaid		8.9				16.5				19.2				
CPT198	396718	6229000	23.5	-29.67	MV Norman Mermaid		6.1			9.4	10.9		13.6	23.5					
CPT199A	405193	6220610	20.7	-26.39	MV Norman Mermaid	0.6	1.6				6.1			17.7					
CPT200	402350	6222030	17.8	-27.47	MV Norman Mermaid	0.6	2.5			4.0	12.9		16.0	17.8					
CPT201C	398350	6204800	23.3	-25.95	MV Norman Mermaid	0.5									23.3				
CPT202	398952	6199810	10.4	-26.34	MV Norman Mermaid	0.5	1.8				3.6				10.4				
CPT203	397203	6198430	11.7	-25.58	MV Norman Mermaid	2.1									11.7				
CPT204A	397203	6198430	21.2	-25.58	MV Norman Mermaid	3.4									16.9				
CPT205	385393	6209140	22.8	-28.06	MV Norman Mermaid	2.3	11..67				16.3				22.8				
CPT206A	416639	6222060	54	-29.59	MV Norman Mermaid						6.2		10.8	25.2					
CPT207	391830	6189090	17.4	-26.91	MV Norman Mermaid										17.4				

Name	Easting [m]	Northing [m]	Total Penetration Depth [m BSF]	Water Depth [m MSL]	Vessel	U10 Depth to Base [m BSF]	U20 Depth to Base [m BSF]	U20a Depth to Base [m BSF]	U20b Depth to Base [m BSF]	U30 Depth to Base [m BSF]	U35 Depth to Base [m BSF]	U36 Depth to Base [m BSF]	U50 Depth to Base [m BSF]	U60 Depth to Base [m BSF]	U65 Depth to Base [m BSF]	U69 Depth to Base [m BSF]	U70 Depth to Base [m BSF]	U90 Depth to Base [m BSF]	BSU Depth to Top [m BSF]
CPT208	395191	6218450	12.4	-29.74	MV Norman Mermaid	0.6	2.2				9.8		12.4						
CPT209	394017	6220270	50.4	-29.52	MV Norman Mermaid		1.7				6.8		9.4		19.6				
CPT210A	372792	6201300	16.2	-35.55	MV Norman Mermaid	1.0									16.2				
CPT211	379447	6204790	25.8	-32.59	MV Norman Mermaid	2.2									25.8				
CPT212	391393	6206360	17.5	-25.86	MV Norman Mermaid	5.0					10.6				15.6				
CPT213	407113	6219970	16.8	-26.54	MV Norman Mermaid	0.6					5.5		10.3	13.2					
CPT214	395449	6204220	13.2	-27.91	MV Norman Mermaid	2.0													
CPT215	389267	6207930	16.6	-26.89	MV Norman Mermaid	2.3	9.8				16.3				16.6				
CPT216A	424735	6224840	54.2	-26.56	MV Norman Mermaid	0.6	2.8				7.0		9.8						
CPT217	422959	6207070	22.5	-27.36	MV Norman Mermaid		2.0				4.1	6.6	11.4	22.5					
CPT218A	395562	6215450	8.3	-27.89	MV Norman Mermaid	1.3	4.2								8.3				
CPT219	416413	6214850	21.1	-29.76	MV Norman Mermaid		0.6				4.0		12.2	21.1					
CPT220	411331	6192260	23.3	-19.95	MV Norman Mermaid	0.5	3.8						12.2		23.3				
CPT221	414313.81	6186769.29			Excalibur														
CPT224	419362	6223710	25.6	-28.79	MV Norman Mermaid	1.1					6.7		14.2	25.6					
CPT225	414883	6197140	23.8	-21.58	MV Norman Mermaid	0.8	6.6				8.5				22.0				
CPT226	393676	6224270	36.7	-30.35	MV Norman Mermaid		5.8				12.4								
CPT227	422503	6192670	29.4	-24.24	MV Norman Mermaid	0.6	4.3				9.6	20.2		29.4					
CPT228	400676	6223720	19.7	-27.82	MV Norman Mermaid		7.7				12.5		14.9	19.7					
CPT229	367995	6189020	6.2	-35.61	MV Norman Mermaid	2.0					6.2				6.2				
CPT230	410596	6222800	30.8	-29.25	MV Norman Mermaid		2.0				9.3		12.4	30.8					
CPT231	398548	6202830	30.2	-26.70	MV Norman Mermaid	1.0					4.8				7.3				
CPT232	406543	6194290	53.7	-20.23	MV Norman Mermaid	0.4	10.9				18.9				53.7				
CPT233	401329	6190100	10.8	-24.53	MV Norman Mermaid	0.4									10.8				
CPT234	410244	6211470	28.1	-24.33	MV Norman Mermaid		6.5				10.0		18.3	28.1					
CPT235	387030	6207490	29.1	-27.28	MV Norman Mermaid	2.8					10.4								
CPT236	411459	6227080	17.3	-31.47	MV Norman Mermaid	2.5				4.5	6.6		11.0	17.3					
CPT237	382017	6194120	26.8	-27.60	MV Norman Mermaid	5.4									26.8				
CPT238	382331	6197250	32.4	-29.54	MV Norman Mermaid	4.7									31.6				
CPT239	388238	6222040	28.4	-28.88	MV Norman Mermaid	0.9	3.2			4.3									
CPT240	389825	6217300	32.2	-27.11	MV Norman Mermaid	2.4	8.0				10.2								
CPT241	378338	6200450	27.7	-32.96	MV Norman Mermaid	1.9									27.7				
CPT242	418516	6212240	13.7	-28.61	MV Norman Mermaid	0.5	1.2				4.2	6.4	12.7	13.7					
CPT243	389321	6194670	25.7	-30.63	MV Norman Mermaid	1.6									25.7				
CPT244	384844	6207010	42.4	-27.86	MV Norman Mermaid	3.1									42.4				
CPT245	402568	6191350	14.4	-22.96	MV Norman Mermaid	2.3	4.0								14.4				
CPT246	386430	6202190	40.4	-31.35	MV Norman Mermaid	1.3									9.9				
CPT247	408820.24	6189689.74			Excalibur														
CPT248	385693	6218440	37.7	-30.59	MV Norman Mermaid	0.9	2.0						4.7		8.2				
CPT249	416302	6203570	21.6	-25.73	MV Norman Mermaid		7.3				10.3		16.3	21.6					
CPT250	408045	6195650	22	-20.08	MV Norman Mermaid	1.4	11.2				21.7								
CPT251	407950.66	6192572.84			Excalibur														
CPT252	401413	6199360	15.6	-24.83	MV Norman Mermaid	0.5									6.7				
CPT253	394561	6230610	13.3	-30.40	MV Norman Mermaid		12.2				13.3								
CPT254	391100	6227730	53.6	-29.84	MV Norman Mermaid		9.0				18.3								
CPT255	400318	6211390	12.7	-25.11	MV Norman Mermaid	1.8	2.2								3.8				
CPT256A	400318	6211390	5.3	-25.11	MV Norman Mermaid	1.6									5.2				
CPT257	378994	6197560	43.7	-30.66	MV Norman Mermaid	3.3									43.7				
CPT258	402636	6202650	27.4	-24.34	MV Norman Mermaid	0.5	16.1				27.0								
CPT260	404102	6216270	53.2	-25.41	MV Norman Mermaid		1.2				10.3		30.3	35.8					
CPT261	382962	6209670	41.3	-29.32	MV Norman Mermaid	3.1									8.9				
CPT262	388397	6196520	20.2	-31.21	MV Norman Mermaid	0.5									20.2				
CPT263	417947.38	6186537.15			Excalibur														
CPT264	394752	6227530	15.1	-31.34	MV Norman Mermaid		7.0			7.6	13.7			15.0					
CPT265	392899	6200570	34.5	-24.50	MV Norman Mermaid	6.1									24.3				
CPT266	402875	6224200	23.4	-27.98	MV Norman Mermaid	0.8	6.7			7.7	12.3		17.7	23.4					
CPT267	416690	6224160	53.6	-29.50	MV Norman Mermaid						5.6		11.6	25.4					
CPT268	411875	6216950	16.7	-28.94	MV Norman Mermaid	0.3	3.9				5.0		13.0	16.7					
CPT269	411724	6204630	24.8	-23.22	MV Norman Mermaid	1.8	13.6				14.4		18.5	24.8					
CPT270	398025	6192430	25	-22.37	MV Norman Mermaid	6.0									22.1				
CPT271	406073	6217720	47.2	-26.10	MV Norman Mermaid		1.9				7.2								
CPT272	419076	6190860	26.7	-21.09	MV Norman Mermaid		3.5				5.9	7.6	20.3	26.7					
CPT273	400416	6215480	20.7	-24.75	MV Norman Mermaid	1.4	3.2				7.2				17.8				
CPT274	388612	6210890	19.8	-26.35	MV Norman Mermaid	3.5	17.5				19.8								
CPT275	407721	6200690	21.1	-20.61	MV Norman Mermaid	2.0	17.1				21.1								
CPT276	416870	6198580	28.6	-22.87	MV Norman Mermaid		13.9				16.6		17.7	28.6					
CPT277	416290	6227130	17.2	-29.75	MV Norman Mermaid	1.2	4.1				6.3		11.9	17.2					
CPT278	419804	6183870	21	-20.95	MV Norman Mermaid		3.7				11.2		19.6	21.0					
CPT279	421493	6222090	15.9	-28.80	MV Norman Mermaid						5.7		13.5	15.9					
CPT280	411675	6195410	31.3	-20.20	MV Norman Mermaid	0.5	7.5								29.5				
CPT281A	396216	6190010	32.1	-22.01	MV Norman Mermaid	6.7									15.8				
CPT282	386628	6194100	15.7	-32.92	MV Norman Mermaid	1.3							8.9		14.3				
CPT283A	399247	6194740	8.4	-24.86	MV Norman Mermaid	2.3									8.6				
CPT284	395490	6212380	15.1	-28.70	MV Norman Mermaid	0.5	9.1				14.8								

Name	Easting [m]	Northing [m]	Total Penetration Depth [m BSF]	Water Depth [m MSL]	Vessel	U10 Depth to Base [m BSF]	U20 Depth to Base [m BSF]	U20a Depth to Base [m BSF]	U20b Depth to Base [m BSF]	U30 Depth to Base [m BSF]	U35 Depth to Base [m BSF]	U36 Depth to Base [m BSF]	U50 Depth to Base [m BSF]	U60 Depth to Base [m BSF]	U65 Depth to Base [m BSF]	U69 Depth to Base [m BSF]	U70 Depth to Base [m BSF]	U90 Depth to Base [m BSF]	BSU Depth to Top [m BSF]
CPT285	377962	6195280	30.2	-34.42	MV Norman Mermaid	1.3									30.2				
CPT286	370210	6196670	14.8	-38.30	MV Norman Mermaid	1.5									14.9				
CPT287	408206	6216150	19.8	-25.01	MV Norman Mermaid		1.2				7.1				19.3				
CPT288	396247	6206390	34.4	-28.59	MV Norman Mermaid	0.5							15.9						
CPT289	380358	6201900	34.7	-32.81	MV Norman Mermaid	0.9									20.7				
CPT290	418485	6195860	30.2	-22.37	MV Norman Mermaid		6.8				12.2		19.5	30.2					
CPT291	385500	6205130	21	-29.65	MV Norman Mermaid	2.1									10.5				
CPT292	422735	6199860	32	-25.92	MV Norman Mermaid		3.4				6.2	19.6		27.9					
CPT293A	386261	6220590	22.5	-30.11	MV Norman Mermaid	1.1	2.0								15.3				
CPT294	408611	6221320	25.5	-26.77	MV Norman Mermaid	0.5	1.7				10.0		14.5	25.5					
CPT295	386786	6199220	14.4	-30.52	MV Norman Mermaid	2.3									14.3				
CPT296	383329	6219960	46.1	-30.72	MV Norman Mermaid	2.6	2.7				6.2		7.1		46.1				
CPT297	394198	6187550	14.3	-22.96	MV Norman Mermaid	3.7									14.3				
CPT298	416645	6191370	41.1	-20.15	MV Norman Mermaid	1.5	6.1				8.6		32.0	41.0					
CPT300	384595	6191580	27.4	-30.33	MV Norman Mermaid	1.6									27.3				
CPT301	391903	6191150	41.1	-26.89	MV Norman Mermaid	1.3									41.1				
CPT302	418242	6218330	16	-29.32	MV Norman Mermaid						6.8		11.6	16.0					
CPT303	419781	6206370	19.7	-27.90	MV Norman Mermaid		1.0				5.4	8.8	13.5	19.7					
CPT304	397353	6226070	30.8	-28.44	MV Norman Mermaid	0.6	8.7				14.2			30.8					
CPT305	384158	6200700	19.1	-32.71	MV Norman Mermaid	1.2							4.2		19.1				
CPT306	415113.64	6189019.06			Excalibur														
CPT307	396425	6219730	21.6	-29.05	MV Norman Mermaid	1.5	4.4				7.8				13.3				
CPT308	418780	6227620	4.8	-29.77	MV Norman Mermaid	0.3	3.7				4.4								
CPT309	399390	6221390	53.1	-26.32	MV Norman Mermaid	1.7	5.2				11.6				39.9				
CPT310	422933	6213220	26.2	-28.25	MV Norman Mermaid	0.9					4.6	6.1	11.4	26.2					
CPT312	412405	6210910	22.1	-26.01	MV Norman Mermaid		7.1				7.6		17.2						
CPT313	391834	6213600	14.7	-27.77	MV Norman Mermaid	1.2	11.5				14.5			14.7					
CPT314	415718.53	6184999.02			Excalibur														
CPT315	383550	6212860	16.4	-29.09	MV Norman Mermaid	2.1	15.9				16.4								
CPT316	411723.58	6189280.74			Excalibur														
CPT318	389130	6219200	17.5	-27.50	MV Norman Mermaid	1.8	3.6								17.5				
CPT319	414082	6225600	33.6	-30.32	MV Norman Mermaid	0.6					7.3		10.2	26.1					
CPT320	414652	6220610	28	-31.09	MV Norman Mermaid						5.9		10.0	27.1					
CPT321	408920	6208080	14.7	-23.17	MV Norman Mermaid	1.5	11.4				14.7								
CPT322	399120	6190630	11.3	-25.17	MV Norman Mermaid	1.3									11.3				
CPT323	383484	6202640	29.9	-33.11	MV Norman Mermaid		1.7								19.0				
CPT324	397355	6196340	28.5	-24.60	MV Norman Mermaid	2.9									23.1				
CPT325	396571	6232040	21.5	-30.42	MV Norman Mermaid		3.9			10.1	13.5		17.9	21.5					
CPT326	376863	6190950	9.9	-33.24	MV Norman Mermaid	1.5					2.7				9.9				
CPT327	420650	6195310	28.7	-23.32	MV Norman Mermaid		9.5				16.1	18.4	20.0	28.7					
CPT328	392238	6203480	23.1	-24.81	MV Norman Mermaid	5.5									23.1				
CPT329	419069	6199060	23.3	-24.55	MV Norman Mermaid		5.7				11.0	16.6	18.5	23.3					
CPT330	407407	6206790	37.1	-22.50	MV Norman Mermaid	1.5	11.8				16.0				29.8				
CPT331	402991	6220130	53.5	-26.48	MV Norman Mermaid	1.0					11.0		26.3	35.0					
CPT332	415469	6200330	34.9	-23.26	MV Norman Mermaid		5.3				7.7		18.6	34.9					
CPT333	394448	6195780	15.5	-22.58	MV Norman Mermaid	5.9									15.5				
CPT334	416742	6194480	13.9	-21.07	MV Norman Mermaid		0.6				2.8		10.2		13.3				
CPT335	422780	6209070	27.8	-27.24	MV Norman Mermaid		1.5				4.5	8.6	12.2	27.8					
CPT336	425716	6194360	11	-24.19	MV Norman Mermaid	0.4	8.7				11.0								
CPT337	401313	6205440	12.8	-24.67	MV Norman Mermaid	0.5	11.6				13.0								
CPT338	411589	6207660	19.9	-24.09	MV Norman Mermaid	0.8	9.7				11.5		17.5	19.9					
CPT339	412260	6198600	37.5	-20.54	MV Norman Mermaid	0.9	4.9						12.8		36.2				
CPT340	397794	6216950	20.8	-24.40	MV Norman Mermaid	2.4	6.3				8.2				20.8				
CPT341	421152	6218950	25.7	-28.56	MV Norman Mermaid						6.9		12.8	25.8					
CPT342	414359	6196000	35.9	-20.58	MV Norman Mermaid	0.7	3.7				5.1				33.7				
CPT343B	380025	6208990	10.6	-33.39	MV Norman Mermaid	0.8									10.5				
CPT344	423009	6216280	25.3	-27.21	MV Norman Mermaid						6.3	8.3	13.2	25.3					
CPT345	399032	6210060	27.7	-23.03	MV Norman Mermaid	3.0	8.3												
CPT346	418922	6217440	34.4	-29.01	MV Norman Mermaid						6.6		11.9	34.4					
CPT347	388375	6203660	25.4	-26.56	MV Norman Mermaid	5.0	5.5								25.4				
CPT348	376577	6206210	23.6	-33.69	MV Norman Mermaid	2.9									23.6				
CPT349	386214	6187860	16.4	-26.07	MV Norman Mermaid	4.3									16.4				
CPT350	390462	6201030	29.5	-24.72	MV Norman Mermaid	5.4									13.5				
CPT351	388098	6224030	34.5	-30.04	MV Norman Mermaid		4.0								30.1				
CPT352	372412	6198190	37	-35.49	MV Norman Mermaid	1.8							30.4		37.0				
CPT353	419029	6220500	25.5	-29.80	MV Norman Mermaid						4.5		17.3	25.5					
CPT354	405986	6222820	19.4	-27.71	MV Norman Mermaid	0.9					7.0		10.1						
CPT355	384750	6189580	6.6	-30.46	MV Norman Mermaid	4.0									6.6				
CPT356	417618	6206930	20.8	-27.71	MV Norman Mermaid		1.3				5.9		13.6	20.8					
CPT357	404214	6189700	18.2	-22.40	MV Norman Mermaid	1.1	4.6								14.8				
CPT358	387768	6213760	15.1	-28.16	MV Norman Mermaid	0.9	10.7				15.1								
CPT360	370461	6190570	18.9	-35.44	MV Norman Mermaid	1.9					4.5		18.3		18.9				
CPT361	386219	6197060	20.2	-30.58	MV Norman Mermaid	1.1									17.8				
CPT362	400695	6201160	31.7	-26.49	MV Norman Mermaid	0.6													

Name	Easting [m]	Northing [m]	Total Penetration Depth [m BSF]	Water Depth [m MSL]	Vessel	U10 Depth to Base [m BSF]	U20 Depth to Base [m BSF]	U20a Depth to Base [m BSF]	U20b Depth to Base [m BSF]	U30 Depth to Base [m BSF]	U35 Depth to Base [m BSF]	U36 Depth to Base [m BSF]	U50 Depth to Base [m BSF]	U60 Depth to Base [m BSF]	U65 Depth to Base [m BSF]	U69 Depth to Base [m BSF]	U70 Depth to Base [m BSF]	U90 Depth to Base [m BSF]	BSU Depth to Top [m BSF]
CPT363	381944	6199180	25.9	-31.23	MV Norman Mermaid	3.5									24.8				
CPT364	396833	6209580	15.5	-26.93	MV Norman Mermaid	1.2	13.7				15.5								
CPT365	390103	6187630	35.2	-29.05	MV Norman Mermaid	1.5									13.9				
CPT366	421108	6186210	26.3	-22.38	MV Norman Mermaid		2.5				10.1		23.5	26.3					
CPT367	384445	6186470	18.5	-26.38	MV Norman Mermaid	4.3					6.5				18.5				
CPT368	423855	6227720	51.2	-26.48	MV Norman Mermaid	1.0					3.8		7.4	15.5	25.8				
CPT369	391816	6219710	50.9	-28.64	MV Norman Mermaid	1.0	3.6				10.5				17.3				
CPT370	414345	6218500	20.8	-30.96	MV Norman Mermaid						6.1		11.0	20.8					
CPT371	383987	6195540	34.8	-30.49	MV Norman Mermaid	3.2									33.6				
CPT372	404248	6206080	16.2	-22.59	MV Norman Mermaid	1.1	12.4				15.8								
CPT373	381979	6215610	16.4	-29.93	MV Norman Mermaid	1.6	15.0				16.3								
CPT374	395125	6193870	16.7	-21.71	MV Norman Mermaid	6.3									16.7				
CPT375	398866	6228480	12.8	-29.61	MV Norman Mermaid		11.7				12.8								
CPT376	403384	6186450	18.7	-23.88	MV Norman Mermaid	0.3	4.9				5.4		12.7		18.7				
CPT377	394756	6197880	20.8	-23.01	MV Norman Mermaid	7.2									16.3				
CPT378	421102	6225080	22.6	-29.49	MV Norman Mermaid	0.5					4.5		11.0	21.4					
CPT379	421121	6202570	14	-26.93	MV Norman Mermaid	0.7	3.0				8.0	11.1	13.1	14.0					
CPT380	394560	6222430	38.5	-30.32	MV Norman Mermaid		5.3				7.3				8.6				
CPT381	391715	6193100	25.3	-25.05	MV Norman Mermaid	4.4									21.6				
CPT382	417947	6201890	29.4	-25.73	MV Norman Mermaid		5.8				8.0		17.3	29.4					
CPT383	393379	6207810	29.9	-28.42	MV Norman Mermaid	2.4	4.1			7.0	14.3				29.9				
CPT384A	402447	6194400	2.7	-24.63	MV Norman Mermaid	3.6									4.5				
CPT385	391440	6230930	26.2	-30.85	MV Norman Mermaid		11.2				14.5		16.5	26.2					
CPT386	400121	6198030	16.5	-25.71	MV Norman Mermaid	0.7									11.8				
CPT387	391735	6209500	17.6	-27.62	MV Norman Mermaid	0.4	14.6				17.6								
CPT388	413744.8	6191758.88			Excalibur														
CPT389	402049	6212760	22.4	-25.70	MV Norman Mermaid		2.5								15.4				
CPT390	406771.41	6186160.96			Excalibur														
CPT391A	405960	6214670	14.7	-24.78	MV Norman Mermaid		2.8				5.3				11.9				
CPT392	398641	6213050	12.5	-23.42	MV Norman Mermaid	3.4	5.5								12.5				
CPT393	379681	6212010	12.2	-33.14	MV Norman Mermaid	0.6	8.2				12.1								
CPT394	410828	6214660	25.5	-25.59	MV Norman Mermaid		2.8				9.6		19.2	25.5					
CPT395	406431	6198320	24.2	-20.65	MV Norman Mermaid	1.5	12.4				18.2								
CPT396	405536	6208360	29.4	-23.11	MV Norman Mermaid	0.5	5.2								29.4				
CPT397	410905	6224910	22.5	-30.35	MV Norman Mermaid	0.5	1.2				8.9		12.4	22.5					
CPT398	384163	6216030	16.1	-28.66	MV Norman Mermaid	0.4	12.3				16.1								
CPT399	398839	6188530	23.2	-23.05	MV Norman Mermaid	4.4									19.3				
SCPT002	393122	6229240	13.5	-29.68	MV Norman Mermaid		7.4			10.5	13.5								
SCPT026C	399883	6218850	21.5	-25.56	MV Norman Mermaid	0.6	2.2				6.1				17.7				
SCPT031	381364	6216780	12.6	-30.14	MV Norman Mermaid	4.2	11.4				12.6								
SCPT033	414238	6216500	20.2	-30.85	MV Norman Mermaid		0.9				3.7		11.1	20.2					
SCPT043B	409954	6213000	31.5	-24.67	MV Norman Mermaid		4.8				9.0				27.2		31.5		
SCPT048	390091	6210160	19.3	-26.68	MV Norman Mermaid	4.9	17.1				19.3								
SCPT053	398511	6208920	15.1	-23.01	MV Norman Mermaid	2.6	14.5				15.1								
SCPT055	420061	6207460	20.6	-27.98	MV Norman Mermaid		1.0				4.5	9.6	13.8	20.6					
SCPT056A	380512	6207120	16.9	-32.77	MV Norman Mermaid	0.5									16.9				
SCPT075	413754	6199930	17.6	-22.10	MV Norman Mermaid		15.9				17.6			17.6					
SCPT084	420074	6196740	12.6	-24.06	MV Norman Mermaid		11.7				12.6			12.5					
SCPT089	402674	6195530	15.5	-24.80	MV Norman Mermaid	2.0									15.5				
SCPT103A	379903	6191550	10.5	-31.67	MV Norman Mermaid	2.3	7.9								10.5				
SCPT113	424040	6187860	23.6	-23.33	MV Norman Mermaid	0.8					11.0	13.7	16.9	23.6					
SCPT117A	390528	6186730	38.1	-28.53	MV Norman Mermaid	1.4									36.5				